Contents

ROMAI J., **4**, 2(2008), 1–6

ON THE GENERALIZED HALLEY METHOD FOR SOLVING NONLINEAR EQUATIONS

Grigore Albeanu

"Spiru Haret" University, Bucharest

galbeanu@gmail.com

Abstract Halley's method is a famous iteration method for solving nonlinear equations $F(X) = 0$. Some Kantorovich-like theorems have been given, including extensions for general spaces. Quasi-Halley methods were proposed too. This paper uses the generalized inverse approach in order to obtain a robust generalized Halley method.

Keywords: nonlinear equations, quasi-Halley method, pseudoinverse.

2000 MSC: 65H10, 65Y99.

1. INTRODUCTION

A famous iteration was presented by Halley [11] in 1694. A large number of papers have been written in time and some interesting extensions were proposed, not only for scalar case but also for multivariate case, for nonlinear systems of equations, even for operator equations in Banach spaces. If f is a function $f : R \to R$ and x^* is a root of f, that is $f(x^*) = 0$, a common approach for obtaining x^* is to use the Newton iteration (also called *the tangent method*):

$$x_{k+1} = x_k - \frac{f(x_k)}{f'(x_k)}, \tag{1}$$

for $k = 0, 1, ...$, generating a sequence of iterations which converges to x^* under some condition. It was shown that the order of convergence for the Newton method is 2.

The Halley's method has a cubic order of convergence. It is known also as *the method of tangent hyperbolas*. The Halley clasic iteration is given by [6, 15, 19, 20]

$$x_{k+1} = x_k - \frac{f(x_k)/f'(x_k)}{1 - \frac{1}{2}\frac{f(x_k)f''(x_k)}{f'(x_k)^2}}, \quad k = 0, 1, ... \tag{2}$$

In this paper we consider the case of nonlinear systems of equations and we extend the Halley method in order to use generalized inverse of the Jacobian matrix. The next section is dedicated to the general basic iterative relation. Algorithmic aspects will be discussed in the third section. The concluding section provides remarks and future possible developments.

2. THE GENERALIZED HALLEY METHOD

Let $F : R^n \to R^n$ generate a system of n equations in n unknowns

$$F(x) = 0, \tag{3}$$

where F is sufficiently smooth and the Jacobian $F'(x^*)$ is nonsingular if x^* is a solution of the system. Consider the Halley class of iterations for solving (1)

$$x_{k+1} = x_k - \left\{ I + \frac{1}{2} L_F(x_k) \left[I - \alpha L_F(x_k) \right]^{-1} \right\} (F'(x_k))^{-1} F(x_k), k = 0, 1, 2, ..., \tag{4}$$

where $L_F(x) = (F'(x))^{-1} F''(x) (F'(x))^{-1} F(x)$ is the degree of logarithmic convexity [12], and α is a real parameter.

For $\alpha = 0$, the classical Chebyshev' s method is obtained

$$x_{k+1} = x_k - \left\{ I + \frac{1}{2} L(x_k) \right\} F'(x_k)^{-1} F(x). \tag{5}$$

When $\alpha = \frac{1}{2}$, we obtain the classical Halley's method. For real-valued function, the iteration is written as in (2). For $\alpha = 1$ is obtained the super-Halley method. It is easy to note that the Newton method is obtained for $\alpha \to -\infty$.

For real valued functions, it was shown that any iterative process given by the expression

$$x_{k+1} = x_k - H(L_F(x_k))(F'(x_k))^{-1} F(x_k), \tag{6}$$

where H is such that $H(0) = 1$, $H'(0) = 1/2$, and $|H''(0)| < \infty$, generates a third order convergence method [9, 19]. An interesting case appears when H is a sum of operators as in the equation

$$H(L) = I + \frac{1}{2} L + \sum_{i=2}^{\infty} A_i L^i, \tag{7}$$

where I is the identity operator, L is the degree of convexity for some function, and $A_i (i = 2, ...,)$ are real constants.

Algorithmic aspects for increasing the confidence in numerical computing of the solution of a system of equations will be detailed in the next section using the two-step iteration model.

3. ALGORITHMIC ASPECTS

In order to implement the computer iteration (2), let us rewrite the equation in the following way (where x_0 is given as a point belonging to a small neighborhood of x^*):
1. solve for u_k: $F'(x_k)u_k = -F(x_k)$;
2. solve for v_k: $(F'(x_k) + \alpha F''(x_k)u_k)v_k = -\frac{1}{2}F''(x_k)u_k u_k$;
3. compute $x_{k+1} = x_k + u_k + v_k$.

In order to have a robust algorithm, without significantly decreasing of the convergence speed, we propose to use Penrose generalized inverse of matrices.

If A is a general real matrix the pseudoinverse $A^\dagger$ of A is defined as the unique matrix satisfying all of the following conditions [5, 16]:

1 $AA^\dagger A = A$;

2 $A^\dagger AA^\dagger = A^\dagger$;

3 $(AA^\dagger)^T = AA^\dagger$;

4 $(A^\dagger A)^T = A^\dagger A$.

. The new iterative process can be described by:

1 compute $u_k = -(F'(x_k))^\dagger F(x_k)$;

2 compute $v_k = -\frac{1}{2}(F'(x_k) + \alpha F''(x_k)u_k)^\dagger F''(x_k)u_k u_k$;

3 compute $x_{k+1} = x_k + u_k + v_k$, for $k = 0, 1, ...$

Such an approach is motivated by the requirement to increase the method reliability while maintaining a degree of convergence greater than 2, even less than 3, when the matrix under inversion did not have a good behaviour. The convergence of the method is guaranteed by theoretical results based on the fact that (2) is an approximation to the Newton equation

$$F'(x_k + u_k)v_k = -F(x_k + u_k), \tag{8}$$

since

$$F(x_k + u_k) \approx F(x_k) + F'(x_k)u_k + \frac{1}{2}F''(x_k)u_k u_k = \frac{1}{2}F''(x_k)u_k u_k,$$

and

$$F'(x_k + u_k) \approx F'(x_k) + \alpha F''(x_k)u_k.$$

From the computational point of view we need second-derivative-free iterations as in the study [14]. In our case $n \geq 1$, and finite difference approximations for the Hessian are required. There are some choices when computing derivatives. The first one consists of establishing a small step $h > 0$ and making differences related to x_k and $x_k \pm h$. The second one can use x_0 as fixed reference point for doing derivatives just like in the univariate case $(f(x_k) - f(x_0))/(x_k - x_0)$. In this case a simplified version like in [2] is used. However, a multipoint approach can be used based on the scheme $(f'(x_k) - f'(x_{k-1}))/(x_k - x_{k-1})$ written for the univariate function f.

Computing generalized inverse is not a difficult task. Some powerful algorithms were already proposed [4, 7, 10, 13, 18] and implementation techniques based on different numerical schemes are available.

The complexity of the generalized Halley method is larger than for the classical iteration, but it is motivated by reliability increasing and robustness of the procedures to be implemented in programming languages.

4. CONCLUSIONS

The Halley's method continues to be an important subject of investigation. In our study we extend the standard iteration in order to obtain robust algorithms based on pseudoinverse computing. There are some options for obtaining second-derivative-free iterations, and it is possible to think about an updating scheme for the Jacobian matrix as in the case of Broyden type methods [1].

References

[1] Albeanu, G., *On the convergence of the quasi Gauss Newton methods for solving nonlinear systems*, Int. J. of Computer Math. **66**(1998), 93-99.

[2] Albeanu, G., *On the modified Gauss-Newton method*, Mathematical Reports, **48**, 3-4(1996), 147-153.

[3] Argyros, I.K., *A note on the Halley method in Banach spaces*, Appl. Math. Comput., **58**(1993), 215-224.

[4] Ben-Israel, A., *An iterative method for computing the generalized inverse of an arbitrary matrix*, Mathematics of Computation **19**, 91(1965), 452-455.

[5] Ben-Israel, A., Greville, T.N.E., *Generalized inverses: Theory and Applications*, Wiley, New York, 1974.

[6] Chen, D., *Ostrowski-Kantorovich theorem and S-order of convergence of Halley method in Banach spaces*, Comment. Math. Univ. Carolinae **34**, 1(1993), 153 - 163.

[7] Eirola, T., Nevanlinna, O., *Rank one updates*, Linear Algebra Appl., **121**(1989), 511-520.

[8] Ezquerro, J. A., Hernández, M. A., Romero, N., *Newton-like methods for operators with bounded second Fréchet derivative*, Tenth Int. Conf. Zaragoza-Pau on Applied Mathematics and Statistics, Jaca, Sept. 15-17, 2008.

[9] Gander, W., *On Halley's iteration method*, Amer. Math. Monthly, **92**(1985), 131-134.

[10] Greville, T. N. E., *The pseudoinverse of a rectangular or singular matrix and the application to the solution of systems of linear equations*, SIAM Rev. **1**(1959), 38-43.

[11] Halley, E., *Methodus nova, accurata et facilis inveniendi radices aequationum quarumcumque generaliter, sine praevia reductione*, Philos. Trans. Roy. Soc. London, **18**(1694), 136-148.

[12] Hernández, M. A., Salanova, M. A., *Indices of convexity and concavity: Application to Halley method*, Appl. Math. Comput., **103**(1999), 27-49.

[13] Ichim, I., *Sur le problème des moindres carrés*, C.R. Acad. Sci. Paris, **326**, Série I(1998), 625-627.

[14] Jisheng, K., Yitian, L., *Third-order iterative methods free from second derivative*, International Mathematical Forum, **2**, 14(2007), 689-698.

[15] Levin, Y., Ben-Israel, A., *Directional Halley and quasi-Halley methods in n variables*, Rutcor Research Report, RRR-28, 2000.

[16] Penrose, R., *A generalized inverse for matrices*, Proc. Camb. Philos. Soc., **51**(1955), 406-413.

[17] Rao, C. R., Mitra, K., *Generalized inverse of matrices and its applications*, Wiley, New York, 1971.

[18] Stanica, D., *A new algorithm for computing the pseudoinverse in Hilbert spaces*, Rev. Roumaine Math. Pures Appl., **50**, 4(2005), 367-371.

[19] Varona, J. L., *Graphic and numerical comparison between iterative methods*, The Mathematical Intelligencer, **24**, 1(2002), 37-46.

[20] Zheng, S., Robbie, D., *A Note on the convergence of Halley's method for solving operator equations*, J. Austral. Math. Soc., Ser. B, **37**(1995), 16-25.

ROMAI J., **4**, 2(2008), 7–28

BIFURCATION AND STABILITY IN THE PROBLEM ON CAPILLARY-GRAVITY ON A SURFACE OF FLOATING DEEP FLUID LAYER

Artyom N. Andronov, Luiza R. Kim-Tyan, Boris V. Loginov

Mordovian State University, Saransk, Russia

Moscow Institute of Steel and Alloys, Russia

Ulyanovsk State Technical University, Russia

arbox@inbox.ru, kim-tyan@yandex.ru, loginov@ulstu.ru

Abstract Potential flows of incompressible heavy capillary floating fluid in 3-dimensional layer of infinite depth with free upper surface are determined. Asymptotics of periodical regimes in spatial layer with free upper boundary close to horizontal plane z=0 bifurcating from the basic flow with constant velocity V in Ox-direction are computed. Their stability is investigated. Methods of group-invariant bifurcation theory and group analysis of differential equations are used. Special attention is paid to cases of high-dimensional ($n \geq 4$) degeneration of the linearized operator.

The obtained results are supported by grant RFBR-Romanian Academy, project No. 07-01-91680a

Keywords: floating deep fluid layer; capillary-gravity surface waves; bifurcation and stability.

2000 MSC: 76B15,76B07, 58E09, 37K45.

1. FORMULATION OF THE PROBLEM

Potential flows of incompressible heavy capillary floating fluid in a spatial layer of infinite depth with free upper boundary are considered. The formulation of these problems goes back to the works of A. I. Nekrasov [1], [2], T. Levi-Civita [3] and D. Struik [4]. In the articles [5] - [10] spatial problems for the layers of finite depth were investigated. In [6] - [8] group stratification, while in [9],[10] – group analysis methods [11] in bifurcation theory problems

[12], developed in [13]-[15], used in a number of surface waves and physics of phase transitions problems [9], [10], [13]-[15], were applied.

Periodical with periods $\frac{2\pi}{a} = a_1$ and $\frac{2\pi}{b} = b_1$ potential flows of a heavy capillary floating deep fluid in spatial layer with free upper boundary close to horizontal plane $z = 0$ are bifurcating from the basic flow with constant velocity V in Ox-direction are considered. Velocity potential has the form $\varphi(x, y, z) = Vx + \Phi(x, y, z)$. In dimensionless variables this problem is described by the system of differential equations

$$\Delta\Phi = 0, -\infty < z < f(x, y); \tag{1}$$

$$\frac{\partial\Phi}{\partial z} - \frac{\partial f}{\partial x} = (\nabla f, \nabla_{xy}\Phi) = \frac{\partial\Phi}{\partial x}\frac{\partial f}{\partial x} + \frac{\partial\Phi}{\partial y}\frac{\partial f}{\partial y}, z = f(x, y); \tag{2}$$

$$\frac{\partial\Phi}{\partial x}+\frac{1}{2}|\nabla\Phi|^2+F^2 f+\frac{k}{\sqrt{1+|\nabla f|^2}}\left[F^2 + (-\nabla f\cdot\nabla_{xy} + \frac{\partial}{\partial z})(\frac{\partial\Phi}{\partial x} + \frac{1}{2}|\nabla\Phi^2|)\right] -$$

$$-\gamma F^2 div(\frac{\nabla f}{\sqrt{1+|\nabla f|^2}}) = const, z = f(x, y), \tag{3}$$

with decreasing conditions of the function Φ and its first derivatives at the infinity. The equality (2) is a kinematic interfacial condition, while (3) describes the force balance (the Bernoulli integral), $F^2 = \frac{gL}{V^2}$ (the Froud number), $\gamma = \frac{\sigma}{\rho g L^2}$(the Bond number), $k = \frac{\rho_0}{\rho L}$.

The system (1)–(3) is invariant to the group of the 2-dimensional shifts $L_\beta g(x, y) = g(x + \beta_1, y + \beta_2)$ and the reflections

$$S_1\colon x \to -x, \Phi(x, y, z) \to -\Phi(-x, y, z), f(x, y) \to f(-x, y),$$
$$S_2\colon y \to -y, \Phi(x, y, z) \to \Phi(x, -y, z), f(x, y) \to f(x, -y)$$

2. CONSTRUCTION OF BRANCHING SYSTEMS

The linearized system can be obtained by straightening the free upper boundary - by performing the change of variables $\zeta = z - f(x, y)$, $\Phi(x, y, \zeta + f(x, y)) = u(x, y, \zeta)$ and setting $F^2 = F_0^2 + \varepsilon$

$$\Delta u = 2u_{x\zeta}f_x + 2u_{y\zeta}f_y + u_\zeta(f_{xx} + f_{yy}) - u_{\zeta\zeta}(f_x^2 + f_y^2) = w^{(0)}(u, f), \tag{4}$$

$$-\infty < \zeta < 0;$$

$$u_\zeta - f_x = u_x f_x + u_y f_y - u_\zeta(f_x^2 + f_y^2) = w^{(1)}(u, f), \zeta = 0; \tag{5}$$

$$u_x + ku_{x\zeta} + F_0^2 f - \gamma F_0^2 \Delta f = u_\zeta f_x - \varepsilon f + \gamma\varepsilon\Delta f - \tfrac{1}{2}(u_x^2 + u_y^2 + u_\zeta^2) +$$
$$+ u_x u_\zeta f_x + u_y u_\zeta f_y - \gamma(F_0^2+\varepsilon)\left[\tfrac{3}{2}(f_x^2 f_{xx} + f_y^2 f_{yy}) + \tfrac{1}{2}(f_x^2 f_{yy} + f_y^2 f_{xx}) +\right.$$
$$\left. + 2 f_x f_y f_{xy}\right] + \tfrac{1}{2}k(F_0^2+\varepsilon)\left(f_x^2 + f_y^2\right) + k\left[-f_y u_{xy} - f_x(u_{xx} + u_{\zeta\zeta}) +\right.$$
$$+ u_x u_{x\zeta} + u_y u_{y\zeta} + u_\zeta u_{\zeta\zeta} + \tfrac{3}{2} f_x^2 u_{x\zeta} + \tfrac{1}{2} f_y^2 u_{x\zeta} +$$
$$+ u_\zeta(f_x f_{xx} + f_y f_{xy} - 2u_{x\zeta} f_x - 2u_{y\zeta} f_y) - u_{xy}(f_x u_y + f_y u_x) -$$
$$\left. - u_{\zeta\zeta}(u_x f_x + u_y f_y) - f_x u_x u_{xx} - f_y u_y u_{yy} + f_x f_y u_{y\zeta}\right] = w^{(2)}(u, f, \varepsilon), \zeta = 0; \tag{6}$$

$$k < \gamma F_0^2, \quad \text{(the ellipticity condition of the Bernoulli integral (6))}, \tag{7}$$

where $w^{(j)}$, $j = 0,\ 1,\ 2$ are small nonlinearities. The system (4)–(6) can be written as the nonlinear functional equation

$$BX = R(X,\varepsilon),\ R(0,\varepsilon) \equiv 0,\ R_x(0,0) = 0,$$

where $X = \{u, f\}$ is the bifurcation point problem with Fredholm [16] operator $B = B_{mn}\colon C^{2+\alpha}(\Pi_0 \times (-\infty, 0]) + C^{2+\alpha}(\Pi_0) \to C^{\alpha}(\Pi_0 \times (-\infty, 0]) + C^{\alpha}(\Pi_0) + C^{\alpha}(\Pi_0)$, $0 < \alpha < 1$, Π_0 being the periodicity rectangle in (x, y) plane. Expanding the function $f(x, y)$ in the Fourier series

$$\sum_{m,n}(a_{mn}\cos max\cos nby + b_{mn}\cos max\sin nby + c_{mn}\sin max\cos nby + d_{mn}\sin max\sin nby),$$

in the homogeneous equation $BX = 0$ we find

$$u(x,y,\zeta) = \sum_{m,n}\frac{mae^{s_{mn}\zeta}}{s_{mn}}\left(c_{mn}\cos max\cos nby + d_{mn}\cos max\sin nby - \right.$$
$$\left. - a_{mn}\sin max\cos nby - b_{mn}\sin max\sin nby\right), \quad s_{mn}^2 = m^2a^2 + n^2b^2, \quad F_{mn}^2 = F_0^2.$$

Then the equation (6) gives the dispersion relation (DR)

$$(k + \frac{1}{s_{mn}})m^2a^2 = F_0^2(1 + \gamma s_{mn}^2), \quad s_{mn}^2 = m^2a^2 + n^2b^2, \quad F_{mn}^2 = F_0^2 \tag{8}$$

(m, n are positive integers, n may be equal zero), which is satisfied for some pairs (m_j, n_j), $j = 1, 2, \ldots, \kappa$, such that the elements of the basis of the zero-subspace $N(B)$ of the linearized operator B have the form

$$\begin{aligned}
\hat\varphi_{1j} &= \{-v_{1j}(\zeta)\sin m_j ax\cos n_j by, v_{2j}\cos m_j ax\cos n_j by\},\\
\hat\varphi_{2j} &= \{-v_{1j}(\zeta)\sin m_j ax\sin n_j by, v_{2j}\cos m_j ax\sin n_j by\},\\
\hat\varphi_{3j} &= \{v_{1j}(\zeta)\cos m_j ax\cos n_j by, v_{2j}\sin m_j ax\cos n_j by\},\\
\hat\varphi_{4j} &= \{v_{1j}(\zeta)\cos m_j ax\sin n_j by, v_{2j}\sin m_j ax\sin n_j by\},
\end{aligned}$$

where $v_{1j}(\zeta) = \dfrac{m_j a\sqrt{ab}}{\pi s_{m_j n_j}} e^{s_{m_j n_j}\zeta}, v_{2j} = \dfrac{\sqrt{ab}}{\pi}$.

Passing to the complex basis the branching equation (BEq) $\hat{t}(\eta, \varepsilon)$ in real variables turns to the BEq in complex variables [8] $\xi_{1,2} = \eta_1 \pm i\eta_2$, $\xi_{3,4} = \eta_3 \pm i\eta_4$

$$t_j(\xi, \varepsilon) = (C^{-1}\hat{t})_j(C\xi, \varepsilon), j = \overline{1,4}. \tag{9}$$

Correspondingly

$$\varphi = C'\hat{\phi}, C = \frac{1}{2}\begin{pmatrix} -i & i & -i & i \\ 1 & 1 & -1 & -1 \\ 1 & 1 & 1 & 1 \\ i & -i & -i & i \end{pmatrix}, C^{-1} = \frac{1}{2}\begin{pmatrix} i & 1 & 1 & i \\ -i & 1 & 1 & i \\ i & -1 & 1 & i \\ -i & -1 & 1 & -i \end{pmatrix};$$

$$\varphi_{1j} = \frac{1}{2}\{v_{1j}(\zeta), -iv_{2j}\}e^{i(m_j ax + n_j by)} = \varphi_{\bar{l}_{1j}} = \frac{1}{2}\{v_{1j}(\zeta), -iv_{2j}\}e^{i\langle \bar{l}_{1j}, q\rangle},$$

$$\varphi_{3j} = \frac{1}{2}\{v_{1j}(\zeta), -iv_{2j}\}e^{i(m_j ax - n_j by)} = \varphi_{\bar{l}_{3j}} = \frac{1}{2}\{v_{1j}(\zeta), -iv_{2j}\}e^{i\langle \bar{l}_{3j}, q\rangle},$$

$$\varphi_{2j} = \varphi_{\bar{l}_{2j}} = \frac{1}{2}\{v_{1j}(\zeta), iv_{2j}\}e^{-i\langle \bar{l}_{1j}, q\rangle}, \quad \varphi_{4j} = \varphi_{\bar{l}_{4j}} = \frac{1}{2}\{v_{1j}(\zeta), iv_{2j}\}e^{-i\langle \bar{l}_{3j}, q\rangle},$$

$$q = (x, y), \quad v_{1j}(\zeta) = \frac{m_j a\sqrt{ab}}{\pi s_j}e^{s_j\zeta}, \quad v_{2j} = \frac{\sqrt{ab}}{\pi}, \quad \bar{l}_{2j} = -\bar{l}_{1j}, \quad \bar{l}_{4j} = -\bar{l}_{3j}.$$

The symmetry of the homogeneous system (4)–(6) operator is proved by standard methods [17]. The same methods, applied to the nonhomogeneous system (4)–(6), result in its solvability conditions, which are used at the construction of BEq

$$-\int\limits_{\Pi_0\times(-\infty,0]} w^{(0)}u_{rj}dxdyd\zeta + \int\limits_{\Pi_0} w^{(1)}\left[u_{rj}(x, y, 0) + k\frac{\partial f_{rj}}{\partial x}\right]dxdy + \int\limits_{\Pi_0} w^{(2)}f_{rj}dxdy = 0,$$

$r = \overline{1,4}, \quad j = 1\ldots\kappa$. In the accepted numeration of basis elements of the subspace N and corresponding vertices of the rectangle $\tilde{\Pi}_0$ in reciprocal lattice group action $\tilde{G}^1$ in variables ξ of the j-th periodical lattice is expressed by the permutations $\xi_{k_j} : p_1 = (1_j, 2_j)(3_j, 4_j), p_2 = (1_j, 3_j)(2_j, 4_j), p_3 = (1_j, 4_j)(2_j, 3_j)$, while the BEq group symmetry in complex basis, by the equalities

$$(p_k t)_r(\xi, \varepsilon) = t_r(p_k\xi, \varepsilon), \quad k = 1, 2, 3. \tag{10}$$

Actually, the transformations of vector basis elements $\varphi_j = \{u_j, f_j\}$ in $N(B)$ at the group action $\tilde{G}^1$ are determined by the formulae

$$p_1\varphi_j = \{p_1 u_j, -p_1 f_j\}, \quad p_2\varphi_j = \{p_2 u_j, p_2 f_j\}, \quad p_3\varphi_j = \{p_3 u_j, -p_3 f_j\},$$

where $p_1 g(x,y) = g(-x,-y)$, $p_2 g(x,y) = g(x,-y)$, $p_3 g(x,y) = g(-x,y)$. BEq also inherits the symmetry of (4)–(6) with respect to the operation J of complex conjugacy. The symmetry with respect to the 2-parameter shifts group is inherited by the BEq as invariance with respect to the 2-parameter rotation group $A_{g(\beta)} \cong SO(2)\times SO(2)$

$$e^{i(l_r,\beta)} t_r(\xi,\varepsilon) = t_r(\ldots, \xi_{1_j} e^{i(l_{1_j},\beta)}, \ldots, \xi_{4_j} e^{i(l_{4_j},\beta)}, \ldots; \varepsilon), \quad r = \overline{1,n}.$$

Basis system of infinitesimal operators ($\partial\xi_k = \partial/\partial\xi_k$, j is the number of symmetry lattice) corresponds to the group $A_{g(\beta)}$

$$X_1 = \sum_j m_j a[-\xi_{1_j}\partial\xi_{1_j} + \xi_{2_j}\partial\xi_{2_j} - \xi_{3_j}\partial\xi_{3_j} + \xi_{4_j}\partial\xi_{4_j} - t_{1_j}\partial t_{1_j} + \tag{11}$$

$$+ t_{2_j}\partial t_{2_j} - t_{3_j}\partial t_{3_j} + t_{4_j}\partial t_{4_j}],$$

$$X_2 = \sum_j n_j b[-\xi_{1_j}\partial\xi_{1_j} + \xi_{2_j}\partial\xi_{2_j} + \xi_{3_j}\partial\xi_{3_j} - \xi_{4_j}\partial\xi_{4_j} - t_{1_j}\partial t_{1_j} + t_{2_j}\partial t_{2_j} +$$

$$+ t_{3_j}\partial t_{3_j} - t_{4_j}\partial t_{4_j}],$$

The general rank $r_*(M)$ of the matrix $M = [\Xi^s_\nu, T^s_\nu]$ of coefficients X_1 and X_2 is equal to 2, if $n_j \neq 0$ for at least one j, and is equal to 1, if $n_j \equiv 0$. The complete system of functionally independent invariants, determined by the equations $X_s I(\xi,t)$, $\quad s = 1,2$, contains n invariants of the form $I_k(\xi,t) = \frac{t_k}{\xi_k}$, $\quad k = \overline{1,n}$, and $\frac{n}{2}$ invariants of the form $I_{n+k}(\xi) = \xi_{2k-1}\xi_{2k}, k = \overline{1,\frac{n}{2}}$. The remaining $2n - r_*(M) - n - \frac{n}{2} = \frac{n}{2} - r_*(M) = \nu_0$ invariants are selected in the form of an invariant monomial of the least possible degrees of ξ. From the form of the matrix M it follows that $T = \{\xi, t | t - t(\xi) = 0\}$ is a nonsingular invariant manifold of group action in the subspace Ξ^{2n} of vectors (ξ,t) and can be represented in the form $\Phi^\sigma(I_1,\ldots,I_{2n-r_*}) = 0$, $\quad \sigma = 1,\ldots,n$. Since $r_*(\Xi,T) = r_*(\Xi)$, the solvability condition $r\left[\frac{\partial I_k}{\partial t_j}\right] = n$ of system with respect to variables t is fulfilled, and we obtain the general form of BEq, expressed by the degrees of invariants $I_{n+\sigma}(\xi), 1 \le \sigma \le \sigma_0 = n - r_*(M)$. In the general case of the analytical BEq of dimension $n > 4$, it is necessary to use additional invariants with the following factorization between the used monomial invariants.

3. FOUR-DIMENSIONAL N(B)

In this case $n = \dim N(B) = 4$ and the branching system has form

$$t_s(\xi,\varepsilon) \equiv a_0^{(s)}(\varepsilon)\xi_s + \sum_q a_q^{(s)}(\varepsilon)\xi_s(\xi_1\xi_2)^{q_1}(\xi_3\xi_4)^{q_2} = 0, \quad s = \overline{1,4},$$

where the relations between the coefficients and the equations are determined by (10). The equalities (10) allow us to express BEqs by the first one

$$t_1(\xi,\varepsilon) \equiv A\xi_1\varepsilon + B\xi_1^2\xi_2 + C\xi_1\xi_3\xi_4 + \cdots = 0,$$

$$A = t^{(1)}_{e_1;1}, \quad B = t^{(1)}_{2e_1+e_2;0}, \quad C = t^{(1)}_{e_1+e_2+e_3}, \quad e_1 = (1,0,0,0), \ldots, e_4 = (0,0,0,1),$$

$$t_k(\xi,\varepsilon) \equiv p_{k-1}t_1(\xi,\varepsilon) = 0, k = 2,3,4,$$

$$t^{(1)}_{\alpha;k} = -\int\limits_{\Pi_0\times(-\infty,0]} w^{(0)}u_2\,dxdyd\zeta + \int\limits_{\Pi_0} w^{(1)}\left[u_2(x,y,0) + k\frac{\partial f_2}{\partial x}\right]dxdy + \int\limits_{\Pi_0} w^{(2)}f_2\,dxdy.$$

Sequentially, we find

$$u_{2e_1;0} = \frac{ima^2b[((k^2+6\gamma)s_{mn} - 5k)s_{mn}e^{2s_{mn}\zeta} - 2(2\gamma s_{mn}^2 - 3ks_{mn} - 1)e^{s_{mn}\zeta}]}{8\pi^2(2\gamma s_{mn}^2 - 3ks_{mn} - 1)}e^{2i(max+nby)},$$
$$f_{2e_1;0} = \frac{abs_{mn}[(k^2+2\gamma)s_{mn}^2 + ks_{mn} + 2]}{8\pi^2(2\gamma s_{mn}^2 - 3ks_{mn} - 1)}e^{2i(max+nby)},$$
$$u_{e_1+e_2;0} = const, \quad f_{e_1+e_2;0} = const; \quad u_{e_3+e_4;0} = const, \quad f_{e_3+e_4;0} = const; \quad u_{e_1+e_4;0} = 0,$$
$$f_{e_1+e_4;0} = \left(\frac{an^2b^3(1+\gamma s_{mn}^2)/s_{mn} - kab(m^2a^2 - n^2b^2)(4\gamma s_{mn}^2 - ks_{mn} + 3)/2}{2\pi^2 s_{mn}(1+4\gamma n^2b^2)(ks_{mn}+1)}\right)e^{2inby};$$

$$u_{e_1+e_3;0} = \frac{ima^2b}{4\pi^2 s_{mn}}\left[\frac{ks_{mn}(ks_{mn}(m^2a^2 - n^2b^2) - 5m^2a^2 - 2\gamma(s_{mn}^2 + 4m^2a^2n^2b^2))}{(ks_{mn}+1)(1+4\gamma m^2a^2)ma - 2s_{mn}(1+2kma)(1+\gamma s_{mn}^2)}e^{2ma\zeta} + \right.$$
$$\left. + \frac{2(3\gamma s_{mn}^2(m^2a^2 - 2n^2b^2) - 2n^2b^2(1-2\gamma n^2b^2)) - 3n^2b^2}{(ks_{mn}+1)(1+4\gamma m^2a^2)ma - 2s_{mn}(1+2kma)(1+\gamma s_{mn}^2)}e^{2ma\zeta} - 2s_{mn}e^{s_{mn}\zeta}\right]e^{2imax};$$

$$f_{e_1+e_3;0} = \frac{ma^2b}{4\pi^2 s_{mn}}\left[\frac{ks_{mn}(ks_{mn}(m^2a^2-n^2b^2)+m^2a^2-3n^2b^2-2\gamma s_{mn}^2)}{(ks_{mn}+1)(1+4\gamma m^2a^2)ma-2s_{mn}(1+2kma)(1+\gamma s_{mn}^2)}+\right.$$
$$\left.+\frac{2(2mas_{mn}-m^2a^2-2n^2b^2)(1+\gamma s_{mn}^2))}{(ks_{mn}+1)(1+4\gamma m^2a^2)ma-2s_{mn}(1+2kma)(1+\gamma s_{mn}^2)}\right]e^{2imax}.$$

Then the non-zero coefficients of the BEq have form

$$A = -(1+\gamma s_{mn}^2) < 0,$$
$$B = \frac{m^2a^3bs_{mn}}{4\pi^2}\left[\frac{ks_{mn}(-6\gamma s_{mn}^2+17)+3}{(2\gamma s_{mn}^2-3ks_{mn}-1)}+\frac{k}{2}(-m^2a^2-3n^2b^2+\frac{4m^2a^2n^2b^2}{s_{mn}^2})+\right.$$
$$\left.-\frac{ks_{mn}^2(ks_{mn}+1)((k^2+2\gamma)s_{mn}^2+ks_{mn}+2)}{(1+\gamma s_{mn}^2)(2\gamma s_{mn}^2-3ks_{mn}-1)}+\frac{3s_{mn}^2\gamma(ks_{mn}+1)}{2(1+\gamma s_{mn}^2)}-1\right],$$
$$C = \frac{m^2a^3b}{2\pi^2}\left[\frac{(3m^2a^2-n^2b^2)ma}{s_{mn}^2(2ma+s_{mn})}U_1+\frac{m^3a^3}{s_{mn}^3}U_2-\frac{4m^2a^2}{s_{mn}}+\frac{2n^2b^2}{s_{mn}}+\frac{2n^2b^2}{s_{mn}^3}U_3+\right.$$
$$+k(-\frac{m^2a^2}{s_{mn}}U_1+\frac{m^3a^3}{s_{mn}^2}U_2-m^2a^2+n^2b^2+\frac{2n^2b^2}{s_{mn}^2}U_3)-\frac{2k(ks_{mn}+1)}{s_{mn}^2(1+\gamma s_{mn}^2)}(m^3a^3U_2-$$
$$-n^2b^2U_3)+\frac{\gamma(ks_{mn}+1)}{2s_{mn}(1+\gamma s_{mn}^2)}(3m^4a^4+3n^4b^4-2m^2a^2n^2b^2)+\frac{8m^3a^3U_1}{s_{mn}^2}-$$
$$\frac{k}{2}(-23m^2a^2+5n^2b^2-\frac{4m^2a^2n^2b^2}{s_{mn}^2}+\frac{2(m^4a^4-n^4b^4)}{s_{mn}^2}+4maU_1+\frac{12m^2a^2U_1}{s_{mn}}-$$
$$\left.-4maU_2+\frac{2m^3a^3U_2}{s_{mn}^2}-\frac{4n^2b^2U_3}{s_{mn}^2})\right],$$

where U_1, U_2, U_3 are defined by the formulae

$$u_{e_1+e_3;0} = \frac{ima^2b}{2\pi^2 s_{mn}}[U_1e^{2ma\zeta}-s_{mn}e^{s_{mn}\zeta}]e^{2imax}, \quad f_{e_1+e_3;0} = \frac{ma^2b}{2\pi^2 s_{mn}}U_2e^{2imax},$$

$$f_{e_1+e_4;0} = \frac{ab}{2\pi^2 s_{mn}}U_3e^{2inby}.$$

The symmetry of the problem with respect to L_β allows us to make a reduction of the BEq $\hat{t}(\eta,\varepsilon)=0$, supposing $\eta_2=\eta_4=0$. Then the main part of the reduced system takes the form

$$A\eta_1\varepsilon + B\eta_1^3 + C\eta_1\eta_3^2 = 0, A\eta_3\varepsilon + C\eta_1^2\eta_3 + B\eta_3^3 = 0.$$

Thus, the following theorem is true.

Theorem 3.1. *The problem* (1)-(3) *in the neighborhood of the bifurcation point $F_0^2 = F_{mn}^2$, which is the four-dimensional eigenvalue, determined by* (8), *has up to the transformation $y \to -y$ two two-parametric families of periodical* *solutions*

$$\{\Phi^{(1)}, f^{(1)}\} = \left[-\frac{A}{B}(F^2 - F_{mn}^2)\right]^{\frac{1}{2}} \left\{\frac{ma\sqrt{ab}}{\pi s_{mn}} e^{s_{mn}\zeta} \cos[ma(x+\beta_1) + nb(y+\beta_2)],\right.$$
$$\left.\frac{\sqrt{ab}}{\pi}\sin[ma(x+\beta_1)+nb(y+\beta_2)]\right\} + O\left(\left|F^2 - F_{mn}^2\right|\right),$$
$$sign(F^2 - F_{mn}^2) = signB,\ \gamma s_{mn}^2 \neq \frac{1}{2}, \zeta = z - f^{(1)}(x,y); \tag{12}$$

$$\{\Phi^{(2)}, f^{(2)}\} = \left\{\frac{2ma\sqrt{ab}}{\pi s_{mn}} e^{s_{mn}\zeta}\cos[ma(x+\beta_1)]\cos[nb(y+\beta_2)],\right.$$
$$\left.\frac{2\sqrt{ab}}{\pi}\sin[ma(x+\beta_1)]\cos[nb(y+\beta_2)]\right\}\left[-\frac{A}{B+C}(F^2 - F_{mn}^2)\right]^{\frac{1}{2}} +$$
$$+O\left(\left|F^2 - F_{mn}^2\right|\right),\ sign(F^2 - F_{mn}^2) = sign(B+C),\ \zeta = z - f^{(2)}(x,y). \tag{13}$$

4. FOUR-DIMENSIONAL N(B). TWO DEGENERATED PERIODICITY LATTICES

First of all, we shall prove the possibility of the existence of physical parameters under which there is a solution with symmetry of two degenerated lattices. Let the DR be fulfilled for two pairs $(m_1, 0)$ and $(m_2, 0)$

$$(km_1a + 1)m_1a = F_0^2(1 + \gamma m_1^2 a^2),$$
$$(km_2a + 1)m_2a = F_0^2(1 + \gamma m_2^2 a^2).$$

Dividing the first equation by the second one, we get the expression for k

$$k = \frac{(1+\gamma m_1^2a^2)(1+\gamma m_2^2a^2)}{m_2^2a^2 - m_1^2a^2}\left[\frac{m_1a}{1+\gamma m_1^2a^2} - \frac{m_2a}{1+\gamma m_2^2a^2}\right].$$

Suppose $m_2 > m_1$ and $f(x) = \dfrac{x}{1+\gamma x^2}$, where $x = ma$. Then $f' = \dfrac{1-\gamma x^2}{(1+\gamma x^2)^2}$ and $f' < 0$ for $\gamma x^2 > 1$, the existence condition for the two degenerated periodicity lattices symmetry.

The one-parameter rotation-reflection group in the space of vectors $\xi = (\xi_1, \xi_2, \xi_3, \xi_4)$ with the diagonal matrix $A(\beta) = diag\{e^{im_1a\beta}, e^{-im_1a\beta}, e^{im_2a\beta}, e^{-im_2a\beta}\}$ corresponds to shifts group with respect to x.

Here $(m_1, 0)$ and $(m_2, 0)$ satisfy the dispersion relation (8). The basis infinitesimal operator $(\partial_{\xi_k} I = \partial I/\partial \xi_k)$

$$X = \left\{\hat{X}(\xi), \hat{X}(t)\right\}, \hat{X}(\xi) = m_1 a\left(-\xi_1\partial_{\xi_1} I + \xi_2\partial_{\xi_2} I\right) + m_2 a\left(-\xi_3\partial_{\xi_3} I + \xi_4\partial_{\xi_4} I\right)$$

corresponds to the group $A(\beta)$.

The differential equation $XI(\xi, t) = 0$ determines the complete system of seven functionally independent invariants

$$I_s(\xi, t) = \frac{t_s}{\xi_s}, s = \overline{1,4}, I_5(\xi) = \xi_1\xi_2, I_6(\xi) = \xi_3\xi_4, I_7(\xi) = \xi_1^{N/m_1}\xi_4^{N/m_2},$$

where N is the least common multiple (L.C.M.) of numbers m_1 and m_2.

By the L.V. Ovsyannikov theorem [11] we obtain the general form of BEq. We suppose BEq to be analytical or sufficiently smooth, therefore while using the constructed complete system of functionally independent invariants some of the monomial terms may be absent. It is necessary to use the additional invariant $I_8 = \xi_2^{N/m_1}\xi_3^{N/m_2}$. Then there occur repetitious summands and it is necessary to make a factorization between the invariants $I_7(\xi)I_8(\xi) = I_5^{N/m_1}(\xi)I_6^{N/m_2}(\xi)$. This factorization is denoted by the symbol $[...]^{out}$. Thus, BEq takes the form

$t_k(\xi, \varepsilon) \equiv$

$$\equiv a_0^{(k)}(\varepsilon)\xi_k + \sum_q a_q^k(\xi)(\xi_1\xi_2)^{q_1}(\xi_3\xi_4)^{q_2}\left[\xi_k\left(\xi_1^{N/m_1}\xi_4^{N/m_2}\right)^{q_3}\left(\xi_2^{N/m_1}\xi_3^{N/m_2}\right)^{q_4}\right]^{out} = 0,$$

$k = \overline{1,4}$ where the symbol $[...]^{out}$ means that the factors in brackets in the form $\xi_{2k-1}\xi_{2k}$ must be omitted.

Particularly, for the coprime numbers m_1 č m_2 the main part of the BEq takes the form

$$\begin{aligned} &A\xi_1\varepsilon + B\xi_2^{m_2-1}\xi_3^{m_1} + \cdots = 0, A\xi_2\varepsilon + B\xi_1^{m_2-1}\xi_4^{m_1} + \cdots = 0,\\ &C\xi_3\varepsilon + D\xi_1^{m_2}\xi_4^{m_1-1} + \cdots = 0, C\xi_4\varepsilon + D\xi_2^{m_2}\xi_3^{m_1-1} + \cdots = 0. \end{aligned} \tag{14}$$

5. SIX-DIMENSIONAL DEGENERATION OF LINEARIZED OPERATOR

The existence of three degeneration periodicity lattices ($n_1 = n_2 = n_3 = 0$) is impossible. Actually, let $m_1 < m_2 < m_3$ and $am_k = s_k$. Then

$$(1+\gamma s_2^2)\frac{s_1}{s_2^2 - s_1^2} - (1+\gamma s_1^2)\frac{s_2}{s_2^2 - s_1^2} = \\ = (1+\gamma s_3^2)\frac{s_1}{s_3^2 - s_1^2} - (1+\gamma s_1^2)\frac{s_3}{s_3^2 - s_1^2} = \\ = (1+\gamma s_3^2)\frac{s_2}{s_3^2 - s_2^2} - (1+\gamma s_2^2)\frac{s_3}{s_3^2 - s_2^2}.$$

Using these relations, we obtain $\gamma = \dfrac{s_3 - s_2}{s_1^2(s_2 - s_3)} = -\dfrac{1}{s_1^2} < 0$, whereas γ must be positive. The regular hexagonal periodicity is also impossible. Actually [9], here $\gamma = \dfrac{s_2 m_1^2(ks_1+1) - s_1 m_2^2(ks_2+1)}{s_1^3 m_2^2(ks_2+1) - s_2^3 m_1^2(ks_1+1)}$, then for $s_1 = s_2$ it will be negative ($\gamma = -\dfrac{1}{s^2}$). We can write two sequential rotations by an angle of $\pi/3$ in the form $m_1 ax + m_1 a\sqrt{3}y \Rightarrow -m_1 ax + \sqrt{3}m_1 ay \Rightarrow -m_1 a(\dfrac{1}{2}x + \dfrac{\sqrt{3}}{2}y) + \sqrt{3}m_1 a(-\dfrac{\sqrt{3}}{2} + \dfrac{1}{2}y) = -2m_1 ax$, such that the assumption $s_1^2 = m_1^2a^2 + 3m_1^2a^2 = 4m_1^2a^2 = s_2^2$ is impossible.

The existence of irregular hexagonal periodicity and also two 4-dimensional periodicity lattices (the next point) can be proved as in [9] (using the DR continuous dependence with respect to k).

For $\dim N(B) = 6$ one of the periodicity rectangles degenerates to the segment. The basis $\{\varphi_i\}_1^6$ of the zero-subspace is numerated by the vectors $\bar{l}(m_i, n_i) = m_i\bar{l}^{(1)} + n_i\bar{l}^{(2)}$ of the reciprocal lattice

$$\varphi_k = \varphi_{\bar{l}_k(m,n)}(\bar{l}^{(1)} = a\bar{e}_1, l^{(2)} = b\bar{e}_2), \quad \bar{l}_1 = \bar{l}_1(m_1, n_1) = m_1\bar{l}_1 + n_1\bar{l}_2, \\ \bar{l}_3 = m_1\bar{l}_1 - n_1\bar{l}_2, \quad \bar{l}_5 = \bar{l}_5(m_2, 0) = m_2\bar{l}_1, \quad \bar{l}_{2j} = -\bar{l}_{2j-1}.$$

At this numeration of basis elements and corresponding vertices $(\pm m_1, \pm n_1)$ č $(\pm m_2, 0)$ of rectangles Π_{01} č Π_{02} in the reciprocal lattice the group action $\tilde{G}^1$ of rectangle symmetry is expressed by the permutation of indices of variables ξ_k, and the group invariance relative to $\tilde{G}^1$ is expressed by the equalities of the type (10). These equalities together with invariance with respect to the operation J of complex conjugation allow us to express the equations of the system in terms of the first and the fifth ones.

In order to construct these equations we use the invariance of the BEq with respect to the 2-dim. shifts group $e^{i(\bar{l}_k,\beta)}t_k(\xi,\varepsilon) = t_k(\xi_1 e^{i(\bar{l}_1,\beta)},\dots,\xi_6 e^{i(\bar{l}_6,\beta)},\varepsilon)$. Then the coefficient $t^{(k)}_{\alpha;j}$ at ξ^α in the k-th equation may be not equal zero, if the equality $\bar{l}_k = \alpha_1\bar{l}_1 + \dots + \alpha_6\bar{l}_6, |\alpha| = r$ is fulfilled.

We consider the case of the six-dimensional branching, when the interaction of lattices occurs at the first step, so there are relations: $\bar{l}_1 = \bar{l}_4 + \bar{l}_5, \bar{l}_3 = \bar{l}_2 + \bar{l}_5, \bar{l}_5 = \bar{l}_1 + \bar{l}_3, \bar{l}_2 = \bar{l}_3 + \bar{l}_6, \bar{l}_4 = \bar{l}_1 + \bar{l}_6, \bar{l}_6 = \bar{l}_2 + \bar{l}_4, m_2 = 2m_1$.

In order to determine the invariants, depending on ξ, we write the system $(\partial_{\xi_k} I = \partial I/\partial\xi_k)$

$$\hat{X}_1(\xi)I \equiv m_1 a\left[-\xi_1\partial_{\xi_1}I + \xi_2\partial_{\xi_2}I - \xi_3\partial_{\xi_3}I + \xi_4\partial_{\xi_4}I\right] + m_2 a\left[-\xi_5\partial_{\xi_5}I + \xi_6\partial_{\xi_6}I\right] = 0$$

$$\hat{X}_2(\xi)I \equiv n_1 b\left[-\xi_1\partial_{\xi_1}I + \xi_2\partial_{\xi_2}I + \xi_3\partial_{\xi_3}I - \xi_4\partial_{\xi_4}I\right] = 0$$

Besides the invariants $I_7 = \xi_1\xi_2, I_8 = \xi_3\xi_4, I_9 = \xi_5\xi_6$, it is necessary to use the additional ones $I_{10} = (\xi_1\xi_3)^{N/2m_1}\xi_6^{N/m_2}, I_{11} = (\xi_2\xi_4)^{N/2m_1}\xi_5^{N/m_2}$, where $N = LCM(2m_1, m_2)$. In this case the functionally independent ones are I_7, I_8, I_9, I_{10}. There is one relationship $I_{10}(\xi)I_{11}(\xi) = (I_7(\xi)I_8(\xi))^{N/2m_1}I_9^{N/m_2}(\xi)$.

Then the first and fifth equations have form

$$t_1(\xi,\varepsilon) \equiv a_0^{(1)}(\varepsilon)\xi_1 + \sum_{q,k} a^{(1)}_{q;k}(\varepsilon)(\xi_1\xi_2)^{q_1}(\xi_3\xi_4)^{q_2}(\xi_5\xi_6)^{q_3}[I_{10}^{q_4}I_{11}^{q_5}\xi_1]^{out} = 0,$$

$$t_5(\xi,\varepsilon) \equiv a_0^{(2)}(\varepsilon)\xi_5 + \sum_{q,k} a^{(2)}_{q;k}(\varepsilon)(\xi_1\xi_2)^{q_1}(\xi_3\xi_4)^{q_2}(\xi_5\xi_6)^{q_3}[I_{10}^{q_4}I_{11}^{q_5}\xi_5]^{out} = 0.$$

The main part of BEq has form

$$\begin{cases} A\xi_1\varepsilon + iB\xi_4\xi_5 = 0, & A\xi_3\varepsilon + iB\xi_2\xi_5 = 0, \quad C\xi_5\varepsilon + iD\xi_1\xi_3 = 0, \\ A\xi_2\varepsilon - iB\xi_3\xi_6 = 0, & A\xi_4\varepsilon - iB\xi_1\xi_6 = 0, \quad C\xi_6\varepsilon - iD\xi_2\xi_4 = 0, \end{cases} \tag{15}$$

where $A = a^1_{01}, C = a^2_{01}, iB = a^{(1;1)}_{0;1}, iD = a^{(2;1)}_{0;1}$, A, B, C, D are real. Transition to real basis in BEq is fulfilled by the formula

$$\hat{t}(\eta,\varepsilon) \equiv (C_1 t)(C_1^{-1}\eta,\varepsilon) = 0,$$

$$\eta = C_1\xi = \frac{1}{2}\begin{pmatrix} -i & i & -i & i & 0 & 0 \\ 1 & 1 & -1 & -1 & 0 & 0 \\ 1 & 1 & 1 & 1 & 0 & 0 \\ i & -i & -i & i & 0 & 0 \\ 0 & 0 & 0 & 0 & -i & i \\ 0 & 0 & 0 & 0 & 1 & 1 \end{pmatrix}\xi, C_1^{-1} = \frac{1}{2}\begin{pmatrix} -i & 1 & 1 & -i & 0 & 0 \\ -i & 1 & 1 & 1 & 0 & 0 \\ i & -1 & 1 & i & 0 & 0 \\ -i & -1 & 1 & -i & 0 & 0 \\ 0 & 0 & 0 & 0 & 2i & 2 \\ 0 & 0 & 0 & 0 & -2i & 2 \end{pmatrix}.$$

The real basis $\hat{\varphi}_j = (\hat{u}_j, \hat{f}_j)$ in $N(B)$ has form

$$\begin{aligned}
&\hat{\varphi}_1 = \{-v_1(\zeta)\sin m_1ax\cos n_1by, v_2\cos m_1ax\cos n_1by\},\\
&\hat{\varphi}_2 = \{-v_1(\zeta)\sin m_1ax\sin n_1by, v_2\cos m_1ax\sin n_1by\},\\
&\hat{\varphi}_3 = \{v_1(\zeta)\cos m_1ax\cos n_1by, v_2\sin m_1ax\cos n_1by\},\\
&\hat{\varphi}_4 = \{v_1(\zeta)\cos m_1ax\sin n_1by, v_2\sin m_1ax\sin n_1by\},\\
&\hat{\varphi}_5 = \{-v_1(\zeta)\sin m_2ax, v_2\cos m_2ax\}, \hat{\varphi}_6 = \{v_1(\zeta)\cos m_2ax, v_2\sin m_2ax\},
\end{aligned}$$

where $v_1(\zeta) = \dfrac{m_2a\sqrt{ab}}{\pi s_{m_2,0}}e^{s_{m_2}\zeta}, v_2 = \dfrac{\sqrt{ab}}{\pi}$. The main part of the BEq in real variables takes the form

$$\begin{aligned}
A\eta_1\varepsilon + B(\eta_1\eta_5 + \eta_3\eta_6) = 0, \quad A\eta_2\varepsilon + B(\eta_2\eta_5 + \eta_4\eta_6) = 0,\\
A\eta_3\varepsilon + B(\eta_1\eta_6 - \eta_3\eta_5) = 0, \quad A\eta_4\varepsilon + B(\eta_2\eta_6 - \eta_4\eta_5) = 0,\\
C\eta_5\varepsilon + \frac{1}{4}D(-\eta_1^2 - \eta_2^2 + \eta_3^2 + \eta_4^2) = 0, \quad C\eta_6\varepsilon + \frac{1}{2}D(-\eta_1\eta_3 - \eta_2\eta_4) = 0.
\end{aligned} \tag{16}$$

Making a reduction of the BEq, supposing $\eta_2 = 0 = \eta_3$, we obtain the branching system

$$\begin{aligned}
\eta_1(A\varepsilon + B\eta_5) = 0, \quad B\eta_4\eta_6 = 0, \quad B\eta_1\eta_6 = 0,\\
\eta_4(A\varepsilon - B\eta_5) = 0, \quad C\eta_5\varepsilon + \frac{1}{4}D(-\eta_1^2 + \eta_4^2) = 0, \quad C\eta_6\varepsilon = 0,
\end{aligned} \tag{17}$$

that has 4 solutions

$$\begin{aligned}
\eta(\varepsilon) = (\pm 2\sqrt{-\frac{AC}{BD}}\varepsilon, 0, 0, 0, -\frac{A}{B}\varepsilon, 0) + o(\varepsilon),\\
\eta(\varepsilon) = (0, 0, 0, \pm 2\sqrt{-\frac{AC}{BD}}\varepsilon, \frac{A}{B}\varepsilon, 0) + o(\varepsilon).
\end{aligned} \tag{18}$$

The combinations of shifts with respect to coordinate x on $\dfrac{\pi}{2m_1a}, \dfrac{\pi}{m_1a}$ and with respect to coordinate y on $\dfrac{\pi}{2n_1b}, \dfrac{\pi}{n_1b}$ generate the transformations

$\{\eta_1 \to \eta_4, \eta_4 \to \eta_1, \eta_5 \to -\eta_5\}, \{\eta_1 \to -\eta_1, \eta_5 \to \eta_5\}, \{\eta_4 \to -\eta_4, \eta_5 \to \eta_5\}$, such that it remains only one solution $\left(2\sqrt{-\dfrac{AC}{BD}}\varepsilon, 0, 0, 0, -\dfrac{A}{B}\varepsilon, 0\right)$.

Taking into account the signs of A and C and the existence of values m_1, n_1, $m_2 = 2m_1$, satisfying $signBD < 0$, we obtain the theorem.

Theorem 5.1. *The problem* (1)-(3) *in the case of two interacting periodicity lattices in the neighborhood of the bifurcation point* $F_0^2 = F_{m_1n_1}^2 = F_{m_20}^2$ *with six-dimensional degeneration of the linearized operator has one two-parametric family of periodical solutions* $\{\Phi^{(1)}, f^{(1)}\} =$

$$= 2\left[-\frac{AC}{BD}\right]^{\frac{1}{2}}(F^2 - F_0^2)\left\{-\frac{m_1a\sqrt{ab}}{\pi s_{m_1n_1}}e^{s_{m_1n_1}\zeta}\sin[m_1a(x+\beta_1)]\cos[n_1b(y+\beta_2)]\,,\right.$$

$$\left.\frac{\sqrt{ab}}{\pi}\cos[m_1a(x+\beta_1)]\cos[n_1b(y+\beta_2)]\right\} - \left\{-\frac{m_2a\sqrt{ab}}{\pi s_{m_20}}e^{s_{m_20}\zeta}\sin[m_2a(x+\beta_1)],\right.$$

$$\left.\frac{\sqrt{ab}}{\pi}\cos[m_2a(x+\beta_1)]\right\}\frac{A}{B}(F^2 - F_0^2) + o(\left|F^2 - F_0^2\right|),$$

$\zeta = z - f^{(1)}(x, y), signBD < 0.$

6. EIGHT-DIMENSIONAL DEGENERATION OF LINEARIZED OPERATOR. TWO PERIODICITY LATTICES

In addition to the proof of such degeneration, mentioned in the previous point, we shall prove this fact for the case of the double rectangle symmetry. Let consider two DRs

$$(k + \frac{1}{s_1})m_1^2a^2 = F_0^2(1 + \gamma s_1^2),$$
$$(k + \frac{1}{2s_1})4m_1^2a^2 = F_0^2(1 + 4\gamma s_1^2).$$

We can get the equation $2\gamma s_1^2 - 3ks_1 - 1 = 0$ implying $(s_1 > 0)$ $s_1 = \dfrac{3k + \sqrt{9k^2 + 8\gamma}}{4\gamma}$, which is the condition of fulfillment.

In the system $X_sI(\xi, t) = 0, \quad s = 1, 2$, where X_1, X_2 are the infinitesimal operators of the Lie algebra we have $n = 8, r = 2, \sigma_0 = 6, \nu_0 = 2$. This system determines 8 invariants in the form $I_k(\xi, t) = \frac{t_k}{\xi_k}, k = \overline{1, 8}$, four invariants in the form $I_{8+k} = \xi_{2k-1}\xi_{2k}, k = \overline{1,4}$ and two invariants $I_{13}(\xi) = (\xi_1\xi_3)^{N_1/m_1}(\xi_6\xi_8)^{N_1/m_2}, I_{14}(\xi) = (\xi_1\xi_4)^{N_2/n_1}(\xi_6\xi_7)^{N_2/n_2}$, where N_1 is the LCM of the numbers m_1 and m_2 and N_2 is the LCM of the numbers n_1 and n_2. Using the additional invariants $I_{15}(\xi) = (\xi_2\xi_4)^{N_1/m_1}(\xi_5\xi_7)^{N_1/m_2}, I_{16}(\xi) = (\xi_2\xi_3)^{N_2/n_1}(\xi_5\xi_8)^{N_2/n_2}$ we write the general form of the BEq

$$t_k(\xi,\varepsilon) \equiv \tag{19}$$

$$\equiv a_0^k(\varepsilon)\xi_k + \sum_q a_q^{(k)}(\varepsilon)(\xi_1\xi_2)^{q_1}\dots(\xi_7\xi_8)^{q_4}\Big[\xi_k((\xi_1\xi_3)^{N_1/m_1}(\xi_6\xi_8)^{N_1/m_2})^{q_5}\times$$
$$\times((\xi_1\xi_4)^{N_2/n_1}(\xi_6\xi_7)^{N_2/n_2})^{q_6}((\xi_2\xi_4)^{N_1/m_1}(\xi_5\xi_7)^{N_1/m_2})^{q_7}$$
$$((\xi_2\xi_3)^{N_2/n_1}(\xi_5\xi_8)^{N_2/n_2})^{q_8}\Big]^{out} = 0, \quad k = \overline{1,8},$$

$$I_{13}(\xi)I_{15}(\xi) = I_9^{N_1/m_1}(\xi)I_{10}^{N_1/m_1}(\xi)I_{11}^{N_1/m_2}(\xi)I_{12}^{N_1/m_2}(\xi),$$
$$I_{14}(\xi)I_{16}(\xi) = I_9^{N_2/n_1}(\xi)I_{10}^{N_2/n_1}(\xi)I_{11}^{N_2/n_2}(\xi)I_{12}^{N_2/n_2}(\xi).$$

The symmetry group of the rectangle is expressed by the permutations of indices of variables ξ_k

$$p_1 = (12)(34)(56)(78), p_2 = (13)(24)(57)(68), p_3 = (14)(23)(58)(67),$$

and the corresponding group symmetry of the BEq, by the equalities of the type (10)

These relations allow us to express all the equations through the first and the fifth ones and yield the coefficients symmetry of BEq

$$t_1(\xi,\varepsilon) = A\xi_1\varepsilon + B\xi_1^2\xi_2 + C\xi_1\xi_3\xi_4 + D\xi_1\xi_5\xi_6 + E\xi_1\xi_7\xi_8 = 0,$$
$$t_5(\xi,\varepsilon) = F\xi_5\varepsilon + G\xi_5^2\xi_6 + H\xi_5\xi_7\xi_8 + K\xi_1\xi_2\xi_5 + L\xi_3\xi_4\xi_5 = 0.$$

Passing to the real basis in $N(B)$, making a reduction of the relevant BEq ($\eta_2 = \eta_3 = 0$), we get the solutions.

7. EIGHT-DIMENSIONAL DEGENERATION OF LINEARIZED OPERATOR. THREE PERIODICITY LATTICES

In order to determine the invariants of ξ for three lattices $(m_1, n_1), (m_2, 0)$ and $(m_3, 0)$ we write the system of differential equations

$$\hat{X}_1(\xi)I \equiv m_1 a\left[-\xi_1\partial_{\xi_1}I + \xi_2\partial_{\xi_2}I - \xi_3\partial_{\xi_3}I + \xi_4\partial_{\xi_4}I\right] + m_2 a\left[-\xi_5\partial_{\xi_5}I + \xi_6\partial_{\xi_6}I\right] + \\ + m_3 a\left[-\xi_7\partial_{\xi_7}I + \xi_8\partial_{\xi_8}I\right] = 0, \\ \hat{X}_2(\xi)I \equiv n_1 b\left[-\xi_1\partial_{\xi_1}I + \xi_2\partial_{\xi_2}I + \xi_3\partial_{\xi_3}I - \xi_4\partial_{\xi_4}I\right] = 0. \tag{20}$$

This system determines eight invariants of the form $\frac{t_k}{\xi_k}$, four invariants of the form $I_9 = \xi_1\xi_2, I_{10} = \xi_3\xi_4, I_{11} = \xi_5\xi_6, I_{12} = \xi_7\xi_8$ and, besides that, two invariants, which can be chosen from following six

$$I_{13}(\xi) = (\xi_1\xi_3)^{N_1/2m_1}\xi_6^{N_1/m_2}, I_{14}(\xi) = (\xi_1\xi_3)^{N_2/2m_1}\xi_8^{N_2/m_3}, I_{15}(\xi) = \xi_5^{N_3/m_2}\xi_8^{N_3/m_3}, \\ I_{16}(\xi) = (\xi_2\xi_4)^{N_1/2m_1}\xi_5^{N_1/m_2}, I_{17}(\xi) = (\xi_2\xi_4)^{N_2/2m_1}\xi_7^{N_2/m_3}, I_{18}(\xi) = \xi_6^{N_3/m_2}\xi_7^{N_3/m_3},$$

where N_1 is $LCM(2m_1, m_2)$, N_2 is $LCM(2m_1, m_3)$ and N_3 is $LCM(m_2, m_3)$.

Making a relationship

$$I_{13}^{\frac{LCM(N_1,N_2)}{N_1}} I_{15}^{\frac{LCM(N_1,N_2)}{N_3}} I_{17}^{\frac{LCM(N_1,N_2)}{N_2}} = (I_9 I_{10})^{\frac{LCM(N_1,N_2)}{2m_1}} I_{11}^{\frac{LCM(N_1,N_2)}{m_2}} I_{12}^{\frac{LCM(N_1,N_2)}{m_3}}, \tag{21}$$

we obtain the BEq

$$t_k(\xi,\varepsilon) \equiv a_0^{(k)}\xi_k + \sum_q a_q^{(k)}(\varepsilon)(\xi_1\xi_2)^{q_1}\ldots(\xi_7\xi_8)^{q_4}\left[\,\xi_k\left((\xi_1\xi_3)^{N_1/2m_1}(\xi_6)^{N_1/m_2}\right)^{q_5}\cdot\right. \\ \left.\cdot\left((\xi_2\xi_4)^{N_2/2m_1}(\xi_7)^{N_2/m_3}\right)^{q_6}\left((\xi_1\xi_3)^{N_3/m_2}(\xi_6)^{N_3/m_3}\right)^{q_7}\,\right]^{out} = 0, \quad k = 1,\ldots,8.$$

The symmetry with respect to the discrete group allows one to express the equation of the branching system in terms of the first, the fifth and the seventh ones, and, thus, it determines the connections between the BEq coefficients $a_q^{(k)}(\varepsilon)$.

Suppose that the interaction of the periodicity lattices occurs at the first step, i.e.

$$l_1 = l_4 + l_5, l_2 = l_3 + l_6, l_3 = l_2 + l_5, l_4 = l_1 + l_6, l_7 = 2l_5, l_8 = 2l_6. \tag{22}$$

The existence of such a situation can be proved by using the DR for the lattices (m_1, n_1), $(2m_1, 0)$, $(4m_1, 0)$. Passing to the real basis in $N(B)$ by means of the formulae of the type (9), making the reduction of the relevant BEq, we obtain the following system

$$A\eta_1\varepsilon + B\eta_1\eta_5 = 0, \quad B\eta_4\eta_6 = 0, \quad B\eta_1\eta_6 = 0, A\eta_4\varepsilon - B\eta_4\eta_5 = 0,$$
$$C\eta_5\varepsilon + \frac{D}{2}(\eta_4^2 - \eta_1^2) + E(\eta_5\eta_7 + \eta_6\eta_8) = 0, \quad C\eta_6\varepsilon + E(\eta_5\eta_8 - \eta_6\eta_7) = 0,$$
$$F\eta_7\varepsilon + G(\eta_6^2 - \eta_5^2) = 0, \quad F\eta_8\varepsilon + 2G\eta_5\eta_6 = 0,$$

which has five solutions, but only three of them are essential.

Theorem 7.1. *The problem* (1)-(3) *in the neighborhood of the bifurcation point* $F_0^2 = F^2_{m_1n_1} = F^2_{m_20} = F^2_{m_30}$ *with eight-dimensional zero-subspace satisfying* (22) *up to a transformation* $y \to -y$ *has one one-parametric and two two-parametric families of solutions*

$$\{\Phi^{(1)}, f^{(1)}\} = \left\{\frac{m_1a\sqrt{ab}}{\pi s_1}e^{s_1\zeta}\cos[m_1a(x+\beta_1)]\sin[n_1b(y+\beta_2)]\right.,$$
$$\left.\frac{\sqrt{ab}}{\pi}\sin[m_1a(x+\beta_1)]\sin[n_1b(y+\beta_2)]\right\}\left[\frac{2A}{BD}(-C-\frac{EA^2G}{FB^2})\right]^{\frac{1}{2}}(F^2-F_0^2)$$
$$+\frac{A}{B}(F^2-F_0^2)\left\{-\frac{m_2a\sqrt{ab}}{\pi s_2}e^{s_2\zeta}\sin[m_2a(x+\beta_1)], \frac{\sqrt{ab}}{\pi}\cos[m_2a(x+\beta_1)]\right\}+$$
$$+\frac{GA^2}{FB^2}(F^2-F_0^2)\left\{-\frac{m_3a\sqrt{ab}}{\pi s_3}e^{s_3\zeta}\sin[m_3a(x+\beta_1)], \ \frac{\sqrt{ab}}{\pi}\cos[m_3a(x+\beta_1)]\right\}+o(|F^2-F_0^2|),$$

$\zeta = z - f^{(1)}(x,y)$,

$$\{\Phi^{(3)}, f^{(3)}\} = \left\{\frac{m_2a\sqrt{ab}}{\pi s_2}e^{s_2\zeta}(-\sin[m_2a(x+\beta_1)]+\cos[m_2a(x+\beta_1)])\right.,$$
$$\left.\frac{\sqrt{ab}}{\pi}(\cos[m_2a(x+\beta_1)]+\sin[m_2a(x+\beta_1)])\right\}\left[-\frac{CF}{2EG}\right]^{\frac{1}{2}}(F^2-F_0^2)+$$
$$+\frac{C}{E}(F^2-F_0^2)\left\{\frac{m_3a\sqrt{ab}}{\pi s_3}e^{s_3\zeta}\cos[m_3a(x+\beta_1)], \frac{\sqrt{ab}}{\pi}\sin[m_3a(x+\beta_1)]\right\}+$$

$+o(|F^2-F_0^2|), \quad \zeta = z - f^{(3)}(x,y),$

$$\{\Phi^{(4)}, f^{(4)}\} =$$
$$= \left[-\frac{CF}{EG}\right]^{\frac{1}{2}}(F^2-F_0^2)\left\{\frac{m_2a\sqrt{ab}}{\pi s_2}e^{s_2\zeta}\cos[m_2a(x+\beta_1)], \frac{\sqrt{ab}}{\pi}\sin[m_2a(x+\beta_1)]\right\}+$$

$$+\frac{C}{E}(F^2-F_0^2)\left\{\frac{m_3a\sqrt{ab}}{\pi s_3}e^{s_3\zeta}\sin[m_3a(x+\beta_1)],\ \frac{\sqrt{ab}}{\pi}\cos[m_3a(x+\beta_1)]\right\}+$$

$$+o(\left|F^2-F_0^2\right|),\quad \zeta=z-f^{(4)}(x,y).$$

8. STABILITY OF SOLUTIONS IN THE CAPILLARY-GRAVITY WAVES PROBLEMS

A. Floating fluid

Consider now the 4-dimensional branching. The stability of the branching solutions (1)-(3) is determined by the stability of stationary solutions of the equation $\frac{d\eta}{dt} = t(\eta,\varepsilon)$, where $t(\eta,\varepsilon)$ is the left-hand side of the branching system, $\varepsilon = F^2 - F_{mn}^2$. The stability of these ones is determined by the signs of the eigenvalues of the Jacobian matrix $J = \left[\frac{\partial \bar{t}_i}{\partial \eta_j}\right]$ for these solutions. The action of the operator $L_{\beta_1\beta_2}$ on the arbitrary element $N(B_{mn})$ is equivalent to the transformation of its coordinates by means of the matrix A_g (here $f_1(\beta_1,\beta_2) = \cos ma\beta_1 \cos nb\beta_2, f_2(\beta_1,\beta_2) = \cos ma\beta_1 \sin nb\beta_2, f_3(\beta_1,\beta_2) = \sin ma\beta_1 \cos nb\beta_2, f_4(\beta_1,\beta_2) = \sin ma\beta_1 \sin nb\beta_2$)

$$A_g = \frac{\pi}{\sqrt{ab}}\begin{pmatrix} f_1(\beta_1,\beta_2) & f_2(\beta_1,\beta_2) & f_3(\beta_1,\beta_2) & f_4(\beta_1,\beta_2) \\ -f_2(\beta_1,\beta_2) & f_1(\beta_1,\beta_2) & -f_4(\beta_1,\beta_2) & f_3(\beta_1,\beta_2) \\ -f_3(\beta_1,\beta_2) & -f_4(\beta_1,\beta_2) & f_1(\beta_1,\beta_2) & f_2(\beta_1,\beta_2) \\ f_4(\beta_1,\beta_2) & -f_3(\beta_1,\beta_2) & -f_2(\beta_1,\beta_2) & f_1(\beta_1,\beta_2) \end{pmatrix}.$$

By using the matrix A_g, the family of solutions is determined as

$\tilde{\eta} = A_g\tilde{\eta}_0(\varepsilon) =$

$$= \frac{\pi}{\sqrt{ab}}(f_1(\beta_1,\beta_2), -f_2(\beta_1,\beta_2), -f_3(\beta_1,\beta_2), f_4(\beta_1,\beta_2))^T\left(-\frac{A}{B}\varepsilon\right)^{1/2} + o(|\varepsilon|^{1/2}),$$

$$\tilde{\eta}_0(\varepsilon) = \begin{pmatrix} 1 \\ 0 \\ 0 \\ 0 \end{pmatrix}\left(-\frac{A}{B}\varepsilon\right)^{1/2} + o(|\varepsilon|^{1/2}),$$

where $\tilde{\eta}_0(\varepsilon)$ is the solution of the reduced BEq ($\beta_1 = \beta_2 = 0$)

$$t_\eta(\tilde{\eta}_0(\varepsilon),\varepsilon)\,[\Lambda_i\tilde{\eta}_0(\varepsilon)]=0, i=1,2, \tag{23}$$

where Λ_i are the infinitesimal operators of the Lie algebra in Ξ^4_φ

$$t_\eta(\tilde{\eta}_0(\varepsilon),\epsilon)=\begin{pmatrix} A\varepsilon-3A\varepsilon & 0 & 0 & 0\\ 0 & 0 & 0 & 0\\ 0 & 0 & 0 & 0\\ 0 & 0 & 0 & A\varepsilon-\frac{CA}{B}\varepsilon\end{pmatrix}, \tag{24}$$

$$\Lambda_1\tilde{\eta}_0(\varepsilon)=\frac{\partial A_\beta}{\partial\beta_1}|_{\beta_1=\beta_2=0}\cdot\tilde{\eta}_0(\varepsilon)=\begin{pmatrix}0\\0\\-v_2m_1a\\0\end{pmatrix}\left(-\frac{A}{B}\varepsilon\right)^{1/2},$$

$$\Lambda_2\tilde{\eta}_0(\varepsilon)=\frac{\partial A_\beta}{\partial\beta_2}|_{\beta_1=\beta_2=0}\cdot\tilde{\eta}_0(\varepsilon)=\begin{pmatrix}0\\-v_2m_1a\\0\\0\end{pmatrix}\left(-\frac{A}{B}\varepsilon\right)^{1/2}.$$

The relations (23) are fulfilled and the stability of the bifurcating solutions $A_\beta\tilde{\eta}_0(\varepsilon)$ is determined by the signs of the main terms with respect to ε of the eigenvalues of the Jacobian matrix J for this solution, which have form ($\tilde{B}=B+C$, $\tilde{C}=3B-C$)

$$\nu_{1,2}=0,\nu_3=-2A\varepsilon,\nu_4=\frac{2A\varepsilon}{\tilde{B}+\tilde{C}}(\tilde{C}-\tilde{B}). \tag{25}$$

Theorem 8.1. *In order for the family of solutions* (12) *be stable it is necessary and sufficient that the condition*

$$sign\varepsilon=signB=sign(\tilde{B}+\tilde{C})=-1$$

be fulfilled

$$\begin{cases}\tilde{B}+\tilde{C}<0\\ \tilde{C}-\tilde{B}>0\end{cases} <=> 0<\frac{|\tilde{C}|}{|\tilde{B}|}<1. \tag{26}$$

Consider the second group of solutions. The main parts of the eigenvalues of the Jacobian matrix J for these solutions are determined from

$$(A\varepsilon - \frac{(3B+C)A\varepsilon}{B+C} - \nu^2)\left[\left(A\varepsilon - \frac{2AB\varepsilon}{B+C} - \nu\right)^2 - \left(\frac{AD\varepsilon}{B+C}\right)^2\right] = 0, \quad (27)$$

$$\nu_{1,2} = -\frac{2AB\varepsilon}{B+C},\ \nu_3 = -\frac{2A\varepsilon}{B+C}(C-B),\ \nu_4 = 0.$$

Theorem 8.2. *In order for the family of solutions* (13) *be stable it is necessary and sufficient that the condition*

$$sign\varepsilon = sign(B+C) = sign\tilde{B} = -1$$

be fulfilled,

$$0 < \frac{|\tilde{B}|}{|\tilde{C}|} < 1. \quad (28)$$

Remark 1. When the inequality (26) (resp. (28)) is satisfied, the family of solutions (12) ((13)) will be stable with respect to perturbations of the same periodicity lattices class. The instability with respect to perturbations of the same periodicity class means the instability in general.

Giving the values to parameters n, b, $q = \frac{ma}{nb}$, we determine $\frac{|\tilde{C}|}{|\tilde{B}|}$. Our results for the first group of solutions are presented in Table 1 (for k=0.8), where the solutions (12) are stable, while the solutions (13) are unstable:

Table 1.

n	b	q	$\lvert\tilde{C}\rvert/\lvert\tilde{B}\rvert$	n	b	q	$\lvert\tilde{C}\rvert/\lvert\tilde{B}\rvert$
1,000	1,000	1,3000	0,850813039	1,000	1,000	1,4500	0,178466137
1,000	1,000	1,3500	0,635714027	1,000	1,000	0,5000	0,131115256
1,000	1,000	1,4000	0,419410516	1,000	1,000	0,5500	0,622709000

The results for the second group of solutions are contained in Table 2, where the solutions (13) are stable, while the solutions (12) are unstable:

Table 2.

n	b	q	$\lvert\tilde{B}\rvert/\lvert\tilde{C}\rvert$		n	b	q	$\lvert\tilde{B}\rvert/\lvert\tilde{C}\rvert$
1,000	1,000	0,8000	0,040375771		2,000	2,000	0,4000	0,122130193
1,000	1,000	0,9000	0,157498907		3,000	3,000	0,1000	0,62698459
1,000	1,000	1,0000	0,301714049		3,000	3,000	0,2000	0,620169486
2,000	2,000	0,1000	0,292847947		3,000	3,000	0,3000	0,538527089
2,000	2,000	0,2000	0,344675422		3,000	3,000	0,4000	0,381837849
2,000	2,000	0,3000	0,272661090		3,000	3,000	0,5000	0,098692584

B. Fluid without flotation (k=0)

Consider the case when k is equal to zero. Our results for the first group of solutions are shown in Table 3, where the solutions (12) are stable, while the solutions (13) are unstable

Table 3.

n	b	q	$\lvert\tilde{C}\rvert/\lvert\tilde{B}\rvert$
2,000	2,000	0,1000	0,595643406
2,000	2,000	0,2000	0,761614822
2,000	2,000	0,3000	0,792834919
2,000	2,000	0,4000	0,765693784
2,000	2,000	0,5000	0,586082036

and for the second one, in Table 4, where the solutions (13) are stable, while the solutions (12) are unstable

Table 4.

n	b	q	$\lvert\tilde{B}\rvert/\lvert\tilde{C}\rvert$		n	b	q	$\lvert\tilde{B}\rvert/\lvert\tilde{C}\rvert$
1,000	1,000	0,6000	0,054693147		2,000	1,000	0,2000	0,077310085
1,000	1,000	0,7000	0,115291056		2,000	1,000	0,3000	0,190900611
1,000	1,000	0,8000	0,170005725		2,000	1,000	0,4000	0,227631315
1,000	1,000	0,9000	0,214241214		2,000	1,000	0,5000	0,156749153
1,000	1,000	1,0000	0,244240961		2,000	1,000	0,6000	0,000648038

Remark 2. For the sake of brevity all tables are shortened.

References

[1] Nekrasov, A. I., *On stationary waves*, Izvestiya of Ivanovo Polytechnical Institute, **6** (1922), 155-171. (Russian)

[2] Nekrasov, A. I., *Exact theory of steady-state type waves on the surface of a heavy fluid*, The USSR Academy of Sciences, Moscow, 1951. (Russian)

[3] Levi-Civita, T., *Determination rigoureuse des ondes permanentes d'ampleur finie*, Math. Annalen, **93** (1925), 264-324.

[4] Struik, D. J., *Determination rigoureuse des ondes irrotationelles periodiques*, Math. Annalen, **95** (1926), 595-634.

[5] Sekerzh-Zenkovich, Ya. I., in "Continuum Mechanics and Related Problems of Analysis", Nauka, Moskva, 1972, 445-458. (Russian)

[6] Loginov, B. V., *Construction of periodic solutions of the three-dimensional problem about waves over the flat bottom*, Doklady Akademii Nauk (Proc. of the Russian Academy of Sciences), USSR, **247**, 2(1979), 324-328. (Russian)

[7] Loginov, B. V., *Periodic solutions of three-dimensional problem about waves over the flat bottom*, Continuum dynamics, **42** (1979), 3-22. (Russian)

[8] Loginov, B. V., *Branching theory of solutions of nonlinear equations under group invariance conditions,* Fan, Tashkent, 1985. (Russian)

[9] Loginov, B. V., Kuznetsov, A. O., *Capillary-gravity waves over the flat surface*, European Journal of Mechanics/B Fluids, **15**, 2 (1996), 259-280.

[10] Loginov, B. V., Karpova, S. A., *Computation of periodic solutions in the problem about capillary-gravity waves in floating fluid spatial layer*, Vestnik of Samara State University, **4(6)** (1997), 69-80. (Russian)

[11] Ovsyannikov, L. V., *Group analysis of differential equations*, Nauka, Moskva, 1978. (Academic Press, New York, 1982). (Russian)

[12] Vainberg, M. M., Trenogin, V. A., *Branching theory of solutions of nonlinear equations*, Nauka, Moskva, 1969. (Russian)

[13] Loginov, B. V., Rakhmatova, Kh. R., Yuldashev, N. N., *On the construction of branching equation by its group symmetry (crystallographic groups)*, in "Mixed type equations and free boundary value problem", Fan, Tashkent, 1987, 183-195. (Russian)

[14] Loginov, B. V., *Group analysis method for construction and investigation of the bifurcation equation*, Applications of Mathematics, **37**, 4(1992), 241-248.

[15] Loginov, B. V., *Branching of solutions of nonlinear equations and group symmetry*, Vestnik of Samara State University, **4**(10)(1998), 15-70. (Russian)

[16] Agranovich, M. S., *Elliptic operators on closed manifolds*, Contemporary Problems in Mathematics. Fundamental directions, VINITI, Moskva, **63** (1990), 5-129. (Russian)

[17] Naimark, M. A., *Linear differential operators*, Nauka, Moskva, 1969. (Russian)

[18] Loginov, B. V., Trenogin, V. A., *On use of group properties for the determination of multiparameter families of solutions of nonlinear equations*, Math. Sbornik, **85**, 3(1971), 440-454. (Russian); Engl. transl. **14**, 3 (1971), 438-452.

[19] Andronov, A. N., *Bifurcating solutions asymptotics in the case of 4-dimensional degeneration in the problem on capillary-gravity waves on a deep fluid surface*, Proc. Middle-Volga Math. Soc., **9**, 2(2007), 9-14. (Russian)

[20] Andronov, A. N., *On the orders of degeneracy of the operator B in the problem on capillary-gravity waves on a deep fluid surface*, Proc. of N.I. Lobachevsky Mathematical Center, Kazan, **36**(2007), 16-18. (Russian)

[21] Loginov, B. V., Rousak, Yu. B., *Generalized Jordan structure in the problem of the stability of bifurcating solutions*, Nonlinear Analysis. TMA, **17**, 3 (1991), 219-231.

ROMAI J., **4**, 2(2008), 29–31

ON CH-QUASIGROUPS OF FINITE SPECIAL RANK

A. Babiy

Tiraspol State University, Chişinău, Republic of Moldova

Abstract CH-quasigroups of finite special rank are characterized by means of various non-medial (or medial) subquasigroups and by means of various non-Abelian (or Abelian) subgroups of their multiplication group.

Keywords: quasigroups, subquasigroups.

2000 MSC: 20N99.

1. INTRODUCTION

By analogy with the group theory [1], the special rank of a quasigroup Q is called the least positive number rQ with the following property: any finitely generated subquasigroup of the quasigroup Q can be generated by rQ elements; if there are not such numbers, then we suppose that $rQ = \infty$.

The theory of commutative Moufang loops (CML's) is one of the deepest and subtlest areas of the present-day theory of quasigroups and loops. It is certainly one of the most interesting areas, mainly because of its many connections with other topics, in particular, with CH-quasigroups [2]-[4]. Such quasigroups are investigated in this paper by means of CML. Concretely, the various equivalent finiteness conditions of special rank of CML and their multiplication groups from [5] are transferred on CH-quasigroups.

Let $(Q, \cdot)$ be a non-empty set Q provided with a binary operation $(x, y) \rightarrow x \cdot y$. One says that $(Q, \cdot)$ is a *TS-quasigroup* if any equality of the form $x \cdot y = z$ remains true under all permutations of x, y, z (equivalently $xy = yx$ and $x{\cdot}xy = y$). A quasigroup is said to be *medial* if $xu{\cdot}xy = xv{\cdot}uy$ holds. $(Q, \cdot)$ is a *CH-quasigroup* iff $(Q, \cdot)$ is a TS-quasigroup such that $xy \cdot xz = xx \cdot yz$ holds. The last condition is equivalent with the following condition: every subquasigroup generated by three elements is medial. For a loop, the identity $xy \cdot xz = xx \cdot yz$ characterizes the CML [2]-[4].

Given four elements x_1, x_2, x_3, k of any quasigroup $(Q, \cdot)$ *the mediator of* x_1, x_2, x_3 *with respect to* k is the element a of Q uniquely determined by the equality $x_1x_2 \cdot kx_3 = x_1a \cdot x_2x_3$. We denote $a = [x_1, x_2, x_3]_k$. We say that *the mediators of weight* i *with respect to* k are the mediators of the form $[x_1, x_2, \ldots, x_{2i+1}]_k$ defined inductively by $\alpha_1 = [x_1, x_2, x_3]_k$ and $\alpha_{i+1} = [\alpha_i, x_{2i+2}, x_{2i+3}]_k$. A quasigroup Q is called medially nilpotent of class n if it satisfies the identity $[x_1, x_2, \ldots, x_{2n+1}]_y = y$, but does not satisfy the identity $[x_1, x_2, \ldots, x_{2n-1}]_y = y$.

The *multiplication group* $\mathfrak{D}$ of a CH-quasigroup $(Q, \cdot)$ is the group generated by all *translations* $L(x)$, where $L(x)y = xy$, $x \in Q$.

Theorem. *For an arbitrary non-medial CH-quasigroup Q with the multiplication group $\mathfrak{D}$ and its subgroup $\mathfrak{D}^0$, consisting of products of even number of translations $L(x)$, $x \in Q$, the following statements are equivalent:*

1) *Q has a finite special rank;*

2) *if Q contains a medially nilpotent subquasigroup of class n, then all its subquasigroups of this type have a finite special rank;*

3) *at least one maximal medial subquasigroup of Q has a finite special rank;*

4) *non-normal medial subquasigroups of Q have a finite special rank;*

5) *normal subquasigroups of Q have a finite special rank;*

6) *$\mathfrak{D}$ (respect. $\mathfrak{D}^0$) has a finite special rank;*

7) *all normal subgroups of $\mathfrak{D}$ (respect. $\mathfrak{D}^0$) have a finite special rank;*

8) *all non-normal Abelian subgroups of $\mathfrak{D}$ (respect. $\mathfrak{D}^0$) have a finite special rank;*

9) *at least one maximal Abelian subgroup of $\mathfrak{D}$ (respect. $\mathfrak{D}^0$) has a finite special rank;*

10) *if $\mathfrak{D}$ (respect. $\mathfrak{D}^0$) contains a nilpotent subgroup of class n, then all its subgroups of this type of $\mathfrak{D}$ have a finite special rank;*

11) *if $\mathfrak{D}$ (respect. $\mathfrak{D}^0$) contains a solvable subgroup of class s, then all its subgroups of this type of $\mathfrak{D}$ have a finite special rank.*

References

[1] Mal'cev, A. I., *About groups of finite rank,* Matem. Sb., **22**, 2(1948), 351 – 352. (Russian)

[2] Manin, Ju. I., *Cubic forms: algebra, geometry, arithmetic,* Moscow, Nauka, 1972. (English translation: North-Holland, Math. Lib. **4**, North-Holland Publishing Go., Amsterdam; American Elsevier, New York, 1974).

[3] Sandu, N. I., *Medially nilpotent distributive quasigroups and CH-quasigroups,* Sibirsk. Math. $\hat{Z}$., **XXVIII**, 2(1987), 159 – 170. (Russian)

[4] Chein, O., Pflugfelder, H. O., Smith, J. D. H., *Quasigroups and loops: Theory and applications,* Helderman, Berlin, 1990.

[5] Babiy, A., Sandu, N., *About commutative Moufang loops of finite special rank,* Bul. Ac. Şt. a Rep. Moldova, Matematica, **1**(50)(2006), 92 – 100.

ROMAI J., **4**, 2(2008), 33–44

GREEN FUNCTION CONSTRUCTION FOR DIVERGENCE PROBLEMS IN AEROELASTICITY

Tatiana E. Badokina, Boris V. Loginov, Olga V. Makeeva

Mordovian State University, Saransk, Russia

Ulyanovsk State Technical University, Russia

Demitrovgrad Technological Inst., branch of Ulyanovsk State Agricultural Academy, Russia

loginov@ulstu.ru

Abstract Buckling of a thin flexible elongated plate subject to supersonic flow of a gas along Ox-axis and compressed or extended by external boundary stresses at the edges $x = 0$ and $x = 1$ is governed by a boundary value problem for a nonlinear ordinary integro-differential equation with two bifurcational (spectral) parameters: one is the external stress and the other is the Mach number. For two types of boundary conditions $w''(0) = 0$, $w'''(0) = 0$, $w(1) = 0$, $w'(1) = 0$ and $w(0) = 0$, $w'(0) = 0$, $w''(1) = 0$, $w'''(1) = 0$ the Green functions for the linearized problems are constructed. The technical difficulties are overcome by means of the bifurcation curves representation through the roots of the relevant characteristic equations [1], [2].

Keywords: aeroelasticity; buckling of an elongated plate; supersonic gas flow; compressing or extending external stresses; linearized problem with two-spectral parameters; Green functions construction.

2000 MSC: 74F20; 34B27; 34C23.

1. INTRODUCTION

The problem on a thin flexible elongated plate (strip-plate) buckling in a supersonic gas flow which is compressed or extended by external boundary stresses along the Ox-axis is investigated (fig.1). In the articles [1], [2] six types of boundary conditions are considered. From them, here we take

B. the left edge is free, the right one is rigidly fixed, $w''(0) = 0$, $w'''(0) = 0$, $w(1) = 0$, $w'(1) = 0$

B′. the right edge is free, the left one is rigidly fixed, $w(0) = 0$, $w'(0) = 0$, $w''(1) = 0$, $w'''(1) = 0$

In dimensionless variables this problem is described by the equation

$$\chi^2 \frac{d^2}{dx^2}\left(\frac{w''}{(1+w'^2)^{3/2}}\right) - T\frac{d^2 w}{dx^2} = kK\left(\frac{dw}{dx}, M, \kappa\right) + \theta w'' \int_0^1 \left[(1+w'^2)^{1/2} - 1\right] dx, \tag{1}$$

where $K(w'_x, M, \kappa) = \left[1 - (1 + \frac{\kappa-1}{2} M w'_x)^{\frac{2\kappa}{\kappa-1}}\right]$ for one-sided flow and $K(w'_x, M, \kappa) = \left[(1 - \frac{\kappa-1}{2} M w'_x)^{\frac{2\kappa}{\kappa-1}} - (1 + \frac{\kappa-1}{2} M w'_x)^{\frac{2\kappa}{\kappa-1}}\right]$ for two-sided flow of the supersonic gas flow along the Ox- axis. Here $w = w(x)$ is the plate deflection, $0 < x < 1$; $x = \frac{x_1}{d}$, $0 \le x_1 \le d$, $-\infty < y_1 < \infty$ are rectangular coordinates; $\chi^2 = \frac{h^2}{12(1-\mu^2)d^2}$, $T = \frac{qd}{Eh}$ and $k = \frac{p_0 d}{Eh}$; d is the width of the plate, h is its thickness; E is the Young module; μ is the Poisson coefficient; $q < 0$ ($q > 0$) is the compressing (extending) stress; M is the Mach number, p_0 is the pressure and κ is the polytropic exponent; the integral term takes into account the complementary force in the middle surface of the buckled plate, $\theta = \frac{1}{1-\mu^2}$. Equation (1) contains this integral, not included in the equation in [1]. In the books [3], [4] and in the article [5] the problem of the rectangular plate divergence is investigated, not subject to the compression/extension stresses. In order to compute the buckled forms in the neighborhoods of parameter critical values, bifurcation theory methods [6] are applied and the terminology and notations are taken from this monograph.

The linearized equation (1) has the form

$$\chi^2 w^{(4)}_{x^4} - T w^{(2)}_{x^2} + \sigma w^{(1)}_x = 0, \qquad \sigma = 1(2)k\kappa M \tag{2}$$

and, together with the boundary conditions B or B’, represents a two-parametric spectral problem, i.e. a spectral two-point boundary value problem. Here the factor 1(2) in the parameter σ corresponds to one-sided (two-sided) supersonic gas flow around the strip-plate. At the investigation of these two-point boundary value problems the following possibilities arise: 1) $4T^3 - 27\sigma^2\chi^2 > 0$, 2) $4T^3 - 27\sigma^2\chi^2 = 0$, 3) $4T^3 - 27\sigma^2\chi^2 < 0$, where $\sigma \ge 0$, $T < 0$ is the compressing stress, $T > 0$ is the extension stress , $T = 0$ corresponds to flow around only.

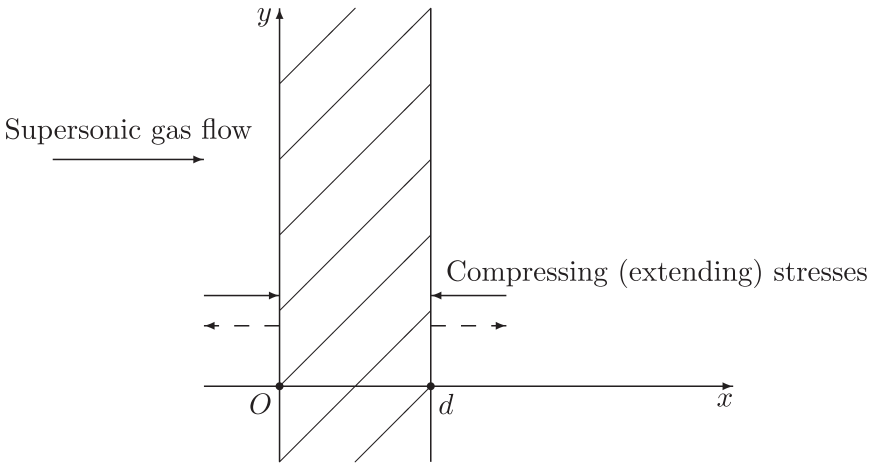

Fig. 1. The problem of strip-plate buckling.

In the first case T is necessarily greater than 0. The characteristic equation

$$f_0(\lambda) = \chi^2\lambda^4 - T\lambda^2 + \sigma\lambda = 0 \tag{3}$$

has one negative root $-\alpha$ and two positive roots $\beta_2 > \beta_1 > 0$ ($\alpha = \beta_1 + \beta_2$). Again T is greater than 0 for $4T^3 - 27\sigma^2\chi^2 = 0$ and (3) has two equal roots $\beta_1 = \beta_2 = \beta > 0$ and one negative root $-\alpha$. It will be useful to indicate here some relations between roots $\beta_2 > \beta_1$ and parameters σ and T

$$\frac{\sigma}{T} < \beta_1, \beta_2 < \frac{3\sigma}{2T}, \quad \beta_2 = \beta_1 + \frac{1}{2\chi\beta_1^{1/2}}\left[\sqrt{T\beta_1 + 3T} - 3\chi\beta_1^{3/2}\right],$$

which follow from the known Viète formulae.

In the third case, which is possible at both extension ($T > 0$) and compression ($T < 0$) of the plate, the roots of (3) are $\gamma \pm \delta i(\gamma, \delta > 0)$ and $-\alpha < 0(\alpha = 2\gamma)$. Here for the buckling investigation it is convenient to introduce the following notation $\delta = \gamma u$, $u = \sqrt{3 - \frac{T}{\gamma^2\chi^2}}$, $\sigma = 2\gamma\chi^2(\gamma^2 + \delta^2) = 2\gamma^3\chi^2(1 + u^2)$. It is not difficult to see that the values

$$0 < u < \sqrt{3} \Rightarrow 2\gamma^3\chi^2 \leq \sigma < 8\gamma^3\chi^2 \tag{4}$$

correspond to the plate extension, and the values

$$u > \sqrt{3} \Rightarrow \sigma > 8\gamma^3\chi^2 \tag{5}$$

respond to the plate compression.

The value $u = \sqrt{3}$ implies $T = 0$, i.e. the extension/compression absence.

The value $u = 0$ corresponds to $4T^3 - 27\sigma^2\chi^2 = 0$.

Note that in the investigation of algebraic equation (3) with two parameters T and σ Sturm method for roots separation was used.

The aim of this article is to construct Green functions for the equation (2) with the boundary conditions B and B′ by using the methods from the monograph [6]. Remark that in [7] the Green functions for aeroelasticity problems were not constructed.

The obtained results are supported by grant RFBR-Romanian Academy No. 07-01-91680-RA_a.

2. GREEN FUNCTIONS FOR THE BOUNDARY CONDITIONS B

2.1 First consider the case $d = 4T^3 - 27\sigma^2\chi^2 > 0 \Rightarrow T > 0$. Here we use the boundary conditions to provide the equation [1], [2]

$$\Delta_B = 0, \tag{6}$$

with

$$\Delta_B = e^{-(\beta_1+\beta_2)}\beta_1\beta_2(\beta_2-\beta_1)+(\beta_1+\beta_2)\beta_2(\beta_1+2\beta_2)e^{\beta_1}-\beta_1(\beta_1+\beta_2)(2\beta_1+\beta_2)e^{\beta_2},$$

which determines possible bifurcation points.

Computational experiment shows [1], [2] that, due to exponential decreasing of the third summand, this equation implicitly defines the unique curve in the region $\beta_2 > \beta_1$ only if $\beta_1 < \beta_0 \approx 1,336358362$.

The conditions of the continuity of the Green function together with derivatives up to the second order

$$G(x,\xi) = \begin{cases} C_1 e^{-\alpha x} + C_2 e^{\beta_1 x} + C_3 e^{\beta_2 x} + C_4, & 0 \le x < \xi,\ \alpha = \beta_1 + \beta_2 \\ D_1 e^{-\alpha x} + D_2 e^{\beta_2 x} + D_3 e^{\beta_2 x} + D_4, & \xi < x \le 1 \end{cases} \tag{7}$$

at the point $x = \xi$ with the jump $-\frac{1}{\chi^2}$ of the third derivative give the linear system with the determinant $\beta_1\beta_2(\beta_2^2 - \beta_1^2)(\beta_1 + 2\beta_2)(2\beta_1 + \beta_2) \neq 0$, from which it follows

$$
\begin{aligned}
D_1 &= C_1 - \frac{e^{(\beta_1+\beta_2)\xi}}{\chi^2(\beta_1+\beta_2)(\beta_1+2\beta_2)(2\beta_1+\beta_2)}, \\
D_2 &= C_2 - \frac{e^{-\beta_1\xi}}{\chi^2\beta_1(\beta_2-\beta_1)(2\beta_1+\beta_2)}, \\
D_3 &= C_3 + \frac{e^{-\beta_2\xi}}{\chi^2\beta_2(\beta_2-\beta_1)(\beta_1+2\beta_2)}, \\
D_4 &= C_4 + \frac{1}{\chi^2\beta_1\beta_2(\beta_1+\beta_2)}.
\end{aligned}
$$

Since apart from equation (1), the Green function (7) must satisfy also the boundary condition B, the functions $C_k(\xi)$, $D_k(\xi)$, $k=\overline{1,4}$ can be determined from the conditions B. Consequently $C_k(\xi), k=\overline{1,4}$ are the solutions of the system

$$
\left\{
\begin{array}{ccccccccc}
\alpha^2 C_1 & + & \beta_1^2 C_2 & + & \beta_2^2 C_3 & & & = & 0, \\
-\alpha^3 C_1 & + & \beta_1^3 C_2 & + & \beta_2^3 C_3 & & & = & 0, \\
e^{-\alpha} C_1 & + & e^{\beta_1} C_2 & + & e^{\beta_2} C_3 & + & C_4 & = & F_1(\xi), \\
-\alpha e^{-\alpha} C_1 & + & \beta_1 e^{\beta_1} C_2 & + & \beta_2 e^{\beta_2} C_3 & & & = & F_2(\xi),
\end{array}
\right. \tag{8}
$$

where

$$
\begin{aligned}
F_1(\xi) &= \frac{1}{\chi^2\beta_1\beta_2(\beta_2^2-\beta_1^2)(2\beta_1+\beta_2)(\beta_1+2\beta_2)}\Big[\beta_1\beta_2(\beta_2-\beta_1)e^{-(\beta_1+\beta_2)(1-\xi)} + \\
&\quad +\beta_2(\beta_1+\beta_2)(\beta_1+2\beta_2)e^{\beta_1(1-\xi)} - \beta_1(\beta_1+\beta_2)(2\beta_1+\beta_2)e^{\beta_2(1-\xi)} - \\
&\quad -(\beta_2-\beta_1)(2\beta_1+\beta_2)(\beta_1+2\beta_2)\Big], \\
F_2(\xi) &= -\frac{e^{-(\beta_1+\beta_2)(1-\xi)}}{\xi^2(2\beta_1+\beta_2)(\beta_1+2\beta_2)} + \frac{e^{\beta_1(1-\xi)}}{\chi^2(\beta_2-\beta_1)(2\beta_1+\beta_2)} - \frac{e^{\beta_2(1-\xi)}}{\chi^2(\beta_2-\beta_1)(\beta_1+2\beta_2)},
\end{aligned}
$$

whence

$$
\begin{aligned}
C_1 &= \frac{\beta_1\beta_2}{\chi^2(\beta_1+\beta_2)(\beta_1+2\beta_2)(2\beta_1+\beta_2)\Delta_B}[(\beta_2-\beta_1)e^{-(\beta_1+\beta_2)(1-\xi)} - \\
&\quad -(\beta_1+2\beta_2)e^{\beta_1(1-\xi)} + (2\beta_1+\beta_2)e^{\beta_2(1-\xi)}],
\end{aligned}
$$

$$
\begin{aligned}
C_2 &= -\frac{(\beta_1+\beta_2)\beta_2}{\chi^2\beta_1(\beta_2-\beta_1)(2\beta_1+\beta_2)\Delta_B}[(\beta_2-\beta_1)e^{-(\beta_1+\beta_2)(1-\xi)}-\\
&\quad -(\beta_1+2\beta_2)e^{\beta_1(1-\xi)}+(2\beta_1+\beta_2)e^{\beta_2(1-\xi)}],\\
C_3 &= \frac{(\beta_1+\beta_2)\beta_1}{\chi^2\beta_2(\beta_2--\beta_1)(\beta_1+2\beta_2)\Delta_B}[(\beta_2-\beta_1)e^{-(\beta_1+\beta_2)(1-\xi)}-\\
&\quad -(\beta_1+2\beta_2)e^{\beta_1(1-\xi)}+(2\beta_1+\beta_2)e^{\beta_2(1-\xi)}],\\
C_4 &= \frac{1}{\chi^2\beta_1\beta_2(\beta_1+\beta_2)\Delta_B}[(\beta_1+\beta_2)(\beta_2^2e^{-\beta_2}-\beta_1^2e^{-\beta_1})e^{(\beta_1+\beta_2)\xi}+\\
&\quad +(\beta_1+\beta_2)^2e^{\beta_1+\beta_2}(\beta_2e^{-\beta_2\xi}-\beta_1e^{-\beta_1\xi})+\\
&\quad +\beta_1\beta_2(\beta_2e^{-\beta_2-\beta_1\xi}-\beta_1e^{-\beta_1-\beta_2\xi})-\Delta_B].
\end{aligned}
$$

Then from (3) it follows

$$
\begin{aligned}
D_1 &= \frac{1}{\chi^2(\beta_1+\beta_2)(2\beta_1+\beta_2)(\beta_1+2\beta_2)\Delta_B}\{\beta_1\beta_2(2\beta_1+\beta_2)e^{\beta_2(1-\xi)}-\\
&\quad -\beta_1\beta_2(\beta_1+2\beta_2)e^{\beta_1(1-\xi)}+\\
&\quad +(\beta_1+\beta_2)e^{(\beta_1+\beta_2)\xi}[\beta_1(2\beta_1+\beta_2)e^{\beta_2}-\beta_2(\beta_1+2\beta_2)e^{\beta_1}]\},\\
D_2 &= -\frac{1}{\chi^2\beta_1(\beta_2-\beta_1)(2\beta_1+\beta_2)\Delta_B}\{\beta_2(\beta_1+\beta_2)(\beta_2-\beta_1)e^{-(\beta_1+\beta_2)(1-\xi)}+\\
&\quad +\beta_1\beta_2(\beta_2-\beta_1)e^{-(\beta_1+\beta_2)-\beta_1\xi}+\beta_2(\beta_1+\beta_2)(2\beta_1+\beta_2)e^{\beta_2(1-\xi)}-\\
&\quad -\beta_1(\beta_1+\beta_2)(2\beta_1+\beta_2)e^{\beta_2-\beta_1\xi})\},\\
D_3 &= \frac{1}{\chi^2\beta_2(\beta_2-\beta_1)(\beta_1+2\beta_2)\Delta_B}\{\beta_1(\beta_1+\beta_2)(\beta_2-\beta_1)e^{-(\beta_1+\beta_2)(1-\xi)}-\\
&\quad -\beta_1(\beta_1+\beta_2)(\beta_1+2\beta_2)e^{\beta_1(1-\xi)}+\beta_1\beta_2(\beta_2-\beta_1)e^{-\beta_1-\beta_2(1+\xi)}+\\
&\quad +\beta_2(\beta_1+\beta_2)(\beta_1+2\beta_2)e^{\beta_1-\beta_2\xi})\},\\
D_4 &= \frac{1}{\chi^2\beta_1\beta_2(\beta_1+\beta_2)\Delta_B}\{(\beta_1+\beta_2)(\beta_2^2e^{-\beta_2}-\beta_1^2e^{-\beta_1})e^{(\beta_1+\beta_2)\xi}+\\
&\quad +(\beta_1+\beta_2)^2(\beta_2e^{-\beta_2\xi}-\beta_1e^{-\beta_1\xi})e^{\beta_1+\beta_2}+\\
&\quad +\beta_1\beta_2(\beta_2e^{-\beta_2-\beta_1\xi}-\beta_1e^{-\beta_1-\beta_2\xi})\}.
\end{aligned}
$$

2.2 If $d = 4T^3 - 27\sigma^2\chi^2 = 0 \Rightarrow T > 0$, the boundary conditions B give the equation [1], [2]

$$\Delta_B = e^{-3\beta} + 8 - 6\beta = 0, \tag{9}$$

which determines only one bifurcation point $\beta \approx 1,336358362$, which, naturally, coincides with the critical value β_0 of the previous case.

The conditions of the continuity of the derivatives up to the second order together with the jump $-\frac{1}{\chi^2}$ of the third derivative at the point ξ for the Green function

$$G(x,\xi)=\begin{cases} C_1e^{-2\beta x}+C_2e^{\beta x}+C_3xe^{\beta x}+C_4, & 0\le x<\xi,\\ D_1e^{-2\beta x}+D_2e^{\beta x}+D_3xe^{\beta x}+D_4, & \xi<x\le 1\end{cases}$$

give the linear system with the determinant $18\beta^5\neq 0$. This system leads to formulae $D_1=C_1-\frac{e^{2\beta\xi}}{18\beta^3\chi^2}$, $D_2=C_2-\frac{2e^{-\beta\xi}}{18\beta^3\chi^2}(4+3\beta\chi)$, $D_3=C_3+\frac{6\beta e^{-\beta\xi}}{18\beta^3\chi^2}$, $D_4=C_4+\frac{9}{18\beta^3\chi^2}$, which, together with the boundary conditions B for the Green function, allow us to determine $C_i(\xi)$, $i=\overline{1,4}$, namely

$$C_1=-\frac{F_2(\xi)}{2\beta e^{\beta}\Delta_B},\ C_2=\frac{28F_2(\xi)}{2\beta e^{\beta}\Delta_B},\ C_3=-\frac{12F_2(\xi)}{2e^{\beta}\Delta_B},$$

$$\begin{aligned} C_4 &= \frac{\beta^3e^{\beta}}{2\beta^5e^{\beta}\Delta_B}\left[2\beta^2F_1(\xi)\Delta_B+\beta F_2(\xi)(e^{-3\beta}-28+12\beta)\right]=\\ &=F_1(\xi)+\frac{1}{2\beta\Delta_B}(e^{-3\beta}+28-12\beta)F_2(\xi),\end{aligned}$$

where

$F_1=\frac{1}{18\beta^3\chi^2}\left\{e^{-2\beta(1-\xi)}+2[4-3\beta(1-\xi)]e^{\beta(1-\xi)}-9\right\}$,

$F_2(\xi)=\frac{-2\beta}{18\beta^3\chi^2}\left\{e^{-2\beta(1-\xi)}+[3\beta(1-\xi)-1]e^{\beta(1-\xi)}\right\}$,

i.e.

$C_4=\frac{9}{18\chi^2\beta^3\Delta_B}\left\{2(2-\beta)e^{-2\beta(1-\xi)}+4(1-\beta\xi)e^{\beta(1-\xi)}+[1-\beta(1-\xi)]e^{-\beta(2+\xi)}-\Delta_B\right\}.$

Consequently

$$\begin{aligned} D_1 &= \frac{1}{18\beta^3\chi^2e^{\beta}\Delta_B}\left\{e^{\beta(1-\xi)}[-1+3\beta(1-\xi)]+2(-4+3\beta)e^{\beta(2\xi+1)}\right\},\\ D_2 &= -\frac{1}{18\beta^3\chi^2e^{\beta}\Delta_B}\left\{28e^{-2\beta(1-\xi)}-36e^{\beta(1-\xi)}(1-\beta\xi)(1+\beta)-2e^{-\beta(2+\xi)}(4+3\beta\xi)\right\},\\ D_3 &= \frac{6\beta}{18\beta^3\chi^2e^{\beta}\Delta_B}\left\{2e^{-2\beta(1-\xi)}+e^{-\beta(2+\xi)}+6(1-\beta\xi)e^{\beta(1-\xi)}\right\},\\ D_4 &= \frac{9}{18\beta^3\chi^2\Delta_B}\left\{2(2-\beta)e^{-2\beta(1-\xi)}+4(1-\beta\xi)e^{\beta(1-\xi)}+[1-\beta(1-\xi)]e^{-\beta(2+\xi)}\right\}.\end{aligned}$$

Remark 2.1. *The passage to limit $\beta_2=\beta_1+a$, $a\to 0$ in case 2.1 gives the result of 2.2, that confirms the computations validity.*

2.3 If $d=4T^3-27\sigma^2\chi^2<0$, the boundary conditions determinant takes the form

$$\Delta_B=2(n^2-3)\sin\delta+8u\cos\delta+u(1+u^2)e^{-3\gamma}=0,\ \ \delta=\gamma u,\ \ \alpha=2\gamma.$$

The continuity and jump conditions for the Green function

$$G(x,\xi)=\begin{cases} C_1e^{-\alpha x}+C_2e^{\gamma x}\cos\delta x+C_3e^{\gamma x}\sin\delta x+C_4, & 0\le x<\xi\\ D_1e^{-\alpha x}+D_2e^{\gamma x}\cos\delta x+D_3e^{\gamma x}\sin\delta x+D_4, & \xi<x\le 1\end{cases}$$

give

$$D_1=C_1-\frac{e^{2\gamma\xi}}{2\chi^2\gamma^3(9+u^2)},\ D_2=C_2-\frac{e^{-\gamma\xi}[(3-u^2)\sin\delta\xi+4u\cos\delta\xi]}{\chi^2\gamma^3u(1+u^2)(9+u^2)},$$

$$D_3=C_3-\frac{e^{-\gamma\xi}[(u^2-3)\cos\delta\xi+4u\sin\delta\xi]}{\chi^2\gamma^3u(1+u^2)(9+u^2)},\ D_4=C_4+\frac{1}{2\chi^2\gamma^3(1+u^2)},$$

and the relevant system is of the form

$$\begin{cases}
-8C_1 & + & (1-3u^2)C_2 & + & u(3-u^2)C_3 & & & = & 0\\
4C_1 & + & (1-u^2)C_2 & + & 2uC_3 & & & = & 0\\
e^{-2\gamma}C_1 & + & (e^{\gamma}\cos\delta)C_2 & + & (e^{\gamma}\sin\delta)C_3 & + & C_4 & = & F_2(x)\\
-2e^{-2\gamma}C_1 & + & (\cos\delta-u\sin\delta)e^{\gamma}C_2 & + & (\sin\delta+u\cos\delta)e^{\gamma}C_3 & & & = & F_1(x)
\end{cases}$$

$$\begin{aligned}
F_1(\xi) &= \frac{1}{\chi^2\gamma^3u(9+u^2)}\big\{-ue^{-2\gamma(1-\xi)}+e^{\gamma(1-\xi)}[u\cos\delta(1-\xi)-3\sin\delta(1-\xi)]\big\},\\
F_2(\xi) &= \frac{1}{2\chi^2\gamma^3u(1+u^2)(9+u^2)}\big\{u(1+u^2)e^{-2\gamma(1-\xi)}+2e^{\gamma(1-\xi)}[(u^2-3)\sin\delta(1-\xi)+\\
&\quad +4u\cos\delta(1-\xi)]-u(9+u^2)\big\},
\end{aligned}$$

whence

$$\begin{aligned}
C_1(\xi) &= \frac{1+u^2}{2\chi^2\gamma^3(9+u^2)\Delta_B}\big\{ue^{-3\gamma+2\gamma\xi}-e^{-\gamma\xi}[u\cos\delta(1-\xi)-3\sin\delta(1-\xi)]\big\},\\
C_2(\xi) &= \frac{2(u^2-7)}{\chi^2\gamma^3(1+u^2)(9+u^2)\Delta_B}\big\{ue^{-3\gamma+2\gamma\xi}-e^{-\gamma\xi}[u\cos\delta(1-\xi)-3\sin\delta(1-\xi)]\big\},\\
C_3(\xi) &= -\frac{2(5u^2-3)}{\chi^2\gamma^3(1+u^2)(9+u^2)\Delta_B}\big\{ue^{-3\gamma+2\gamma\xi}-e^{-\gamma\xi}[u\cos\delta(1-\xi)-3\sin\delta(1-\xi)]\big\},\\
C_4(\xi) &= \frac{1}{2\chi^2\gamma^3(1+u^2)\Delta_B}\big\{-u(1+u^2)e^{-3\gamma}+(1+u^2)e^{-\gamma(2+\xi)}[u\cos\delta(1-\xi)-\\
&\quad -\sin\delta(1-\xi)]+2e^{-2\gamma(1-\xi)}[2u\cos\delta-(1-u^2)\sin\delta]-\\
&\quad -2[4u\cos\delta+(u^2-3)\sin\delta]+4e^{\gamma(1-\xi)}(u\cos\delta\xi-\sin\delta\xi)\big\},
\end{aligned}$$

implying the following formulae for $D_i(\xi), i = \overline{1,4}$,

$$\begin{aligned}
D_1(\xi) &= \frac{-1}{2\chi^2\gamma^3(9+u^2)\Delta_B}\big\{(1+u^2)e^{-\gamma\xi}[u\cos\delta(1-\xi) - 3\sin\delta(1-\xi)] + \\
&+2e^{2\gamma\xi}[4u\cos\delta + (u^2-3)\sin\delta]\big\}, \\
D_2(\xi) &= \frac{e^{-\gamma\xi}}{\chi^2\gamma^3 u(1+u^2)(9+u^2)\Delta_B}\big\{2u(u^2-7)[ue^{-3\gamma(1-\xi)} - \\
&-u\cos\delta(1-\xi) + 3\sin\delta(1-\xi)] + \\
&+[(u^2-3)\sin\delta\xi - 4u\cos\delta\xi)][u(1+u^2)e^{-3\gamma} + 8u\cos\delta + 2(u^2-3)\sin\delta]\big\}, \\
D_3(\xi) &= \frac{e^{-\gamma\xi}}{\chi^2\gamma^3 u(1+u^2)(9+u^2)\Delta_B}\big\{-2u(5u^2-3)[ue^{-3\gamma(1-\xi)} - \\
&-u\cos\delta(1-\xi) + 3\sin\delta(1-\xi)] - \\
&-[(u^2-3)\cos\delta\xi + 4u\sin\delta\xi][u(1+u^2)e^{-3\gamma} + 8u\cos\delta + 2(u^2-3)\sin\delta]\big\}, \\
D_4(\xi) &= \frac{1}{2\chi^2\gamma^3(1+u^2)\Delta_B}\big\{(1+u^2)e^{-\gamma(2+\xi)}[u\cos\delta(1-\xi) - \sin\delta(1-\xi)] + \\
&+2e^{-2\gamma(1-\xi)}[2u\cos\delta - (1-u^2)\sin\delta] + 4e^{\gamma(1-\xi)}(u\cos\delta\xi - \sin\delta\xi)\big\}.
\end{aligned}$$

Remark 2.2. *The passage to the limit $u \to 0$ gives the result of 2.2, that confirms the validity of computations of 2.2.*

3. GREEN FUNCTIONS FOR THE BOUNDARY CONDITIONS B′

For this case we give the final result without any details of computations.
3.1. If $d = 4T^3 - 27\sigma^2\chi^2 > 0 \Rightarrow T > 0$, the conditions of continuity of the Green function together with derivatives up to the second order imply

$$G(x,\xi) = \begin{cases} C_1e^{-\alpha x} + C_2e^{\beta_1 x} + C_3e^{\beta_2 x} + C_4, & 0 \le x < \xi \\ D_1e^{-\alpha x} + D_2e^{\beta_2 x} + D_3e^{\beta_2 x} + D_4, & \xi < x \le 1 \end{cases}$$

at the point $x = \xi$, while the conditions of the jump $-\frac{1}{\chi^2}$ of the third derivative give the linear system, where

$$\Delta_{B'} = \beta_1\beta_2(\beta_2-\beta_1)e^{\beta_1+\beta_2} + (\beta_1+\beta_2)\left[\beta_2(\beta_1+2\beta_2)e^{-\beta_1} - \beta_1(2\beta_1+\beta_2)e^{-\beta_2}\right],$$

yielding

$$
\begin{aligned}
C_1(\xi) &= \frac{1}{\chi^2(\beta_1+\beta_2)(\beta_1+2\beta_2)(2\beta_1+\beta_2)\Delta_{B'}}\big\{(\beta_1+\beta_2)\big[\beta_2(\beta_1+2\beta_2)e^{-\beta_1+(\beta_1+\beta_2)\xi} - \\
&\quad -\beta_1(2\beta_1+\beta_2)e^{-\beta_2+(\beta_1+\beta_2)\xi}\big] + \\
&\quad +\beta_1\beta_2\big[(\beta_1+2\beta_2)e^{\beta_2+\beta_1(1-\xi)} - (2\beta_1+\beta_2)e^{\beta_1+\beta_2(1-\xi)}\big]\big\}, \\
C_2(\xi) &= \frac{1}{\chi^2\beta_1(\beta_2-\beta_1)(2\beta_1+\beta_2)\Delta_{B'}}\big\{\beta_2(\beta_2-\beta_1)\big[(\beta_1+\beta_2)e^{-\beta_1+(\beta_1+\beta_2)\xi} + \\
&\quad +\beta_1 e^{\beta_2+\beta_1(1-\xi)}\big] + (\beta_1+\beta_2)(2\beta_1+\beta_2)\big[\beta_2 e^{-\beta_1-\beta_2\xi} - \beta_1 e^{-\beta_2-\beta_1\xi}\big]\big\}, \\
C_3(\xi) &= \frac{1}{\chi^2\beta_2(\beta_2-\beta_1)(\beta_1+2\beta_2)\Delta_{B'}}\big\{(\beta_1+\beta_2)(\beta_1+2\beta_2)\big[\beta_1 e^{-\beta_2-\beta_1\xi} - \beta_2 e^{-\beta_1-\beta_2\xi}\big] - \\
&\quad -\beta_1(\beta_2-\beta_1)\big[(\beta_1+\beta_2)e^{-\beta_2+(\beta_1+\beta_2)\xi} + \beta_2 e^{\beta_1+\beta_2(1-\xi)}\big]\big\}, \\
C_4(\xi) &= -\frac{1}{\chi^2\beta_1\beta_2(\beta_2^2-\beta_1^2)(\beta_1+2\beta_2)(2\beta_1+\beta_2)\Delta_{B'}}\big\{(\beta_2^2-\beta_1^2)\big[\beta_1\beta_2\Big(\beta_2^2 e^{-\beta_1} - \\
&\quad -\beta_1^2 e^{-\beta_2} + (\beta_1+\beta_2)(\beta_2 e^{-\beta_1} - \beta_1 e^{-\beta_2})\Big) + \\
&\quad +(\beta_1+\beta_2)(\beta_2^3 e^{-\beta_1} - \beta_1^3 e^{-\beta_2})\big]e^{(\beta_1+\beta_2)\xi} + \\
&\quad +\beta_1\beta_2^2(\beta_1+2\beta_2)(\beta_2^2+2\beta_1\beta_2-\beta_1^2)e^{\beta_2+\beta_1(1-\xi)} + \\
&\quad +\beta_1^2\beta_2(2\beta_1+\beta_2)(\beta_1^2+2\beta_1\beta_2-\beta_2^2)e^{\beta_1+\beta_2(1-\xi)} - \\
&\quad -(\beta_1+\beta_2)[\beta_2^4(2\beta_1+\beta_2)e^{\beta_2(2-\xi)} + \beta_1^4(\beta_1+2\beta_2)e^{\beta_1(2-\xi)}] + \\
&\quad +(\beta_1+\beta_2)(\beta_2^2-\beta_1^2)(2\beta_1+\beta_2)(\beta_1+2\beta_2)[\beta_2 e^{-\beta_1-\beta_2\xi} - \beta_1 e^{-\beta_2-\beta_1\xi}]\big\},
\end{aligned}
$$

and

$$
\begin{aligned}
D_1(\xi) &= \frac{\beta_1\beta_2}{\chi^2(\beta_1+\beta_2)(2\beta_1+\beta_2)(\beta_1+2\beta_2)\Delta_{B'}}\big\{(\beta_1+2\beta_2)e^{\beta_2+\beta_1(1-\xi)} - \\
&\quad -(2\beta_1+\beta_2)e^{\beta_1+\beta_2(1-\xi)} - (\beta_2-\beta_1)e^{(\beta_1+\beta_2)(1-\xi)}\big\}, \\
D_2(\xi) &= \frac{\beta_2(\beta_1+\beta_2)}{\chi^2\beta_1(\beta_2-\beta_1)(2\beta_1+\beta_2)\Delta_{B'}}\big\{(\beta_2-\beta_1)e^{-\beta_1+(\beta_1+\beta_2)\xi} + \\
&\quad +(2\beta_1+\beta_2)e^{-\beta_1-\beta_2\xi} - (\beta_1+2\beta_2)e^{-\beta_1(1+\xi)}\big\}, \\
D_3(\xi) &= \frac{\beta_1(\beta_1+\beta_2)}{\chi^2\beta_2(\beta_2-\beta_1)(\beta_1+2\beta_2)\Delta_{B'}}\big\{(\beta_1+2\beta_2)e^{-\beta_2-\beta_1\xi} - \\
&\quad -(2\beta_1+\beta_2)e^{-\beta_2(1+\xi)} - (\beta_2-\beta_1)e^{-\beta_2+(\beta_1+\beta_2)\xi}\big\},
\end{aligned}
$$

$$\begin{aligned} D_4(\xi) = & \frac{1}{\chi^2\beta_1\beta_2(\beta_2^2-\beta_1^2)(\beta_1+2\beta_2)(2\beta_1+\beta_2)\Delta_{B'}}\Big\{-\big[\beta_1\beta_2\Big(\beta_2^2e^{-\beta_1}-\beta_1^2e^{-\beta_2}+ \\ & +(\beta_1+\beta_2)(\beta_2e^{-\beta_1}-\beta_1e^{-\beta_2})\Big)+(\beta_1+\beta_2)(\beta_2^3e^{-\beta_1}-\beta_1^3e^{-\beta_2})\big](\beta_2^2-\beta_1^2)e^{(\beta_1+\beta_2)\xi}- \\ & -\beta_1\beta_2^2(\beta_1+2\beta_2)(\beta_2^2+2\beta_1\beta_2-\beta_1^2)e^{\beta_2+\beta_1(1-\xi)}- \\ & -\beta_1^2\beta_2(2\beta_1+\beta_2)(\beta_1^2+2\beta_1\beta_2-\beta_2^2)e^{\beta_1+\beta_2(1-\xi)}+ \\ & +(\beta_1+\beta_2)[\beta_2^4(2\beta_1+\beta_2)e^{\beta_2(2-\xi)}+\beta_1^4(\beta_1+2\beta_2)e^{\beta_1(2-\xi)}]- \\ & -(\beta_1+\beta_2)(\beta_2^2-\beta_1^2)(2\beta_1+\beta_2)(\beta_1+2\beta_2)[\beta_2e^{-\beta_1-\beta_2\xi}-\beta_1e^{-\beta_2-\beta_1\xi}]+ \\ & +(\beta_2-\beta_1)(\beta_1+2\beta_2)(2\beta_1+\beta_2)\big[\beta_1\beta_2(\beta_2-\beta_1)e^{\beta_1+\beta_2}+ \\ & +\beta_2(\beta_1+\beta_2)(\beta_1+2\beta_2)e^{-\beta_1}-\beta_1(\beta_1+\beta_2)(2\beta_1+\beta_2)e^{-\beta_2}\big]\Big\}. \end{aligned}$$

3.2. If $d = 4T^3 - 27\sigma^2\chi^2 = 0$, the boundary conditions B′ give the equality

$$\Delta_{B'} = 1 + (8 + 6\beta)e^{-3\beta} > 0$$

while the divergence is absent [2].

3.3. If $d = 4T^3 - 27\sigma^2\chi^2 < 0$, the boundary conditions B′ give the equality [2]

$$\begin{aligned} \Delta_{B'} &= 2(3-u^2)\sin\gamma u + 8u\cos\gamma u + u(1+u^2)e^{3\gamma} = \\ &= ue^{3\gamma}\big[\big(2(3-u^2)\frac{\sin u}{u} + 8\cos\gamma u\big)e^{-3\gamma} + (1+u^2)\big], \end{aligned}$$

whence its positivity for small u. For the large u and γ the third summand grows faster than two first ones. Consequently $\Delta_{B'} > 0$ and the divergence is absent again.

References

[1] B. V. Loginov, A. V. Tsyganov, O. V. Kožhevnikova, *Strip-plate divergence as bifurcation problem with two spectral parameters*, Trends in Applications of Mathematics to Mechanics, Proc. of Intern. Symp. STAMM-2004, Wang Y., Hutter K. (eds), Seeheim-Darmstadt, Germany, August 22-28, 2004, Shaker-Verlag, Aachen: Berichte aus der Mathematik, 235-245 (2005).

[2] K. M. Petrov, A. V. Tsyganov, B. V. Loginov, *On the divergence stability loss of elongated plate in supersonic gas flow subjected to compressing or extending stresses*, Izvestiya Irkutskogo Gos. Universiteta, ser. Mathematika, **1**, 1 (2007), 212-235.

[3] A. S. Vol'mir, *Stability of deformed systems*, Nauka, Moscow, 1964.

[4] A.S. Vol'mir, *Shells in fluid and gas flows. Aeroelasticity problems*, Nauka, Moscow, 1976.

[5] B. V. Loginov, O. V. Kozhevnikova, *Computation of eigen-bending forms and branching solutions asymptotics for bifurcation problem on rectangular plate divergence*, Izvestiya RAEN, **2**(3)(1998), 112-120.

[6] M. M. Vainberg, V. A.Trenogin, *Branching theory of solutions of nonlinear equations*, Nauka, Moscow, 1969 Engl.transl. Volters-Noordorf, Leiden, 1974.

[7] M. A. Naimark, *Linear differential operators*, Nauka, Moscow, 1969.

[8] Yu. A. Melnikov, *Influence functions and matrices*, Mech. Engng **119**, M. Dekker, 1999.

ROMAI J., **4**, 2(2008), 45–56

A NUMERICAL STUDY BY FEM AND FVM OF A PROBLEM WHICH PRESENTS A SIMPLE LIMIT POINT

Cătălin Liviu Bichir

ROSTIREA MATHS RESEARCH, Galaţi

catalinliviubichir@yahoo.com

Abstract A problem, which presents a simple limit point, is approximated by finite element method (FEM) and by finite volume method (FVM). In order to obtain the branch of solutions, an arc-length-continuation method and Newton's method are used. Numerical results obtained by two computer programs, based on FEM and FVM, are presented.

Keywords: simple limit point, finite element method, finite volume method.

2000 MSC: 37G10, 34K28, 65L60, 90C53.

1. INTRODUCTION

Let $\Omega = (0,1) \times (0,1)$ and consider the following problem in $(\lambda, u) \in \mathbb{R} \times H_0^1(\Omega)$

$$\begin{aligned} -\ \triangle u &= \lambda e^u \text{ in } \Omega\,, \\ u &= 0 \text{ on } \partial\Omega\,, \end{aligned} \tag{1}$$

where λ is the parameter.

In order to solve problem (1), Glowinski [6] proposed the algorithm presented in the sequel, based on arc-length-continuation methods, for the problem in $(\lambda, u) \in \mathbb{R} \times H_0^1(\Omega)$

$$\begin{aligned} -\ \triangle u &= \lambda T(u) \text{ in } \Omega\,, \\ u &= 0 \text{ on } \partial\Omega\,, \end{aligned} \tag{2}$$

which generalizes (1). $\Omega \subset \mathbb{R}^N$ is a bounded domain with smooth boundary $\partial\Omega$ and T is a nonlinear operator from $H_0^1(\Omega)$ to $H^{-1}(\Omega)$.

Glowinski [6] followed H. B. Keller [10], [11] in order to use arc-length-continuation methods to solve nonlinear problems and so to associate to (2) the continuation equation

$$\int_\Omega |\nabla \frac{\partial u}{\partial s}|^2 d\Omega + (\frac{d\lambda}{ds})^2 = 1\,, \tag{3}$$

where s is the curvilinear abscissa.

In order to solve (2), the extended system formed by (2) and (3), parametrized by s, was considered. Let $\triangle s$ be an arc-length step and $u^n \cong u(n\triangle s)$. The following algorithm was formulated ([6]): take $\lambda^0 = 0$, $u^0 = 0$ and suppose that $\frac{d\lambda(0)}{ds}$, $\frac{\partial u(0)}{\partial s}$ are given; for $n \geq 0$, assuming that λ^{n-1}, u^{n-1}, λ^n, u^n are known, $(\lambda^{n+1}, u^{n+1}) \in \mathbb{R} \times H_0^1(\Omega)$ is obtained from

$$\begin{aligned} &-\triangle u^{n+1} = \lambda^{n+1} T(u^{n+1}) \text{ in } \Omega\,, \\ &u^{n+1} = 0 \text{ on } \partial\Omega\,, \end{aligned} \tag{4}$$

and

$$\begin{aligned} &\int_\Omega \nabla(u^1 - u^0)\cdot\nabla(\frac{\partial u(0)}{\partial s})d\Omega + (\lambda^1 - \lambda^0)\frac{d\lambda(0)}{ds} = \triangle s \text{ if } n = 0\,, \\ &\int_\Omega \nabla(u^{n+1} - u^n)\cdot\nabla(\frac{u^n - u^{n-1}}{\triangle s})d\Omega + (\lambda^{n+1} - \lambda^n)(\frac{\lambda^{n+j} - \lambda^{n+j-1}}{\triangle s}) = \\ &\quad = \triangle s \text{ with } j = 0 \text{ or } 1, \text{ if } n \geq 1\,. \end{aligned} \tag{5}$$

From (2), it follows

$$\begin{aligned} &-\triangle\frac{\partial u(0)}{\partial s} = \frac{d\lambda(0)}{ds} T(0) \text{ in } \Omega\,, \\ &\frac{\partial u(0)}{\partial s} = 0 \text{ on } \partial\Omega\,, \end{aligned} \tag{6}$$

while $\frac{d\lambda(0)}{ds}$, $\frac{\partial u(0)}{\partial s}$ are deduced from

$$(\frac{d\lambda(0)}{ds})^2(1 + \int_\Omega |\nabla\hat{u}|^2 d\Omega) = 1\,, \tag{7}$$

$$\frac{\partial u(0)}{\partial s} = \frac{d\lambda(0)}{ds}\hat{u}\,, \tag{8}$$

where $\hat{u} \in H_0^1(\Omega)$ is the solution of

$$\begin{aligned} &-\triangle\hat{u} = T(0) \text{ in } \Omega\,, \\ &\hat{u} = 0 \text{ on } \partial\Omega\,. \end{aligned} \tag{9}$$

For (1), $T(v) = e^v$, $v \in H_0^1(\Omega)$, and $T(0) = 1$.

Glowinski [6] approximated (1) by using the FEM, taking a triangulation $\mathcal{T}_h$ of Ω by 512 triangles and considering the approximation of u by u_h, $u_h \in V_h^1$, where

$$V_h^i = \{v_h \in C^0(\bar{\Omega}), v_h|_{\partial\Omega} = 0 \text{ and } v_h|_K \in P_i(K), \forall K \in \mathcal{T}_h\}, \quad i = 1, 2\,, \tag{10}$$

and $P_i(K)$ is the space of polynomials in x and y of degree less than or equal to i defined on K. Such a triangle K is defined by the nodal points A_1, A_3, A_5 in fig. 1 and a basis functions of the space $P_1(K)$ is defined by these three nodal points.

For $\lambda > 0$, Glowinski [6] solved, the obtained approximate equations corresponding to (4), (5) by the Polak-Ribière version of the conjugate gradient method. He took $\triangle s = 0.1$ and $j = 0$ and obtained the computed simple limit point (turning point) at $\lambda = 6.8591\ldots$. Glowinski also quoted H.B.Keller [10], [11] who used Newton's and quasi-Newton's methods in order to solve nonlinear problems by arc-length-continuation methods.

2. NEWTON'S METHOD FOR (4), (5)

Let us consider the weak formulation of (1) as the problem in $(\lambda, u) \in \mathbb{R} \times V$, $V = H_0^1(\Omega) \cap C^0(\bar{\Omega})$,

$$\int_\Omega \nabla u \cdot \nabla v \, d\Omega = \lambda \int_\Omega e^u v \, d\Omega\,, \ \forall\, v \in H_0^1(\Omega)\,. \tag{11}$$

For $\lambda \leq 0$, problem (11) possesses a unique solution u. If $\lambda = 0$, then $u = 0$. There exists a positive number $\widetilde{\lambda}$ such that for $\lambda > \widetilde{\lambda}$, problem (11) has no solution. For $0 \leq \lambda < \widetilde{\lambda}$, problem (11) possesses a positive minimal solution $u(\lambda)$, $(\lambda, u(\lambda))$ is a regular point of (11) and the mapping $\lambda \to u(\lambda)$ is increasing in the following sense: if $\lambda_1 < \lambda_2$ then $u(\lambda_1) < u(\lambda_2)$ in Ω. For $\lambda = \widetilde{\lambda}$, there exists a unique $\widetilde{u} \in V$ such that $(\widetilde{\lambda}, \widetilde{u})$ is solution of (11). $(\widetilde{\lambda}, \widetilde{u})$ is a nondegenerate simple limit point (a turning point) of problem (11) ([1]). Other theoretical results from [1] lead to the conclusion that there exists $\widetilde{\lambda}_1$, $0 < \widetilde{\lambda}_1 < \widetilde{\lambda}$, such that for $\widetilde{\lambda}_1 < \lambda < \widetilde{\lambda}$, each of the two solutions (λ, u') and (λ, u'') of problem (11) are regular. Under the conditions from [1], which relates the exact problem (11) to an approximate problem of (11), $(\widetilde{\lambda}, \widetilde{u})$ is approximated by a nondegenerate simple limit point of the approximate problem.

In (5), let us denote $u^* = u^0$, $\lambda^* = \lambda^0$, $u^{**} = \frac{\partial u(0)}{\partial s}$, $\lambda^{**} = \frac{d\lambda(0)}{ds}$ if $n = 0$ and $u^* = u^n$, $\lambda^* = \lambda^n$, $u^{**} = \frac{u^n - u^{n-1}}{\triangle s}$, $\lambda^{**} = \frac{\lambda^n - \lambda^{n-1}}{\triangle s}$ if $n \geq 1$. We take $j = 0$.

We propose to construct the branch of solution, for $\lambda \geq 0$, for an approximate problem corresponding to problem (1), using an algorithm based on the above algorithm for (4), (5) and on Newton's method. We obtain the approximate problem in two ways: by FEM and by FVM.

In order to apply Newton's method, it is necessary to know if the solutions obtained by (4), (5) are regular. It remains to verify that the kernel of the differential of the function from (4), (5), with respect of $(\widetilde{\lambda}, \widetilde{u})$, is $\{0\}$, that is the following equation in $(\mu, w) \in \mathbb{R} \times V$ has only the solution $(\mu, w) = (0, 0)$

$$\begin{aligned} &\int_\Omega \nabla w \cdot \nabla v \, d\Omega - \widetilde{\lambda} \int_\Omega e^{\widetilde{u}} w v \, d\Omega - \mu \int_\Omega e^{\widetilde{u}} v \, d\Omega = 0 \,, \ \forall \, v \in H_0^1(\Omega) \,, \\ &\int_\Omega \nabla w \cdot \nabla u^{**} \, d\Omega + \mu \lambda^{**} = 0 \,, \end{aligned} \tag{12}$$

For the first equation from (12), there exists a solution $(0, \widetilde{w}) \neq (0, 0)$, $\widetilde{w} > 0$ in Ω ([1]). In addition, all solutions of this equation are of the form $(0, \alpha\widetilde{w})$, $\alpha \in \mathbb{R}$. For $(\mu, w) = (0, \widetilde{w})$, (12) becomes

$$\begin{aligned} &\int_\Omega \nabla \widetilde{w} \cdot \nabla v \, d\Omega - \widetilde{\lambda} \int_\Omega e^{\widetilde{u}} \widetilde{w} v \, d\Omega = 0 \,, \ \forall \, v \in H_0^1(\Omega) \,, \\ &\int_\Omega \nabla \widetilde{w} \cdot \nabla u^{**} \, d\Omega = 0 \,. \end{aligned} \tag{13}$$

If $\widetilde{w}$ is a solution of (13), it follows that $\int_\Omega e^{\widetilde{u}} \widetilde{w} u^{**} \, d\Omega = 0$. This is not possible since $e^{\widetilde{u}} \widetilde{w} u^{**} > 0$ or $e^{\widetilde{u}} \widetilde{w} u^{**} < 0$ in Ω ($u^{**} > 0$ or $u^{**} < 0$ in Ω) so the kernel of the differential of the function from (4), (5), with respect of $(\widetilde{\lambda}, \widetilde{u})$, is $\{0\}$ and we can apply Newton's method.

We now formulate the algorithm which we will use to construct the branch of solution for an approximate problem corresponding to problem (1):

1. solve (9) (with $T(0) = 1$) to obtain $\hat{u} \in H_0^1(\Omega)$;
2. obtain $\frac{d\lambda(0)}{ds}$ from (7) and $\frac{\partial u(0)}{\partial s}$ from (8) ;

3. let $\lambda^0 = 0$, $u^0 = 0$; for $n \geq 0$, taking λ^n, u^n as initial iteration, the following algorithm based on the Newton's method calculates λ^{n+1}, u^{n+1} : obtain $(\lambda^{m+1}, u^{m+1}) \in \mathbb{R} \times V$ using

$$\begin{aligned}
&\int_\Omega \nabla u^{m+1} \cdot \nabla v \, d\Omega - \int_\Omega \lambda^m e^{u^m} u^{m+1} v \, d\Omega - \lambda^{m+1} \int_\Omega e^{u^m} v \, d\Omega \\
&= - \int_\Omega \lambda^m e^{u^m} u^m v \, d\Omega \, , \; \forall \, v \in H_0^1(\Omega) \, , \\
&\int_\Omega \nabla u^{m+1} \cdot \nabla u^{**} \, d\Omega + \lambda^{m+1} \lambda^{**} = \int_\Omega \nabla u^* \cdot \nabla u^{**} \, d\Omega + \lambda^* \lambda^{**} + \triangle s \, .
\end{aligned} \tag{14}$$

4. the algorithm is stopped after an imposed number of iterations for n.

3. THE APPROXIMATE PROBLEM OBTAINED BY FEM

We formulate an approximate problem corresponding to (14) using the finite element method (FEM). Let us consider a triangulation $\mathcal{T}_h$ of $\Omega = (0,1) \times (0,1)$ by N triangles K. We approximate the component u of the solution of (14) by $u_h \in V_h^2$. The elements $K \in \mathcal{T}_h$, for the definition of V_h^2, are triangles with six nodal points: the three vertices and the three mid-points of sides. Such a triangle K is defined by the nodal points A_1, A_3, A_5 in fig. 1 and a nodal point i is A_i, $i = 1, \ldots, 6$.

A certain fixed numeration of these nodal points, with $i \in J_K = \{1, 2, 3, 4, 5, 6\}$, represents the local numeration for the nodes of K. A certain fixed numeration of all the nodal points of Ω, with $j \in J = \{1, \ldots, M\}$, represents the global numeration for the nodes of Ω. The two numerations are related by a matrix L whose elements are elements $j \in J$ (from the global numeration) as function of the elements $K \in \mathcal{T}_h$ (by the number of the element K in a certain fixed numeration with elements from the set $\{1, \ldots, N\}$) and of the elements $i \in J_K$ (from the local numeration), that is $j = L(K, i)$.

Denote by ψ_i, $i \in J_K$, the basis functions of the space $P_2(K)$ corresponding to the nodal points i in the local numeration of K. The functions ψ_i define a

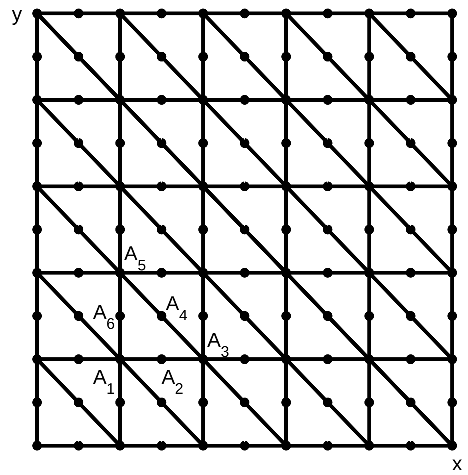

Fig. 1. Triangulation.

basis functions ϕ_j, $j \in J$, of V_h^2. Let us represent $u_h \in V_h^2$ by

$$u_h(x,y) = \sum_{j=1}^{M} u_j \phi_j(x,y)\,, \tag{15}$$

where u_j are the values of $u_h(x,y)$ at the nodes j. Taking $u = u_h$, u_h given by (15), and $v = \phi_j$, $j \in J$, in (14), we obtain the discrete variant of problem (14) as the following problem in $(\lambda, u_1, \ldots, u_M) \in \mathbb{R}^{M+1}$, written suitable for the assembly process,

$$\begin{aligned} &\sum_{K\in\, \mathcal{T}_h} \Big\{ \sum_{i\in\ J_K,\, j=L(K,i)} u_j^{m+1} \int_K \nabla\psi_i \cdot \nabla\psi_\ell \, dK \\ &- \sum_{i\in\ J_K,\, j=L(K,i)} u_j^{m+1} \int_K \lambda^m e^{u^m} \psi_i\, \psi_\ell \, dK - \lambda^{m+1} \int_K e^{u^m}\ \psi_\ell \, dK \Big\} \\ &= - \sum_{K\in\, \mathcal{T}_h} \int_K \lambda^m e^{u^m} u^m\ \psi_\ell \, dK\,, \end{aligned} \tag{16}$$

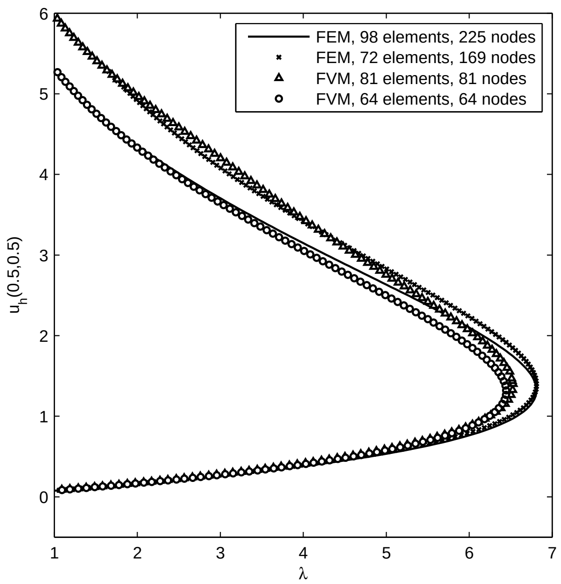

Fig. 2. u_h, in $x = y = 0.5$, as function of λ.

$$\sum_{K\in \mathfrak{T}_h} \sum_{i\in J_K,\, j=L(K,i)} u_j^{m+1} \int_K \nabla\psi_i \cdot \nabla u^{**}\, dK + \lambda^{m+1}\lambda^{**}$$
$$= \sum_{K\in \mathfrak{T}_h} \int_K \nabla u^* \cdot \nabla u^{**}\, dK + \lambda^*\lambda^{**} + \triangle s\,, \tag{17}$$
$$u_j^{m+1} = 0 \text{ for nodal points } j \text{ on } \partial\Omega\,,$$

for all $\ell \in J_K$, for all $K \in \mathfrak{T}_h$.

The algorithm of Section 2 for problem (16)-(17) was transcribed in a computer program. We took $\triangle s = 0.1$ and considered two cases:

1. 98 elements, 225 nodes; it was obtained $\widetilde{\lambda}_{computed} = 6.8101870809$;
2. 72 elements, 169 nodes; it was obtained $\widetilde{\lambda}_{computed} = 6.8105122120$,

where $\widetilde{\lambda}_{computed}$ is maximum of λ^n obtained by numerical calculation.
In fig. 2, we present u_h, in $x = y = 0.5$, as function of λ. In fig. 3, we present $\|u_h\|$ as function of λ. Here and in Section 4, $\|u_h\| \cong \|u\| = (\int_\Omega |\nabla u|^2 d\Omega)^{1/2}$.

Our results agree with the computed solution u_h, in $x = y = 0.5$, as function of λ, obtained by Glowinski [6] for the case presented at the end of Section 1.

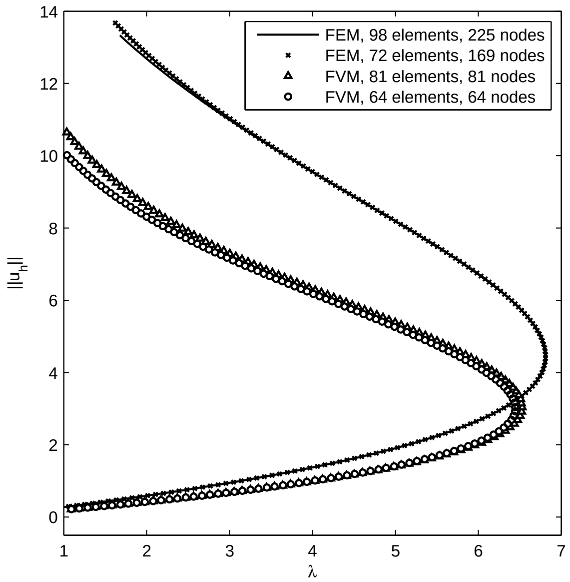

Fig. 3. $\|u_h\|$ as function of λ.

4. THE APPROXIMATE PROBLEM OBTAINED BY FVM

In the sequel, we will retain the weak formulation of (1) without partial integration in the term $\int\limits_\Omega \triangle u\, v\, d\Omega$. Then (14) becomes the following problem in $(\lambda^{m+1}, u^{m+1}) \in \mathbb{R} \times (H^2(\Omega) \cap C^0(\bar{\Omega}))$

$$\begin{aligned} &\int\limits_\Omega \triangle u^{m+1}\, v\, d\Omega + \int\limits_\Omega \lambda^m e^{u^m} u^{m+1}\, v\, d\Omega + \lambda^{m+1} \int\limits_\Omega e^{u^m}\, v\, d\Omega \\ &= \int\limits_\Omega \lambda^m e^{u^m} u^m\, v\, d\Omega\,,\ \forall\, v \in L^2(\Omega)\,, \\ &u^{m+1} = 0 \text{ on } \partial\Omega\,, \\ &\int\limits_\Omega \nabla u^{m+1} \cdot \nabla u^{**}\, d\Omega + \lambda^{m+1}\lambda^{**} = \int\limits_\Omega \nabla u^* \cdot \nabla u^{**}\, d\Omega + \lambda^* \lambda^{**} + \triangle s\,. \end{aligned} \tag{18}$$

We formulate an approximate problem corresponding to problem (18) using the FVM.

For $\Omega = (0,1) \times (0,1)$, let us consider a rectangular mesh defined by the points of coordinates (x_i, y_j), where $x_i = i\triangle x$, $y_j = j\triangle y$, $0 \le i \le N_1$,

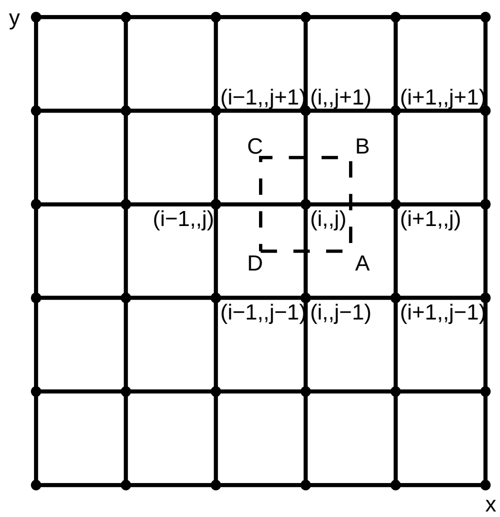

Fig. 4. Rectangular mesh.

$0 \le j \le N_2$, $x_{N_1} = 1.0$, $y_{N_2} = 1.0$ (fig. 4). Let us associate a subdomain K_{ij} to each nodal point (i, j) of coordinates (x_i, y_j). K_{ij} is a rectangle $ABCD$ (fig. 4), where the points A, B, C, D have coordinates of the type $x_i \pm 0.5\triangle x$, $y_j \pm 0.5\triangle y$. Denote $\mathcal{T}_h$ the triangulation formed by K_{ij} and by Γ_{ij} the boundary of K_{ij}.

Let us replace v in (18) by functions defined by $v_{ij} : \bar{\Omega} \to \mathbb{R}$,

$$
\begin{aligned}
&v_{ij}(x, y) = 0 \text{ if } (x, y) \notin \bar{K}_{ij} \\
&v_{ij}(x, y) = 1 \text{ if } (x, y) \in \bar{K}_{ij} \; .
\end{aligned}
\tag{19}
$$

The problem (18) becomes the following problem in $(\lambda^{m+1}, u^{m+1}) \in \mathbb{R} \times (H^2(\Omega) \cap C^0(\bar{\Omega}))$

$$
\begin{aligned}
&\int\limits_{K_{ij}} \triangle u^{m+1} \, dK + \int\limits_{K_{ij}} \lambda^m e^{u^m} u^{m+1} \, dK + \lambda^{m+1} \int\limits_{K_{ij}} e^{u^m} \, dK \\
&= \int\limits_{K_{ij}} \lambda^m e^{u^m} u^m \, dK \;, \text{ for all } \; K_{ij} \in \; \mathcal{T}_h \;,
\end{aligned}
\tag{20}
$$

$$\sum_{K_{ij}\in \mathcal{T}_h} \int_{K_{ij}} \nabla u^{m+1} \cdot \nabla u^{**} \, dK + \lambda^{m+1}\lambda^{**}$$
$$= \sum_{K_{ij}\in \mathcal{T}_h} \int_{K_{ij}} \nabla u^{*} \cdot \nabla u^{**} \, dK + \lambda^{*}\lambda^{**} + \triangle s \ ,$$
$$u^{m+1} = 0 \text{ on } \partial\Omega \ ,$$

Let $\mathbf{H} = (f,g) = (\frac{\partial u}{\partial x}, \frac{\partial u}{\partial y})$, $\mathbf{V} = (u,0) = u\mathbf{1}_x$, $\mathbf{W} = (0,u) = u\mathbf{1}_y$, $\mathbf{V}^* = (u^*,0) = u^*\mathbf{1}_x$, $\mathbf{W}^* = (0,u^*) = u^*\mathbf{1}_y$, $\mathbf{V}^{**} = (u^{**},0) = u^{**}\mathbf{1}_x$, $\mathbf{W}^{**} = (0,u^{**}) = u^{**}\mathbf{1}_y$, where $\mathbf{1}_x$, $\mathbf{1}_y$ are the unit vectors along the x , y directions. Denote by $\mathbf{n}$ the unit outward normal to Γ_{ij}.

Applying Gauss's formula, $\int_{K_{ij}} \nabla \cdot \mathbf{H} \, dK = \int_{\Gamma_{ij}} \mathbf{H} \cdot \mathbf{n} \, ds$, considering that u_{ij} is the average value of u over K_{ij} and that u_{ij} is located at the nodal point (i,j), we obtain a approximate variant of (20) as the following problem in (λ, $u_{0,0}$, ..., u_{N_1,N_2}) $\in \mathbb{R}^{1+(N_1+1)(N_2+1)}$

$$\begin{aligned}
&\int_{\Gamma_{ij}} \mathbf{H}^{m+1} \cdot \mathbf{n} \, ds + u_{ij}^{m+1} \, \lambda^m \, e^{u_{ij}^m} \, area(K_{ij}) + \lambda^{m+1} \, e^{u_{ij}^m} \, area(K_{ij}) \\
&= \lambda^m \, e^{u_{ij}^m} \, u_{ij}^m \, area(K_{ij}) \ , \text{ for all } \ K_{ij} \in \mathcal{T}_h \\
&\sum_{K_{ij}\in \mathcal{T}_h} \{ \frac{\partial u_{ij}^{**}}{\partial x} \int_{\Gamma_{ij}} \mathbf{V}^{m+1} \cdot \mathbf{n} \, ds + \frac{\partial u_{ij}^{**}}{\partial y} \int_{\Gamma_{ij}} \mathbf{W}^{m+1} \cdot \mathbf{n} \, ds \} \\
&+ \lambda^{m+1}\lambda^{**} = \sum_{K_{ij}\in \mathcal{T}_h} \nabla u_{ij}^{*} \cdot \nabla u_{ij}^{**} \, area(K_{ij}) + \lambda^{*}\lambda^{**} + \triangle s \ , \\
&u_{ij}^{m+1} = 0 \text{ for nodal points } (i,j) \text{ on } \partial\Omega \ ,
\end{aligned} \tag{21}$$

The terms in this equation are evaluated by the following relations

$$\begin{aligned}
&\int_{\Gamma_{ij}} \mathbf{H} \cdot \mathbf{n} ds = \\
&= f_{AB}(y_B - y_A) - g_{AB}(x_B - x_A) + f_{BC}(y_C - y_B) - g_{BC}(x_C - x_B) \\
&+ f_{CD}(y_D - y_C) - g_{CD}(x_D - x_C) + f_{DA}(y_A - y_D) - g_{DA}(x_A - x_D) \, ,
\end{aligned}$$

$$f_{AB} = \frac{1}{2}(f_A + f_B), \quad g_{AB} = \frac{1}{2}(g_A + g_B), \quad u_{AB} = \frac{1}{2}(u_A + u_B), \quad \ldots .$$

$$\int_{\Gamma_{ij}} \mathbf{V}\cdot\mathbf{n}ds =$$
$$= u_{AB}(y_B - y_A) + u_{BC}(y_C - y_B) + u_{CD}(y_D - y_C) + u_{DA}(y_A - y_D)\,,$$

$$\int_{\Gamma_{ij}} \mathbf{W}\cdot\mathbf{n}ds =$$
$$= -u_{AB}(x_B - x_A) - u_{BC}(x_C - x_B) - u_{CD}(x_D - x_C) - u_{DA}(x_A - x_D)\,.$$

$$u_A = \sum_{I\in S_A} u_I n_I(x_A, y_A),\ u_B = \sum_{I\in S_B} u_I n_I(x_B, y_B),$$
$$u_C = \sum_{I\in S_C} u_I n_I(x_C, y_C),\ u_D = \sum_{I\in S_D} u_I n_I(x_D, y_D),$$
$$f_A = \frac{\partial u_A}{\partial x} = \sum_{I\in S_A} u_I \frac{\partial n_I(x_A, y_A)}{\partial x},$$
$$g_A = \frac{\partial u_A}{\partial y} = \sum_{I\in S_A} u_I \frac{\partial n_I(x_A, y_A)}{\partial y},\ldots,$$
$$S_A = \{(i, j-1), (i+1, j-1), (i+1, j), (i, j)\},$$
$$S_B = \{(i, j), (i+1, j), (i+1, j+1), (i, j+1)\},$$
$$S_C = \{(i-1, j), (i, j), (i, j+1), (i-1, j+1)\},$$
$$S_D = \{(i-1, j-1), (i, j-1), (i, j), (i-1, j)\}.$$

We used finite element interpolation on the rectangles of vertices (i, j) in order to evaluate the value of u in points such as A, B, C, D. N_I are the shape functions on these rectangular finite elements. They are also used to evaluate $\|u_h\|$, where u_h has the value u_{ij} in (i, j).

$$\frac{\partial u^*_{ij}}{\partial x} = \frac{1}{area(K_{ij})}\int_{K_{ij}} \frac{\partial u^*}{\partial x}\,dK = \frac{1}{area(K_{ij})}\int_{\Gamma_{ij}} \mathbf{V}^*\cdot\mathbf{n}\,ds\,,$$
$$\frac{\partial u^*_{ij}}{\partial y} = \frac{1}{area(K_{ij})}\int_{K_{ij}} \frac{\partial u^*}{\partial y}\,dK = \frac{1}{area(K_{ij})}\int_{\Gamma_{ij}} \mathbf{W}^*\cdot\mathbf{n}\,ds\,,$$

and the same if we replace u^*_{ij} by u^{**}_{ij}.

The algorithm of Section 2 and problem (21) was transcribed in a computer program. We took $\triangle s = 0.1$ and considered two cases:
1. 81 elements, 81 nodes; it was obtained $\widetilde{\lambda}_{computed} = 6.5301245953$;
2. 64 elements, 64 nodes; it was obtained $\widetilde{\lambda}_{computed} = 6.4448260233$,
where $\widetilde{\lambda}_{computed}$ is maximum of λ^n obtained by numerical calculation. In fig. 2, we present u_h, in $x = y = 0.5$, as function of λ. In fig. 3, we present $\|u_h\|$ as function of λ.

References

[1] M. Crouzeix, J. Rappaz, *On Numerical approximation in bifurcation theory*, Masson-Paris, Springer-Berlin, 1990.

[2] C. Cuvelier, A. Segal, A. A. van Steenhoven, *Finite element methods and Navier-Stokes equations*, Reidel, Amsterdam, 1986.

[3] C. A. J. Fletcher, *Computational techniques for fluid dynamics*, **1**, **2**, Springer, Berlin, 1991.

[4] A. Georgescu, M. Moroianu, I. Oprea, *Bifurcation theory. Principles and applications*, Applied and Industrial Mathematics Series, **1**, University of Piteşti, 1999.

[5] V. Girault, P.-A. Raviart, *Finite element methods for Navier-Stokes Equations. Theory and algorithms*, Springer, Berlin, 1986.

[6] R. Glowinski, *Numerical methods for nonlinear variational problems*, Springer, New York, 1984.

[7] C. Hirsch, *Numerical computation of internal and external flows, Volume 1: Fundamentals of numerical discretization*, John Wiley & Sons, Chichester, 1988.

[8] C. Hirsch, *Numerical computation of internal and external flows, Volume 2: Computational methods for inviscid and viscous flows*, John Wiley & Sons, Chichester, 1990.

[9] T. Hughes, C. Taylor, *Finite element programming of the Navier-Stokes equations*, Pineridge Press, Swansea, U.K., 1981.

[10] H. B. Keller, *Numerical solution of bifurcation eigenvalue problems*, in *Applications in bifurcation theory*, ed. by P. Rabinowitz, Academic, New York, 1977.

[11] H. B. Keller, *Global homotopies and Newton methods*, in *Recent advances in numerical methods*, ed. by C. de Boor, G. H. Golub, Academic, New York, 1978.

[12] R. Peyret, T. D. Taylor, *Computational methods for fluid flow*, Springer, Berlin, 1983.

ROMAI J., **4**, 2(2008), 57–60

ON A SUBCLASS OF ANALYTIC FUNCTIONS DEFINED BY A GENERALIZED SĂLĂGEAN OPERATOR

Adriana Cătaş, Alina Alb Lupaş

Department of Mathematics and Computer Science, University of Oradea

dalb@uoradea.ro, acatas@uoradea.ro

Abstract By means of a generalized Sălăgean differential operator we define a new class $\mathcal{BO}(n,\mu,\alpha,\lambda)$ involving functions $f \in \mathcal{A}$. Parallel results, for some related classes including the class of starlike and convex functions respectively, are obtained too.

Keywords: analytic function, starlike function, convex function, generalized Sălăgean operator.

2000 MSC: 30C45.

1. INTRODUCTION AND DEFINITIONS

Let $\mathcal{A}$ denote the class of functions of the form $f(z) = z + \sum_{j=2}^{\infty} a_j z^j$, which are analytic in the open unit disc $U = \{z : |z| < 1\}$ and $\mathcal{H}(U)$ the space of holomorphic functions in U. Let

$$\mathcal{A}_n = \{f \in \mathcal{H}(U),\ f(z) = z + a_{n+1}z^{n+1} + \ldots,\ z \in U\}$$

with $\mathcal{A}_1 = \mathcal{A}$ and

$$\mathcal{H}[a,n] = \{f \in \mathcal{H}(U),\ f(z) = a + a_n z^n + a_{n+1}z^{n+1} + \ldots,\ z \in U\}$$

for $a \in \mathbb{C}$ and $n \in \mathbb{N}$.

Let $\mathcal{S}$ denote the subclass of functions that are univalent in U.

By $\mathcal{S}^*(\alpha)$ we denote a subclass of $\mathcal{A}$ consisting of starlike univalent functions of order α, $0 \le \alpha < 1$ which satisfies $\mathrm{Re}\left(\frac{zf'(z)}{f(z)}\right) > \alpha$, $z \in U$.

Further, a function f belonging to $\mathcal{S}$ is said to be convex of order α in U, if and only if $\mathrm{Re}\left(\frac{zf''(z)}{f'(z)} + 1\right) > \alpha$, $z \in U$, for some α, $0 \le \alpha < 1$. We denote by

$\mathcal{K}(\alpha)$ the class of functions in $\mathcal{S}$ which are convex of order α in U and denote by $\mathcal{R}(\alpha)$ the class of functions in $\mathcal{A}$ which satisfy $\operatorname{Re} f'(z) > \alpha$, $z \in U$.

It is well-known that $\mathcal{K}(\alpha) \subset \mathcal{S}^*(\alpha) \subset \mathcal{S}$.

If f and g are analytic functions in U, we say that f is subordinate to g, written $f \prec g$, if there is a function w analytic in U, with $w(0) = 0$, $|w(z)| < 1$, for all $z \in U$ such that $f(z) = g(w(z))$ for all $z \in U$. If g is univalent, then $f \prec g$ if and only if $f(0) = g(0)$ and $f(U) \subseteq g(U)$.

Let D^n be a generalized Sălăgean operator introduced by Al-Oboudi in [1], $D^n : \mathcal{A} \to \mathcal{A}$, $n \in \mathbb{N}$, defined as

$$\begin{aligned} D^0 f(z) &= f(z), \\ D^1 f(z) &= (1-\lambda) f(z) + \lambda z f'(z) = D_\lambda f(z), \quad \lambda > 0 \\ D^n f(z) &= D_\lambda(D^{n-1} f(z)), \quad z \in U. \end{aligned}$$

We note that if $f \in \mathcal{A}$, then

$$D^n f(z) = z + \sum_{j=2}^{\infty} [1 + (j-1)\lambda]^n a_j z^j, \quad z \in U.$$

For $\lambda = 1$, we get the Sălăgean operator [5].

In order to prove our main theorem we need the following lemma.

Lemma 1.1. [4]. *Let p be analytic in U with $p(0) = 1$ and suppose that*

$$\operatorname{Re}\left(1 + \frac{zp'(z)}{p(z)}\right) > \frac{3\alpha - 1}{2\alpha}, \quad z \in U.$$

Then $\operatorname{Re} p(z) > \alpha$ *for* $z \in U$ *and* $1/2 \le \alpha < 1$.

2. MAIN RESULTS

Definition 1. *We say that a function $f \in \mathcal{A}$ is in the class $\mathcal{BO}(n, \mu, \alpha, \lambda)$, $n \in \mathbb{N}$, $\mu \ge 0$, $\lambda \ge 0$, $\alpha \in [0, 1)$ if*

$$\left| \frac{D_\lambda^{n+1} f(z)}{z} \left(\frac{z}{D_\lambda^n f(z)} \right)^\mu - 1 \right| < 1 - \alpha, \qquad z \in U.$$

Remark. The family $\mathcal{BO}(n, \mu, \alpha, \lambda)$ is a new comprehensive class of analytic functions which includes various new classes of analytic univalent functions as well as some very well-known ones. For example, $\mathcal{BO}(0, 1, \alpha, 1) \equiv$

$\mathcal{S}^*(\alpha)$, $\mathcal{BO}(1,1,\alpha,1) \equiv \mathcal{K}(\alpha)$ and $\mathcal{BO}(0,0,\alpha,1) \equiv \mathcal{R}(\alpha)$. Another interesting subclasses are the special case $\mathcal{BO}(0,2,\alpha,1) \equiv \mathcal{B}(\alpha)$ which has been introduced in [3], the class $\mathcal{BO}(0,\mu,\alpha,1) \equiv \mathcal{B}(\mu,\alpha)$ introduced in [4] and the class $\mathcal{BO}(n,\mu,\alpha,1)$ introduced and studied in [2].

In this note we provide a sufficient condition for functions to be in the class $\mathcal{BO}(n,\mu,\alpha,\lambda)$. Consequently, as a special case, we show that convex functions of order $1/2$ are also members of the above defined family.

Theorem 2.1. *If for the function $f \in \mathcal{A}$, $n \in \mathbb{N}$, $\mu \geq 0$, $\lambda > 0$, $1/2 \leq \alpha < 1$ we have*

$$\frac{1}{\lambda}\frac{D_\lambda^{n+2}f(z)}{D_\lambda^{n+1}f(z)} - \frac{\mu}{\lambda}\frac{D_\lambda^{n+1}f(z)}{D_\lambda^{n}f(z)} + \frac{\mu-1}{\lambda} + 1 \prec 1 + \beta z, \quad z \in U, \tag{1}$$

where $\beta = \frac{3\alpha-1}{2\alpha}$, then $f \in \mathcal{BO}(n,\mu,\alpha,\lambda)$.

Proof. Consider $p(z) = \frac{D_\lambda^{n+1}f(z)}{z}\left(\frac{z}{D_\lambda^n f(z)}\right)^\mu$. Then $p(z)$ is analytic in U with $p(0) = 1$. A simple differentiation yields

$$\frac{zp'(z)}{p(z)} = \frac{1}{\lambda}\frac{D_\lambda^{n+2}f(z)}{D_\lambda^{n+1}f(z)} - \frac{\mu}{\lambda}\frac{D_\lambda^{n+1}f(z)}{D_\lambda^{n}f(z)} + \frac{\mu-1}{\lambda}.$$

Using (1) we get $\mathrm{Re}\left(1 + \frac{zp'(z)}{p(z)}\right) > \frac{3\alpha-1}{2\alpha}$. Thus, by Lemma 1.1, we deduce that $\mathrm{Re}\left\{\frac{D_\lambda^{n+1}f(z)}{z}\left(\frac{z}{D_\lambda^n f(z)}\right)^\mu\right\} > \alpha$. Therefore, $f \in \mathcal{BO}(n,\mu,\alpha,\lambda)$, by Definition 1. ∎

As consequences of the above theorem we have the following corollaries.

Corollary 1. *If $f \in \mathcal{A}$ and $\mathrm{Re}\left\{\frac{2zf''(z)+z^2f'''(z)}{f'(z)+zf''(z)} - \frac{zf''(z)}{f'(z)}\right\} > -\frac{1}{2}$, $z \in U$, then $f \in \mathcal{BO}(1,1,1/2,1)$, hence $\mathrm{Re}\left\{1 + \frac{zf''(z)}{f'(z)}\right\} > \frac{1}{2}$, $z \in U$. That is, f is convex of order $\frac{1}{2}$.*

Corollary 2. *If $f \in \mathcal{A}$ and $\mathrm{Re}\left\{1 + \frac{zf''(z)}{f'(z)}\right\} > \frac{1}{2}$, $z \in U$ then $\mathrm{Re}\, f'(z) > \frac{1}{2}$, $z \in U$. In other words, if the function f is convex of order $\frac{1}{2}$, then $f \in \mathcal{BO}(0,0,\frac{1}{2},1) \equiv \mathcal{R}\left(\frac{1}{2}\right)$.*

Corollary 3. *If $f \in \mathcal{A}$ and $\mathrm{Re}\left\{\frac{f(z)+3zf'(z)+z^2f''(z)}{f'(z)+zf'(z)} - \frac{zf'(z)}{f'(z)}\right\} > \frac{1}{2}$, $z \in U$, then $\mathrm{Re}\left\{\frac{zf'(z)}{f(z)}\right\} > 0$, $\quad z \in U$. That is, f is a starlike function.*

Corollary 4. *If $f \in \mathcal{A}$ and $\mathrm{Re}\left\{\frac{-f(z)+5zf'(z)+z^2f''(z)}{f(z)+zf(z)}\right\} > -\frac{1}{2}$, $z \in U$, then $\mathrm{Re}\left\{\frac{f(z)}{z} + f'(z) - 2\right\} > 2$, $z \in U$.*

References

[1] F. M. Al-Oboudi, *On univalent functions defined by generalized Sălăgean operator*, Internat. J. Math. and Math. Sci., **27**(2004), 1429-1436.

[2] A. Cătaş, A.Alb Lupaş, *On a subclass of analytic functions defined by differential Sălăgean operator*, (to appear).

[3] B. A. Frasin, M. Darus, *On certain analytic univalent functions*, Internat. J. Math. and Math. Sci., **25**(5)(2001), 305-310.

[4] B. A. Frasin, J. M. Jahangiri, *A new and comprehensive class of analytic functions*, Analele Universităţii din Oradea, **XV**, 2008.

[5] G. St. Sălăgean, *Subclasses of univalent functions*, Lecture Notes in Math., Springer, Berlin, **1013**(1983), 362-372.

ROMAI J., **4**, 2(2008), 61–72

THE SIMILARITY OF XML-BASED DOCUMENTS IN FINDING THE LEGAL INFORMATION

Sorina Cornoiu

Legislative Council, Bucharest

sorina_c_2000@yahoo.com

Abstract In this paper, we propose to integrate semantic similarity assessment in an edit distance algorithm, seeking to amend similarity judgments when comparing XML-based legal documents[3].

Keywords: information retrieval, XML, semantic, legal information.

2000 MSC: 68P20, 05C05, 03D55, 68Q55.

1. INTRODUCTION

In the legal information retrieval systems, the information is usually searched by means of a full text search, every term in the texts of the documents can function as a search key [4].

In the past few years, XML has been established as an effective mean for information management, and has been widely exploited for complex data representation[1]. We propose developing efficient techniques for comparing XML-based legal documents to become essential in information retrieval (IR) research, integrating IR semantic similarity assessment in an edit distance algorithm, seeking to amend similarity judgments when comparing XML-based legal documents. Our approach consists of an original edit distance operation cost model, introducing semantic relatedness of XML element/attribute labels, in traditional edit distance computations[1].

In recent years, W3C's XML (eXtensible Mark-up Language) has been accepted as a major mean for efficient data management and exchange. The use of XML ranges over information formatting and storage, database information interchange, data filtering, as well as web services interaction. Due to the ever-increasing web exploitation of XML, an efficient approach to compare XML-based legal documents becomes crucial in information retrieval [3]. Legal documents play an important role in all activities related to the legal domain. In particular they represent an efficient human communication mean to transmit legal knowledge. Legislations are often complex and prone to change. Organizations that base their daily work on a set of legal documents have to deal with a massive amount of legal and numerous legal updates[7]. Legal documents typically combine structured and unstructured information. The structured information is increasingly tagged with markup languages such as XML (Extensible Markup Language) [6] . A range of algorithms for comparing semi-structured data, e.g. XML documents, have been proposed in the literature. All of these approaches focus exclusively on the structure of documents, ignoring the semantics involved. However, in the legal information retrieval systems, estimating semantic similarity between legal documents is of key importance to improving search results[1].

Semantic similarity IR for legal information, incited us to expand existing XML structural similarity so as to take into account semantic relatedness while comparing XML documents [1].

2. BACKGROUND

2.1. LEGAL XML DATA MODEL

Legal documents typically combine structured and unstructured information, the former, for instance, referring to common document architectures, reference structures and metadata information the latter involving the natural language texts. The structured information is increasingly tagged with markup languages such as XML [6].

XML documents represent a hierarchically structured information and can be modeled as Ordered Labeled Trees (OLTs). Nodes in a traditional DOM (Document Object Model) ordered labeled tree represent document elements and are labeled with corresponding element tag names. Element attributes mark the nodes of their containing elements [1].

The Community Official Journal texts, which constitute our working base, consist of many types of texts grouped in two main categories: legislation, information and notices. In this paper, we focus on regulations, directives, decisions and recommendations regardless of their category [5]. Legislative documents have a hierarchical structure in which elements with detailed content are nested in larger elements[1]. In [4] we can find recommendations and legislative techniques for structuring the document.

Community acts are generally drafted according to a standard structure (fig. 1):

Fig. 1. Basic structure of legislative acts

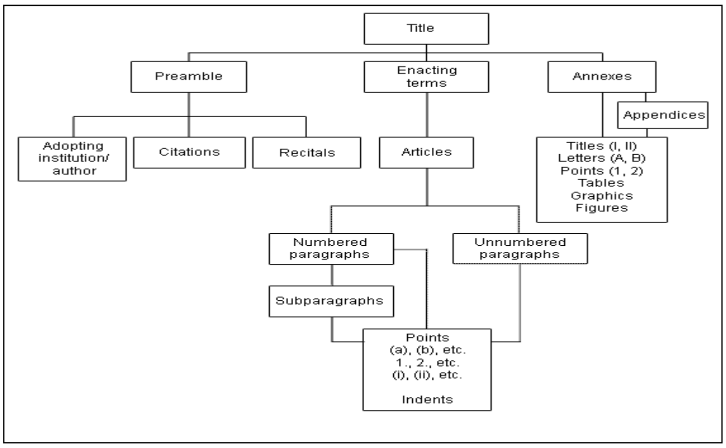

1. the "Title" comprises all the information in the heading of the act which serves to identify it. It may be followed by certain technical data (reference to the authentic language version, relevance for the EEA, serial number) which are inserted, where appropriate, between the title proper and the preamble [4];
2. "preamble" means everything between the title and the enacting terms of the act, namely the citations, the recitals and the solemn forms which precede and follow them [4]. Citations: at the beginning of the preamble, they indicate the legal basis of the act, the proposals, recommendations, initiatives, drafts... that must be obtained, and certain opinions and other non-mandatory pro-

cedural steps. Citations are generally introduced by the dedicated expression 'Having regard to" or "Acting in accordance with" [5]. Recitals: are the parts of the act containing the statement of reasons for the act; they are placed between the citations and the enacting terms. Recitals are introduced by the word "Whereas : " and continue with numbered points comprising one or more complete sentences [5];

3. the "enacting terms" are the legislative part of the act. They are composed of articles, which may be grouped in titles, chapters and sections, and may be accompanied by annexes [5].

4. annex: "where necessary annex" and is spread out until the end of document. In case where many annexes are necessary, each annex has a heading like the one cited above and is numbered [5].

2.2. XML STRUCTURAL SIMILARITY

An XML document can be modeled as an ordered labeled tree, each node in the tree corresponding to an element in the document and is labeled with the element tag name. Let us consider the following XML documents (fig. 2).

Fig. 2. Example of XML documents

```
<act>
  < element>
    <article>
      <title></tile>
      <paragraph></paragraph>
    </article>
  </element>
</act>
```

Tree A

```
<document>
  <element>
    <article>
        <section></section>
    </article>
  </element>
</document>
```

Tree B

```
<legal_document>
  <element>
    <article>
        <chapter></chapter>
    </article>
  </element>
</legal_document>
```

Tree C

Using traditional edit distance computations, the same structural similarity value is obtained when document A is compared to documents B and C. However, despite having similar structural characteristics, one can obviously recognize that sample document A shares more semantic characteristics with document B than with C. For example, in fig. 2 pairs act-document and paragraph-section, from documents A and B, are semantically similar while paragraph-chapter, from documents A and C, are semantically different [3]. For this reason we integrate semantic similarity assessment in a structured XML similarity approach, in order to provide an improved XML similarity measure for comparing heterogeneous XML documents [1].

In order to determine structural similarities between hierarchically structured data, particularly XML documents, we can use various methods : Tree Edit Distance (TED) Similarity, Tag Similarity, Fourier Transform Similarity Metric.

Several authors have provided algorithms for computing the optimal edit distance between two trees. In general, the edit distance measures the minimum number of node insertions, deletions, and updates required to convert one tree into another [2]

$$TED(D_i, D_j) = \frac{editDist(D_i, D_j)}{max(|N_i|, |N_j|)}, \tag{1}$$

where : N_i is the set of nodes in the tree representation of document D_i and N_j is the set of nodes in the tree representation of document D_j. Chawathe restricts insertion and deletion operations to leaf nodes, and changes to trees using three basic tree edit operations : insertion of leaf nodes - Ins(x, i, p, λ(x)) , deletion of leaf nodes - Del(x, p) , update internal/leaf nodes - Upd(x, y) [3] . By associating costs with each edit operation, Chawathe defines the cost of an edit script (sequence of edit operations) to be the sum of the costs of its component operations [1]. Similarity measures based on edit (or metric) distance are generally computed as [3]

$$sim(A, B) = \frac{1}{1 + dist(A, B)}. \tag{2}$$

We can to find the cheapest sequence of edit operations that can transform one tree into another.

Chawathe employed the ld-pair representation of a tree node. It is defined as the pair (l, d) where: l and d are the node label and depth in the tree [3], respectively. We use p.l and p.d to refer to the label and the depth of an ld-pair p respectively. For example, we have the following representation for the tree A :

A=((act,0),(enact,1),(article,2),(title,3),(paragraph,3))

We can assign identical costs to insertion and deletion operations (CostIns = CostDel = 1), as well as to update operations only when the newly assigned label is different from the node current label (CostUpd(a ,b) = 1 when a.l $\neq$ b.l, otherwise, when the labels are the same, CostUpd = 0, underlining that no changes are to be made to the label of node a).

Applying Chawathe's approach we obtain

Edit script= Upd (A[1],B[1]) , Upd (A[4],B[4]) , Del (A[5],A[3])

Dist(A,B)=Dist(A,C)=3.

Using (2) , we obtain : Sim(A, B) = Sim(A, C) = 0.25.

The corresponding edit distance computations are shown in Table 1. The minimum-cost ES contribution to the edit distance computation process is emphasized in bold format.

Table 1 Computing minimum edit distance for XML trees A and B

	0	B[1]/(document,0)	B[2]/(element,1)	B[3]/(article,2)	B[4]/(section,3)
0	0	1	2	3	4
A[1](act,0)	1	1	2	3	4
A[2](element,1)	2	2	1	2	3
A[3](article,2)	3	3	2	1	2
A[4](title,3)	4	4	3	2	2
A[5](paragraph,3)	5	5	4	3	3

Intuitive cost models do not affect the correctness of Chawathe's structural similarity algorithm. However, they fail to capture the semantics of XML documents. we propose to complement the structure-based similarity algorithm, with a cost model integrating semantic assessment (semantic similarity) in the comparison process [1].

So far we spoke about how we can enhance existing XML comparison approaches in order to take into consideration both structural and semantic characteristics of XML documents.

3. INTEGRATED SEMANTIC AND STRUCTURE BASED SIMILARITY

In order to take into account semantic meaning while comparing XML documents, we propose to complement Chawathe's edit distance algorithm with the following semantic cost model (SCM)

$$Cost_{Op}(x, y) = Cost_{SemOp}(x, y) \times Cost_{DepthOp}(x) \in [0, 1] \tag{3}$$

where Op designates an insertion, deletion or update operation, Cost_{SemOp}(x, y) is the label semantic similarity cost and represents the operation costs according to the semantic of concerned nodes, $\text{Cost}_{DepthOp}$(x) represents the node depth.
In our case, using (3) we have

Cost_{Op}(A,B)= Cost_{SemOp}(A,B) $\times$ $\text{Cost}_{DepthOp}$(A)

3.1. LABEL SEMANTIC SIMILARITY COST

The label semantic similarity cost Cost_{SemOp}(x, y) represents the operation costs according to the semantic of the concerned nodes

$$Cost_{SemOp}(x, y) = 1 - Sim_{SemOp}(x.l, y.l) \tag{4}$$

where Sim_{SemOp}(x.l, y.l) represents the label semantic similarity that use Lin's semantic similarity measure.

For calculate Lin's measure WordNet-based semantic similarity. The WordNet (WordNet Search - 3.0) is a lexical database that provides a combination between the traditional lexicographical information and modern computing. WordNet contains more than 118000 different word forms and more than 90000 different word senses and include synonymy (same-name) , antonymy (opposite-name), hyponymy (sub-name), hypernymy (super-name), meronymy (part-name) and holonymy (whole-name) relations. The lexical database WordNet is particularly suited for similarity measures, since it organizes nouns and verbs into hierarchies of "is-a" relations. Using the CPAN(Comprehensive Perl Archive Network) module, we are able to measure the semantic similarities between words by use of algorithms. There will be used the Lin's algorithm that is based on the information content of the least common subsumer (LCS) of concepts A and B. Information content is a measure of the specificity of a concept, and the LCS of concepts A and B is the most specific concept that is an ancestor of both A and B. The Lin measure augments the information content of the LCS with the sum of the information content of concepts A and B themselves. The Lin measure scales the information content of the LCS by this sum [8].

Following Lin, the semantic similarity between two words (expressions) can be computed as

$$Sim_{Sem}(w1, w2) = Sim_{Sem}(c1, c2) = \frac{2logp(c_0)}{logp(c_1) + logp(c_2)} \tag{5}$$

where:
- c1 and c2 are concepts, in a knowledge base of hierarchical structure (taxonomy), subsuming words w1 and w2 respectively;
- c0 is the most specific common ancestor of concepts c1 and c2;
- p(c) denotes the occurrence probability of words corresponding to concept c. It can be computed as the relative frequency: p(c) = freq(c) / N, freq(c) = Σcount(w) and N: total number of words in the corpus.

We can have the following three situations:

$$update : Cost_{SemUpd}(x, y) = 1 - Sim_{Sem}(x.l, y.l) \tag{6}$$

where x is an node from an XML document and x.l is the node label x, y is an node from an XML document and y.l is the node label y.

When labels are identical, the semantic similarity is of maximum value, Sim_{Sem}(x.l, y.l) = 1, yielding Cost_{Upd}(x, y) = 0 (no changes to be made). When labels are completely different, the semantic similarity is of minimum value, Sim_{Sem}(x.l, y.l) = 0, which brings us to Cost_{Upd}(x, y) = 1 [3];

$$insert : Cost_{SemIns}(x, i, p, \lambda(x)) = 1 - Sim_{Sem}(\lambda(x), p.l) \tag{7}$$

$$delete : Cost_{SemDel}(x, p) = 1 - Sim_{Sem}(x.l, p.l). \tag{8}$$

In order to insert deletion operation, when labels are identical or completely different, insertion/deletion costs would be equal to 0 or 1 [3].

3.2. NODE DEPTH COST

Information becomes increasingly specific as one descends in the XML tree hierarchy. For example, consider the XML sample tree A in fig. 2. Editing node A[1] (A[1].l = act) by changing its label to "book", would semantically affect tree A a lot more than deleting node A[4] (A[4].l = title), changing A's whole semantic context. Therefore, it would be relevant to vary operation costs following node depths, assuming that operations near the root node have higher impact than operations further down the hierarchy. The following formula, adapted from, could be used for that matter [1]

$$Cost_{DepthOp}(x) = \frac{1}{1 + x.d} \in [0, 1] \tag{9}$$

where Op is an insert, delete or update operation, x.d is the depth of node considered for insertion, deletion or updating.
Editing the root node of a document tree involves $\text{Cost}_{DepthOp}$(root) = 1.

3.3. SEMANTIC COST MODEL(SCM)

In order to enrich formula (2) with semantic meaning, we propose the following cost model [1]

$$Cost_{Op}(x, y) = Cost_{SemOp} \times Cost_{Depth}(x) \tag{10}$$

where Op designates an insertion, updating or deletion operation. In this case we have

$$sim(A, B) = \frac{1}{1 + distSCM(A, B)}. \tag{11}$$

First we must obtain word semantic similarities, computed by following Lin's measure (Table 2).

Table 2 Word semantic similarities, computed by following Lin's measure.

Word pairs		SimLin	Wordpairs		SimLin
act	document	0.8391	article	chapter	0.3693
act	legal_document	0.8746	title	paragraph	0.5029
act	element	0.1067	title	section	06028
act	article	0.3768	title	chapter	0.5642
act	title	0.5758	title	document	0.6637
act	paragraph	0.5229	title	legal_document	0.6444
act	section	0.6316	paragraph	document	0.5944
act	chapter	0.5895	paragraph	section	0.5451
element	document	0.1252	paragraph	legal_document	0.5789
element	legal_document	0.1211	paragraph	chapter	0.5134
element	article	0.1017	chapter	legal_document	0.6616
element	section	0.1123	chapter	document	0.682
element	chapter	0.1043	section	legal_document	0.7152
element	title	0.1017	document	legal_document	0.9637
element	paragraph	0.0918	document	section	0.7391
article	legal_document	0.4218	document	article	0.4344
article	title	0.3611	article	section	0.3945
article	paragraph	0.3292			

The results attained by applying the semantic cost model to compare sample XML documents A, B and C are shown in Tables 3 and 4.

For example, $\mathrm{Dist}_{SCM(A[1],B[1])}$= (1-SimLin(A[1], B[1])) = 1-0.8391=0.1609.

Table 3 Computing minimum edit distance for XML trees A and B; $\mathrm{dist}_{SCM(A,B)}$=0.1014.

	B[1]/(document,0)	B[2]/(element,1)	B[3]/(article,2)	B[4]/(section,3)
A[1](act,0)	0.1609	0.8933	0.6232	0.3684
A[2](element,1)	0.4374	0.1609	04491	0.4438
A[3](article,2)	0.1885	0.2994	0.1609	0.2018
A[4](title,3)	0.0840	0.2245	0.1597	0.0993
A[5](paragraph,3)	0.1014	0.2270	0.1677	0.1137

Table 4 Computing minimum edit distance for XML trees A and C; $\mathrm{dist}_{SCM(A,C)}$=0.1254.

	C[1]/(legal_document,0)	C[2]/(element,1)	C[3]/(article,2)	C[4]/(chapter,3)
A[1](act,0)	0.1254	0.8933	0.6232	0.4105
A[2](element,1)	0.4374	0.1254	04491	0.4438
A[3](article,2)	0.1927	0.2994	0.1254	0.2102
A[4](title,3)	0.0889	0.2245	0.1597	0.1089
A[5](paragraph,3)	0.1052	0.2270	0.1677	0.1216

By using (11), we obtain: Sim $_{SCM(A,B)}$ = 1/(1+0.1014)= 0.907 and Sim $_{SCM(A,C)}$ = 1/(1+0.1254)= 0.888.

Considering semantic relatedness, in the comparison process, reflects the fact that sample documents A and B are more similar than A and C (SimSCM(A, B) > SimSCM(A,C)), in spite of sharing identical structural similarities [3]. In order to compare XML legal documents we use a structure-based (edit distance) similarity algorithm, which seems to capture semantic meaning effectively.

4. CONCLUSION

The database community has proposed several languages for quering XML, such as XML-QL, XQuery, XQL. These language are based on exact matching and do not support ranked queries. For this reason we propose using semantic cost model which takes in consideration both structural and semantic characteristics of XML legal documents.

References

[1] J. Tekli, R. Chbeir, K. Yétongnon, *A hybrid approach for XML similarity*, 33rd International Conference on Current Trends in Theory and Practice of Computer Science (SOFSEM)pringer Verlag Incs, Harrachov, Czech Republic, January 2007, 783-795.

[2] D. Buttler, *A short survey of document structure similarity algorithms*, The 5th International Conference on Internet Computing, Las Vegas, NV, United States, June 21, 2004.

[3] J. Tekli, R. Chbeir, K. Yétongnon, *Semantic and Structure Based XML Similarity-AnIntegratedApproach*, 13th International Conference on Management of Data (COMAD'06), Delhi, India, December 2006.

[4] *Joint practical guide for the drafting of community legislation*, http://reterei.eu/rete/GPC_en.pdf.

[5] F. Fady, R. Rousselot, *DARES: Documents annotation and recombining system-Application to the European law*, Artificial Intelligence and Law, Springer, **15**,(2)(2007), 83-102.

[6] M.F. Moens, *Retrieval of legal documents: combining structured and unstructured information*, Proceedings ELPUB2005 Conference on Electronic Publishing, Kath. Univ. Leuven, June 2005.

[7] O. Vasutiu, D. Jouve, Y. Amghar, J.M. Pinon, *XML based legal document drafting information system*, Standards for Legislative XML Workshop, Amsterdam, December 15, 2007.

[8] T. Pedersen, J. Michelizzi , *Wordnet: Similarity - measuring the relatedness of concepts*, Proceedings of the Nineteenth National Conference on Artificial Intelligence (AAAI-04), 2004.

ROMAI J., **4**, 2(2008), 73–80

APPROXIMATE LIMIT CYCLES FOR THE RAYLEIGH MODEL

Adelina Georgescu, Petre Băzăvan, Mihaela Sterpu

Academy of Romanian Scientists, Bucharest

Department of Mathematics and Computer Science, University of Craiova

Department of Mathematics and Computer Science, University of Craiova

adelinageorgescu@yahoo.com, bazavan@yahoo.com, mihaelas@central.ucv.ro

Abstract By using asymptotic methods the approximate limit cycle of the periodically forced Rayleigh oscillator is deduced for $g \ll 1$, where g is the amplitude of the forcing. The limiting limit cycle as $g \to 0$ is also constructed. The theoretical results agree with the numerical ones deduced by means of one of the authors (P. B.) method.

Keywords: Rayleigh equation, limit cycle, asymptotic approximation.

2000 MSC: 34C05, 41A60.

1. THE RAYLEIGH MODEL

By the Rayleigh model we mean the Cauchy problem

$$x(0) = x_0, \quad \dot{x}\,(0) = y_0, \tag{1}$$

for the (generalized) Rayleigh equation

$$\varepsilon\,\ddot{x} + \frac{1}{3}\,\dot{x}^3 - \dot{x} + ax = g \sin \omega t \tag{2}$$

where $x : \mathbb{R} \to \mathbb{R}$, $x = x\,(t)$, is the unknown (state) function, t is the time, ε, a, g and ω are positive parameters and the dot over quantities stands for the differentiation with respect to time. The generalized Rayleigh equation without forcing ($g = 0$) reads

$$\ddot{x} + \frac{1}{3}\dot{x}^3 - \dot{x} + x = 0. \tag{3}$$

For $\varepsilon = a = 1$, the equation (3) becomes the equation introduced by Rayleigh in 1883 to study the oscillations of the violin chords. The dynamics generated by it is closed to the dynamics generated by the Van der Pol equation

$$\ddot{x} + (x^2 - 1)\dot{x} + x = 0. \tag{4}$$

Indeed, by differentiating the original Rayleigh equation with respect to time and by using the notation $\dot{x} = y$, we obtain just the Van der Pol equation.

In its form (2) the Rayleigh equation was introduced in 1979 by Diener in order to study the duck (French canard) phenomenon [6], [7]. Subsequently, it was found that, for certain values of the parameters, the dynamics generated by (2) can be very complicated, presenting cascades of bifurcations and chaotic regions. In addition, the model (1), (2), as well as the van der Pol model, was applied to electronics and physiology in a series of papers, e.g. [1], [2], [5], [8], [11], [12], [13], [15], [16], [17]. Especially it was investigated numerically and theoretically the existence and uniqueness of limit cycles corresponding to periodic oscillations, the attractors the most important for applications.

In this paper, by using asymptotic methods, [9], [10], we extended the studies from [15], [16] concerning the construction of approximate limit cycles for the Rayleigh model with or without forcing. We neglected the higher harmonics as suggested in [14].

The equation (2) was transformed into the following system of two nonautonomous ordinary differential equations (ODEs)

$$\begin{cases} \dot{x} = y, \\ \dot{y} = -\frac{a}{\varepsilon}x + \frac{1}{\varepsilon}\left(y - \frac{1}{3}y^3\right) + \frac{g}{\varepsilon}\sin\omega t, \end{cases} \tag{5}$$

or to the following system of three autonomous ODEs in $\mathbb{R}^3$

$$\begin{cases} \dot{x} = y, \\ \dot{y} = -\frac{a}{\varepsilon}x + \frac{1}{\varepsilon}\left(y - \frac{1}{3}y^3\right) + \frac{g}{\varepsilon}\cdot\sin z, \\ \dot{z} = \omega. \end{cases} \tag{6}$$

First we used the first order asymptotic approximation of (5) as $g \to 0$ to derive the so-called averaged system associated with (5)

$$\begin{cases} \dot{x}= y, \\ \dot{y}= \frac{1}{\varepsilon}\left(-ax + y - \frac{1}{3}y^3\right), \end{cases} \tag{7}$$

which coincides with the system (5) without forcing.

With system (7) a two-dimensional dynamical system is associated while the dynamics generated by (5) or (6) is three-dimensional.

In [16], it is proved that the system (7) without forcing possesses a limit cycle passing through the point $\left(0, -\sqrt{3}\right)$. In Section 2 we derive an asymptotic approximation of the limit cycle of (5) and in Section 3 we give comparative graphical representations of the exact or approximate limit cycle.

2. APPROXIMATE LIMIT CYCLE

The unique limit cycle of (7) passing through $\left(0, -\sqrt{3}\right)$ represents an approximate limit cycle for (5). Another approximation corresponds to limit cycles of the form

$$\begin{cases} x\,(t) = \gamma(t) + \alpha(t)\cos\omega t + \beta(t)\sin\omega t, \\ y(t) = \dot{\gamma}(t) + [\dot{\alpha}(t) + \omega\beta(t)]\cos\omega t + \left[\dot{\beta}(t) - \omega\alpha(t)\right]\sin\omega t. \end{cases} \tag{8}$$

Introducing (8) into (5), neglecting the higher harmonics (e.g. $\cos^2\omega t = \frac{\cos 2\omega t + 1}{2} \sim \frac{1}{2}$) and the derivatives $\ddot{\alpha}$ and $\ddot{\beta}$ and using the notation $\dot{\gamma} = \delta$, we obtain

$$\begin{cases} \dot{\gamma} = \delta, \\ \varepsilon\dot{\delta} + \frac{1}{3}\delta^3 + \delta\left[\frac{1}{2}A - 1\right] + a\gamma = 0, \\ \varepsilon\omega(2\dot{\beta} - \omega\alpha) + (\dot{\alpha} + \omega\beta)\left[\frac{1}{4}A + (\dot{\gamma}^2 - 1)\right] + a\alpha = 0, \\ -\varepsilon\omega(2\dot{\alpha} + \omega\beta) + (\dot{\beta} - \omega\alpha)\left[\frac{1}{4}A + (\dot{\gamma}^2 - 1)\right] + a\beta - g = 0, \end{cases} \tag{9}$$

where $A = (\dot{\alpha} + \omega\beta)^2 + (\dot{\beta} - \omega\alpha)^2$.

The equilibria of (9) correspond to periodic solutions of period $\frac{2\pi}{\omega}$ of (5), hence to the limit cycles of the associated dynamical system. These equilibria satisfy the algebraic system

$$\begin{cases} \delta = 0, \\ \gamma = 0, \\ \left(a - \varepsilon\omega^2\right)\alpha + \omega\left[\frac{1}{4}\omega^2\left(\alpha^2 + \beta^2\right) - 1\right]\beta = 0, \\ -\omega\left[\frac{1}{4}\omega^2\left(\alpha^2 + \beta^2\right) - 1\right]\alpha + \left(a - \varepsilon\omega^2\right)\beta = g, \end{cases} \tag{10}$$

which has the solution $(\alpha, \beta, \gamma, \delta) = (\alpha, \beta, 0, 0)$. Since $\gamma = 0$, $\dot{\gamma} = 0$, (8) becomes

$$\begin{cases} x(t) = \alpha \cos \omega t + \beta \sin \omega t, \\ y(t) = \beta \omega \cos \omega t - \alpha \omega \sin \omega t, \end{cases} \tag{11}$$

where, with the notation $r^2 = \alpha^2 + \beta^2$, from (10) we deduced $\alpha = \frac{1}{\Delta} \omega g \left(1 - \frac{\omega^2 r^2}{4}\right)$, $\beta = \frac{1}{\Delta} g \left(a - \varepsilon \omega^2\right)$, $\Delta = \left(a - \varepsilon \omega^2\right)^2 + \omega^2 \left[1 - \frac{1}{4} \omega^2 r^2\right]^2$ and r is a real solution of equation

$$r^2 \left[\left(a - \varepsilon \omega^2\right)^2 + \omega^2 \left(1 - \frac{1}{4} \omega^2 r^2\right)^2\right] = g^2, \tag{12}$$

or, equivalently,

$$r^2 \Delta = g^2. \tag{13}$$

The equation (12) was deduced from $(10)_3^2 + (10)_4^2 = 0$.

Case $g = 0$. In this case (12) implies

$$\omega^2 r^2 = 4, \quad \omega^2 \varepsilon = a \tag{14}$$

i.e.

$$\omega = \sqrt{\frac{a}{\varepsilon}}, \quad r = 2\sqrt{\frac{\varepsilon}{a}}. \tag{15}$$

From (11) we have

$$\alpha = x(0), \quad \beta = \frac{y(0)}{\omega}, \tag{16}$$

and this relation holds also for the case $g > 0$. In addition, we have

$$x^2(0) + \frac{y^2(0)}{\omega^2} = r^2. \tag{17}$$

The simplest approximate form for the ellipse (11) corresponds to $\beta = 0$ and, hence, $\alpha = r = 2\sqrt{\frac{\varepsilon}{a}}$ and it is

$$\begin{cases} x(t) = 2\sqrt{\frac{\varepsilon}{a}} \cos \sqrt{\frac{a}{\varepsilon}} t, \\ y(t) = -2 \sin \sqrt{\frac{a}{\varepsilon}} t, \end{cases} \tag{18}$$

This is the only approximate limit cycle considered in [16]. It passes through the point $\left(2\sqrt{\frac{a}{\varepsilon}}, 0\right)$. However, we do not know a priori if this point belongs or not to the approximate limit cycle. In fact, the ellipse through $\left(2\sqrt{\frac{a}{\varepsilon}}, 0\right)$ is only one among the infinity of ellipses of the form

$$\begin{cases} x(t) = x(0) \cos \sqrt{\frac{a}{\varepsilon}} t + \frac{y(0)}{\omega} \sin \sqrt{\frac{a}{\varepsilon}} t, \\ y(t) = y(0) \cos \sqrt{\frac{a}{\varepsilon}} t - \omega x(0) \sin \sqrt{\frac{a}{\varepsilon}} t, \end{cases} \tag{19}$$

where $x(0)$ and $y(0)$ satisfy (17). From this set we must choose the approximate limit cycle.

The philosophy under our choice is: the approximate limit cycle from the case $g = 0$ is that which is equal to the limit cycle from the case $g > 0$ as $g \to 0$.

Case $g > 0$**.** In order to deduce the limiting limit cycle (11) as $g \to 0$ we must derive asymptotic expansions for α, β, r, ω and Δ as $g \to 0$. The main idea, suggested by (14), is

$$\varepsilon\omega^2 \sim a + a_0 g + a_1 g^2 + ..., \quad \omega^2 r^2 - 4 \sim 4r_0^2 g + 4r_1^2 g^2 + ..., \quad as \quad g \to 0. \tag{20}$$

The expansion $(20)_1$ shows that $\omega = O(1)$ as $g \to 0$ and $(20)_2$ implies that $r = O(1)$ as $g \to 0$ too. From (20) we have as $g \to 0$

$$\begin{aligned}
&\omega^2 \sim \tfrac{a}{\varepsilon} + \tfrac{a_0}{\varepsilon} g + \tfrac{a_1}{\varepsilon} g^2 + ..., \quad \omega \sim \sqrt{\tfrac{a}{\varepsilon}} \left(1 + \tfrac{a_0}{2a} g + ...\right), \\
&\tfrac{1}{\omega^2} \sim \sqrt{\tfrac{a}{\varepsilon}} \left(1 - \tfrac{a_0}{a} g + ...\right), \\
&r^2 \sim \left(4 + 4r_0^2 g + ...\right) \tfrac{\varepsilon}{a} \left(1 - \tfrac{a_0}{a} g + ...\right) \sim \tfrac{4\varepsilon}{a} \left[1 + g\left(r_0^2 - \tfrac{a_0}{a}\right)\right] + ... \\
&\Delta \sim g^2 \left[a_0^2 + 2a_0 a_1 g + \left(\tfrac{a}{\varepsilon} + \tfrac{a_0}{\varepsilon} g\right)\left(r_0^4 + 2r_0^2 r_1^2 g\right)\right] + ... \\
&\quad \sim g^2 \left[a_0^2 + r_0^4 \tfrac{a}{\varepsilon} + g\left(r_0^4 \tfrac{a}{\varepsilon} + 2r_0^2 r_1^2 \tfrac{a}{\varepsilon} + 2a_0 a_1\right)\right] + ...
\end{aligned} \tag{21}$$

Introducing (20) into (12) and taking into account (21) it follows that, up to terms of order g, we have $\frac{4}{\omega^2}\left(1 + r_0^2 g\right)\Delta \sim g^2$, i.e.

$$4\left(1 + r_0^2 g\right)\frac{\varepsilon}{a}\left(1 - \frac{a_0}{a} g\right) g^2 \left[a_0^2 + r_0^4 \frac{a}{\varepsilon} + g\left(r_0^4 \frac{a}{\varepsilon} + 2r_0^2 r_1^2 \frac{a}{\varepsilon} + 2a_0 a_1\right)\right] + ... \sim g^2$$

or, equivalently,

$$\frac{4\varepsilon}{a}\left(a_0^2 + r_0^4 \frac{a}{\varepsilon}\right) + \frac{4\varepsilon}{a} g \left[\left(a_0^2 + r_0^4 \frac{a}{\varepsilon}\right)\left(r_0^2 - \frac{a_0}{a}\right) + r_0^4 \frac{a}{\varepsilon} + 2r_0^2 r_1^2 \frac{a}{\varepsilon} + 2a_0 a_1\right] + ... \sim 1. \tag{22}$$

After the matching, from (22) we obtain

$$\frac{4\varepsilon}{a}\left(a_0^2 + r_0^4 \frac{a}{\varepsilon}\right) = 1, \tag{23}$$

$$\left(a_0^2 + r_0^4 \frac{a}{\varepsilon}\right)\left(r_0^2 - \frac{a_0}{a}\right) + r_0^4 \frac{a_0}{\varepsilon} + 2r_0^2 r_1^2 \frac{a}{\varepsilon} + 2a_0 a_1 = 0. \tag{24}$$

On the other hand, taking into account (23), (24) and the above quoted expansions for α and β we have, up to terms in g, as $g \to 0$,

$$\alpha \sim -\frac{1}{a_0^2 + r_0^4 \frac{a}{\varepsilon}} \sqrt{\frac{a}{\varepsilon}} \left(1 + \frac{a_0}{2a} g\right)\left(r_0^2 + r_1^2 g\right)\left[1 + g\left(r_0^2 - \frac{a_0}{a}\right)\right] \tag{25}$$

$$\sim -4\sqrt{\frac{\varepsilon}{a}}\left[r_0^2+g\left(r_0^4-\frac{a_0}{2a}r_0^2+r_1^2\right)\right],$$

$$\beta \sim -\frac{1}{a_0^2+r_0^4\frac{a}{\varepsilon}}\left(a_0+a_1 g\right)\left[1+g\left(r_0^2-\frac{a_0}{a}\right)\right] \tag{26}$$

$$\sim -\frac{4\varepsilon}{a}\left[a_0+g\left(a_1+a_0 r_0^2-\frac{a_0^2}{a}\right)\right].$$

Taking into account the initial conditions (16), then (25) and (26) yield

$$x(0)=-4\sqrt{\frac{\varepsilon}{a}}r_0^2 \tag{27}$$

$$r_0^4-r_0^2\frac{a_0}{2a}+r_1^2=0, \tag{28}$$

$$\frac{y\left(0\right)}{\omega}=-\frac{4\varepsilon}{a}a_0, \tag{29}$$

$$a_1+a_0 r_0^2-\frac{a_0^2}{a}=0. \tag{30}$$

The unique solution of (23), (24), (28) and (30) reads

$$a_0^2=\frac{a^2}{4\left(a\varepsilon+1\right)},\quad a_1=0,\quad r_0^2=\frac{1}{2\sqrt{a\varepsilon+1}},\quad r_1^2=-\frac{1}{8\left(a\varepsilon+1\right)}, \tag{31}$$

Numerical computations revealed that the appropriate route for a_0 is $a_0 = -\frac{a}{2\sqrt{a\varepsilon+1}}$. Then

$$\alpha=-\frac{2\sqrt{\varepsilon/a}}{\sqrt{a\varepsilon+1}},\quad \beta=-\frac{2\varepsilon}{\sqrt{a\varepsilon+1}},\quad \omega\sim\sqrt{\frac{a}{\varepsilon}}-\frac{\sqrt{a/\varepsilon}}{4\sqrt{a\varepsilon+1}}g \tag{32}$$

and to the approximate limit cycle for $g \ll 1$

$$\begin{cases} x\left(t\right)=-\frac{2\sqrt{\varepsilon/a}}{\sqrt{a\varepsilon+1}}\cos\left(\sqrt{\frac{a}{\varepsilon}}-\frac{g\sqrt{a/\varepsilon}}{4\sqrt{a\varepsilon+1}}\right)t-\frac{2\varepsilon}{\sqrt{a\varepsilon+1}}\sin\left(\sqrt{\frac{a}{\varepsilon}}-\frac{g\sqrt{a/\varepsilon}}{4\sqrt{a\varepsilon+1}}\right)t, \\ y\left(t\right)=-\left[\frac{2\sqrt{a\varepsilon}}{\sqrt{a\varepsilon+1}}+\frac{g\sqrt{a\varepsilon}}{a\varepsilon+1}\right]\cos\left(\sqrt{\frac{a}{\varepsilon}}-\frac{g\sqrt{a/\varepsilon}}{4\sqrt{a\varepsilon+1}}\right)t+ \\ \qquad +\left[\frac{2}{\sqrt{a\varepsilon+1}}+\frac{g}{a\varepsilon+1}\right]\sin\left(\sqrt{\frac{a}{\varepsilon}}-\frac{g\sqrt{a/\varepsilon}}{4\sqrt{a\varepsilon+1}}\right)t. \end{cases} \tag{33}$$

This ellipse passes through the point $\left(-\frac{2}{\sqrt{a\varepsilon+1}}\sqrt{\frac{\varepsilon}{a}}, -\frac{2\sqrt{a\varepsilon}}{\sqrt{a\varepsilon+1}}-\frac{\sqrt{a\varepsilon}}{a\varepsilon+1}g\right)$. As $g \to 0$ this ellipse tends to the ellipse

$$\begin{cases} x\left(t\right)=-\frac{2\sqrt{\varepsilon/a}}{\sqrt{a\varepsilon+1}}\cos\sqrt{\frac{a}{\varepsilon}}t-\frac{2\varepsilon}{\sqrt{a\varepsilon+1}}\sin\sqrt{\frac{a}{\varepsilon}}t, \\ y\left(t\right)=-\frac{2\sqrt{a\varepsilon}}{\sqrt{a\varepsilon+1}}\cos\sqrt{\frac{a}{\varepsilon}}t+\frac{2}{\sqrt{a\varepsilon+1}}\sin\sqrt{\frac{a}{\varepsilon}}t, \end{cases} \tag{34}$$

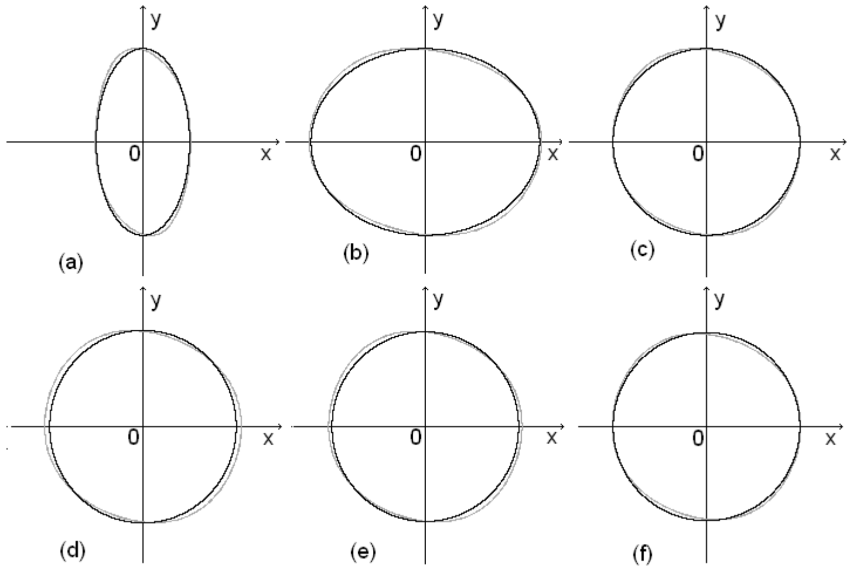

Fig. 1. The approximate limit cycle of (5). Case $g = 0$: (a) $\varepsilon = 1$, $a = 4$; (b) $\varepsilon = 3$, $a = 2$; (c) $\varepsilon = 3$, $a = 3$. Case $g > 0$: (d) $\varepsilon = 3$, $a = 3$, $\omega = 0.985$, $g = 0.2$; (e) $\varepsilon = 3$, $a = 3$, $\omega = 0.990$, $g = 0.1$; (f) $\varepsilon = 3$, $a = 3$, $\omega = 0.992$, $g = 0.05$.

which passes through the point

$$(x_0, y_0) = \left(-\frac{2\sqrt{\varepsilon/a}}{\sqrt{a\varepsilon + 1}}, -\frac{2\sqrt{a\varepsilon}}{\sqrt{a\varepsilon + 1}} \right). \tag{35}$$

As expected, the ellipse (34) is of the form (19), where the initial point is (35), and it is the approximate limit cycle of (5) as $g \to 0$.

3. NUMERICAL RESULTS

In fig. 1 we give comparative numerical results on the approximate limit cycle of (5). In figs. 1a-c we represent the orbit through $(0, -\sqrt{3})$ of (7) (black color) and the orbit (34). They show the good approximation realized.

In figs. 1d-e we give numerical results on the approximate limit cycle (33) for various values of the parameters and $g \ll 1$.

The numerical method used was that from [4], [3].

References

[1] Barnes, B., Grimshaw, R., *Analytical and numerical studies of the Bonhoeffer van der Pol system*, Aust. Math. Soc. Series B, **38** (1997), 427-453.

[2] Barnes, B., Grimshaw, R., *Numerical studies of the periodically forced Bonhoeffer van der Pol oscillator*, Int. J. Bifurcation and Chaos, **7,** 12 (1997), 2653-2689.

[3] Băzăvan, P. : *The dynamical system generated by a variable step-size algorithm for Runge-Kutta methods*, Int. J. Chaos Theory Appl., **4,** 4 (1999), 21-28.

[4] Băzăvan, P., *A variable step-size algorithm for Runge-Kutta methods*, Rom. J. Inf. Sch. Tech., **3**, 2(2000), 105-112.

[5] Băzăvan, P., *Numerical study of the succession of attractors in the periodically forced Rayleigh system*, Annals of the University of Craiova, Math. Comp. Sci. Ser., **33** (2006), 241-250.

[6] Diener, M., *Nessie et les canards*, IRMA, Strasbourg, 1979.

[7] Diener, M., *Quelques examples de bifurcations et les canards*, IRMA, Strasbourg, 1979, 1979-1985.

[8] Flaherty, J. E., Hoppensteadt, F. C., *Frequency entrainemment of a forced van der Pol oscillator*, Studies Appl. Math., **58** (1978), 5-15.

[9] Georgescu, A., *Aproximaţii asimptotice*, Ed. Tehnică, Bucureşti, 1989.

[10] Georgescu, A., *Asymptotic treatment of differential equations*, Chapman & Hall, London, 1995.

[11] Jordan, D. W., Smith, P., *Nonlinear ordinary differential equations*, Clarendon, Oxford, 1989.

[12] Mettin, R., Parlitz, U., Lauterborn, W., *Bifurcation structure of the driven van der Pol oscillator*, Int. J. Bifurcation and Chaos, **3,** 6 (1993), 1529-1555.

[13] Rajasekar, S., Lakshmanan, M., *Period-doubling bifurcations, chaos, phase-locking and the devils staircase in the Bonhoeffer van der Pol oscillator*, Physica D**, 32** (1988), 146-152.

[14] Reithmeier, E., *Periodic solutions of nonlinear dynamical systems*, Springer Berlin, 1991.

[15] Sterpu, M., Băzăvan, P., *Study on a Rayleigh equation*, Bul. St. Univ. Piteşti, Seria Matematică-Informatică, **3** (1999), 429-434.

[16] Sterpu, M., Georgescu, A., Băzăvan, P., *Dynamics generated by the generalized Rayleigh equation II. Periodic solutions*, Mathematical Reports, **2**(52), **3**(2000), 367-378.

[17] Wang, W., *Bifurcations and Chaos of the Bonhoeffer van der Pol model*, J. Phys. A: Math. Gen., **22** (1989), L627-L632.

ROMAI J., **4**, 2(2008), 81–98

LYAPUNOV STABILITY ANALYSIS IN TAYLOR-DEAN SYSTEMS

Adelina Georgescu, Florica Ioana Dragomirescu

Academy of Romanian Scientists, Bucharest

Department of Mathematics, University "Politehnica" of Timişoara

adelinageorgescu@yahoo.com, ioana_dragomirescu@yahoo.com

Abstract The Taylor-Dean viscous fluid flow between two rotating cylinders is a combination of a circular Couette flow and azimuthal Poiseuille flow. Its linear stability was investigated analytically and numerically, among others, in the case when the size of the gap between the two cylinders was taken into account [4], [21], [19]. When this parameter becomes important, the existence of a large variety of patterns bifurcated from the Taylor-Dean flow depends on the strata determined in the parameter space. The main interest in most of these studies is for the critical instability conditions. In this paper, the eigenvalue problem governing the Lyapunov stability of the basic Taylor-Dean flow against rotationally symmetric perturbations, previously investigated in [14] by using isoperimetric inequalities, is studied along with some other examples from [24], by means of spectral methods based on Legendre polynomials [12]. In each case the critical Taylor number at which the instability sets in is obtained. All our numerical results agree with those existing in the literature.
Acknowledgement. This work was supported by the Grant 12/11.02.2008 within the framework of the Russian Foundation for Basic Research - Romanian Academy collaboration.

Keywords: Taylor-Dean system, spectral methods, Taylor number, eigenvalue problem.

2000 MSC: 176E06, 65L60, 41A10.

1. STATEMENT OF THE PROBLEM

The simplest example of a steady-circular flow of a viscous fluid between two-rotating cylinders is the Taylor-Couette flow for which the laminar basic state is the circular Couette flow. In the absence of viscosity, the first criterion of stability was given by Rayleigh [23], i.e., a stratification of angular momentum about an axis is stable if and only if increases monotonically outward. For the case of a viscous Couette flow, theoretical and experimental investigations were performed for the first time by G.I. Taylor (1923) [26] for the case of a small gap d ($d = R_2 - R_1$) between the rotating cylinders compared to the mean radius ($(R_1 + R_2)/2$). The analytical expression of its criterion is given in terms of the Taylor number, a dimensionless parameter that characterizes the importance of the centrifugal forces due to rotation of fluid about vertical axis, relative to viscous forces. In the case when the inner cylinder rotates and the outer cylinders is stationary, he found [26] that the flow becomes unstable when the parameter $Re(d/R_1)^{1/2}$ exceeds the value of about 41, where the spacing between the cylinders is small compared to the inner radius R_1 and the disturbances were assumed axisymmetric. Here Re represents the Reynolds number. Chandrasekhar [4] also investigated the eigenvalue problem arising in the Lyapunov stability study and obtained expressions for the secular equations leading to the neutral manifolds that separate the stability and instability domains.

Another motion of great interest from the engineering point of view is the Taylor-Couette flow of a viscous fluid in a fully filled annulus of concentric rotating cylinders. Applications from bearing lubrification and viscometry need analytical and numerical results on this motion [1]. Practical applications of the system from [1] exist in the textile industry or paper fabrication.

When a viscous fluid flows in a curved channel under a pressure gradient acting round the cylinders a pumping velocity distribution occur. This type of instability was first considered by Dean (1928)[7], also in the case of a thin annulus compared to the mean radius. Further analytical and numerical investigations of the resulting eigenvalue problems were given by DiPrima [10], Reid [24], Hammerlin [16], to quote but a few of the first works.

In the following we present some results from previous works concerning the Taylor-Dean system, pointing out in each case that the main interest was on the influence of the various fields or of the physical parameters (the gap space for instance) on the stability of the system or on the numerical evaluations of the critical values of the Taylor number.

For a viscous flow between two rotating cylinders in which the basic motion is a combination of a circular Couette flow and an azimuthal Poisseuille flow the system becomes a Taylor-Dean one. Experimental investigations of the Taylor-Dean problem in the case of a small gap between the cylinders compared to the mean radius were first conducted by Brewster and Nissan [2] and then also theoretically and experimentally by Brewster, Grosberg and Nissan in [3]. For the case when the outer cylinder is at rest the analytical investigation of the problem was performed by DiPrima [10] using Fourier series expansions in order to obtain critical values of the Taylor number. In this paper the theoretical analysis of this problem [10] is performed using spectral methods based on Legendre and Chebyshev polynomials expansions and the numerical results are compared to the ones from [10], proving to be similar.

Linear stability analysis were conducted for the arbitrary gap spacing case also. At first, Chen and Chang [5] conducted a complete analysis for the onset of secondary motion of Taylor-Dean flow in between two infinitely long rotating cylinders in the small gap approximation theory. In [6] Chen found, for the arbitrary gap spacing case, that the most stable state correspond either to the case when the instability is about to change from a nonaxisymmetric mode into a symmetric mode, as the pumping velocity is increasing, or when a nonaxisymmetric mode changes both its azimuthal wavelength and its direction of travelling. The numerical evaluations of the two-point eigenvalue problem was based on a shooting technique together with a unit-disturbance method [6].

In [21] the linear and weakly nonlinear analysis of the Taylor-Dean system which consists of the flow between two rotating cylinders in the horizontal position is presented. The numerical computations of the critical Taylor number, wavenumbers and wave speeds for the primary transitions are given at first for a finite gap system and then compared with results obtained in the small gap approximation. The weakly nonlinear analysis of the transition towards the spirals or the stationary rolls shows that this transition is always supercritical if the Poisseuille-Couette flow is induced by a partial filling. When an external pumping is present, however, a supercritical bifurcation for specific values of the rotation ratio is induced leading to the conclusion that these two configurations are not always equivalent either for linear or nonlinear analysis.

In [22] the flow of a Bingham fluid between two rotating cylinders with a pressure gradient in the tangential direction is considered. A nonlinear stability analysis of the Taylor-Couette flow, along with a theoretical study of the Taylor-Dean configuration, are performed. The critical parameters characterizing the occurrence of the instability in the Taylor-Dean configuration for a Bingham fluid were computed.

Hills and Bassom [18], [19] were concerned with a large wavenumber perturbations in small-gap Taylor-Dean flow. They proved that a consistent solution of the governing equations in the main body of the fluid can be constructed by a WKB analysis which links the Taylor and Dean instabilities at exponentially small orders. Although their studies concerned high wavenumbers, the observed asymptotic behaviours could be use to interpret the neutral curves behaviours obtained by Kachoyan [20].

In [8] a linear stability analysis of a viscous flow driven by a constant azimuthal pressure gradient between two horizontal radial temperature concentric porous cylinders when a radial temperature gradient is given. The influence of the temperature field is pointed out for both outflow and inflow cases.

A modified Taylor-Dean system is considered in [13]. The flow of a viscous fluid take place between a inner cylinder, which is rotating about its fixed axis and, in general, the outer cylinder is fixed and noncircular. The gap space is assumed to be small compared to the radius of the inner cylinder. The streamwise growth of a steady disturbance is calculated with a given method that involves considering a steady-state small disturbance of the base flow. Stability characteristic and critical values of the Taylor number are obtained. It is proven that the more the gap width increases in the direction of the flux of the basic flow the more unstable the flow becomes, and conversely when the gap width correspondingly decreases.

The Taylor-Dean flow configurations when the annulus is only partially filled have multiple engineering applications such as rotating drum filter, in electrogalvanizing line in the steel making industry which uses a roller-type cell to plate zinc onto the surface of a steel strip. It has been shown that wall curvature can have a significant effect on the performance of film cooling over turbine blades [1].

2. SPECTRAL METHODS

The general Taylor-Dean stability problem leads to the following two-point boundary value problem [10]

$$\begin{cases} (D^2 - a^2)^2 U = F(x)V, \\ (D^2 - a^2)V = -a^2 T G(x) U \end{cases} \tag{1}$$

and the boundary conditions

$$U = DU = V = 0 \text{ at } x = 0, 1, \tag{2}$$

where D denote the differentiation with respect to the variable x, i.e. $D = \dfrac{d}{dx}$, $F(x)$ and $G(x)$ are known continuous, indefinitely derivable functions, a is the wavenumber and T is the Taylor number. The unknown functions U and V stand for the amplitude of the perturbation fields of the radial and azimuthal velocity, respectively. In (1)-(2) the vector (U, V) represents the eigenvector and T is the corresponding eigenvalue. The classical Taylor stability problem is of the form (1) - (2) with $g(x) = 1$, $f(x) = 1 - (1 - \mu)x$, $\mu < 1$, $\mu = \dfrac{\Omega_2}{\Omega_1}$ with Ω_1 and Ω_2 the angular velocities of rotation about the axis of the inner and the outer cylinders. In the general case, the basic mathematical problem is: *given $F(x)$ and $G(x)$, determine the smallest value of T for $a > 0$ such that a solution of (1) - (2) exists.* We are interested in the critical value of the Taylor number T for positive values of the wavenumber at which instability sets in.

The main reason for the use of spectral methods is their exponential accuracy. Large classes of eigenvalue problems can be solved numerically using spectral methods, where, typically, the various unknown fields are expanded upon sets of orthogonal polynomials or functions. The convergence of such methods is in most cases easy to assure and they are efficient, accurate and fast. Our numerical study is performed using a weighted residual (Galerkin type) spectral method.

One of the most important characteristic of the Galerkin projection is that the boundary conditions of the problem are treated implicitly by building them into the base functions. In these conditions, the basis functions must be chosen such that each of the functions satisfies the boundary conditions which imply that they are satisfied by a linear combination of such functions also in the case of the linear stability problems from hydrodynamic stability characterized by linear and homogeneous boundary conditions.

Following [17], let us consider the complete orthogonal sets of functions

$$\{\phi_i\}_{i=1,2,...,n} \in L^2(0,1) : \phi_i(x) = \int_0^x Q_i(t)dt,$$

with ϕ_i, $i = 1, 2, ..., n$ satisfying boundary conditions of the type $\phi_i(0) = \phi_i(1) = 0$ and

$$\{\beta_i\}_{i=1,2,...,n} \in L^2(0,1) : \beta_i(x) = \int_0^x \int_0^s Q_i(t)dtds,$$

with β_i, $i = 1, 2, ..., n$ satisfying boundary conditions of the type $\beta_i(0) = \beta_i(1) = \beta_i'(0) = \beta_i'(1) = 0$.

we denoted by Q the classical Legendre polynomials defined on $(-1, 1)$.

Let us write the unknown functions U and V as series of the form

$$U = \sum_{i=1}^{n} U_i \beta_i(x), \quad V = \sum_{i=1}^{n} V_i \phi_i(x). \tag{3}$$

In this way, the functions U and V satisfy all boundary conditions imposed on them since each of the expansion function satisfies automatically the boundary conditions.

Replacing the expressions (3) in the system of ordinary differential equations that define the eigenvalue problem (1), we obtain the following algebraic system in the expansion functions

$$\begin{cases} \sum\limits_{i=1}^{n} U_i (D^2 - a^2)^2 \beta_i - \sum\limits_{i=1}^{n} V_i F(x) \phi_i = 0, \\ \sum\limits_{i=1}^{n} V_i (D^2 - a^2) \phi_i + a^2 T \sum\limits_{i=1}^{n} U_i G(x) \beta_i = 0. \end{cases} \tag{4}$$

Following [17], we impose the condition that the equations in (4) be orthogonal on the vector (β_k, ϕ_k), $k = 1, 2, ..., n$. We get

$$\begin{cases} \sum_{i=1}^{n} [U_i\Big((D^2 - a^2)^2\beta_i, \beta_k\Big) - V_i(F((x)\phi_i, \beta_k)] = 0, \\ \sum_{i=1}^{n} [V_i\Big((D^2 - a^2)\phi_i, \phi_k\Big) + a^2 T U_i(G(x)\beta_i, \phi_k)] = 0. \end{cases} \tag{5}$$

The secular equation, which yields the critical value of the Taylor number T is obtained by imposing the condition that the determinant of the system (5) vanish, i.e.

$$\begin{vmatrix} ((D^2 - a^2)^2\beta_i, \beta_k) & (F(x)\phi_i, \beta_k) \\ & \\ a^2 T(G(x)\beta_i, \phi_k) & ((D^2 - a^2)\phi_i, \phi_k) \end{vmatrix} = 0. \tag{6}$$

The unknown vector field (U, V) from (1) can also be expanded upon complete sequences of functions in $L^2(0, 1)$ defined by using Chebyshev polynomials that satisfy the boundary conditions of the problem. Keeping the above notations, the functions ϕ_i, $i = 1, 2, ..., N$ are defined, for instance, by $\phi_i(x) = T_i^*(x) - T_{i+2}^*(x)$ and β_i, $i = 1, 2, ..., n$ by $\beta_i(n) = T_i^*(x) - \dfrac{2(i+2)}{i+3}T_{i+2}^*(x) + \dfrac{i+1}{i+3}T_{i+4}^*(x)$ [25] with T_i^*, $i = 1, 2, ..., n$, the shifted Chebyshev polynomials on $(0, 1)$ defined in a similar manner as the shifted Legendre polynomials. All the evaluations of the scalar products were based on the orthogonality relation

$$\int_0^1 T_n^*(z)T_m^*(x)w^*(z)dz = \begin{cases} \dfrac{\pi}{2}c_n\delta_{nm}, \text{ if } i = j, \\ 0, \text{ if } i \neq j, \end{cases} \tag{7}$$

with respect to the weight function $w^*(x) = \dfrac{1}{\sqrt{x(1-x))}}$.

Remark. We could also work with original Legendre or Chebyshev polynomials by transforming the defined interval on $(a, b) = (-1, 1)$. However, the choice $(a, b) = (0, 1)$ led us to simplified numerical evaluations.

3. A VARIATIONAL APPROACH

Since $F(x)$, $G(x) \in \mathcal{C}^\infty$ and $V \in \mathcal{C}^2$, from $(1)_1$ we get that $U \in \mathcal{C}^6$, then $(1)_2$ implies that $V \in \mathcal{C}^4$ and, again from $(1)_1$ it follows that $U \in \mathcal{C}^8$ and so on such that $U, V \in \mathcal{C}^\infty$. As they are defined on a compact set it follows that they are bounded hence U^2, V^2 are Lebesgue integrable. The problem (1) - (2) can also be written in the form

$$A\mathbf{X} = TB\mathbf{X}, \quad \mathbf{X} \in \mathcal{D}(A - TB),$$

where $\mathbf{X} = (U, V)^t$, the expressions of the matricial differential operators A and B are $A = \begin{pmatrix} (D^2 - a^2)^2 & 0 \\ 0 & D^2 - a^2 \end{pmatrix}$, $B = \begin{pmatrix} 0 & F(x) \\ -a^2 G(x) & 0 \end{pmatrix}$ and $\mathcal{D}(A - TB)$, the domain of definition of the operator $A - TB$, is defined by $\mathcal{D}(A - TB) = \mathcal{D}(A) \cap \mathcal{D}(B)$,

$\mathcal{D}(A) = \{\mathbf{X} \in \overline{\mathcal{C}}^\infty \times \overline{\mathcal{C}}^\infty | U, V \text{ satisfy the boundary conditions (2)}\}$, $\mathcal{D}(B) = \overline{\mathcal{C}}^\infty$,

therefore $\mathcal{D}(A - TB) = \mathcal{D}(A)$, with $\overline{\mathcal{C}}^\infty = \mathcal{C}^\infty(\overline{(0,1)}; \mathbb{R})$ the space of functions $\widetilde{f} : (0,1) \to \mathbb{R}$ which, together with all their derivatives can be prolonged by continuity on $[0,1]$.

Since $\mathcal{C}_0^\infty$ is dense in L^2, the operators A and B may be extended to operators in L^2 densely defined on some Hilbert subspace $\mathcal{H}$ of L^2 obtained by the closure of $\mathcal{D}(A)$ in L^2. It can be proved immediately that $A = A^*$ and $B^* = B^t$, A^* and B^* being the adjoint operators for A and B and that for

$$A\mathbf{X} = TB\mathbf{X}, \ \mathbf{X} \in \mathcal{H} \tag{8}$$

its adjoint reads

$$A\mathbf{X}^* = TB^t\mathbf{X}^*, \ \mathbf{X}^* \in \mathcal{H}. \tag{9}$$

A necessary condition for the existence of the eigenvector $\mathbf{X}$ of (8) is

$$Q_1(\mathbf{X}, \mathbf{X}^*) = ((A - TB)\mathbf{X}, \mathbf{X}^*) = 0, \tag{10}$$

where $\mathbf{X}^*$ is the eigenvector of (9).

The following variational principle for the linear nonselfadjoint operator $A - TB$ holds[9], [27]

$(T, \mathbf{X})$ and $(T^*, \mathbf{X}^*)$ are the eigenvalues and eigenvectors of problem (8) and (9) respectively iff $T = extQ$ where $Q : \mathcal{H} \times \mathcal{H} \to \mathbb{R}$ is the functional $Q(\mathbf{X}, \mathbf{X}^*) = \dfrac{(A\mathbf{X}, \mathbf{X}^*)}{(B\mathbf{X}, \mathbf{X}^*)}$ and ext stands for the extremum value of Q. (11)

This reduces the calculation of the eigenvalues and eigenvectors of (8) and (9) to the solution of the variational problem $extQ$ in $\mathcal{H} \times \mathcal{H}$.

Due to the complicate form of Q it is preferable to transform the variational problem without constraints (11) into the isoperimetric problem:

extremal (stationary) points of Q in $\mathcal{H} \times \mathcal{H}$ are equal to the extremal (stationary)

points of the functional Q_1 in $\mathcal{H}_1 \times \mathcal{H}_1 = \{(\mathbf{X}, \mathbf{X}^*)|(B\mathbf{X}, \mathbf{X}^*) = 1\}$.

If $\mathbf{X} = (U, V)$ and $\mathbf{X}^* = (U^*, V^*)$ are represented by series, e.g. $U = \sum\limits_{i=1}^{n} U_i\beta_i(x)$, $V = \sum\limits_{i=1}^{n} V_i\phi_i(x)$, $U^* = \sum\limits_{i=1}^{n} U_i^*\beta_i(x)$, $V^* = \sum\limits_{i=1}^{n} V_i^*\phi_i(x)$, then Q_1 becomes a function of $4n$ variable $U_1, U_2, ..., U_n$, $V_1, ..., V_n$, $U_1^*, ..., U_n^*$, $V_1^*, ..., V_n^*$ such that in order for Q_1 to achieve an extremum value it is necessary that

$$\frac{\partial Q_1}{\partial U_i} = \frac{\partial Q_1}{\partial V_i} = \frac{\partial Q_1}{\partial U_i^*} = \frac{\partial Q_1}{\partial V_i^*} = 0, \quad i = 1, 2, ..., n. \tag{12}$$

The evaluations can be simplified by halving the order of differentiation if the expression of Q_1 from (10) is integrated by parts and then taking into account the boundary conditions on U, V, U^*, V^*, i.e. $U = DU = V = 0$, $U^* = DU^* = V^* = 0$ at $x = 0$ and $x = 1$. We get

$$Q_1(\mathbf{X}, \mathbf{X}^*) = \int_0^1 \{D^2UD^2U^* + 2a^2DUDU^* + a^4UU^* - F(x)VU^* - DVDV^* -$$

$$-a^2VV^* + a^2TG(x)UV^*\}dx = 0. \tag{13}$$

Since $Q_1(\mathbf{X}, \mathbf{X}^*)$ is then equal to

$$Q_1(U_1, .., U_n, V_1, .., V_n, U_1^*, ..., U_n^*, V_1^*, ..., V_n^*) = \sum_{i=1}^{n}\sum_{j=1}^{n} U_iU_j^*((D^2\beta_i, D^2\beta_j)+$$

$$+2a^2(D\beta_i, D\beta_j) + a^4(\beta_i, \beta_j)) - V_iU_j^*(F(x)\phi_i, \beta_j) - V_iV_j^*((D\phi_i, D\phi_j)) + a^2(\phi_i, \phi_j)+$$

$$+a^2TU_iV_j^*(G(x)\beta_i, \phi_j) = 0 \tag{14}$$

(12) will lead to the following relation $detM \cdot detM^t = 0$, where M is a simplified form of the determinant in (6).

4. NUMERICAL EVALUATIONS

Some particular examples of (1)-(2) are numerically treated using the spectral method based on polynomials presented in Section 2.

Let be a viscous flow between two concentric cylinders due to a pressure gradient acting round the cylinders. The z axis is the cylinders axis. In the narrow gap approximation and if the principle of exchange of stabilities holds, the stability of the basic flow to rotationally symmetric perturbations, specially periodic in the z-direction is governed by the system [14], [24]

$$\begin{cases} (D^2-a^2)^2u = a^2T(4x-4x^2)v, \\ (D^2-a^2)v = (1-2x)u \end{cases} \tag{15}$$

and the boundary conditions

$$v = u = Du = 0 \text{ at } x = 0, 1. \tag{16}$$

In [14] Joseph's method is applied in order to obtain bounds for the stability problem (15)-(16).

Multiplying $(15)_2$ by $-a^2T$ the system (15) is reduced to the general form (1), i.e.

$$\begin{cases} (D^2-a^2)^2\Psi = (4x^2-4x)v, \\ (D^2-a^2)v = -a^2T(1-2x)\Psi. \end{cases} \tag{17}$$

Here, and in all the examples below, $\Psi(x) = \begin{pmatrix} u(x) \\ v(x) \end{pmatrix}$ is the vector perturbation function and it represents the eigenfunction in the above eigenvalue problem.

Representing the unknown functions as in the above spectral method, the secular equation is obtained allowing us to obtain numerical evaluations on the critical Taylor number. These numerical results are presented in comparison with the ones from [24] in Table 1.

In [10] DiPrima studied the stability of a viscous flow between rotating cylinders when the inner cylinder is rotating (the Taylor problem) and at the same time the fluid is being pumped round the annulus (the Dean problem), with the possibility of pumping in the direction of rotation or opposed to it. Introducing a pumping parameter $Q = 3(1+a)\dfrac{V_p}{V_r}$, with the quantities V_p and V_r being the average velocities due to rotation and pumping, respectively, he obtained numerical values of the critical Taylor number for different wavenumbers for axisymmetric modes in a small-gap approximation, for various values of the parameter Q.

The stability problem for this type of velocity distribution has the form [10]

$$\begin{cases} (D^2-a^2)^2u = \{(1-x)-Q(x^2-x)\}v, \\ (D^2-a^2)v = -Ta^2\{1+Q(2x-1)\}u \end{cases} \tag{18}$$

with the boundary conditions (16). The eigenvalue problem (18) -(16) is solved in [10] using a method from Chandrasekhar [4]. Our numerical evaluations, based on shifted Legendre and Chebyshev polynomials, presented in Table 2, are similar to those from [10].

In [15] the linear stability of the Taylor-Dean flow was investigated in the case of a partially filled rotating confinement and subject to circumferential drop pressure. The eigenvalue problem is defined by a nonselfadjoint matrix differential operators with variable coefficients which lead to the application of numerical methods (e.g. shooting method was used by Mutabazi, Normand, Peerhossainti, Wesfried) rather than towards analytical approaches.

The flow of an incompressible viscous fluid between two coaxial horizontal cylinders rotating in the same direction in the presence of a circumferential pressure gradient is investigated [15]. More over, two cases are analyzed: one case when both cylinders are rotating and another when only the inner cylinder is rotating and the outer one is at rest. In the first one, the problem governing the linear stability of the basic flow $(U, V, W, P) = (0, V(x), 0, P(x))$, where $V(x) = 3(1+\mu)x^2 - 2(2+\mu)x + 1$, with respect to infinitesimal perturbations of the form $f(x, y) = f(y)e^{i\sigma x}$, can be written in the classical form [15]

$$\begin{cases} (D^2-a^2)^2u = Vv, \\ (D^2-a^2)v = -2a^2TDVu, \qquad x \in [0,1] \end{cases} \tag{19}$$

where $D = d/dx$, $u \in \mathcal{C}^4([0,1], \mathbb{R})$, $v \in \mathcal{C}^2([0,1], \mathbb{R})$, $\mu \in [0,1]$, $T > 0$, $a \in \mathbb{R}_+$. Here μ is the rotation velocities ratio.

For the case when the inner cylinder is rotating with the angular velocity Ω_1 and the other cylinder is at rest, the basic flow velocity distribution is a quadratic polynomial

$$V_0(x) = 2\alpha(1-x) + 6(1-\alpha)(x-x^2) \tag{20}$$

where α is the dimensionless measure of the relative strength of the velocities due to the rotation and the pressure gradient.

The eigenvalue problem has then the form [15]

$$\begin{cases} (D^2 - a^2)^2 u = a^2 T V_0 v, \\ (D^2 - a^2) v = 0.5 D V_0 u \end{cases} \tag{21}$$

with the boundary conditions (16).

The problem was investigated analytically and numerically in [15] using the Chandrasekhar method. The azimuthal eigenfunction $v(x)$ is expanded in a Fourier sine series $v(x) = \sum_{n=1}^{\infty} v_n \sin(n\pi x)$ that satisfies all boundary conditions on v. The radial eigenfunction $u(x)$ is obtained by replacing $v(x)$ in $(21)_1$ and solve the obtained ordinary differential equation. Then the functions $u(x)$ and $v(x)$ are replaced in $(21)_2$ and imposing the condition that the left-hand side of the obtained equation to be orthogonal on $\sin(m\pi x)$, $m = 1, 2, ...,$ an algebraic infinite system of equations is obtained. Since the solution of this system is nontrivial, the conditions that the determinant of the system to vanish is imposed. The secular equation of the form $F(T, a, \alpha) = 0$ is obtained. The same method was also used in [20]. In [20] it is shown also that the values of the wavenumber on some intervals lead to some discontinuities; in this case the lowest stationary mode does not exists.It is clear that the method we used lead to a simplification not only of the numerical computations but also on the symbolic written.

The numerical results for all the presented cases are given in Tables 1-4. In the following we give the notations used for the tables headings: T_L-corresponding to the numerical results obtained here using shifted Legendre polynomials, T_C-corresponding to the numerical results obtained here using shifted Legendre polynomials, $T_{[cited\ reference]}$-corresponding to the numerical results obtained in the cited reference. The accuracy of the spectral methods used here is proven also by the small number of terms in the expansion series, $n \leq 6$. Obviously, we performed numerical evaluations for a larger number of terms, but the obtained improvements of the numerical evaluations did not justified the much larger computational time.

a	T_L	T_C	$T_{[24]}$
1	126320.1329	122194.722	117835.7058
2	41110.9207	40176.220	38786.6952
2.5	31570.5941	31045.954	30007.6002
3	27007.4955	26728.576	25869.0258
3.8	24449.0427	24480.515	23764.18005
3.9	24443.38079	24452.04647	23748.48592
4	25051.82227	24467.073	23774.64568
4.5	25550.4704	25120.706	23840.10808
5	26893.4293	26612.164	26005.6818
5.5	28976.0245	28849.428	28298.2050
6	31758.7613	31802.477	31375.1250
8	50185.97265	51218.709	51520.5000

Table 1 **Numerical values of the critical Taylor number for various values of the wavenumber for the model (15)-(16).**

Q	a	T_L	T_C	$T_{[10]}$
-2	3.80	13576.5545	12098.7883	12594.1346
-0.5	3.17	4279.4433	4291.879	4182.021
0	3.12	3474.8687	3532.390395	3393.6866
0.5	3.13	2915.5634	2975.603180	2845.6975
3	3.14	1525.6674	1582.064085	1480.5318
10	3.45	472.0859	484.4711193	455.6961
21	3.70	154.8957	157.1818753	149.0145

Table 2 **Numerical values of the critical Taylor number for various values of the parameters Q and a for the model (18)-(16).**

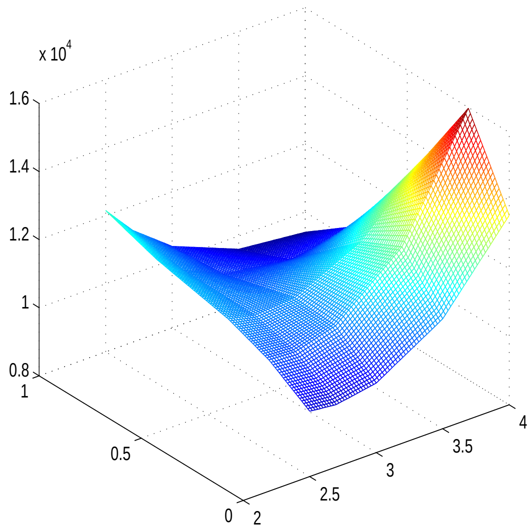

Fig.1.: Neutral surface for the model (19)-(16).

The neutral surface separating the stability and instability domain is presented in Figure 1. It was obtained in MATLAB using a two dimensional

μ	a	T_L	T_C
0	2.5	9919.7149	11460.31073
0	2.7	9835.469	11532.63127
0	3	10045.964	12016.05962
0.2	3	10995.292	12409.86652
0.2	4	15979.639	16915.09562
0.4	2.7	10998.024	11539.55249
0.4	2.8	10984.887	11554.30105
0.4	3	11088.561	11707.50378
0.75	3	10504.836	9860.645306
0.75	3.5	10224.794	9790.854202
0.75	3.75	10301.214	9968.810226
1	3	10395.189	8801.452055
1	4	9403.829	8387.847645
1	4.15	9426.951	8480.124589
1	4.5	9606.823	8819.413100

Table 3 **Numerical values of the critical Taylor number for various values of the parameters μ and a for the model (19)-(16).**

α	a	$T\times 10^3_{[20]}$	$T\times 10^3_L$	$T\times 10^3_C$
0.125	3.68	4.75	4.9569	5.05001
0.5	3.14	2.96	3.0513	3.17117
0.75	3.13	2.162	2.222	2.29017
1.5	3.24	1.205	1.233	1.20967
3	3.80	0.731	0.7542	0.62713
-3	5.7	2.553	6.358	2.41603

Table 4 **Numerical values of the critical Taylor number for various values of the parameters α and a for the model (21)-(16).**

interpolation procedure. The graphical representation gives us the critical Taylor number as a function of a and μ, $T = T(a,\mu)$. It can be noticed that for fixed values of μ (a projection on this space) the neutral curve given by $T = T(a)$ has the classical well known form from [4].

5. CONCLUSIONS

In this paper we present a few models of Taylor-Dean system, the analytical and numerical investigation performed on them. The practical importance of these models was pointed out and the physical characteristics on each case are emphasized. We were interested in the critical values of the Taylor number, T_c (proportional to the inner cylinder rate) at which the system changes from a spatially uniform state to a travelling wave state. We also completed some of them with our analytical and numerical results. The evaluations were each time compared to the existing ones and they proved to be similar.

We can conclude that an experimental, analytical and numerical study is of great theoretical and practical interest due to the large variety of patterns that this system exhibits.

References

[1] Ait Aider, A., Skali, S., Brancher, J.P., *Laminar-turbulent transition in Taylor-Dean flow*, J of Phys. Conf. Series, **14**(2005), 118-127.

[2] Brewster, D.B., Nissan, A.H., *The hydrodynamics of flow between horizontal concentric cylinders*, Chem. Eng. Sci., **7** (1958), 215-221.

[3] Brewster, D.B., Grosberg, P., Nissan, A.H., *The stability of viscous flow between horizontal concentric cylinders*, Proc. R. Soc. London A, Math.Phys.Sci., **251**(1959), 76-91.

[4] Chandrasekar, S., *Hydrodynamic and hydromagnetic stability*, Oxford University Press, 1961.

[5] Chen, F., Chang, M.H., *Stability of Taylor-Dean flow in a small gap between rotating cylinders*, J. Fluid Mech., **243**(1992), 443-455.

[6] Chen, F., *Stability of Taylor-Dean flow in an annulus with arbitrary gap spacing*, Phys. Rev.E, **48** (1993), 1036-1045.

[7] Dean, W.R., *Fluid motion in a curved channel*, Proc. R. Soc. London, **A121**(1928), 402-420.

[8] Deka, R.K., Gupta, A.S., Das, S.K., *Stability of viscous flow driven by an azimuthal pressure gradient between two porous concentric cylinders with radial flow and a radial temperature gradient*, Acta Mecanica, **189**(2007), 73-86.

[9] Didwania, A.K., Gooddard, J.L., *A note on the generalized Rayleigh quotient for non-selfadjoint linear stability operators*, Phys. Fluids A **5**, 5(1993), 1269–.

[10] DiPrima, R.C., *Application of the Galerkin method to problems in hydrodynamic stability*, Quart. Appl. Math., **13**(1955), 55-62.

[11] DiPrima, R.C., *The stability of viscous flow between rotating concentric cylinders with a pressure gradient acting round the cylinders*, J of Fluid Mech., **6**(1959), 462-468.

[12] Dragomirescu, F. I., *Shifted polynomials in a convection problem*, Appl. Math. and Inf. Sci., **2** (2), 2008, 163-172.

[13] Eagles, P.M., *On a modified Taylor-Dean stability problem where the small gap between the cylinders varies in the azimuthal direction*, Phys. Fluids, **16**, 3(2004), 546-550.

[14] Georgescu, A., *Stability of spiral flow and of the flow in a curved channel*, Rev Roum. de Math. Pures and Appl., **XVII**, 3(1972), 353-357.

[15] Georgescu, A., Mutabazi, I., *Direct and variational methods to study Taylor-Dean problem*, ????

[16] Hämmerlin, G., *Die stabilität der strömung in einem gekrümmten kanal*, Arch. Rat. Mech. Anal., **1**, 212-24 (1958), 109-111.

[17] Hill, A.A., Straughan, B., *A Legendre spectral element method for eigenvalues in hydromagnetic stability*, J. of Computational and Applied Mathematics, **193** (2003), 363-381.

[18] Hills, C.P. Bassom, A.P., *The simultaneous onset and interaction of Taylor and Dean instabilities in a Couette geometry*, J of Phys.: Conf. Series, **14** (2005), 101-112.

[19] Hills, C.P., Bassom, A.P., *The asymptotics of neutral curve crossing in Taylor-Dean flow*, ZAMP, **57**(2006), 76-93.

[20] Kachoyan, B.J., *Neutral curve behaviour in Taylor-Dean flow*, J. of Appl. Math. and Phys. (ZAMP), **38**(1987), 905-924.

[21] Laure, P., Mutabazi, I., *Nonlinear analysis of instability modes in the Taylor-Dean system*, Phys. Fluids, **6** (11), 1994, 3630-3642.

[22] Nsom, B., Mangel, H., *Stability of Taylor-Dean flow of Bingham fluid*, 12^{th} Int.Couette-Taylor Workshop, 6-8Sept.2001, Evanstaon, IL USA.

[23] Lord Rayleigh, *On the dynamics of revolving fluids*, Scientific papers, **6**, 447-453, Cambridge, England, 1920.

[24] Reid, W.H., *On the stability of viscous flow in a curved channel*, Proc. Roy. Soc., A, **244** (1958), 186-198.

[25] Shen, J., *Efficient spectral-Galerkin method II, Direct solvers of second and fourth order equations by using Chebyshev polynomials*, SIAM J.Sci. Stat. Comput., **16** (1995), 74-87.

[26] Taylor, G.I., *Stability of a viscous liquid contained between two rotating cylinders*, Phil. Trans.Roy. Soc. (London)A, **223**, 1923, 289-343.

[27] Weinberger, H.F., *Variational methods of eigenvalue approximation*, Soc. Ind. Appl. Math., Philadelphia, 1974.

ROMAI J., **4**, 2(2008), 99–104

STABILITY AND BIFURCATION IN A GENERAL PREDATOR-PREY MODEL

Raluca-Mihaela Georgescu

Department of Mathematics, University of Pitesti

gemiral@yahoo.com

Abstract A mathematical model from biology describing the evolution of two species being in a predator-pray relationship is analyzed. The model is a Cauchy problem for a system consisting of two first order ordinary differential equations with quadratic nonlinearities and containing six real parameters. Two parameters are the growth rates of the involved species, other two are the carrying capacities of the species and the last two parameters represent the action of one species on the other. The phase functions are assumed to be positive and the only last two parameters are allowed to vary. Numerically it is found that the only candidates for the Lyapunov asymptotically stable or unstable sets governing the phase portrait are the equilibrium points, so that their type was investigated by means of the spectrum of the matrix defining the linearized equations around the equilibrium. In the case of nonhyperbolic equilibria the Lyapunov-Perron theorem upon the first approximation is no longer valid. This is why in this paper the normal form method is applied to get a nonhyperbolic Lyapunov asymptotically unstable nondegenerate saddle-node mainly responsable for the phase plane. The corresponding global dynamic bifurcation diagram is carried out numerically.

Acknowledgement. This work was supported by the Grant 12/11.02.2008 within the framework of the Russian Foundation for Basic Research - Romanian Academy collaboration.

Keywords: dynamical system, Lyapunov stability, normal form.

2000 MSC: 34D20, 37N25.

1. INTRODUCTION

There are many instances in nature where one species of animal feeds on another species of animal, which in turn feeds on other things. The first species is called the predator and the second is called the prey. In a predator-prey situation the growth rate of one population is decreased and the other increased. There are more s.o.d.e.s which represent the predator-prey model. We study here only one of them [3], i.e.

$$\begin{cases} \dot{x} &= r_1 x(1 - x/K_1 - p_{12}y/K_1), \\ \dot{y} &= r_2 y(1 - y/K_2 + p_{21}x/K_2), \end{cases} \tag{1}$$

where x, y represent the two species (x is the prey and y is the predator), $r_1 < 0$, $r_2 > 0$ - the growth rates of these species, K_1, K_2 -the carrying capacity of every species, $p_{12} > 0$ - the effect of species y on the growth of species x and $p_{21} > 0$ - the the effect of species x on the growth of species y. In this study we consider r_1, r_2, K_1 and K_2 as fixed, hence in (1) only two parameters, p_{12} and p_{21}, occur.

Due to physical reasons, the phase space must be the first quadrant (without axes of coordinates). However, for theoretical reasons we consider these half-axes too.

2. THE EQUILIBRIUM POINTS

The system (1) has the following equilibria: $O(0,0)$, $E_1(K_1, 0)$, $E_2(0, K_2)$, $E_3\left(\dfrac{K_1 - K_2p_{12}}{1 + p_{12}p_{21}}, \dfrac{K_2 + K_1p_{21}}{1 + p_{12}p_{21}}\right)$. From biological viewpoint, this last equilibrium point must be in the first quadrant, i.e. $\dfrac{K_1 - K_2p_{12}}{1 + p_{12}p_{21}} > 0$ and $\dfrac{K_2 + K_1p_{21}}{1 + p_{12}p_{21}} > 0$. It follows that $K_1 - K_2p_{12} > 0$, i.e. $p_{12} < K_1/K_2$.

By the Lyapunov-Perron linearization principle, the Lyapunov asymptotic stability of a hyperbolic equilibrium point, say $(x*, y*)$, depends on the eigenvalues of the matrix of the system linearized around the point [2]. More exactly, the attractivity of (x^*, y^*) corresponds to the eigenvalues of the matrix

$$\left.\begin{pmatrix} r_1\left(1 - 2x/K_1 - p_{12}y/K_1\right) & -r_1p_{12}x/K_1 \\ r_2p_{21}y/K_2 & r_2\left(1 - 2y/K_2 + p_{21}x/K_2\right) \end{pmatrix}\right|_{(x^*,y^*)}. \tag{2}$$

In the following we analyze the nature of the equilibrium points and their attractivity for all possible values of the parameters p_{12} and p_{21}. Since in our case the Lyapunov stability (instability) implies attractivity (repulsivity) and, conversely, for the sake of simplicity in the sequel we refer only to attractivity and repulsivity.

$\mathbf{p_{12} < K_1/K_2}$. In this case there exist four equilibria; the equilibrium O is a repulsive node, because the eigenvalues of the matrix (2) are $\lambda_1 = r_1 > 0$, $\lambda_2 = r_2 > 0$. For the equilibrium point E_1 the eigenvalues of the matrix (2) are $\lambda_1 = -r_1 < 0$, $\lambda_2 = r_2(1 + p_{21}K_1/K_2) > 0$, therefore E_1 is a saddle. Similarly, for the equilibrium point E_2 the eigenvalues of the matrix (2) are $\lambda_1 = -r_2 < 0$, $\lambda_2 = r_1(1 - p_{12}K_2/K_1) > 0$, hence E_2 is a saddle, too.

For the fourth equilibrium point, E_3, the eigenvalues of the matrix (2) are the roots of the characteristic equation $\lambda^2 - \mathrm{tr}\ \mathbf{A}\ \lambda + \det \mathbf{A} = 0$, where

$$\mathbf{A} = \frac{1}{1 + p_{12}p_{21}} \begin{pmatrix} r_1 \left(p_{12}K_2 - K_1\right)/K_1 & r_1 p_{12} \left(p_{12}K_2 - K_1\right)/K_1 \\ r_2 p_{21} \left(p_{21}K_1 + K_2\right)/K_2 & -r_2 \left(p_{21}K_1 + K_2\right)/K_2 \end{pmatrix}. \tag{3}$$

We have

$$\det \mathbf{A} = -\frac{r_1 r_2}{K_1 K_2} \cdot \frac{(p_{12}K_2 - K_1)(p_{21}K_1 + K_2)}{1 + p_{12}p_{21}} > 0, \tag{4}$$

therefore λ_1 şi λ_2 have the same sign (if they are real), so, we have to study the sign of $\mathrm{tr}\mathbf{A}$, too. We have

$$\mathrm{tr}\mathbf{A} = \frac{1}{1 + p_{12}p_{21}} \left[\frac{r_1(p_{12}K_2 - K_1)}{K_1} - \frac{r_2(p_{21}K_1 + K_2)}{K_2} \right].$$

The curve H of the Hopf bifurcation values is the straight line defined by $\mathrm{tr}\mathbf{A} = 0$, i.e. by the equation $p_{21} = K_2/(r_2K_1)(r_1K_2p_{12}/K_1 - r_1 - r_2)$, which for $p_{12} < K_1/K_2$ have $p_{21} < 0$, therefore this is not in the first quadrant. It follows that for positive parameters p_{12}, p_{21} there are no Hopf singularities. For $p_{12} < K_1/K_2$ we have $\mathrm{tr}\mathbf{A} < 0$. Since $\det \mathbf{A} > 0$, it follows that E_3 is an attractive node.

$\mathbf{p_{12} = p_{21} = 0}$. The equilibria are: $O(0,0)$, $E_1(K_1, 0)$, $E_2(0, K_2)$, $E_3(K_1, K_2)$.

$\mathbf{p_{12} = 0}$, $\mathbf{p_{21} \neq 0}$. The equilibria are: $O(0,0)$, $E_1(K_1, 0)$, $E_2(0, K_2)$ and $E_3(K_1, K_1p_{21} + K_2)$.

$\mathbf{p_{12} \neq 0}$, $\mathbf{p_{21} = 0}$. The equilibria are: $O(0,0)$, $E_1(K_1, 0)$, $E_2(0, K_2)$ and $E_3(K_1 - p_{12}K_2, K_2)$. In all these situations the equilibria have the same type as in the case $p_{12} < K_1/K_2$.

$\mathbf{p_{12} > K_1/K_2}$. In this case, from the biological viewpoint, there exist only three equilibria, the fourth equilibrium point being in the second quadrant.

The equilibrium O is an repulsive node (the eigenvalues of the matrix (2) being $\lambda_1 = r_1 > 0,\ \lambda_2 = r_2 > 0$). The equilibrium point E_1 is a saddle (the eigenvalues of the matrix (2) are $\lambda_1 = -r_1 > 0,\ \lambda_2 = r_2(1 + p_{21}K_1/K_2) > 0$); E_2 is an attractive node (the eigenvalues of the matrix (2) being $\lambda_1 = -r_2 < 0,\ \lambda_2 = r_1(1 - p_{12}K_2/K_1) > 0$). The fourth equilibrium point (which has only a mathematical existence) is a saddle.

$\mathbf{p_{12} = K_1/K_2}$. In this case (1) assumes the form

$$\begin{cases} \dot{x} &= r_1 x\,(1 - x/K_1 - y/K_2)\,, \\ \dot{y} &= r_2 y\,(1 - y/K_2 - p_{21}x/K_2)\,. \end{cases} \tag{5}$$

The equilibria of the (5) are: $O(0,0)$ (repulsive node), $E_1(K_1, 0)$ (saddle) and $E_2(0, K_2)$ (saddle-node, it is a double point appeared when E_3 and E_2 coalesce).

In the following we study the nature of the saddle-node using the normal form method [1].

Proposition 2.1. *The normal form of (5) at the point $E_2(0, K_2)$ is*

$$\begin{cases} \dot{n}_1 &= r_1\,(p_{21}/K_2 + 1/K_1)\,n_1^2 + O(\mathbf{n}^3), \\ \dot{n}_2 &= -r_2 n_2 + [p_{21}(r_1 - r_2)/K_2]n_1 n_2 + O(\mathbf{n}^3), \end{cases} \tag{6}$$

therefore, E_2 is a nondegenerated saddle-node equilibrium.

Proof. First, we translate the point E_2 at the origin by means of the change $u_1 = x,\ u_2 = y - K_2$. Let $\mathbf{u} = (u_1, u_2)^T$. Then, in $\mathbf{u}$, (5) reads

$$\begin{cases} \dot{u}_1 &= -(r_1/K_1)u_1^2 - (r_1/K_2)u_1 u_2, \\ \dot{u}_2 &= r_2 p_{21} u_1 - r_2 u_2 + (r_2 p_{21}/K_2)u_1 u_2 - (r_2/K_2)u_2^2. \end{cases} \tag{7}$$

The eigenvalues of the matrix defining the linear terms in (7) are $\lambda_1 = 0$, $\lambda_2 = -r_2$ and the corresponding eigenvectors read $\mathbf{u}_{\lambda_1} = (1, p_{21})^T$ and $\mathbf{u}_{\lambda_2} = (0, 1)^T$. Thus, with the change of coordinates $\begin{pmatrix} u_1 \\ u_2 \end{pmatrix} = \begin{pmatrix} 1 & 0 \\ p_{21} & 1 \end{pmatrix} \begin{pmatrix} v_1 \\ v_2 \end{pmatrix}$, (7) achieves the form

$$\begin{cases} \dot{v}_1 &= -Bv_1^2 - (r_1/K_2)v_1 v_2, \\ \dot{v}_2 &= -r_2 v_2 + p_{21}Bv_1^2 - Cv_1 v_2 - (r_2/K_2)v_2^2, \end{cases} \tag{8}$$

where $B = r_1\,(p_{21}/K_2 + 1/K_1)$ and $C = p_{21}(r_2 - r_1)/K_2$, such that the matrix defining the linear part is diagonal. In order to reduce the second order non-resonant terms in (8) we determine the transformation $\mathbf{v} = \mathbf{n} + \mathbf{h}(\mathbf{n})$, where $\mathbf{v} = (v_1, v_2)^T$ and $\mathbf{n} = (n_1, n_2)^T$, suggested by the Table 1, found by applying the normal form method.

m_1	m_2	$X_{\mathbf{m},1}$	$X_{\mathbf{m},2}$	$\Lambda_{\mathbf{m},1}$	$\Lambda_{\mathbf{m},2}$	$h_{\mathbf{m},1}$	$h_{\mathbf{m},2}$
2	0	$-B$	$p_{21}B$	0	r_2	-	$p_{21}B/r_2$
1	1	$-r_1/K_2$	$-C$	$-r_2$	0	$r_1/(r_2K_2)$	-
0	2	0	$-r_2/K_2$	$-2r_2$	$-r_2$	0	$1/K_2$

Table 1.

Here $\Lambda_{\mathbf{m},1}$, $\Lambda_{\mathbf{m},2}$ are the eigenvalues of the associated Lie operator, while $X_{\mathbf{m}}$ is the second order homogenous vector polynomial in (8).

We find the transformation

$$\begin{cases} v_1 &= n_1 + [r_1/(r_2K_2)]n_1n_2, \\ v_2 &= n_2 + (Bp_{21}/r_2)n_1^2 + (1/K_2)n_2^2, \end{cases}$$

carrying (8) into (6). We have $r_1(p_{21}/K_2 + 1/K_1) \neq 0$. By [1], the equilibrium point E_2 corresponding the dynamical system generated by a s.o.d.e. of the form (6) is a nondegenerated saddle-node. ∎

3. THE DYNAMIC BIFURCATION DIAGRAM

From Section 2 it follows that the strata of the parameter space are determined by the curves $S = \{(p_{12}, p_{21}) | p_{12} = K_1/K_2\}$ and $H_{\mathbb{R}} = \{(p_{12}, p_{21}) | p_{21} = K_2/(r_2K_1)(r_1K_2p_{12}/K1 - r_1 - r_2)$.

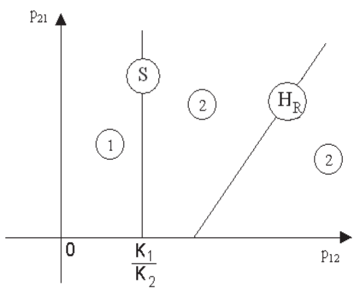

Fig. 1. The parametric portrait.

In fig. 1 the parametric portrait is represented. The regions 1 and 2 contain the axes, too.

In fig. 2 the phase portraits corresponding to the strata from the parametric portrait are presented. The coordinate axes represent the two species: x the abscissa, and y the ordinate. The portraits from the zone 2 and the zone $H_{\mathbb{R}}$ are topological equivalent (in the zone 2 the point E_3 is a saddle, while on the curve $H_{\mathbb{R}}$ it is a neutral saddle).

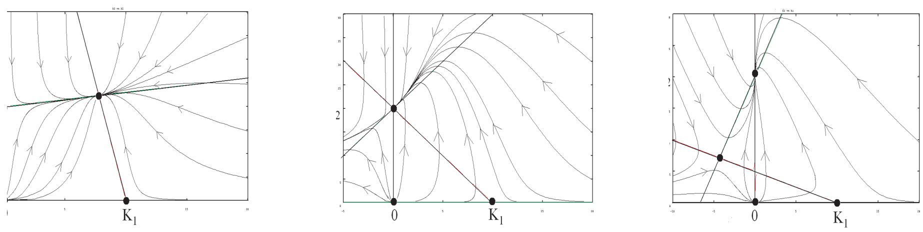

Fig. 2. The phase portraits for the strata from fig. 1.

Examining the phase portrait we conclude that for some values of the parameters p_{12} and p_{21} the two species go to a coexistence situation (zone 1). However, for other values of the same parameter, in time, the prey population x will be exterminated by the predator population y (zones S, 2 and $H_{\mathbb{R}}$).

References

[1] Arrowsmith, D. K., Place, C. M., *Ordinary differential equations*, Chapman and Hall, London, 1982.

[2] Georgescu, A., Moroianu, M., Oprea, I. *Bifurcation theory. Principles and applications*, Ed. Univ. Pitesti, Pitesti, 1999. (Romanian)

[3] Giurgiţeanu, N., *Computational economical and biological dynamics*, Europa, Craiova, 1997. (Romanian)

[4] Murray, J. D., *Mathematical biology, 2nd corr. ed.*, Springer, Berlin, 1993 (first ed. 1989).

ROMAI J., **4**, 2(2008), 105–114

LYAPUNOV STABILITY OF THE ZERO SOLUTION OF A PERTURBED ABSTRACT PARABOLIC NON-AUTONOMOUS EQUATION

Anca-Veronica Ion

"Gh. Mihoc-C. Iacob" Institute of Mathematical Statistics

and Applied Mathematics of the Romanian Academy, Bucharest

averionro@yahoo.com

Abstract A perturbed parabolic non-autonomous abstract equation in a Banach space is considered. The asymptotic stability of the zero solution of the non-perturbed equation was studied in [5] and [6]. Here, in the hypotheses from [5] and by assuming that the perturbation is of sufficient small norm, we establish the Lyapunov stability and the asymptotic stability of the zero solution of the perturbed equation. The result is applied to an abstract delay differential equation.

Keywords: abstract evolution equations, stability.

2000 MSC: 35B35, 35K90.

1. INTRODUCTION

In [5] and [6] the abstract parabolic non-autonomous equation

$$\dot{x} = Ax + R(t, x), \tag{1}$$

in a Banach space $(X, \|\cdot\|)$, is considered in the following hypotheses:

H1. *$A : \mathcal{D}(A) \subset X \to X$ is a closed linear operator, with $\mathcal{D}(A)$ dense in X. It generates a strongly continuous semigroup on X, $T(t)$, exponentially decreasing, that is, there exist $M > 0$ and $\alpha > 0$ such that $\|T(t)\| \leq Me^{-\alpha t}$, for any $t \in \mathbb{R}^+$;*

H2. *the nonlinear mapping R, defined on the Cartesian product of $\mathbb{R}^+$ with a neighborhood of 0 in X, is continuous, $R(t, 0) = 0$ for all $t \in \mathbb{R}^+$ and there is a $\beta > 0$ and a continuous function $C : \mathbb{R}^+ \mapsto (0, \infty)$ such that for all $t \in \mathbb{R}^+$*

and x_1, x_2 in a neighborhood of 0 *in X, the inequality*

$$||R(t,x_1) - R(t,x_2)|| \leq C(t)max^{\beta}(||x_1||, ||x_2||)||x_1 - x_2|| \tag{2}$$

holds.

In [5], in the hypothesis that $C(\cdot)$ is bounded, it is proved that the Cauchy problem (1), $x(0) = x_0$, has an unique generalized (mild) solution, provided x_0 is sufficiently small, solution that is exponentially decreasing to zero as time tends to infinity, hence the local asymptotic stability of the zero (mild) solution. If a Hölder condition in t is imposed to $R(t,x)$, the mild solution is proved to be the classical solution for eq. (1). It follows that the classical solution $x(t) = 0$ is locally asymptotical stable.

We consider a perturbed form of equation [5], that is

$$\dot{x} = Ax + Bx + R(t,x), \quad t \in \mathbb{R}, \tag{3}$$

with the initial condition (for some fixed $s \in \mathbb{R}$)

$$x(s) = a. \tag{4}$$

H3. *$B : X \mapsto X$ is a bounded linear operator with the property that*

$$L := \frac{M}{\alpha}\|B\|_{\mathcal{L}(X,X)} < 1. \tag{5}$$

For problem (3), (4) we assume $t \in \mathbb{R}$. The operator A satisfies hypothesis **H1**, while R satisfies the hypothesis **H2'**, obtained by **H2** by replacing $\mathbb{R}^+$ by $\mathbb{R}$. We assume also that

H4. *there is a $C > 0$ such that $C(t) \leq C$ for every $t \in \mathbb{R}$.*

Obviously $x(t) = 0$ is a solution of equation (3). We study its stability (in the sense made precise below).

2. DEFINITIONS

With the non-autonomous equation (3) we associate the integral equation

$$x(t) = T(t-s)a + \int_s^t T(t-\theta)Bx(\theta)d\theta + \int_s^t T(t-\theta)R(\theta, x(\theta))d\theta. \tag{6}$$

Let s' be a real number with $s' > s$.

Definition 1. *We say that a function $x(.;s,a):[s,s')\mapsto X$ is an A-mild solution of problem (3), (4) on $[s,s')$ if it is a solution of (6), for any $t\in[s,s')$.*

Obviously, a classical solution of (3), (4) on $[s,s')$ (i.e. a C^1 function from $[s,s')$ to $\mathcal{D}(A)$ satisfying (3), (4)), is also a solution of (6), hence an A-mild solution of the above problem.

For our non-autonomous problem, we adopt the following definition of the Lyapunov stability.

Definition 2 [4]. *A classical (resp. A-mild) solution $x(.;s_0,a_0)$ of problem (3), (4) is called stable if for every $\epsilon>0$ and every $s>s_0$ there is a $\delta=\delta(\epsilon,s)$ such that for every $y\in X$ with $\|y-x(s;s_0,a_0)\|\leq\delta$, the classical (resp. A-mild) solution $x(\cdot,\,s,y)$ exists, is defined on $[s,\infty)$, and*

$$\|x(t;s_0,a_0)-x(t;s,y)\|<\epsilon$$

for every $t\geq s$.

For the asymptotic stability we take the following definition.

Definition 3. *A classical (resp. A-mild) solution $x(.;s_0,a_0)$ of problem (3), (4) is called asymptotically stable if it is stable and, for every $s>s_0$, there is a $\delta=\delta(s)>0$ such that for $y\in X$ with $\|y-x(s;s_0,a_0)\|<\delta$, the classical (resp. A-mild) solution $x(\cdot;s,y)$ exists, is defined on $[s,\,\infty)$, and*

$$\|x(t;s_0,a_0)-x(t;s,y)\|\to 0$$

as $t\to\infty$.

3. STABILITY OF THE ZERO SOLUTION OF THE PERTURBED PROBLEM

The proof of the stability of the zero solution of problem (3), (4) follows the main lines of the similar proof for the non-perturbed problem, given in [5].

We consider $\mathcal{C}_b=\mathcal{C}_b([0,\infty),X)$ - the space of continuous bounded functions from $[0,\infty)$ to X, endowed with the supremum norm $\|x\|_0=\sup_{t\geq 0}\|x(t)\|$. We define the operators D, E, F_s as follows:

$$D:X\mapsto\mathcal{C}_b$$

associating with $a \in X$ the function $D(a)$ given by $D(a)(\tau) = T(\tau)a$, $\tau \geq 0$;

$$E : \mathcal{C}_b \mapsto \mathcal{C}_b$$

given by $E(x)(\tau) = \int_0^\tau T(\tau - \theta)Bx(\theta)d\theta$; and, for every $s \in \mathbb{R}$,

$$F_s : \mathcal{C}_b \mapsto \mathcal{C}_b,$$

defined by $F_s(x)(\tau) = \int_0^\tau T(\tau - \theta)R(s + \theta, x(\theta))d\theta$.

The fact that the operators D and F_s take values in the space $\mathcal{C}_b$ is a consequence of Lemmas 1 and 2 from [5]. There, the space of functions used is $\mathcal{C}_\alpha = \{x : [0, \infty) \mapsto X; \sup_{t\geq 0} \|x(t)\|e^{\alpha t} < \infty\}$, but the results are immediately translated to our case. More than that, the following inequalities

$$\|D\|_{\mathcal{L}(X,\mathcal{C}_b)} \leq M, \tag{7}$$

$$\|F_s x\|_0 \leq K\|x\|_0^{\beta+1},\ (\forall)x \in \mathcal{C}_b, \tag{8}$$

$$\|F_s(x) - F_s(y)\|_0 \leq Kmax\{\|x\|_0^\beta,\ \|y\|_0^\beta\}\|x - y\|_0,\ (\forall)x,\ y \in \mathcal{C}_b, \tag{9}$$

with $K = MC/\alpha$, can be proved as the similar ones in [5].

The hypotheses on B imply, for a $x \in \mathcal{C}_b$,

$$\begin{aligned} \|E(x)(\tau)\| &\leq \int_0^\tau \|T(\tau - \theta)Bx(\theta)d\theta\| \\ &\leq \int_0^\tau Me^{-\alpha(\tau-\theta)}\|Bx(\theta)\|d\theta \\ &\leq \frac{M}{\alpha}\|B\|_{\mathcal{L}(X,X)}\|x\|_0 = L\|x\|_0, \end{aligned}$$

and, by taking the supremum for $\tau \in [0, \infty)$, we obtain

$$\|E(x)\|_0 \leq L\|x\|_0. \tag{10}$$

The same method leads us to

$$\|E(x_1) - E(x_2)\|_0 \leq L\|x_1 - x_2\|_0,\ (\forall)x_1,\ x_2 \in \mathcal{C}_b. \tag{11}$$

In the integral equation (6), (where $t > s$), let us set $t - s = \tau$, and make the change of variables $\theta - s = \theta'$ in the two integrals of the equation. We obtain

$$x(s+\tau) = T(\tau)a + \int_0^\tau T(\tau-\theta')Bx(s+\theta')d\theta' + \int_0^\tau T(\tau-\theta')R(s+\theta', x(s+\theta'))d\theta'. \tag{12}$$

For every continuous function $x : \mathbb{R} \mapsto X$ and every $s \in \mathbb{R}$, we define the function $x|_s : [0, \infty) \mapsto X$, by $x|_s(\theta) = x(s+\theta)$, such that the previous integral equation may be written as

$$x|_s = Da + E(x|_s) + F_s(x|_s). \tag{13}$$

Since $x|_s$ belongs to $\mathcal{C}_b$, equation (13) is equivalent to the fixed point problem

$$\phi = \Phi(a, \phi), \tag{14}$$

where $\Phi(\cdot, \cdot) : X \times \mathcal{C}_b \mapsto \mathcal{C}_b$ is given by $\Phi(a, \phi) = Da + E(\phi) + F_s(\phi)$.

Theorem 1. *Let $r_1 < [(1-L)/K]^{1/\beta}$. If $\|a\| < \frac{r_1}{M}(1 - L - Kr_1^\beta)$, the mapping $\Phi(a, \cdot)$ is an uniform contraction from $B(0, r_1) \subset \mathcal{C}_b$ to itself.*

Proof. For any $a \in X$ and any ϕ_1, $\phi_2 \in B(0, r) \subset \mathcal{C}_b$, we have

$$\|\Phi(a, \phi_1) - \Phi(a, \phi_2)\|_0 \leq [L + Kr^\beta]\|\phi_1 - \phi_2\|_0.$$

We choose a positive real number r_1 satisfying the condition $L + Kr_1^\beta < 1 \Leftrightarrow r_1 < [(1-L)/K]^{1/\beta}$ and find that, for $\|\phi\|_0 \leq r_1$, $\Phi(a, \phi)$ is an uniform contraction with respect to a. If $\|a\| \leq r_0$, $\|\phi\|_0 < r_1$, then

$$\|\Phi(a, \phi)\|_0 \leq Mr_0 + (L + Kr_1^\beta)r_1.$$

By imposing this last quantity to be less than r_1, we find the restriction

$$r_0 < \frac{r_1}{M}(1 - L - Kr_1^\beta).$$

The assertion of the theorem is proved.□

Proposition 1. *For every $s \in \mathbb{R}$ and every $\|a\|$ small enough, there is an unique A-mild solution of problem (3), (4).*

Proof. Consider $\|a\| < r_0$, with r_0 defined in the proof of Theorem 1. Then, Theorem 1 and The Uniform Contraction Principle imply the existence of an unique fixed point $\phi^*(a) \in B(0, r_1) \subset \mathcal{C}_b$ of the mapping $\Phi(a, \cdot)$. We define the function $x : [s, \infty) \mapsto X$, $x(t; s, a) = \phi^*(a)(t - s)$, $t \geq s$. This is the solution of problem (6), that is, the A-mild solution of problem (3), (4).□

Proposition 2. *The A- mild solution $x(t) = 0$, $t \in \mathbb{R}$, of equation (3) is stable.*

Proof. The solution $x(t) = 0$ is both A-mild and classical and it can be regarded as $x(\cdot; s_0, 0)$, for any $s_0 \in \mathbb{R}$.

For a given $s \in \mathbb{R}$ and an $\epsilon > 0$, we take $\delta < \min\{\epsilon, [(1-L)/K]^{1/\beta}\}$ and $\delta_1 = \min\{\delta, \delta(1-L-K\delta^\beta)/M\}$. Now, by Theorem 1, for $\|a\| < \delta_1$ the A-mild solution $x(t;s,a)$ exists for $t \geq s$, is unique, and $\|x(t;s,a)\| < \epsilon$, for every $t \geq s$.□

4. ASYMPTOTIC STABILITY OF THE ZERO SOLUTION OF THE PERTURBED EQUATION

Proposition 3. *The A- mild solution $x(\cdot;s,0) = 0$ of equation (3) is asymptotically stable.*

Proof. We take some $s \in \mathbb{R}$. Let $\epsilon > 0$ be given such that $K\epsilon^\beta < \frac{1-L}{3}$. We take δ_1 as in the proof of Proposition 2 and a with $\|a\| < \delta_1$. By Proposition 1, there is an unique A- mild solution $x(\cdot;s,a)$. Below we denote it by $x(\cdot)$.

In eq. (12) we take the norm (of X) and successively obtain

$$\|x(s+\tau)\| \leq \|T(\tau)a\| + \|\int_0^\tau T(\tau-\theta')Bx(s+\theta')d\theta'\| + \|\int_0^\tau T(\tau-\theta')R(s+\theta', x(s+\theta'))d\theta'\|$$

$$\leq Me^{-\alpha\tau}\|a\| + L\|x|_s\|_0 + K\|x|_s\|_0^{\beta+1}.$$

From the proof of Proposition 2 it follows that $\|x|_s\|_0 < \epsilon$, and thus

$$\|x(s+\tau)\| \leq Me^{-\alpha\tau}\|a\| + L\epsilon + K\epsilon^{\beta+1}.$$

We choose τ_1 such that $Me^{-\alpha\tau_1} < \frac{1-L}{3}$. Then, for $\tau \geq \tau_1$,

$$\|x(s+\tau)\| \leq 2\frac{1-L}{3}\epsilon + L\epsilon = (\frac{2}{3} + \frac{L}{3})\epsilon$$

Hence, for $\tau \geq \tau_1$ we have

$$\|x(s+\tau)\| \leq q\,\epsilon, \;\; q = \frac{2}{3} + \frac{L}{3} < 1,$$

that is $\|x|_{s+\tau_1}\|_0 \leq q\,\epsilon$. Now, returning to the integral equation (12), we obtain as above,

$$\|x(s+\tau_1+\tau)\| \leq Me^{-\alpha\tau}\|x(s+\tau_1)\| + L\|x|_{s+\tau_1}\|_0 + K\|x|_{s+\tau_1}\|_0^{\beta+1}$$

and

$$\|x(s+\tau_1+\tau)\| \leq q^2\epsilon$$

for $\tau > \tau_1$. That is $\|x|_{s+2\tau_1}\|_0 \leq q^2\epsilon$.

By induction we obtain that for $t > s + n\tau_1$ the inequality $\|x(t)\| \leq q^n \epsilon$ holds, implying that $\|x(t; s, x_s)\| \to 0$, as $t \to \infty$, and, by Definition 3, the A-mild null solution is asymptotically stable.□

5. A HÖLDER TYPE CONDITION ON R; THE EXISTENCE OF THE CLASSICAL SOLUTION OF THE PERTURBED PROBLEM

In the spirit of [5], we impose to the nonlinear operator R a new hypothesis
H5. *There is a $\delta \in [0, 1)$ such that for any $t \in \mathbb{R}$, $h \in \mathbb{R}$ the inequality*

$$\|R(t + h, x) - R(t, x)\| \leq C\|x\|h^\delta$$

holds.
By using the properties of operator E, with minor modifications due to the use of the space $\mathcal{C}_b$ instead of $\mathcal{C}_\alpha$ and to the presence of the perturbing term, by the same reasonings as in [5], the following result may be proved.
Theorem 2. *If the hypotheses **H1**, **H2'**, **H3-H5** are assumed, then the A-mild solution $x(.; s, a)$ is also a classical solution of problem (3), (4).*

It follows, from the above results, that the classical zero solution is asymptotically stable too.

Remark. If in equation (3) we take $R(t, x) = 0$ we obtain a linear autonomous equation $\dot{x} = Ax + Bx$, to which we attach the initial condition $x(0) = a$. By following the lines of the reasoning for the general nonlinear equation, (with the simplifications due to the fact that this new equation is autonomous), we obtain that the above equation has, for every $a \in X$, an unique classical solution. Hence we can define the semigroup of operators $\{S(t)\}_{t\geq 0}$ by $S(t)a = x(t; a)$ where $x(t, a)$ is the solution of the above problem. Moreover, we obtain that $S(t)a \to 0$ as $t \to \infty$. In [1], [2] a similar result is proved for a Miyadera-type perturbation, that is an operator B that satisfies

$$\int_0^t \|BT(s)x\|ds \leq L\|x\|, \quad 0 < L < 1.$$

Our hypotheses **H1** and **H3** imply the above inequality. In the above cited works a class of semigroups larger than that described by Hypothesis **H1** is considered. However, the mathematical tools used by us here are much more elementary than those from [1], [2].

6. AN ABSTRACT EQUATION WITH DELAY

Let X be a Banach space and A, R two operators satisfying the hypotheses **H1**, **H2'**, **H4**. For $r > 0$, consider the space of functions $\mathcal{E} = L^p([-r,0],X)$ endowed with the natural norm and the bounded linear operator $\Phi : W^{1,p}([-r,0],X) \to X$. Assume that the norm of this operator is small enough, in a sense made precise later.

For $x : \mathbb{R} \to X$, define the functions x_t by $x_t(\tau) = x(t+\tau)$, $\tau \in [-r,0]$.

Consider the problem

$$\dot{x} = Ax + \Phi x_t + R(t,x), \tag{15}$$

$$x(s) = a;\ x_s = \phi,\ \ \phi \in \mathcal{E}, \tag{16}$$

and denote its solution by $x(t;s,a,\phi)$. Obviously, $x(t) = 0$, $t \in \mathbb{R}$, is a solution of eq. (15), corresponding to the initial conditions $x(s) = 0$, $x_s = 0$. We are interested in the stability of this solution. We regard the term Φx_t as a perturbing term for the equation (1), but, since the operator Φ is defined on $W^{1,p}([-r,0],X)$ and takes values in X, we have to reformulate the problem in order to have operators with definition domain and range in the same space. We use the construction from [1].

We consider the Banach space $Y = X \times \mathcal{E}$, the linear operators

$$\mathcal{A} = \begin{pmatrix} A & 0 \\ 0 & \frac{d}{ds} \end{pmatrix},$$

with definition domain $D(\mathcal{A}) = \left\{ \begin{pmatrix} x \\ \phi \end{pmatrix} \in \mathcal{D}(A) \times W^{1,p}([-r,0],X); \phi(0) = x \right\}$,

$$\Psi = \begin{pmatrix} 0 & \Phi \\ 0 & 0 \end{pmatrix}$$

defined on Y, and the nonlinear mapping

$$\mathcal{R}(t,x,\phi) = \begin{pmatrix} R(t,x) \\ 0 \end{pmatrix}$$

defined for all $t \in \mathbb{R}$, x in a neighborhood of 0 in X and all ϕ in $\mathcal{E}$.

We also put $u(t) = \begin{pmatrix} x(t) \\ x_t \end{pmatrix}$, where $x : \mathbb{R} \to X$, and consider the problem

$$\dot{u} = \mathcal{A}u + \Psi u + \mathcal{R}(t, u), \tag{17}$$

$$u(s) = \begin{pmatrix} a \\ \phi \end{pmatrix}. \tag{18}$$

Following the method from [1], where an autonomous problem is considered, it can be easily shown that the two problems are equivalent, in the following sense:

i) given $\begin{pmatrix} a \\ \phi \end{pmatrix} \in D(\mathcal{A})$ and $x : [s-r, \infty) \mapsto X$ a solution of (15), (16), the map

$$t \mapsto \begin{pmatrix} x(t) \\ x_t \end{pmatrix}$$

is a classical solution of problem (17), (18);

ii) conversely, given $\begin{pmatrix} a \\ \phi \end{pmatrix} \in D(\mathcal{A})$ and $u : [s, \infty) \mapsto Y$, $u(t) = \begin{pmatrix} z(t) \\ v(t) \end{pmatrix}$ a classical solution of (17), (18), the function $x : [s-r, \infty) \mapsto X$,

$$x(t) = \begin{cases} z(t), & t > s, \\ \phi(t), & t \in [s-r, s] \end{cases}$$

is a classical solution of (15), (16) and $x_t = v(t)$.

Thus, we may concentrate on problem (17), (18). In order to apply to it the results from the previous sections, we need to know the semigroup of operators generated by $\mathcal{A}$. In [1] it is proved that $\mathcal{A}$ is the infinitesimal generator of the semigroup of operators $\{\mathcal{T}(t)\}_{t \geq 0}$ on Y, such that

$$\mathcal{T}(t) = \begin{pmatrix} T(t) & 0 \\ T_t & \widetilde{T}(t), \end{pmatrix}, \tag{19}$$

where $(T_t a)(\tau) = \begin{cases} T(t+\tau)a, & t+\tau > 0, \\ 0, & t+\tau < 0, \end{cases}$ $\tau \in [-r, 0]$ and $\widetilde{T}$ is the so-called left-shift semigroup on $L^p([-r, 0], X)$ defined [3] by

$$(\widetilde{T}(t)\phi)(\tau) = \begin{cases} \phi(t+\tau), & t+\tau \leq 0, \\ 0, & t+\tau > 0, \end{cases} \qquad \tau \in [-r, 0].$$

For an element y of Y, $y = \begin{pmatrix} a \\ \phi \end{pmatrix}$, we have

$$\|\mathcal{T}(t)y\|_Y = \|T(t)a\|_X + \|T_t a + \widetilde{T}(t)\phi\|_{\mathcal{E}} \le Me^{-\alpha t}\|a\| + \|T_t a\|_{\mathcal{E}} + \|\widetilde{T}(t)\phi\|_{\mathcal{E}}.$$

Since

$$\|T_t a\|_{\mathcal{E}} = \left(\int_{-r}^{0} \|T(t+\tau)a\|^p d\tau\right)^{1/p} \le \left(\int_{-r}^{0} M^p e^{-\alpha p(t+\tau)}\|a\|^p d\tau\right)^{1/p}$$

$$\le Me^{-\alpha t}\left(\int_{-r}^{0} e^{-\alpha p\tau} d\tau\right)^{1/p}\|a\| \le \frac{M}{(\alpha p)^{1/p}} e^{\alpha r} e^{-\alpha t}\|a\| = M' e^{-\alpha t}\|a\|,$$

with $M' = \frac{M}{(\alpha p)^{1/p}} e^{\alpha r}$, and, since $\|\widetilde{T}(t)\phi\|_{\mathcal{E}} = 0$ for $t > r$, we have

$$\|\mathcal{T}(t)(y)\|_Y \le M_1 e^{-\alpha t}\|a\| \le M_1 e^{-\alpha t}\|y\|_Y, \text{ for } t > r,$$

where $M_1 = M + M'$.

Hence the operator $\mathcal{A}$ satisfies hypothesis **H1**. It is easily seen that the hypotheses **H2'** and **H4** on the mapping $\mathcal{R}$ are fulfilled.

As far as the operator Φ is concerned, in order to satisfy the hypothesis **H3**, we must have $\frac{M_1}{\alpha}\|\Phi\|_{\mathcal{L}(\mathcal{E},X)} < 1$. Hence, if this inequality holds, the results from Sections 3-5 hold for problem (15)-(16).

References

[1] A. Bátkai, S. Piazzera, *Semigroups and linear partial differential equations with delay*, J. Math. Anal. Appl., **264**(2001), 1-20.

[2] V. Casarino, S. Piazzera, *On the asymptotic behaviour of perturbed semigroups*, Ulmer Seminare, **3**(1998).

[3] K.-J. Engel, R. Nagel, *One-parameter semigroups for linear evolution equations*, Springer, Berlin, 1999.

[4] G. Guhring, F. Rabiger, *Linearized stability for semilinear non-autonomous evolution equations with applications to retarded differential equations*, Ulmer Seminare, **2**(1997).

[5] V. A. Trenogin, *Lyapunov theorem about the stability by linear approximation as the consequence of the implicit operators theorem*, Doklady Academii Nauk, **407**(2006), 742-746. (in Russian)

[6] V. A. Trenogin, *Asymptotic stability of trivial solution of differential equations with unbounded linearity, in Banach spaces*, ROMAI Journal, **3**, 1(2007), 207-212.

ROMAI J., **4**, 2(2008), 115–125

NEW FEATURES IN SIMULATING THE BEHAVIOR OF TURBULENT FLOWS

Adela Ionescu

Faculty of Engineering and Management of Technological Systems, University of Craiova, branch Drobeta-Turnu Severin

adaion@hotmail.coms

Abstract This paper continues the previous work in the turbulent mixing field. The mixing theory is a modern theory in the field of flow kinematics. Its mathematical methods and techniques developed the significant relation between turbulence and chaos. The turbulence is an important feature of dynamic systems with few freedom degrees, the so-called far from equilibrium systems. These are widespread between the models of excitable media.

Studying a mixing for a flow implies the analysis of successive stretching and folding phenomena for its particles, the influence of parameters and initial conditions. In the previous works, [1,2], the 3D non-periodic models exhibited a quite complicated behavior. In agreement with experiments [4], they involved some significant events - the so-called rare events. The variation of parameters had a great influence on the length and surface deformations. The 2D (periodic) case was simpler, but significant events can issue for irrational values of the length and surface unit vectors, as was the situation in 3D case. The periodic case analysis was recently started, in order to establish some statistic features of the mixing flow behavior. The aim of this paper is to get a new approach of numeric simulation of turbulent mixing. Namely, specific plotting new procedures of Maple11 soft are tested, such as the Interactive Plot Builder. A graphical comparative analysis between the discrete and the continuous time case is realized, for the same unit vector irrational values. The results should be used for further numerical study.

Keywords: turbulent mixing, numeric simulation.

2000 MSC: 76F25, 37E35.

1. INTRODUCTION

In turbulence theory, two important features are generally distinguished: the transition theory from smooth laminar flows to chaotic flows (characteristic to turbulence) and the statistic studies of the completely developed turbulent systems.

The statistical point of view of a flow has the following representation

$$x = \Phi_t(X) \quad \text{with} \quad X = \Phi_t(t=0)(X) \tag{1}$$

which must be of class C^k. From the dynamic point of view the map

$$\Phi_t(X) \longrightarrow x \tag{2}$$

is a diffeomorphism of class C^k and (1) must satisfy the relation

$$0 < J < \infty,\ J = \det\left(\frac{\partial x_i}{\partial X_j}\right),\ J = det(D\Phi_t(X)) \tag{3}$$

where D denotes the differentiation with respect to the reference configuration, in this case X. The relation (3) implies two particles, X_1 and X_2, which occupy the same position x at a moment. Non-topological behavior (like break up, for example) *is not allowed.*

Define the basic measure for the deformation, namely the *deformation gradient*, **F**

$$\mathbf{F} = \left(\nabla_X \Phi_t(\mathbf{X})\right)^T,\ F_{ij} = \left(\frac{\partial x_i}{\partial X_j}\right),\ \text{or}\ \mathbf{F} = D\Phi_t(\mathbf{X}) \tag{4}$$

where ∇_X denotes differentiation with respect to X. According to (3), **F** is not singular. The basic measure for the deformation with respect to x is the *velocity gradient* (∇_x denote differentiation with respect to x).

By differentiation of x with respect to X there are obtained the basic deformation for a material filament, and for the area of an infinitesimal material surface.

In what follows we focus on the basic deformation measures: the *length deformation* λ and *surface deformation* η, defined by the relations [5]

$$\lambda = (C : MM)^{\frac{1}{2}}, \ \eta = (\det F) \cdot \left(C^{-1} : NN\right)^{\frac{1}{2}}, \tag{5}$$

with $\mathbf{C}(= \mathbf{F}^T\mathbf{F})$ the Cauchy-Green deformation tensor, and the length and surface vectors M, N defined by

$$\mathbf{M} = d\mathbf{X}/\left|d\mathbf{X}\right|, \ \mathbf{N} = d\mathbf{A}/\left|d\mathbf{A}\right|. \tag{6}$$

The relation (5) has the following scalar form

$$\lambda = C_{ij} \cdot M_i \cdot N_j, \quad \eta = (\det F) \cdot \left(C_{ij}^{-1} \cdot N_i \cdot N_j\right) \tag{7}$$

with $\sum M_i^2 = 1$, $\sum N_j^2 = 1$.

The deformation tensor $\mathbf{F}$ and the associated tensors $\mathbf{C}$, $\mathbf{C}^{-1}$ represent the basic quantities in the deformation analysis for the infinitesimal elements.

In this framework, the mixing concept implies the stretching and folding of the material elements. If at an initial location P there is a material filament dX and an area element dA, the specific length and surface deformations are given by the relations

$$\frac{D(\ln\lambda)}{Dt} = \mathbf{D} : \mathbf{mm}, \quad \frac{D(\ln\eta)}{Dt} = \nabla\mathbf{v} - \mathbf{D} : \mathbf{nn}, \tag{8}$$

where $\mathbf{D}$ is the deformation tensor, obtained by decomposing the velocity gradient in its symmetric and non-symmetric part.

2. THE PERIODIC 2D MIXING MODEL. COMPARATIVE ANALYSIS

Studying a mixing for a flow implies the analysis of successive *stretching* and *folding* phenomena for its particles, the influence of parameters and initial conditions [4,5]. In the previous works, the study of the 3D non-periodic models exhibited a quite complicated behavior [1]. Recently the behavior of the mixing flow in 2D case was started, both for periodic [3] and non-periodic case [2]. In what follows we continue this analysis, with a different point of view. Some irrational values of the length and surface unit vectors are also chosen, like in previous works, in order to search some significant events, and compare them to 3D case.

Let us start with the following periodic 2D mixing model [5]

$$v_x = -\varepsilon \cdot x, \tag{9}$$

$$v_y = \varepsilon \cdot y, \quad 0 < t < T_{ext}$$

$$v_r = 0, \tag{10}$$

$$v_\theta = -\omega\left(r\right), T_{ext} < t < T_{ext} + T_{rot}$$

with $-1 < K < 1$, $0 < G < 1$.

In the above relations, the first part represents the extensional part and the second, the rotational part of the so- called t*endril-whorl (TW) model*.

As shown in [5], two-dimensional flows increase their length by forming two basic kinds of structures: *tendrils* and *whorls* and their combinations. The tendril-whorl flow (TW) introduced by Khakhar, Rising and Ottino (1987) is a discontinuous succession of extensional flows and twist maps. Even the simplest case is complex enough. The physical motivation for this flow is that locally, a velocity field can be decomposed into extension and rotation.

The above model is the simplest case of the TW model, where the velocity field over a single period is given by its extensional and rotational part, where T_{ext} denotes the duration of the extensional component and T_{rot} the duration of rotational component.

For the moment we study only the extensional component. So, for the system (9) the solution of the model

$$x = X \cdot \exp\left(-\varepsilon \cdot T_{ext}\right), \tag{11}$$

$$y = Y \cdot \exp\left(\varepsilon \cdot T_{ext}\right)$$

leads to the gradient deformation F and the Cauchy-Green tensors C, C^{-1} of quite simple forms. Therefore the deformations in length and surface λ^2 and η^2 has the following similar forms [3]

$$e_\lambda = 2\varepsilon \cdot \left(1 - \frac{2\exp\left(-2\varepsilon T_{ext}\right) \cdot M_1^2}{\exp\left(-2\varepsilon T_{ext}\right) \cdot M_1^2 + \exp\left(2\varepsilon T_{ext}\right) \cdot M_2^2}\right), \tag{12}$$

$$e_\eta = 2\varepsilon \cdot \left(1 - \frac{2\exp\left(-2\varepsilon T_{ext}\right) \cdot N_2^2}{\exp\left(-2\varepsilon T_{ext}\right) \cdot N_2^2 + \exp\left(2\varepsilon T_{ext}\right) \cdot N_1^2}\right), \tag{13}$$

where the condition $M_1^2 + M_2^2 = 1$, $N_1^2 + N_2^2 = 1$ must be satisfied for the length and surface unit vectors.

In what follows, the behavior of e_λ and e_η is analysed, using a new Maple11 tool, namely *Interactive Plot Builder.* Its calling sequence is the following

interactive(expr, variables), with the parameters:

expr - (optional) expression;

variables - (optional) expression of the form variables=varset.

The *interactive* command is part of the plots package. It allows us to build plots interactively.

If *expr* is an algebraic expression or a list, it is taken to be a single expression to be plotted. If expr is a set of algebraic expressions or lists, these are taken to be separate expressions to be plotted in the same graph.

If present, the *variables* option provides a complete list of the variables used in plotting.

The *Interactive Plot Builder* generates interactive plots, using *continuous time intervals.* Therefore the analysis of the mixing behavior produces useful informations, comparing to discrete case [2,3].

The recent experience revealed interesting events for irrational values of the length and surface unit vectors. Therefore, some irrational unit vectors values were chosen for this analysis, namely

(a) $(M_1, M_2) = (N_1, N_2) = \left(-\frac{1}{\sqrt{2}}, \frac{1}{\sqrt{2}}\right)$; (b) $(M_1, M_2) = (N_1, N_2) = \left(\frac{1}{\sqrt{3}}, \frac{\sqrt{2}}{\sqrt{3}}\right)$; (c) $(M_1, M_2) = (N_1, N_2) = \left(\frac{1}{\sqrt{5}}, \frac{2}{\sqrt{5}}\right)$.

For the parameter $0 < \varepsilon < 1$ there were considered two values: $\varepsilon_1 = 0.05$, $\varepsilon_2 = 0.08$. Thus, the following situations were identified:

(a1) the case (a) with ε_1; (a2) the case (a) with ε_2;

(b1) the case (b) with ε_1; (b2) the case (b) with ε_2;

(c1) the case (c) with ε_1; (c2) the case (c) with ε_2.

For each of these six cases, calculating e_λ and e_η , following the formulae (11) and (12) respectively, 12 differential equations follow [3].

The behavior of the expressions (11) and (12) was analyzed and plotted with *Interactive Plot Builder.* Between the 12 plots which have resulted, a few plots were chosen for identifying some special events. The plots were labeled according to the case of simulation.

Fig. 1- the surface deformation in the case a1)

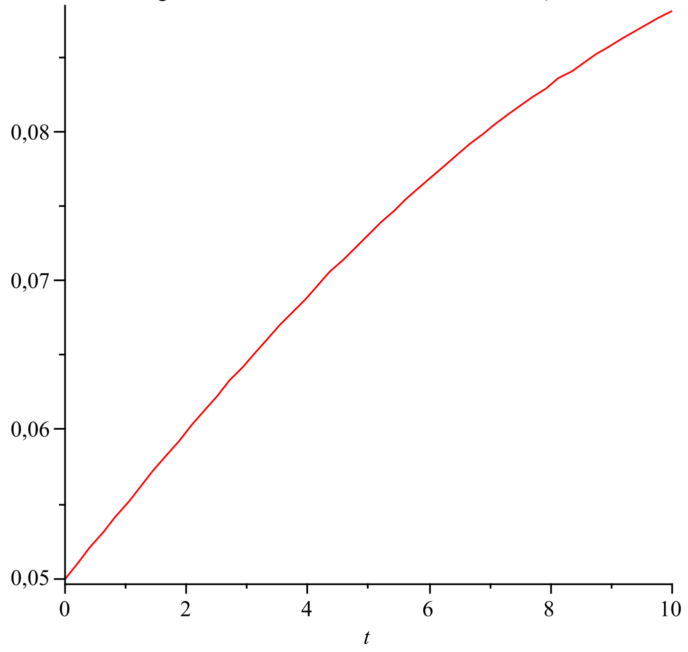

Fig.2 The surface deformation in the case a2)

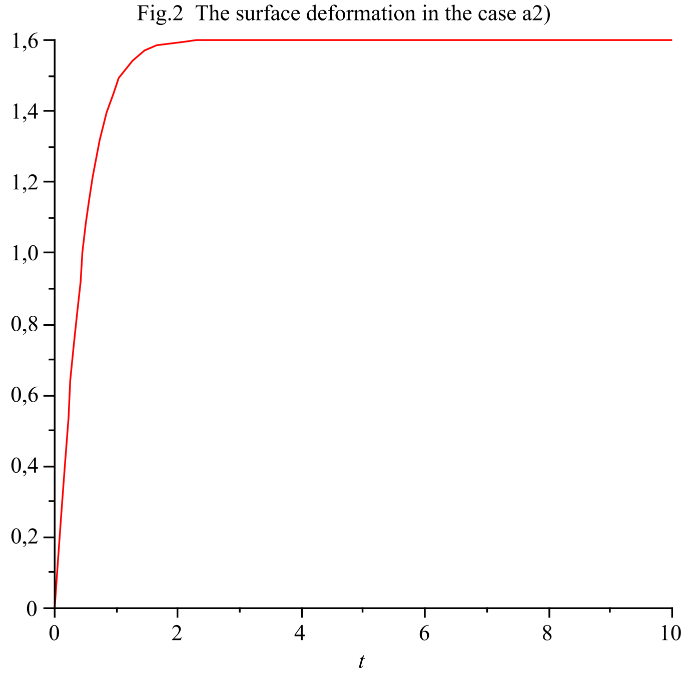

Fig. 3 The length deformation in the case b1)

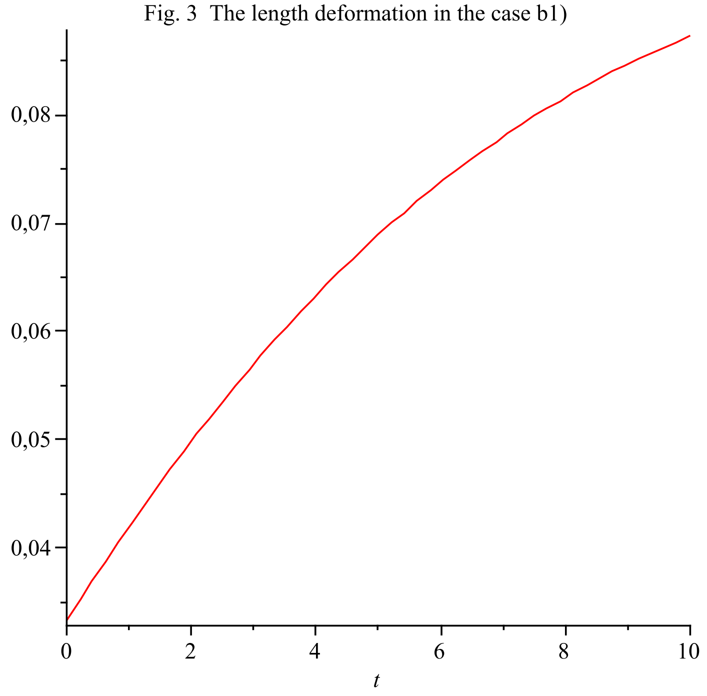

Fig. 4 The surface deformation in the case b1)

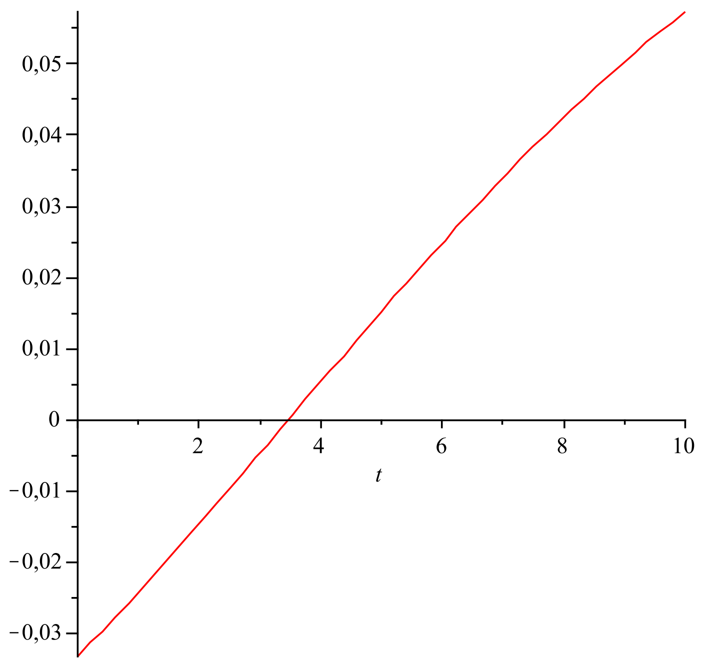

Fig. 5 The surface deformation in the case b2)

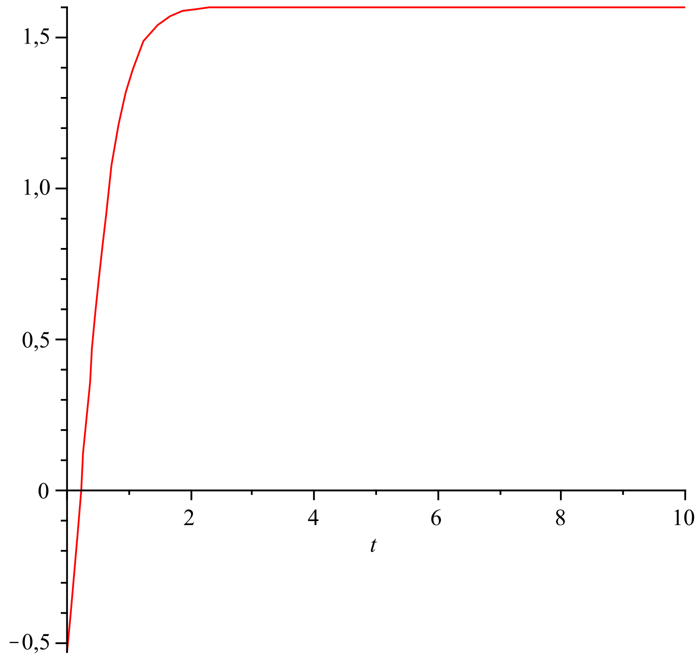

Fig. 6 The surfece deformation in the case c2)

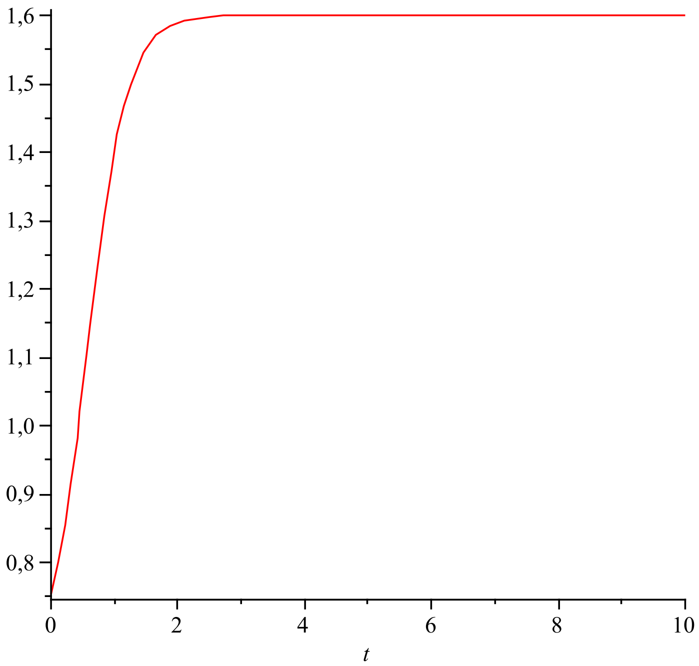

3. CONCLUSIONS. REMARKS

1.Compared to the discrete case, in the continuous time interval case, the behavior of both length and surface deformation seems to be linear. Despite this fact, the deformation is not always linear. It suffices to take into account the cases a1) and b1) for e_λ, b2) for e_η, respectively, as in [3]. The plots are as follows

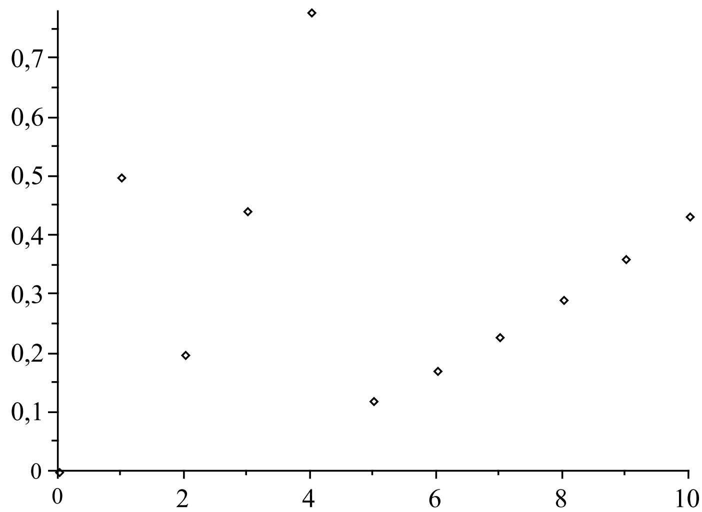

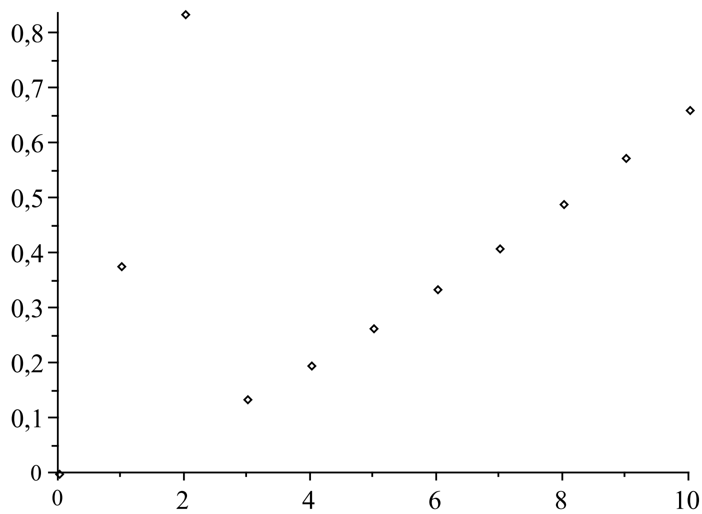

Looking at the above plots, it seems surprising *that the same expression, with the same parameter values, when studied in discrete time interval produces*

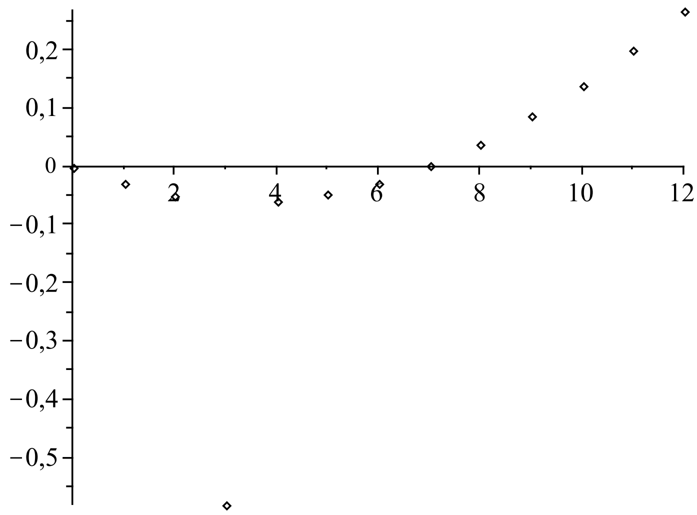

a specific output type, and when studied in continuous time produces another output type.

2. It happens that both the length and surface deformation have a *negative behavior*, although only a small time scale was considered, a 0..10 scale. Thus, comparing to the cases studied in [1], it can be assessed that there can issue significant differences between output data for two plot builders. The Interactive Plot Builder is not more accurate than the discrete plot builder, in spite of the fact that it is faster.

3. It can be assessed, as for 2D periodic case [2], that there *irrational unit vector values* could produce nonlinear phenomena. As an immediate aim, more irrational unit vectors values will be taken into account. That will be useful also for studying the efficiency of deformations, in length and also in surface. As perturbing the initial model, the calculus could become quite complex, therefore a parametric approach would be very useful.

4. The analysis of the length and surface deformation for more irrational values in the periodic case, could match the experiments in [6], as was the situation in 3D case. Moreover, *reiterative events* can be observed. This allows us to take into account the possibility of building some fractal sets. This is a next aim.

References

[1] Ionescu, A., *The structural stability of biological oscillators. Analytical contributions*, Ph.D. Thesis., Politechnic University of Bucharest, 2002.

[2] Ionescu, A., Costescu, M., *Some qualitative features of 2D periodic mixing model*, Acta Universitatis Apulensis (Mathematics-Informatics), **15**(2008), Univ. of Alba-Iulia, 387-396.

[3] Ionescu, A., Costescu, M., *Computational aspects in excitable media. The case of vortex phenomena*, Int. J. of Computing, Communications, Control, **1**(2006), Suppl. Issue: Proceedings of ICCCC2006, 280-284.

[4] Ottino, J. M., Ranz W. E., Macosko C. W., *A framework for the mechanical mixing of fluids*, AlChE J., **27**(1981), 565-577.

[5] Ottino, J. M., *The kinematics of mixing: stretching, chaos and transport*, Cambridge University Press, 1989.

[6] Săvulescu, St. N., *Applications of multiple flows in a vortex tube closed at one end*, Internal Reports, CCTE, IEA, Bucharest, (1996-1998).

ROMAI J., **4**, 2(2008), 127–134

AVOIDING BANKRUPTCY AT ALL COSTS

Mario Lefebvre

Department of Mathematics and Industrial Engineering, École Polytechnique,

Montréal, Canada

mlefebvre@polymtl.ca

Abstract Assuming that the value of the stock of a company at time t can be represented as a controlled one-dimensional Bessel process, we consider the problem of finding the control that minimizes the mathematical expectation of a cost function with quadratic control costs on the way. Two terminal cost functions, which are infinite if the process hits the origin before a given positive boundary, are used and the optimal control is obtained explicitly in each case.

Keywords: Bessel process, optimal control, Brownian motion, first-passage time.

2000 MSC: 93E20.

1. INTRODUCTION

Let $\{X(t), t \geq 0\}$ be a one-dimensional controlled Bessel process defined by the stochastic differential equation

$$dX(t) = \frac{\beta - 1}{2X(t)}\,dt + bu(t)\,dt + dB(t), \tag{1}$$

where $\{B(t), t \geq 0\}$ is a standard Brownian motion, $u(t)$ is the control variable and $\beta > 0$ and $b \neq 0$ are constants. We want to find the value of the control $u^*(t)$ that minimizes the expected value of the cost criterion

$$J(x) = \int_0^{T(x)} \tfrac{1}{2} q u^2(t)\,dt + K[X(T), T],$$

where $x = X(0)$, $T(x)$ is a random variable, q is a positive constant and K is the termination cost function.

Using a result due to Whittle ([4], p. 289), we can state that

$$u^* \; (= u^*(0)) = \frac{1}{b}\frac{G'(x)}{G(x)} \tag{2}$$

with

$$G(x) := E\left[\exp\{-\alpha K[x(\tau), \tau]\} \mid x(0) = x\right], \tag{3}$$

in which

$$\alpha := \frac{b^2}{q},$$

$\{x(t), t \geq 0\}$ is the *uncontrolled* process that corresponds to $\{X(t), t \geq 0\}$ [that is, we set $u(t) \equiv 0$ in (1)] and τ is the same as T, but for $\{x(t), t \geq 0\}$.

Remark. In fact, the condition $P[\tau(x) < \infty] = 1$ must hold for (2) to be valid.

In [3], the author defined the random variable

$$T(x) = \inf\{t > 0 : X(t) = d \mid X(0) = x < d\}$$

and he chose (in particular)

$$K[X(T), T] = K(T) = \begin{cases} 0 & \text{if } T \geq t_0, \\ \infty & \text{if } T < t_0. \end{cases}$$

Hence, the aim was to force the controlled process $\{X(t), t \geq 0\}$ to stay in the continuation region $C := (-\infty, d)$ until a fixed time t_0. We find that

$$u^* = \frac{1}{b} \frac{H'(x)}{H(x)},$$

where

$$H(x) := P[\tau(x) \geq t_0] = 1 - F_{\tau(x)}(t_0).$$

Thus, the optimal control u^* was obtained from the distribution function $F_{\tau(x)}$ of the random variable $\tau(x)$.

In the present paper, we consider the controlled process $\{X(t), t \geq 0\}$ in the interval $[c, d]$, where $c \geq 0$. We want the process to leave the continuation region through its right-hand side d. If $X(t)$ represents the value of the stock of a certain company at time t, and if we choose $c = 0$, then the aim is to find the value of $u(t)$ that enables the company to avoid bankruptcy (corresponding to $X(t) = 0$), while taking the quadratic control costs $\frac{1}{2} q u^2(t)$ into account. In this application, $u(t)$ would be the amount of capital that must be invested in the company to prevent it from going bankrupt.

In Section 2, we will define

$$T(x) = \inf\{t > 0 : X(t) = c \text{ or } d \mid X(0) = x\} \tag{4}$$

and we will take

$$K[X(T), T] = K[X(T)] = -\lambda \ln[X(T)], \tag{5}$$

where $\lambda > 0$. If $c = 0$, we see that we give an infinite penalty if $X(t)$ reaches the origin (before d). The constant d can be chosen as large as we want. The larger it is, the longer it will take $X(t)$ to attain this value, which means that the company will be in business for a long period of time.

By giving an infinite penalty if the final value of $X(t)$ is equal to c, we force the process to avoid this boundary. We assume that there are no constraints on the control variable $u(t)$. Thus, we can state that we are ready to avoid bankruptcy at all costs.

Next, in Section 3, we will change the definition of the final time $T(x)$ to

$$T(x) = \inf\{t > 0 : \{X(t) = d\} \cap \{X(s) \neq c \; \forall s \in (0,t)\} \mid X(0) = x \in (c,d)\}. \tag{6}$$

That is, $T(x)$ is now the time it takes $\{X(t), t \geq 0\}$ to reach the boundary at d, without having ever touched the boundary at c. Moreover, we will choose

$$K[X(T), T] = K(T) = \lambda T, \tag{7}$$

where, as above, $\lambda > 0$.

Remark. If the controlled process $\{X(t), t \geq 0\}$ actually hits c before d, we set $T = \infty$ (because the joint event $\{X(t) = d\} \cap \{X(s) \neq c \; \forall s \in (0,t)\}$ will never occur). Therefore, once again, we give an infinite penalty when $X(T) = c$.

We will obtain an explicit formula for the optimal control u^* in the two cases mentioned above, and we will conclude this work with a few remarks in Section 4.

2. OPTIMAL CONTROL WHEN $\boldsymbol{K[X(T), T] = -\lambda \ln[X(T)]}$

First, we mention that if we want the constant c to take the value 0 in the definition (4) of $T(x)$, then the constant β in (1) must be in the interval $[0, 2)$. Indeed, when $0 < \beta < 2$, the origin is a regular boundary for the Bessel process $\{x(t), t \geq 0\}$ defined by

$$dx(t) = \frac{\beta - 1}{2x(t)} dt + dB(t), \tag{8}$$

while it is an exit boundary if $\beta = 0$ ([2], p. 239). In both cases, $\{x(t), t \geq 0\}$ can reach the origin. However, if $\beta \geq 2$, then 0 is an entrance boundary, which is not attainable in finite expected time.

Remarks. i) In the case $\beta = 1$, $\{x(t), t \geq 0\}$ is a standard Brownian motion defined on $[c, d]$, with $c \geq 0$. Actually, $\{x(t), t \geq 0\}$ is the absolute value of a Brownian motion process if $\beta = 1$.

ii) We could generalize Eq. (8) by multiplying $dB(t)$ by a positive constant σ. However, a Bessel process is traditionally defined with $\sigma = 1$.

Because the interval $[c, d]$ is bounded, it is not difficult to justify that the condition $P[\tau(x) < \infty] = 1$ is satisfied. Therefore, we can get the optimal control u^* from (2).

With the termination cost function defined in (5), the function $G(x)$ in (3) becomes

$$G(x) = E\left[x^{\alpha\lambda}(\tau) \mid x(0) = x\right].$$

We can write that

$$G(x) = c^{\alpha\lambda} P[x(\tau) = c \mid x(0) = x] + d^{\alpha\lambda} P[x(\tau) = d \mid x(0) = x].$$

Let $\pi_d(x) := P[x(\tau) = d \mid x(0) = x]$. The function π_d satisfies the Kolmogorov backward equation

$$\pi_d''(x) + \frac{\beta - 1}{x} \pi_d'(x) = 0,$$

and is such that

$$\pi_d(c) = 0 \quad \text{and} \quad \pi_d(d) = 1.$$

We easily find that, if $\beta \neq 2$,

$$\pi_d(x) = \frac{c^{2-\beta} - x^{2-\beta}}{c^{2-\beta} - d^{2-\beta}} \quad \text{for } c \leq x \leq d.$$

When $\beta = 2$, we obtain that

$$\pi_d(x) = \frac{\ln x - \ln c}{\ln d - \ln c} \quad \text{for } c \leq x \leq d.$$

Since $P[x(\tau) = c \mid x(0) = x] = 1 - \pi_d(x)$, we have

$$G(x) = c^{\alpha\lambda} \left(\frac{x^{2-\beta} - d^{2-\beta}}{c^{2-\beta} - d^{2-\beta}} \right) + d^{\alpha\lambda} \left(\frac{c^{2-\beta} - x^{2-\beta}}{c^{2-\beta} - d^{2-\beta}} \right) \quad \text{if } \beta \neq 2$$

and

$$G(x) = \frac{c^{\alpha\lambda}(\ln d - \ln x) + d^{\alpha\lambda}(\ln x - \ln c)}{\ln d - \ln c} \quad \text{if } \beta = 2.$$

Making use of (2), we can now state the following proposition.

Proposition 2.1. *The optimal control, when the termination cost function is the one defined in (5), is given, for $c < x < d$, by*

$$u^* = \frac{1}{b} \frac{\left(c^{\alpha\lambda} - d^{\alpha\lambda}\right)(2-\beta)x^{1-\beta}}{c^{\alpha\lambda}\left(x^{2-\beta} - d^{2-\beta}\right) + d^{\alpha\lambda}\left(c^{2-\beta} - x^{2-\beta}\right)} \quad \textit{if } \beta \neq 2 \qquad (9)$$

and

$$u^* = \frac{1}{bx} \frac{d^{\alpha\lambda} - c^{\alpha\lambda}}{c^{\alpha\lambda}\ln(d/x) + d^{\alpha\lambda}\ln(x/c)} \quad \textit{if } \beta = 2.$$

Remarks. i) If $\beta \in [0, 2)$, we can set $c = 0$. Then (9) reduces to

$$u^* = \frac{1}{b} \frac{2-\beta}{x} \quad \text{for } 0 < x < d.$$

Moreover, in the case when $\{x(t), t \geq 0\}$ is a standard Brownian motion (so that $\beta = 1$), the optimal control is simply $u^* = 1/(bx)$.

ii) If $\beta \in [0, 2)$ and $c = 0$, the optimally controlled process $\{X^*(t), t \geq 0\}$ satisfies the stochastic differential equation

$$dX^*(t) = \frac{3-\beta}{2X^*(t)} dt + dB(t).$$

Hence, we can state that $\{X^*(t), t \geq 0\}$ is also a Bessel process, with $\beta^* = 4 - \beta$. Notice that $\beta^* \in (2, 4]$. Therefore, $\{X^*(t), t \geq 0\}$ cannot reach the origin.

In the next section, the case when $K[X(T), T] = K(T) = \lambda T$ will be treated.

3. OPTIMAL CONTROL WHEN $K[X(T), T] = \lambda T$

When the termination cost function $K[X(T), T]$ is given by λT, where λ is a positive constant and T is now the random variable defined in (6), we must calculate $G(x) = E\left[e^{-\gamma\tau} \mid x(0) = x\right]$, where $\gamma := \alpha\lambda$ (> 0). That is, we need the moment generating function of the random variable

$$\tau = \inf\{t > 0 : \{x(t) = d\} \cap \{x(s) \neq c \; \forall s \in (0, t)\} \mid x(0) = x \in (c, d)\}.$$

The function G satisfies the Kolmogorov backward equation

$$\frac{1}{2}G''(x) + \frac{\beta - 1}{2x}G'(x) = \gamma G(x) \quad \text{for } c < x < d, \tag{10}$$

subject to $G(c) = 0$ and $G(d) = 1$. We find that

$$G(x) = \frac{d^{\theta} K_{\theta}(\sqrt{2\gamma}c)\, I_{\theta}(\sqrt{2\gamma}x)}{x^{\theta}\left[K_{\theta}(\sqrt{2\gamma}c)\, I_{\theta}(\sqrt{2\gamma}d) - K_{\theta}(\sqrt{2\gamma}d)\, I_{\theta}(\sqrt{2\gamma}c)\right]} \quad \text{for } c \le x \le d,$$

where

$$\theta := \frac{\beta}{2} - 1$$

and K_{θ} and I_{θ} are modified Bessel functions ([1], p. 374).

Proposition 3.1. *When the termination cost function is $K[X(T), T] = \lambda T$, with T defined in (6), the optimal control u^* is given by (2), where the function $G(x)$ has been calculated above.*

Because the general explicit expression for u^* is rather involved, for the sake of simplicity we will present only some particular cases.

I) First, if $\beta = 1$ (so that $\{x(t), t \ge 0\}$ is a standard Brownian motion), we obtain that

$$G(x) = \frac{\sinh[\sqrt{2\gamma}\,(x - c)]}{\sinh[\sqrt{2\gamma}\,(d - c)]} \quad \text{for } c \le x \le d.$$

Hence,

$$u^* = \frac{\sqrt{2\gamma}}{b}\coth[\sqrt{2\gamma}\,(x - c)] \quad \text{for } c < x < d,$$

in which $c \ge 0$.

II) Next, assume that $\beta = 1/2$. Then, with $c = 0$, we calculate

$$G(x) = \left(\frac{x}{d}\right)^{3/4}\frac{I_{3/4}(\sqrt{2\gamma}x)}{I_{3/4}(\sqrt{2\gamma}d)} \quad \text{for } 0 \le x \le d$$

and

$$u^* = \frac{\sqrt{2\gamma}}{b}\frac{I_{-1/4}(\sqrt{2\gamma}x)}{I_{3/4}(\sqrt{2\gamma}x)} \quad \text{for } 0 < x < d.$$

Making use of the following formula, which is valid as z tends to zero ([1], p. 375):

$$I_{\nu}(z) \sim \left(\frac{z}{2}\right)^{\nu}\frac{1}{\Gamma(\nu + 1)} \quad (\text{for } \nu \ne -1, -2, \ldots),$$

we can write that, for x very small,

$$u^* \simeq \frac{3}{2bx}.$$

III) Now, with $\beta = 3/2$ and $c = 0$, we get that

$$G(x) = \left(\frac{x}{d}\right)^{1/4} \frac{I_{1/4}(\sqrt{2\gamma}x)}{I_{1/4}(\sqrt{2\gamma}d)} \quad \text{for } 0 \leq x \leq d,$$

from which we deduce that

$$u^* = \frac{\sqrt{2\gamma}}{b} \frac{I_{-3/4}(\sqrt{2\gamma}x)}{I_{1/4}(\sqrt{2\gamma}x)} \quad \text{for } 0 < x < d.$$

This time, we obtain (if x is very small) that

$$u^* \simeq \frac{1}{2bx}.$$

IV) Finally, if we take $\beta = 2$ (and $c > 0$), the function $G(x)$ is given by

$$G(x) = \frac{I_0(\sqrt{2\gamma}c)\,K_0(\sqrt{2\gamma}x) - K_0(\sqrt{2\gamma}c)\,I_0(\sqrt{2\gamma}x)}{I_0(\sqrt{2\gamma}c)\,K_0(\sqrt{2\gamma}d) - K_0(\sqrt{2\gamma}c)\,I_0(\sqrt{2\gamma}d)} \quad \text{for } c \leq x \leq d.$$

It follows that

$$u^* = \frac{\sqrt{2\gamma}}{b} \frac{K_0(\sqrt{2\gamma}c)\,I_1(\sqrt{2\gamma}x) + I_0(\sqrt{2\gamma}c)\,K_1(\sqrt{2\gamma}x)}{K_0(\sqrt{2\gamma}c)\,I_0(\sqrt{2\gamma}x) - I_0(\sqrt{2\gamma}c)\,K_0(\sqrt{2\gamma}x)} \quad \text{for } c < x < d.$$

As $z \to 0$ ([1], p. 375),

$$I_0(z) \sim 1 \quad \text{and} \quad K_0(z) \sim -\ln z,$$

while

$$I_1(z) \sim \frac{z}{2} \quad \text{and} \quad K_1(z) \sim \frac{1}{z}.$$

Hence, if x and c are both small enough, then we can write that

$$u^* \simeq \frac{1}{2bx} \left[\frac{2 - x^2 \ln(\sqrt{2\gamma}c)}{\ln(x/c)}\right].$$

4. CONCLUSION

We have obtained (exact and) explicit expressions for the optimal control of a Bessel diffusion process when the objective is to prevent the process from ever hitting a boundary at $x = c$ (≥ 0). This work is related to the one presented in [3].

Hitting the boundary at $x = 0$ (if $\beta \in [0, 2)$) meant, in the application mentioned in Section 1, that the company went bankrupt.

The stochastic differential equation (1) could serve as a model in other situations, and the objective could then be to avoid hitting the boundary at $x = d$ instead. We could also consider the same problem, but in the infinite interval $[c, \infty)$. In that case, we would give a reward for survival in the continuation region $[c, \infty)$. To apply the result due to Whittle, one should make sure that $P[\tau(x) < \infty] = 1$. That is, the uncontrolled process must be certain to eventually hit the boundary at $x = c$. Because the interval $[c, \infty)$ is infinite, it is not obvious that $\{x(t), t \geq 0\}$ will necessarily end up at $x = c$.

Finally, we could try to solve the same type of problem as the one presented in the current paper, but for a two-dimensional diffusion process. For example, the continuation region could be a circle centered at the origin and $T(x, y)$ be the first time that the controlled process hits the boundary of this circle. The random variable $X(T)$ would then be a continuous rather than discrete random variable, and computing its mathematical expectation could prove quite difficult.

Acknowledgments

This work was supported by the Natural Sciences and Engineering Research Council of Canada.

References

[1] M. Abramowitz, I. A. Stegun, *Handbook of mathematical functions with formulas, graphs, and mathematical tables*, Dover, New York, 1965.

[2] S. Karlin, H. Taylor, *A Second course in stochastic processes*, Academic Press, New York, 1981.

[3] M. Lefebvre, *Forcing a stochastic process to stay in or to leave a given region*, Ann. Appl. Probab. **1** (1991), 167-172.

[4] P. Whittle, *Optimization over time*, **I**, Wiley, Chichester, 1982.

ROMAI J., **4**, 2(2008), 135–143

INTERACTION BETWEEN ECONOMIC DYNAMICAL SYSTEMS

Constantin Pătrăşcoiu

Faculty of Engineering and Management of Technological Systems, University of Craiova, branch Drobeta-Turnu Severin

patrascoiu@yahoo.com

Abstract The paper deals with economic dynamical systems, the state spaces of which are Riemannian manifolds. Between two economic dynamical systems, global feedforward and the feedback interaction is defined and the connection between their linearization or prolongation by derivation is discussed.

Keywords: economic dynamical system, feedforward, feedback, linearization.

2000 MSC: 91B28, 91B64.

1. FEEDFORWARD AND FEEDBACK

All mathematical objects used in this paper (manifolds, functions, tensor fields, connections etc.) are smooth (of class C^{∞}).

Consider two economic dynamical systems with configuration (or state space) Riemann manifolds (M, g), respectively $(N, g\prime)$; let (U, φ) be a local chart on $M, x \in U, \varphi(x) = (x^1, x^2, ..., x^m) \in \varphi(U) \subset \mathbb{R}^m$ and let (V, ψ) be a local chart on $N, y \in V, \psi(y) = (y^1, y^2, ..., y^n) \in \psi(V) \subset \mathbb{R}^n$.

All possible behaviors of the two economic dynamical systems can be described locally by the set of continuous and smooth, time dependent configuration coordinates

$$x^i = x^i(t), i = 1, 2, ..., m, \tag{1}$$

$$y^k = y^k(t), k = 1, 2, ..., n. \tag{2}$$

Suppose that the feedforward command of the first economic dynamical system upon the second one is defined by the smooth map $f : M \longrightarrow N$, which in local coordinates is given by the nonlinear functional transformation

$$y^k = f^k(x^i), k = 1, 2, ..., n; i = 1, 2, ..., m. \tag{3}$$

Its inverse, the feedback map from the second dynamical system to the first, is defined by the smooth map $h = f^{-1} : N \longrightarrow M$, which in local coordinates is given by the nonlinear functional transformation

$$x^i = h^i(y^k), k = 1, 2, ..., n; i = 1, 2, ..., m. \tag{4}$$

So far the coordinate transformations (3) and (4) are completely general, nonlinear and unknown, while the corresponding transformations of velocities are linear and homogeneous

$$\dot{y}^k = \sum_{i=1}^{m} \frac{\partial f^k}{\partial x^i} \dot{x}^i, \ k = 1, 2, ..., n; \ i = 1, 2, ..., m, \tag{5}$$

$$\dot{x}^i = \sum_{k=1}^{n} \frac{\partial f^k}{\partial y^k} \dot{y}^k, \ k = 1, 2, ..., n; \ i = 1, 2, ..., m. \tag{6}$$

Representing two autonomous economic dynamical systems, given by two sets of ordinary differential equations, relations (5) and (6) define two velocity vector fields.

The solution of the above equations system gives the flow, consisting of integral curves of the vector field, such that all vectors from the vector field are tangent to the integral curves at different points.

Geometrically, a velocity vector field is defined as a cross-section of the tangent bundle of the manifold.

In our case, the velocity vector-field with coordinates

$$X^i = \dot{x}^i(x^i, t), i = 1, 2, ..., m,$$

represents a cross-section of the tangent bundle (TM, π_M, M), i.e. $X : M \longrightarrow TM$ and $\pi_M \circ X = id_M$.

The velocity vector-field with coordinates

$$Y^k = \dot{y}^k(y^k, t), \ k = 1, 2, ..., n$$

represents a cross-section of the tangent bundle (TN, π_N, N), i.e. $Y : N \longrightarrow TN$ and $\pi_N \circ Y = id_N$.

In this way, two local velocity vector fields, X and Y, give local representation for the following two global tangent maps

$$Tf : TM \longrightarrow TN \text{ and } Th : TN \longrightarrow TM.$$

Obviously, the diagrams

$$\begin{array}{ccc} TM & \xrightarrow{Tf} & TN \\ X\uparrow & & \uparrow Y \\ M & \xrightarrow{f} & N \end{array}, \qquad \begin{array}{ccc} TM & \xleftarrow{Th} & TN \\ X\uparrow & & \uparrow Y \\ M & \xleftarrow{h} & N \end{array} \tag{7}$$

commute.

The acceleration vector field is defined as the absolute time derivative, of the velocity vector field. The corresponding acceleration vector fields A and B, as time rates of change of the two velocity vector fields X and Y in local coordinates, are given by

$$A^i = \dot{X}^i(x^i, \dot{x}^i, t), i = 1, 2, ..., m,$$
$$B^k = \dot{Y}^k(y^k, \dot{y}^k, t), k = 1, 2, ..., n.$$

Recall that if M is a manifold, there exist a connection on M, i.e. a map

$$\nabla : X(M) \times\ X(M) \to X(M), \nabla(X_1, X_2) = \nabla_{X_1} X_2$$

such that the following conditions

$$\nabla_{f_1X_1+f_2X_2} X_3 = f_{1X_1} X_3 + f_2 \nabla_{f_2X_2} X_3;$$
$$\nabla_{X_1}(X_2 + X_3) = \nabla_{X_1} X_2 + \nabla_{X_1} X_3;$$
$$\nabla_{X_1}(fX_2) = (X_1 f)X_2 + f \nabla_{X_1} X_2;$$

hold for all vector fields $X_1, X_2, X_3 \in$X(M), and for all differentiable real function f_1, f_2, on M.

In our case, (M, g) is a Riemannian manifold, hence there exists a unique connection $\nabla_{X_1} X_2 - \nabla_{X_2} X_1 = [X_1, X_2]$ symmetric and compatible with the metric g, $(X_1 g(X_2, X_3) = g(\nabla_{X_1} X_2, X_3) + g(X_2, \nabla_{X_1} X_3))$, called the Levi-Civita connection.

We shall use the Levi-Civita connection on the Riemann manifolds M and N.

Let (U, φ) be a local coordinates (local map) around a point $x \in M$. The absolute (or covariant) time derivative of a contravariant vector field X on M, with local coordinates (X^i) along a curve, $x^i = x^i(t)$, $i = 1, 2, ..., m$, is given by

$$\nabla_{\dot{x}(t)} X = \sum_{i=1}^{m} (\dot{X}^i + \sum_{j,s=1}^{m} \Gamma^i_{js} \dot{x}^j X^s) \frac{\partial}{\partial x^i} = \sum_{i=1}^{m} (\ddot{x}^i + \sum_{j,s=1}^{m} \Gamma^i_{js} \dot{x}^i \dot{x}^s) \frac{\partial}{\partial x^i}, \tag{8}$$

where the m^3 differentiable functions $\Gamma^i_{js} : U \longrightarrow \mathbb{R}$, are the Christoffel symbols defined by

$$\nabla_{\frac{\partial}{\partial x^j}} \frac{\partial}{\partial x^s} = \sum_{i=1}^{m} \Gamma^i_{js} \frac{\partial}{\partial x^i}. \tag{9}$$

In our case (because ∇ is the Levi-Civita connection) we have

$$\Gamma^i_{js} = \frac{1}{2} \sum_{l=1}^{m} g^{il} \left(\frac{\partial g_{lj}}{\partial x^s} + \frac{\partial g_{ls}}{\partial x^j} + \frac{\partial g_{js}}{\partial x^l} \right), \text{ where } (g^{il}) = (g_{il})^{-1}. \tag{10}$$

So, locally, the acceleration vector field A is given by

$$A = \sum_{i=1}^{m} (\ddot{x}^i + \sum_{j,s=1}^{m} \Gamma^i_{js} \dot{x}^j \dot{x}^s) \frac{\partial}{\partial x^i}. \tag{11}$$

Similarly the acceleration vector-field B defined on the manifold N, in local coordinates $(y^1, y^2, ..., y^n)$, is given by

$$B = \sum_{q=1}^{n} (\ddot{y}^q + \sum_{j,s=1}^{n} \Gamma^q_{js} \dot{y}^j \dot{y}^s) \frac{\partial}{\partial x^i}, \tag{12}$$

where Γ^q_{js} denote the second-order Christoffel symbols of the Levi-Civita connections on the manifold N, determined by the Riemann structure of configuration manifold N.

Geometrically, an acceleration vector field is defined as a cross-section of a second tangent bundle of the manifold. In our case the acceleration vector field A, represents a cross-section of the second tangent bundle (TTM, π_{TM}, TM), i.e. $A : TM \longrightarrow TTM$ and $\pi_{TM} \circ A = id_{TM}$, while the acceleration vector field B, represents a cross-section of the second tangent bundle (TTN, π_{TN}, TN), i.e., $B : TN \longrightarrow TTN$ and $\pi_{TN} \circ B = id_{TN}$.

The diagrams: $\begin{array}{ccc} TTM & \xrightarrow{TTf} & TTN \\ A\uparrow & & \uparrow B \\ TM & \xrightarrow{Tf} & TN \end{array}$, $\begin{array}{ccc} TTM & \xleftarrow{TTh} & TTN \\ A\uparrow & & \uparrow B \\ TM & \xleftarrow{Th} & TN \end{array}$ commute.

Finally, the two following commutative diagrams

$$\begin{array}{ccc} TTM & \xrightarrow{TTf} & TTN \\ A\uparrow & & \uparrow B \\ TM & \xrightarrow{Tf} & TN \\ X\uparrow & & \uparrow Y \\ M & \xrightarrow{f} & N \end{array} , \qquad \begin{array}{ccc} TTM & \xleftarrow{TTh} & TTN \\ A\uparrow & & \uparrow B \\ TM & \xleftarrow{Th} & TN \\ X\uparrow & & \uparrow Y \\ M & \xleftarrow{h} & N \end{array} \tag{13}$$

formally define the global feedforward and feedback interaction between two economic dynamical systems given by: $\dot{x} = X(x)$ and $\dot{y} = Y(y)$ on the Riemann manifolds M and N.

Remark. We used a Riemannian structure on configuration manifolds M and N. If (N, g) is a Riemannian manifold and $f : M \longrightarrow N$ is an immersion, then f^*g is a Riemannian metric in M (the induced metric) and we can use this Riemannian structure on the configuration manifold M. Recall that if (M, g) and (N, g') are Riemannian manifolds, a diffeomorphism $f : M \longrightarrow N$ is said to be an isometry if $g = f^*g'$. So, we can use isometric Riemannian structure on the configuration manifolds M and N if the feedforward command of the first dynamical system upon the second dynamical system is a diffeomorphism.

2. PROLONGATION BY DERIVATION AND LINEARIZATION OF AN AUTONOMOUS ECONOMIC DYNAMICAL SYSTEM

Let (M, g) be a semi-Riemannian manifold. Recall that a semi -Riemannian structure on the $m-$dimensional manifold M is defined by a semi- Riemannian metric g on M, i.e. a smooth symmetric tensor field of type $(0, 2)$, which to each point $x \in M$ assigns a nondegenerate inner product $g(x)$ on the tangent space T_xM, of signature (r, s), $r + s = m$.

Let X be a vector field on the manifold M and the autonomous economic dynamical system given by

$$\dot{x} = X(x). \tag{14}$$

The function $f : M \longrightarrow \mathbb{R}$, $f(x) = \frac{1}{2} g(X(x), X(x))$ determined by the semi-Riemannian metric g and the vector field X is called [4] energy density of the vector field X.

Let ∇ be the Levi-Civita connection of the semi-Riemannian structure (M, g). The differential system

$$\frac{\nabla \dot{x}}{dt} = \nabla_{\dot{x}} X \tag{15}$$

obtained using the semi-Riemannian version of the covariant derivative operator defined by the Levi-Civita connection is the prolongation by derivation of the differential system (14).

Remark. Differential system (15) is also the prolongation by derivation of any perturbation of system (14) obtained by adding to the right-hand side, a vector field parallel with respect to the covariant derivative, which illustrates a progression from stable to unstable flows.

Writing $\nabla X = \nabla X - g^{-1} \otimes g(\nabla X) + g^{-1} \otimes g(\nabla X)$, and putting $F = \nabla X - g^{-1} \otimes g(\nabla X)$, differential system (15) can be written in the equivalent form

$$\frac{\nabla \dot{x}}{dt} = F(\dot{x}) + g^{-1} \otimes g(\nabla X)(\dot{x}) \tag{16}$$

The external distinguished $(1,1)-$tensor field F, (characterizing the helicity of the vector field X and its flow), determined by the geometrical objects X, g, ∇, in the local coordinates $(x^1, x^2, ..., x^m)$, is given by

$$F^i_j = \nabla_j X^i - \sum_{h,k=1}^{m} g^{ik} g_{hj} \nabla_k X^h \text{ with } i, j, h, k = 1, 2, ..., m. \tag{17}$$

Differential system (15) can by modified [4] as follows

$$\frac{\nabla \dot{x}}{dt} = F(\dot{x}) + g^{-1} \otimes g(\nabla X)(X). \tag{18}$$

In the local coordinates $(x^1, x^2, ..., x^m)$, if Γ^i_{jk} represents the components of Levy- Civita connection ∇ of g, system (18) can be written

$$\frac{d^2x^i}{dt^2} + \sum_{j,k=1}^{m} \Gamma^i_{jk} \frac{dx^j}{dt}\frac{dx^k}{dt} = \sum_{j=1}^{m} F^i_j \frac{dx^j}{dt} + \nabla^i f,\ i = 1, 2, ..., m, \tag{19}$$

where $\Gamma^i_{jk}\ \frac{dx^j}{dt}$ is the gyroscopic term, and $\nabla^i f = \sum_{j,h,k=1}^{m} g^{ih} g_{kj} (\nabla_h X^k) X^j$ are the contavariant components of the gradient of energy f and represent the conservative part of the gyroscopic force.

Differential system (18) is also the prolongation of the first order differential system (14) and describes a conservative dynamics of the vector field X.

Since $g^{-1} \otimes g(\nabla X)(X) = \nabla f$, the differential system (18) can be written as

$$\frac{\nabla \dot{x}}{dt} = F(\dot{x}) + \nabla f \tag{20}$$

If $F \neq 0$, system (20) is a non-potential dynamical system with m degrees of freedom. If $F = 0$, system (20) is a potential dynamical system with m degrees of freedom.

Remark. The dynamical systems (20) is conservative because identifying the tangent bundle TM with the cotangent bundle T^*M using the semi–Riemann metric g the trajectories of the dynamical system (20) are the extremals of the Lagrangian: $L = \frac{1}{2}g(\dot{x} - X, \dot{x} - X) = \frac{1}{2}g(\dot{x}, \dot{x}) - g(X, \dot{x}) + f(x)$ and the associated Hamiltonian $H = \frac{1}{2}g(\dot{x}, \dot{x}) - f(x)$.

The linearization of an autonomous economic dynamical system given by (14) on the Euclidian space around an equilibrium point $(0, 0..0)$ is of the form $\dot{x} = Cx$, where C is a Jacobian matrix computed at equilibrium point and the linearization of its prolongation (Udriste [4]) is given by: $\frac{d^2x}{dt^2} = (C - C^t)\frac{dx}{dt} + C^tCx$

Example. The Linearization of Tobin-Benhabib-Myao economic flow along a trajectory. The configuration Riemann manifold $(\mathbb{R}^3_+, \delta_{ij})$.

This economic dynamical system reads

$$\begin{cases} \frac{dk}{dt} = sf(k) - (1-s)(\theta - q)m - nk, \\ \frac{dm}{dt} = m(\theta - \bar{p} - n), \\ \frac{dq}{dt} = \mu(\bar{p} - q)\mu(\bar{p} - q), \end{cases} \tag{21}$$

where k = the capital/work ratio; m = the money stock per head; q = the expected rate of inflation; $\bar{p} = \varepsilon(m - l(k, q)) + q$ the actual rate of inflation; $s, \theta, n, \mu, \varepsilon,$ are parameters representing saving ratio, rate of money expansion, population growth rate, speed of adjustment of expectation, speed of adjustment of price level.

The real functions $f(k)$ and $l(k, q)$ are differentiable functions.

Let $(k_0(t), m_0(t), q_0(t))$ be a trajectory of system (21). Assume that the motion of nonlinear system (21) in the neighborhood of this trajectory is

$$\begin{cases} k(t) = k_0(t) + \Delta k(t), \\ m(t) = m_0(t) + \Delta m(t), \\ q(t) = q_0(t) + \Delta q(t), \end{cases} \tag{22}$$

where $\Delta k(t)$, $\Delta m(t)$, $\Delta q(t)$ represents a small quantity. Putting

$$x(t)=\begin{pmatrix} k(t)\\ m(t)\\ q(t)\end{pmatrix},\ x_0(t)=\begin{pmatrix} k_0(t)\\ m_0(t)\\ q_0(t)\end{pmatrix},\ \Delta x(t)=\begin{pmatrix} \Delta k(t)\\ \Delta m(t)\\ \Delta q(t)\end{pmatrix},$$

,

$$F(x)=\begin{pmatrix} sf(k)-(1-s)(\theta-q)m-nk\\ m(\theta-\bar{p}-n)\\ \mu(\bar{p}-q)\end{pmatrix},$$

we obtain a matrix form of system (21)

$$\frac{d}{dt}x(t)=F(x(t)). \tag{23}$$

But $x(t)=x_0(t)+\Delta x(t)$ and because $(k_0(t),m_0(t),q_0(t))$ is a solution of system (21) we have the identity $\frac{d}{dt}x_0(t)=F(x_0(t))$. So,

$$\frac{d}{dt}x(t)=\frac{d}{dt}x_0(t)+\frac{d}{dt}\Delta x(t)=F(x_0(t)+\Delta x(t))=$$

$$=F(x_0(t))+\left(\frac{\partial F}{\partial x}\right)_{x_0(t)}\Delta x(t)+higher\,order\,terms.$$

Neglecting the higher order terms (because they contain at least quadratic quantities of Δx) we obtain the linearized system

$$\frac{d}{dt}\Delta x(t)=\left(\frac{\partial F}{\partial x}\right)_{x_0(t)}\Delta x(t),\ \Delta x(t)=x(t)-x_0(t) \tag{24}$$

where the partial derivative represents the Jacobian matrix given by

$$\left(\frac{\partial F}{\partial x}\right)_{x_0(t)}=\left\|\begin{matrix} \frac{\partial F_1}{\partial k} & \frac{\partial F_1}{\partial m} & \frac{\partial F_1}{\partial q}\\ \frac{\partial F_2}{\partial k} & \frac{\partial F_2}{\partial m} & \frac{\partial F_2}{\partial q}\\ \frac{\partial F_3}{\partial k} & \frac{\partial F_3}{\partial m} & \frac{\partial F_3}{\partial q}\end{matrix}\right\|_{x_0(t)}=$$

$$=\left\|\begin{matrix} sf'-n & -(1-s)(\theta-q) & (1-s)m\\ \varepsilon m\frac{\partial l}{\partial k} & -2\varepsilon m & m(\varepsilon\frac{\partial l}{\partial q}-1)\\ \mu\varepsilon\frac{\partial l}{\partial k} & \mu\varepsilon & -\mu\varepsilon\frac{\partial l}{\partial q}\end{matrix}\right\|_{x_0(t)}. \tag{25}$$

CONCLUSIONS. Taking account of first section, the global feedforward and feedback interaction between the economic dynamical systems $\dot{x}=X(x)$, on the Riemann manifolds M, and $\dot{y}=y(y)$, on the Riemann manifolds N, given by diagrams (13), contains the levels of the feedforward and feedback interaction between the prolongation by derivation of this systems.

Because the feedforward and feedback at the level of velocities are linear and homogenous, it is most advantageous to begin with the search of the linear function between the tangent spaces of configuration manifolds which satisfies the conditions (5), (6).

The calculations simplify if the feedforward is an isometry of configuration Riemann manifolds.

References

[1] Hirsch, M. W., Smale, S., *Differential equations, dynamical systems and linear algebra*, Academic Press, New York, 1974.

[2] Ivancevic, V., Ivancevic, T., *Applied differential geometry, a modern introduction*, World Scientific, Singapore, 2006.

[3] Pătrăşcoiu, C., Bordeaşu, I., Săceanu, C., *Command and control in interaction between two dynamical systems*, Bul. Şt. al Univ. " Politehnica" Timişoara, Seria Mecanică, Transactions on Mechanics, **53(67)**, 1(2008).

[4] Udrişte, C., Ferrara, M., Opriş, D., *Economic geometric dynamics*, Geometry Balkan Press, Bucharest, 2004.

[5] Wiggins, S., *Introduction to applied dynamical system and chaos*, Springer, New York, 1990.

ROMAI J., **4**, 2(2008), 146–168

MATHEMATICAL AND NUMERICAL MODEL OF ROCK/CONCRETE MECHANICAL BEHAVIOR IN A MULTI-PLANE FRAMEWORK

Seyed Amirodin Sadrnejad

Faculty of Civil Engineering, K.N.Toosi University of Technology,

Tehran, Iran

sadrnejad@kntu.ac.ir

Abstract Among the various mathematical and numerical simulating models of plane concrete, the multi-planes models have an excellent position. These models are not as complicated as microscopic models, such as discrete particles models, and do not have the shortcomings of macroscopic models based on the stress or strain invariants. The object of this study is the presentation of a developed multi-planes damage based model of plane concrete through a 3D finite elements code to show its abilities in crack/damage analysis of actual rock/concrete/concrete structures such as a double curvature arch dam. The proposed code not only is able to predict the crack line, but also determines which combination of loading conditions occurs on damaged multi-planes.

The presented multi-plane based model is capable of seeing both dynamic and elastoplastic behavior of rock/concretes and concrete, with a particular focus on semi-micromechanical behavior of geo-materials. The constitutive equations of this model is derived within the context of elastic behavior of the whole medium and plastic sliding of interfaces of predefined multi-plane, not missing the directional effects. The formulation incorporates explicitly the notion of the preferred direction, with a description of the medium as an assembly of discrete polyhedron elements that support the overall applied loads through contact friction and cohesion. The overall mechanical response ideally may be described on the basis of micro-mechanical behavior of discrete polyhedron elements interconnections.

According to this model, the overall deformation of any small part of the medium is composed of total elastic response and an appropriate summation of sliding, separation/closing phenomenon under the current effective normal and shear stresses on sampling planes. These assumptions adopt overall sliding, separation/closing of inter-granular points of grains included in one structural unit (discrete polyhedron elements) are summed up and contributed as the result of sliding, separation/closing surrounding boundary planes. This simply implies yielding/failure or even ill-conditioning, bifurcation response damage and fragmentation phenomena to be possible over any of the randomly oriented sampling planes. Consequently, plasticity control such as yielding should be checked at each of the planes and those of the planes that are sliding will contribute to plastic deformation. Therefore, the geo-material mass has an infinite number of yield functions usually one for each of the planes in the physical space. Compact and isotropic synthetic media are generated automatically and are used to investigate the mechanical behavior of these low-porosity materials. In the case of micro-mechanics, the model considers the two-phase, aggregate and cement medium, at a macroscopic scale.

The proposed multi-plane based model is capable of predicting the behavior of materials under different orientation of bedding plane, history of strain progression during the application of any stress/strain paths, based on five types of planar behavior of sampling planes. Validity of the proposed model is investigated through a few standard benchmark examples.

Keywords: mechanics of geo-materials, micromechanical behavior.

2000 MSC: 74L05, 74L10.

1. INTRODUCTION

A survey through the published scientific papers deals with the object of constitutive modeling of geo-materials. All models are categorized into two main classes: continuous and discontinuous models. In the first class, it is postulated that the overall mass of material is continuous and no crack/rupture/gap or fracture are allowed. On the other hand, in the last class, the material is assumed to act as an assemblage of the discrete particles, which can affect on the movements of each others. In turn, the continuous models consist of two large groups: macroscopic models in the context of damage and plasticity theory or combination of both and mesoscopic models such as micro-plane or multi-laminate models. However discontinuous models are placed into one category as microscopic models such as discrete particle models. The macroscopic models concern the definition of relation between stress and strain tensors (structural scale) and the meso-scopic models deal with the same object but in a different way. The later captures this goal by assigning of the relation between the stress and strain components of the different planes with prescribed orientations called "micro or multi planes". Finally, the microscopic models concern the discrete particle models consisting of convex polygons that are able to withstand a limited cohesion (granular scale). A description of contacts of particles as well as a bond formulation between them could lead to forces induced by particle movements. These forces are inserted into the equations of motion, which are solved numerically based on the discrete element methodology.

A technique for modeling degraded planes and enabling conventional stress/strain analysis of a multidirectional laminate through rock/concrete media including different mechanical behavior aspects, such as the induced anisotropy, softening and strength reduction, and the localization distribution at any location is presented. For the analysis, degraded planes are replaced by a continuum model with a lower stiffness matrix. The degree of stiffness reduction is estimated by acoustic emission like method by considering semi-micromechanics effective stiffness of a laminate having degraded sliding or opening through change of properties.

Given the intrinsic oriented nature of geo-material fabric similar to rock/concrete, it is important to include the effect of anisotropy in a rational way. In this respect, the major obstacles, are our ability to properly define the spatial and temporal variations of the material properties, deformability, hardening/softening and boundary conditions. The value of a model lies primarily in its ability to capture the basic trends in the material behavior and thereby provide a more realistic representation of the problem.

2. FROM SLIP PLANES TO MICRO PLANES

The basic idea, namely that of the constitutive material behavior as a relationship between strain and stress tensors which can be "assembled" from the behavior of material, on the planes with different orientations within the material such as slip planes, micro cracks, particle contacts etc., might be traced back to the failure envelopes of Mohr (1900) and the "slip theory of plasticity" of G. I. Taylor (1938) who was the first that implemented this mentioned theory for modeling the behavior of polycrystalline metals. Taylor's idea was formulated in detail by Batdorf and Budiansky (1949). This theory was soon recognized as the most realistic constitutive model for plastic-hardening metals. It was refined in a number of subsequent works (e.g. Lin and Ito 1965, 1966, Kröner 1961, Budianski and Wu 1962, Hill, 1965, 1966, Rice, 1970). It was used in arguments about the physical origin of strain hardening, and was shown to allow easy modeling of anisotropy as well as the vertex effects for loading increment to the side of a radial path in stress space. All formulations considered that only the inelastic shear strains ('slips'), with no inelastic normal strain, were taking place on what is now called the 'micro-planes'. The theory was also adapted to anisotropic rocks and soils under the name "multi laminate model" (Zienkiewicz and Pande 1977, Pande and Sharma 1981, 1982; Pande and Xiong 1982).

In these works there is a common assumption that the planes of plastic slip in the material (in those studies called the 'slip-planes' and in this article called the 'micro-planes') are constrained statically to the stress ('macro-stress') tensorσ_{ij} (i.e. the stress vector on each 'micro-plane' was the projection ofσ_{ij}). The static constraint formulation was extensively used under the name of slip theory for metals or multi-laminate theory for anisotropic rocks until the first application of this theory by Bažant and Gambarova in 1984 and Bažant in 1984, to continuum damage mechanics and cohesive-frictional materials, who, for the first time, changed its name from slip theory or multi-laminate theory to micro-plane theory.

In all multi-plane models, such as slip-planes or multi-laminate models, first the macro-stress tensor was projected on the micro-planes and then by introducing on-plane constitutive laws, the micro-strain components were calculated and finally the macro-strain tensor was identified by superposition of on-plane micro-strain components upon any of sampling plane transformation matrix obtained through direction cosines of sampling points on the surface of a unit sphere

$$\int_{\Omega} f\,(x, y, z)\, d\Omega = 4\pi \sum_{p} W_p f\,(x_p, y_p, z_p). \tag{1}$$

Now consider the stress tensor σ_{ij} in the macro-level state at the center of the unit sphere as always is used in the micro-plane models. Then, we are going to project this tensor on the planes, which are tangent to the surface of the sphere at the prescribed points. The number and position of these points are determined depending on the numerical integration formulation which was elected for doing integration of an arbitrary function over the surface of the unit sphere. It is worth noting that the origin of the initiation and propagation of the multi-plane models including micro-plane or multi-laminate models are used as this mathematical numerical formulation for integration. Here, for this job, we use a precise formulation of 26 integration points. In Table 1, direction cosines and weights of the integration points and in fig. 1, their positions on the surface of the unit sphere are shown. If we project the stress tensor to the surface of the sphere, we have

$$\begin{gathered} \sigma_N = N_{ij}\sigma_{ij},\ N_{ij} = n_i n_j, \\ \sigma_M = M_{ij}\sigma_{ij},\ M_{ij} = \left(m_i n_j + m_j n_i\right)/2, \\ \sigma_L = L_{ij}\sigma_{ij},\ L_{ij} = \left(l_i n_j + l_j n_i\right)/2 \end{gathered} \tag{2}$$

where n_i, $\quad i = 1,2,3$ are the direction cosines of the unit vector normal to the plane and m_i, l_i, $\quad i = 1,2,3$ are the direction cosines of two orthogonal unit vectors tangent to the plane.

Direction Cosines			Weight	Direction cosins			Weight
ℓ_i	m_i	n_i	W_i	ℓ_i	m_i	n_i	W_i
$\sqrt{1/3}$	$\sqrt{1/3}$	$\sqrt{1/3}$	27/840	$\sqrt{1/3}$	$-\sqrt{1/3}$	$\sqrt{1/3}$	27/840
$-\sqrt{1/3}$	$\sqrt{1/3}$	$\sqrt{1/3}$	27/840	$-\sqrt{1/3}$	$-\sqrt{1/3}$	$\sqrt{1/3}$	27/840
$\sqrt{1/2}$	$\sqrt{1/2}$	0.0	32/840	$-\sqrt{1/2}$	$\sqrt{1/2}$	0.0	32/840
$\sqrt{1/2}$	0.0	$\sqrt{1/2}$	32/840	$-\sqrt{1/2}$	0.0	$\sqrt{1/2}$	32/840
0.0	$-\sqrt{1/2}$	$\sqrt{1/2}$	32/840	0.0	$+\sqrt{1/2}$	$\sqrt{1/2}$	32/840
1.0	0.0	0.0	40/840	0.0	1.0	0.0	40/840
0.0	0.0	1.0	40/840				

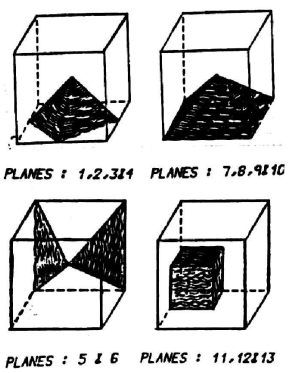

Fig. 1. Definition of micro-planes.

For convenience of calculations, one of the unit vectors tangent to the plane is assumed to be horizontal (parallel to $x - y$ plane). For instance, the projection of the stress tensor on the plane number 1 results in

$$\sigma_N = \frac{1}{3}\left(\sigma_x + \sigma_y + \sigma_z\right) + \frac{2}{3}\left(\tau_{xy} + \tau_{yz} + \tau_{zx}\right),$$
$$\sigma_M = \frac{1}{\sqrt{6}}\left(-\sigma_x + \sigma_y + \tau_{yz} - \tau_{zx}\right), \quad (3)$$
$$\sigma_L = \frac{1}{\sqrt{18}}\left(\sigma_x + \sigma_y - 2\sigma_z + 2\tau_{xy} - \tau_{yz} - \tau_{zx}\right),$$

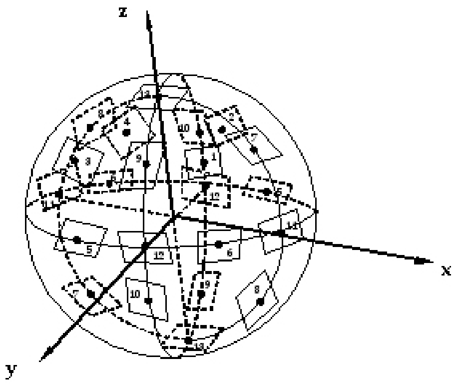

Fig. 2. Position of integration points on the unit sphere' surface.

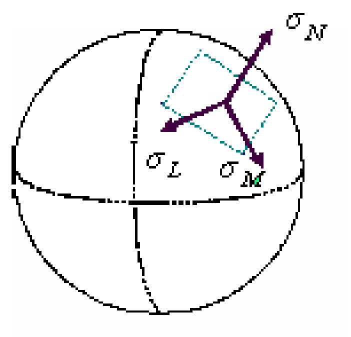

Fig. 3. Projection of stress tensor on the surface of unit sphere.

In order to obtain the original stress tensor from its projections on the micro-planes, first necessary to transfer every stress vector on the micro-plane from local coordinate to the global coordinate system and then we can add them up according to their weightings. Obviously, the result must be equal to numerical integration of the on-plane stress tensor. This numerical integration is a crucial step in the construction of any micro-plane model. In order to transfer every micro-stress vector to the macro state the following transition matrix can be written

$$T_p = \begin{bmatrix} N_{11} & M_{11} & L_{11} \\ N_{22} & M_{22} & L_{22} \\ N_{33} & M_{33} & L_{33} \\ N_{12} & M_{12} & L_{12} \\ N_{23} & M_{23} & L_{23} \\ N_{13} & M_{13} & L_{13} \end{bmatrix}_p . \tag{4}$$

The subscript p denotes any specified micro-plane. So, we can write

$$\hat{\sigma}_p = T_p.\bar{\sigma} = T_p.\sigma : N_p, \tag{5}$$

$$\sigma : N_p = \begin{bmatrix} n_1 & n_2 & n_3 \\ m_1 & m_2 & m_3 \\ l_1 & l_2 & l_3 \end{bmatrix} \begin{bmatrix} \sigma_x & \tau_{xy} & \tau_{xz} \\ \tau_{xy} & \sigma_y & \tau_{yz} \\ \tau_{xz} & \tau_{yz} & \sigma_z \end{bmatrix} \begin{bmatrix} n_1 \\ n_2 \\ n_3 \end{bmatrix} . \tag{6}$$

For example, by transforming the micro-stress vector of the plane 1 to the macro level, we reach to the following six components vector

$$\hat{\sigma}_1 = \frac{1}{6} \left\{ \begin{array}{l} 2\left(\sigma_x + \tau_{xy} + \tau_{xz}\right) \\ 2\left(\sigma_y + \tau_{xy} + \tau_{yz}\right) \\ 2\left(\sigma_z + \tau_{zy} + \tau_{xz}\right) \\ \sigma_x + \sigma_y + 2\tau_{xy} + \tau_{yz} + \tau_{xz} \\ \sigma_y + \sigma_z + \tau_{xy} + 2\tau_{yz} + \tau_{xz} \\ \sigma_x + \sigma_z + \tau_{xy} + \tau_{yz} + 2\tau_{xz} \end{array} \right\} . \tag{7}$$

By summing up the transformed six component vectors according of their weighting functions, we obtain

$$\sum_{p=1}^{26} W_p \hat{\sigma}_P = \frac{1}{3} \left\{ \begin{array}{cccccc} \sigma_x & \sigma_y & \sigma_z & \tau_{xy} & \tau_{yz} & \tau_{zx} \end{array} \right\}^T , \tag{8}$$

where the subscript p denotes any specified micro-plane.

As a general rule for the numerical integration of an arbitrary function $f(x, y, z)$ over the surface of unit sphere, we can use the following 26 sampling point equations

$$\int_{\Omega} f(x, y, z)\, d\Omega = 4\pi \sum_{p=1}^{26} W_p f(x_p, y_p, z_p). \tag{9}$$

Comparing equations (8) and (9) we can write

$$\int_{\Omega} \mathbf{T}.\boldsymbol{\sigma} : N\, d\Omega = \int_{\Omega} \hat{\boldsymbol{\sigma}}\, d\Omega = 4\pi \sum_{p=1}^{26} W_p \hat{\sigma}_p = \frac{4\pi}{3} \left\{\sigma_x \ \sigma_y \ \sigma_z \ \tau_{xy} \ \tau_{yz} \ \tau_{zx}\right\}^T. \tag{10}$$

So, in order to obtain the original stress tensor we can write the equation

$$\sigma_{ij} = \frac{3}{4\pi} \int_{\Omega} \left(\sigma_N.N_{ij} + \sigma_M.M_{ij} + \sigma_L.L_{ij}\right) d\Omega, \tag{11}$$

$$\begin{aligned} \sigma_{ij} &= 3 \sum_{p=1}^{26} W_p \left(\sigma_N.N_{ij} + \sigma_M.M_{ij} + \sigma_L.L_{ij}\right) = \\ &= 6 \sum_{p=1}^{13} W_p \left(\sigma_N.N_{ij} + \sigma_M.M_{ij} + \sigma_L.L_{ij}\right). \end{aligned} \tag{12}$$

This comparison shows that the pre-multiplier in equations (12) and (1) for superimposition is not the same hence it is not correct.

Furthermore, it is worth noting that in the static constraint approach, the equilibrium of the forces at a point are satisfied automatically because of the projection of the stress tensor to the planes, but the compatibility condition of strain tensor is met only in particular cases. In other words, the micro-strain components acting on the planes may not be always the projection of the strain tensor, because the way of the superimposition of micro-strain components which are used in the static constraint approach (relation (1)) does not guarantee to be the same as the summation of the projections of macro-strain tensor obtained on every plane.

3. A NOVEL MICRO-PLANE DAMAGE FORMULATION

After the above argument which has been done about the theory of the micro-plane approach, in this section we present a new formulation of the micro-plane model in the area of damage theory which is going to be applied for the simulation of the behavior of the plane concrete. This formulation has some specifications distinct from the other micro-plane damage models.

In order to satisfy both the static equilibrium and compatibility conditions, we have considered a new method of projecting the stress tensor to the micro-planes as described earlier in this article. Then, we derived the strain tensor in terms of the stress tensor based on a well-capable constitutive relation in an ordinary three-dimensional coordinate system. In the second case, the derived strain tensor was projected to or transformed on the micro-planes. So, at this stage, by comparing the components of the stress and strain on the micro-planes we must be able to define the equal microscopic constitutive relations in such a way that both the stress and strain components on each micro-plane are the projections of the corresponding stress and strain tensors. In fact, this situation is the double constraint formulation in which the equilibrium of forces and compatibility of displacements in every integration points are satisfied one by one.

In order to attain the double constraint aspect, after analogy of the projections of stress and strain tensors to the micro-planes obtained in the manner that was explained in the previous section, it was certain that it is necessary to separate the behavior of the material into two distinct parts namely as deviatory and volumetric. So, if firstly we discretize the strain tensor as the volumetric and deviatory parts and then project each of them to the micro-planes separately, we may try to obtain the deviatory part of the modules matrix from the behaviors on the micro-planes whereas the volumetric one, which is not affected by the direction characteristics and essentially is isotropic, is obtained in the ordinary coordinate system and summed up to the deviatory part at the end of each step of loading. Therefore, we can write

$$D_{ijkl} = \frac{3}{4\pi}\int_{\Omega}\left(\frac{E}{1+\nu}\right)\left[\left(N_{ij}-\frac{\delta_{ij}}{3}\right)\left(N_{kl}-\frac{\delta_{kl}}{3}\right)+M_{ij}M_{kl}+L_{ij}L_{kl}\right]d\Omega+$$

$$+\frac{E}{1-2\nu}\frac{\delta_{kl}}{3}\delta_{ij}. \tag{13}$$

4. NEW ANISOTROPY DAMAGE FUNCTION FORMULATION

The total deviatory part of constitutive matrices is computed from superposition of its counterparts on the micro-planes. In turn, these counterparts are calculated based on the damages occurred on each plane depending on its specific loading conditions. This damage is evaluated according to the five separate damage functions; each of them belongs to the particular loading states. This five loading conditions are

1) hydrostatic compression, 2) hydrostatic extension, 3) pure shear, 4)shear + compression, 5)shear + extension.

On each micro-plane, at each time of loading history, there exists one specific loading situation that may be in one of the five mentioned basic loading conditions. For every five mood, a specific damage function according to the authoritative laboratory test results available in the literature is assigned. Then, for each state of on-plane loading, one of the five introduced damage functions will be computed with respect to the history of micro-stress and strain components.

In this formulation we consider just two basic material parameters for ease as elasticity and Poisson's coefficients.

5. UNIAXIAL COMPRESSION (UC) TEST

As can be seen in fig. 4, there is a good agreement between the results obtained by using the proposed model and experimental evidences. The material parameters used in the above analysis are: $E = 25000\, MPa$, $\nu = 0.20$.

In fig. 5, the volumetric changes of the concrete specimen under uniaxial compressive loading have been compared with the experimental observations experienced by Kupfer and his co-workers in 1969. As it is shown, there exists an excellent coincidence between analytical and laboratory data.

In order to show more confidence on the capability of the micro-planes during uniaxial compression test, in figs. 6 - 11, the variation of micro-stress normal and tangential component values are represented versus the total axial compressive stress. It can be seen that, during the application of the uniax-

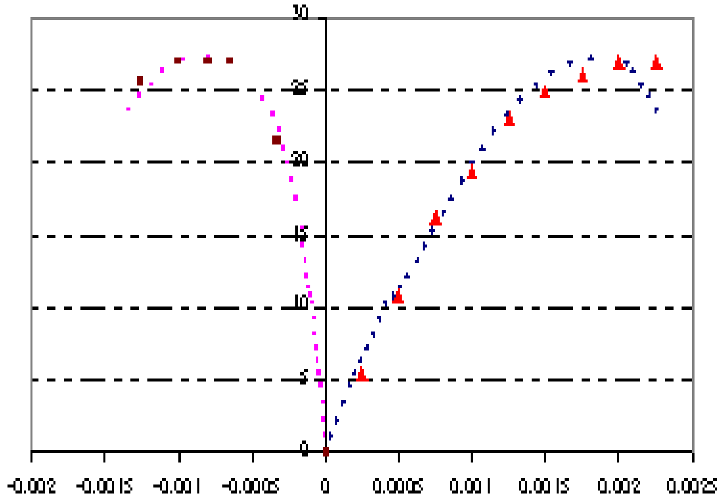

Fig. 4. Axial and lateral strains in mm/mm (right and respectively left horizontal semi-axis) versus axial stress in MPa (vertical axis) in uniaxial compression test of concrete obtained by means of the proposed micro-plane damage model ($f_c' = 27MPa$); red triangles at right and black squares at left represent experimental data from Kupfer et al., 1969.

ial compressive load on the x-axis, the micro-plane number 11 is under just the compressive stress, whereas the micro- planes numbers 9,10,12,13, which geometrically are located normal to the load direction on the unit sphere, are only under the tensile stress. The compressive stress accompanied with shear affects the other remaining planes. During the increase of the uniaxial compressive load, the compressive and shear stress components acting on the micro-planes number 1 to 8 first increase together with the shear stress, but near the peak stress (f_c'), the compressive stress decreases suddenly.

Fig. 12 shows the growth of the damage function values of different micro-planes during uniaxial compression test of concrete obtained with the proposed model. Namely, the damage evolutes on the micro-planes number 9,10,12,13 on the unit sphere faster than the other planes. This is due to the existence of different modes of loading on those planes. In the uniaxial compression test done by the proposed model, the axial compressive load is applied to the x-axes that are normal to the micro-plane number 11. So, on this plane, there exists only a normal compressive load (mode I) for which no damage could

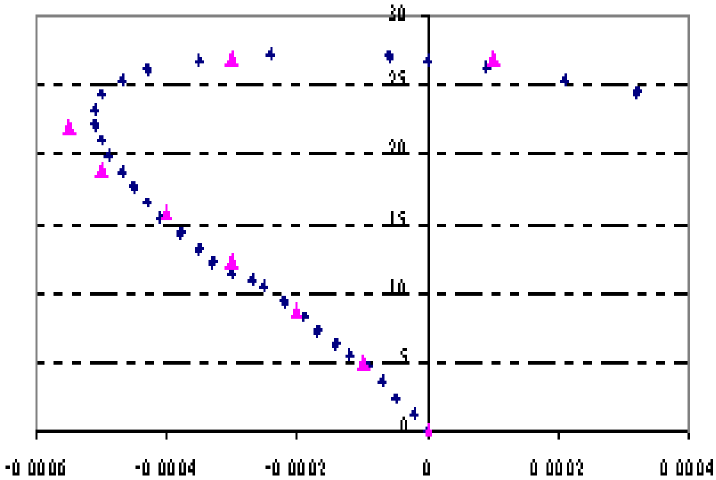

Fig. 5. Volumetric behavior of concrete (on the horizontal axis - compression at the left, dilation at the right of 0) under uniaxial compressive loading (on the vertical axis); violet triangles represent experimental data from Kupfer et al., 1969 ($f'_c = 27MPa$).

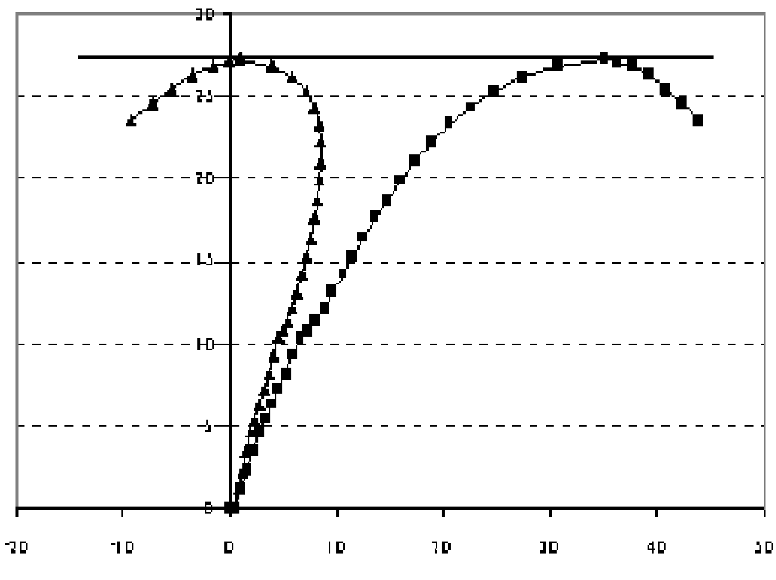

Fig. 6. Variation of micro stress components acting on the micro planes number 1,2,3,4 during uniaxial compression test. On the horizontal axis - the micro stress components (MPa), on the vertical axis - axial compressive stress; the left branch - normal component, the right branch - tangential component.

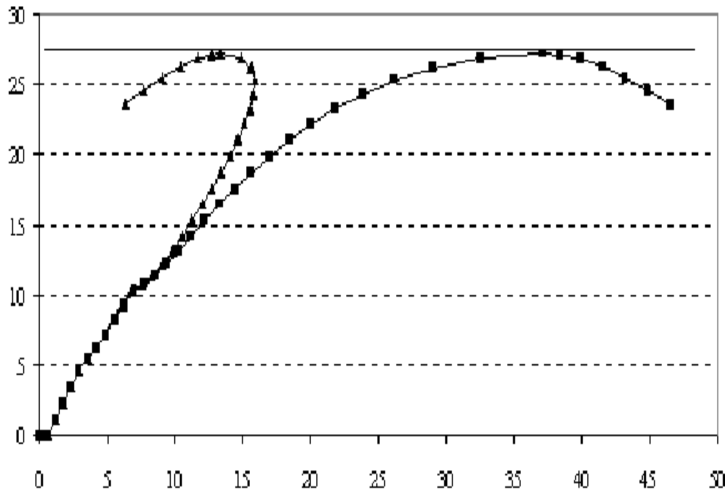

Fig. 7. Variation of micro stress components acting on the micro planes number 5, 6 during uniaxial compression test. On the horizontal axis- the micro stress components (MPa), on the vertical axis- axial compressive stress (MPa); the left branch - normal component, the right branch - tangential component.

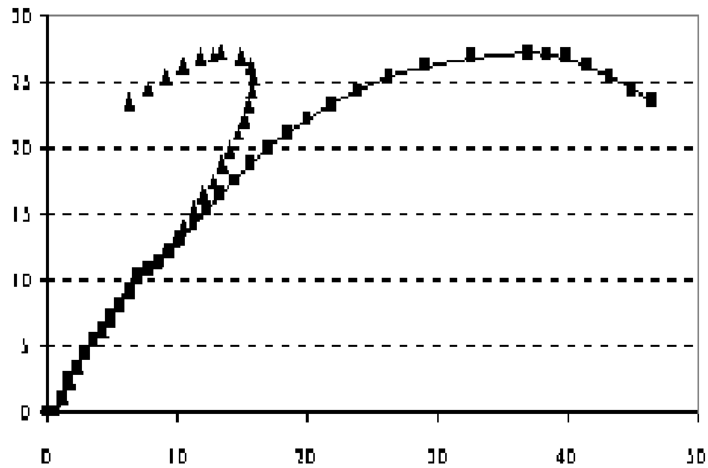

Fig. 8. Variation of micro stress components acting on the micro planes number 7, 8 during uniaxial compression test. On the horizontal axis- the micro stress components (MPa), on the vertical axis- axial compressive stress (MPa); the left branch - normal component, the right branch - tangential component.

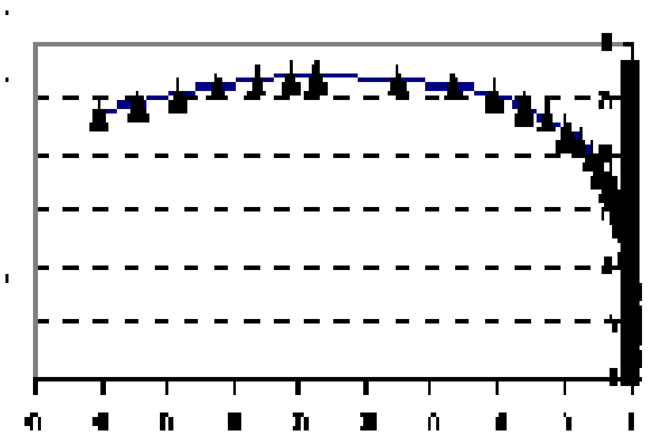

Fig. 9. Variation of micro stress components acting on the micro planes number 9, 10 during uniaxial compression test. On the horizontal axis- the micro stress components (MPa), on the vertical axis- axial compressive stress (MPa); the left branch - normal component, the vertical branch - tangential component.

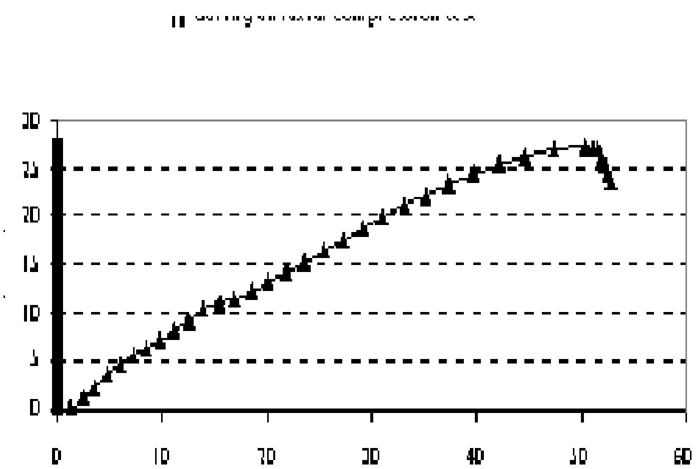

Fig. 10. Variation of micro stress components acting on the micro plane number 11 during uniaxial compression test. On the horizontal axis- the micro stress components (MPa), on the vertical axis- axial compressive stress (MPa); the right branch - normal component, the vertical branch - tangential component.

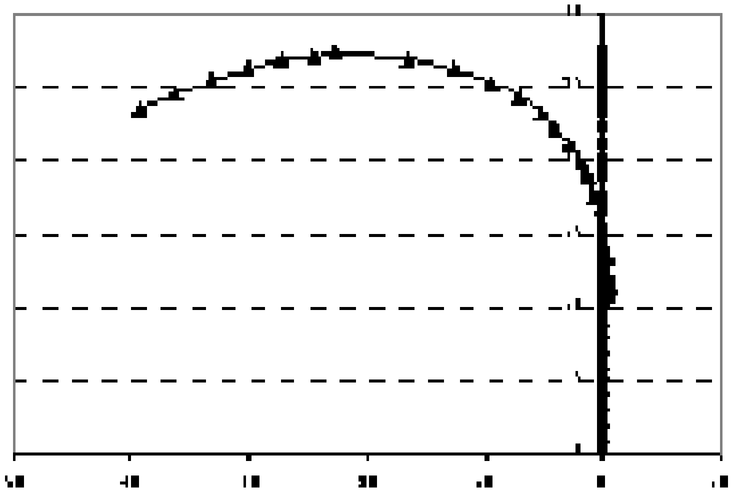

Fig. 11. Variation of micro stress components acting on the micro planes number 12, 13 during uniaxial compression test. On the horizontal axis- the micro stress components (MPa), on the vertical axis- axial compressive stress (MPa); the left branch - normal component, the vertical branch - tangential component.

occur on it. On the micro-planes number 5,6,7,8 there is a shear combined with the normal compressive load (mode IV) causing damages less than the micro-planes 1,2,3,4 on which there exists the same mode of loading (mode III). This is because of the fact that on the micro-planes number 1, 2, 3 and 4 the magnitude of the compressive stress component is less than the same component value on the micro-planes number 5 to 8 (figs. 6- 12), so damage growths faster.

Finally, on the micro-planes number 9,10,12,13 there exists only normal tension loading (mode II), which causes the damage growths faster than the all other planes (figs. 9-11).

From the above behaviors of the micro-planes, obtained by using the proposed model, we conclude that in the uniaxial compression test, the damages or cracks can appear first on the micro-planes number 9,10,12,13 and then on the micro-planes number 1, 2, 3 and 4. This can be observed in the real situation of the laboratory on the cylindrical concrete specimen. If there is no friction restraint between the surfaces of the loading top/bottom plates and the specimen, then the cracks will appear differently on the positions of the micro-planes number 9,10,12,13 of the proposed model. Else if the damages on the micro-planes number 1, 2, 3 and 4 will be greater and cracks will be initiated first on these planes. As a result, the effect of lateral confining pressures on the compressive cylindrical strength of concrete specimens simulated by the proposed model has been compared with experimental data of Ansari and Li (1998) in fig. 14.

Fig. 15 exhibits the behavior of concrete specimen under conventional triaxial extension (CTE) test that is presented by the proposed model.

6. CONVENTIONAL TRIAXIAL COMPRESSION (CTC) TEST

In this test, at first the hydrostatic pressure is applied to the specimen to a certain level and then the axial compression is increased while the lateral or confining pressure is held constant. So, in this test, up to certain level of hydrostatic compression, there must be no shear forces on the micro-planes. This can be seen in fig. 12 that shows the evolution of the micro-stress components on different micro-planes during CTC test. In fig. 13, the axial stress-strain curves of cylindrical concrete specimen under two different Uniaxial Compression (UC) test and Conventional Triaxial Compression (CTC) test obtained by using the proposed micro-plane damage model have been compared.

The stress-strain response of the concrete cylindrical specimen under UT test that is depicted in fig. 16. In fig. 17 the proposed model prediction under hydrostatic tension (HT) test is depicted. The load capacity of the sample under the hydrostatic tension is greater than the same value in the UT test because in the UT test the cause of the damage is the compromise of tension and shear stress while in the HT test, the pure tensile stress acting on the planes. The prediction of the proposed micro-planes for the HT test is shown in the fig. 18. As it can be noticed, the behavior of all micro-planes under this loading is the same. The reason is that in the hydrostatic loading, the same condition of stress distributions is imposed around the physical point and

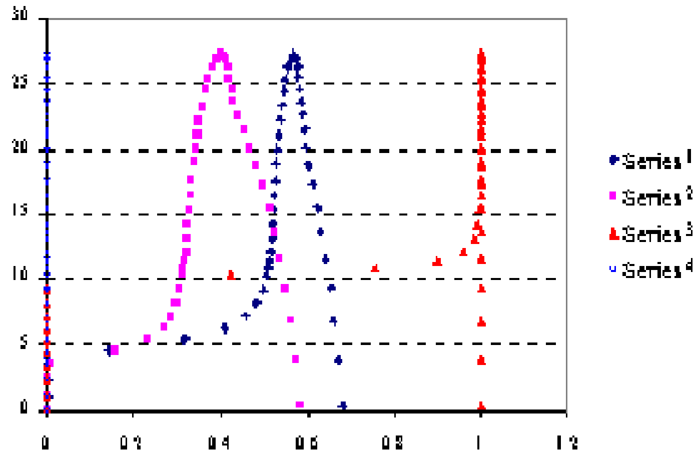

Fig. 12. Comparison of the damage evolution functions on the various micro-planes during the axial compressive loading. On the horizontal axis- the damage evolution function value, on the vertical axis- the axial stress (MPa).

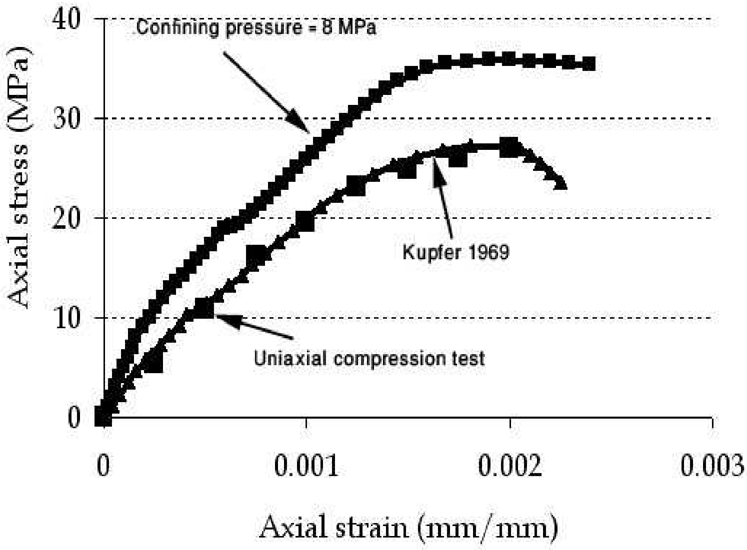

Fig. 13. Comparison of axial stress-strain curves of concrete in UC and CTC tests.

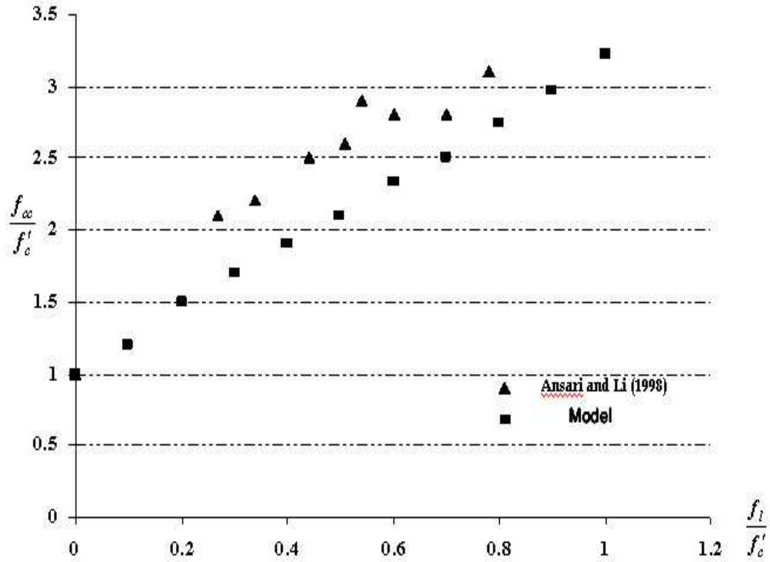

Fig. 14. Different triaxial compression strengths f_{cc} obtained for different lateral confining pressures f_l.

therefore the anisotropy could not appear. Furthermore, as it is anticipated, there is no shear stress on the planes.

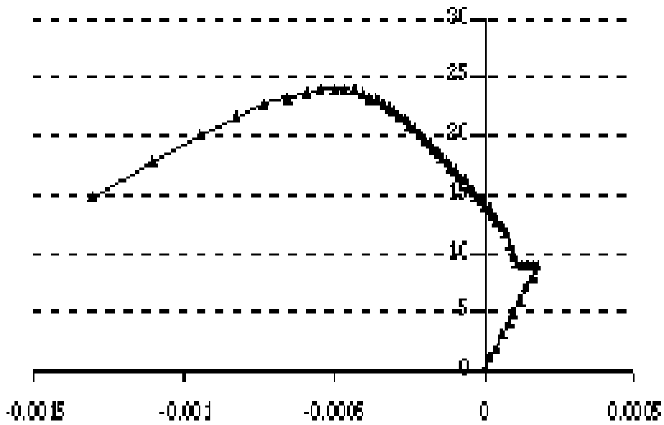

Fig. 15. Behavior of the cylindrical concrete specimen under (CTE) test obtained by using the proposed micro-plane damage model.

The expected response of concrete cylindrical specimen under hydrostatic compression (HC) test, associated with the increase of bearing capacity unlimitedly. Simulation of this response under the HC test is presented in fig. 19, 20. As in the case of HT test, the behavior of the whole planes under the HC test is the same.

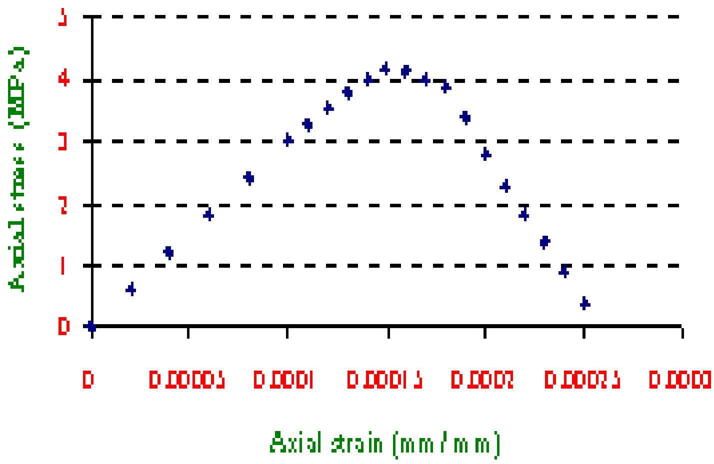

Fig. 16. Behavior of the cylindrical concrete specimen under uniaxial tension test obtained by using the proposed micro-plane damage model.

7. CYCLIC LOADING

Generally, the most damage models fail to reproduce the irreversible strains and the slopes of the curve in the unloading and reloading regions.

In fig.21, the predicted response of the model under cyclic compression test is compared with the experimental results of B. P. Sinha, K. H. Gerstle and L. G. Tulin (1964). A good agreement between the analytical and experimental data is seen. Also, in fig. 22, the behavior of concrete simulated by using the proposed model under complete cyclic loading is shown.

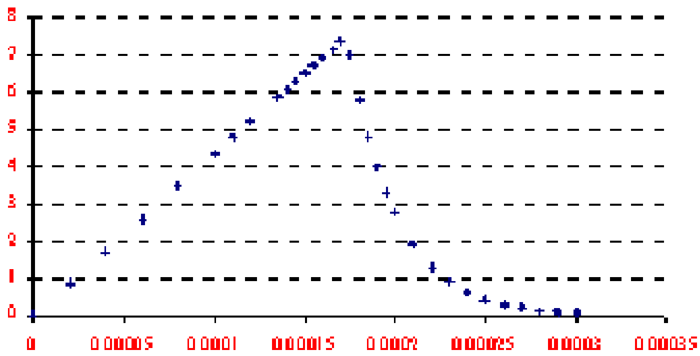

Fig. 17. Behavior of the cylindrical concrete specimen under HT test obtained by using the proposed micro-plane damage model; axial strain (mm/mm) - on the horizontal axis, axial tensile stress (MPa) - on the vertical axis.

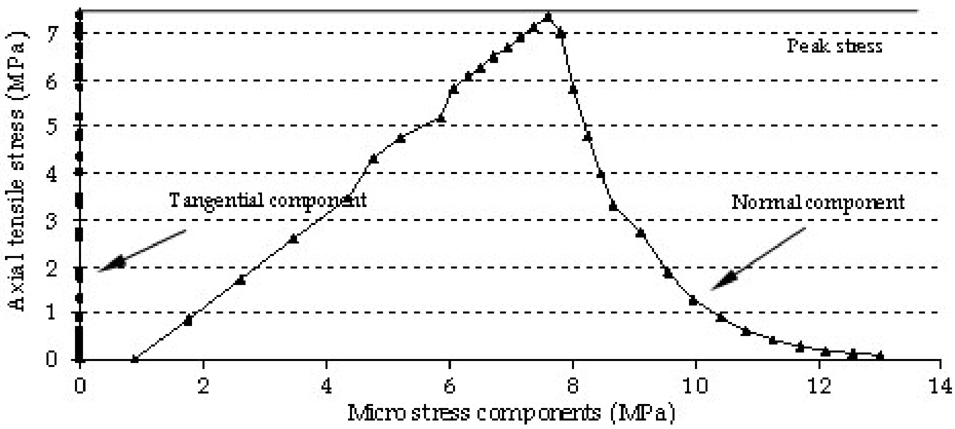

Fig. 18. Variation of micro-stress component values acting on the micro-planes number 1 to 13 during the HT test.

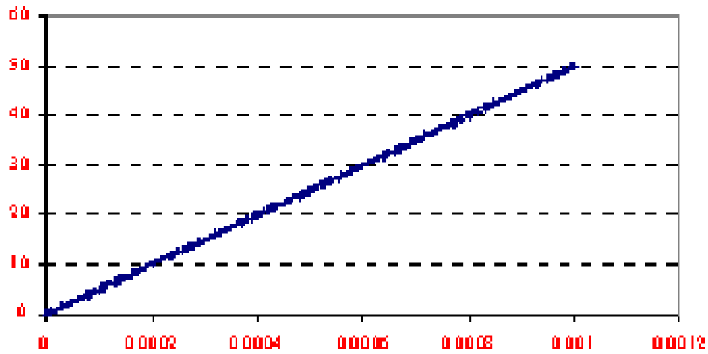

Fig. 19. Behavior of the cylindrical concrete specimen under the HC test obtained by using the proposed micro-plane damage model; axial strain (mm/mm) - on the horizontal axis, axial tensile stress (MPa) - on the vertical axis.

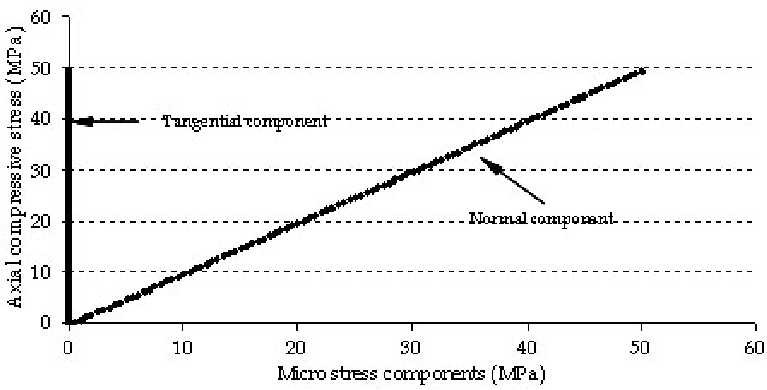

Fig. 20. Variation of micro-stress component values acting on the micro-planes number 1 to 13 during the HC test.

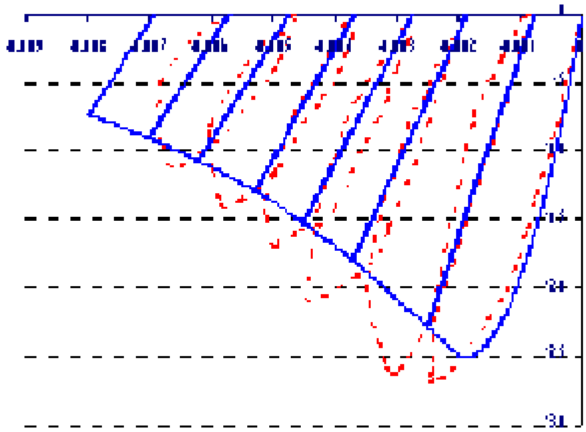

Fig. 21. Cyclic compression test simulation; axial strain (mm/mm) on the horizontal axis, axial stress (MPa) on the vertical axis, blue continuous line - proposed model, red dotted line- experimental results.

8. CONCLUSIONS

A constitutive damage model for the mechanical behavior of concrete/rock under arbitrary loadings was developed using the composition of the theoretical framework of micro-plane and damage approaches. A new damage formulation has been employed into the micro-plane model. Accordingly, an arbitrary change of six strain/stress on cube element led to combination of five conditions introduced on plane. Therefore, the proposed model is capable of predicting the concrete behavior under an arbitrary strain/stress path. These five force conditions are: *1)hydrostatic compression, 2)hydrostatic extension, 3)pure shear, 4)shear + compression, 5)shear + extension.* The five damage evolution functions, all of them functions of equivalent strain, were formulated for any of the five force conditions. This novel micro-plane damage model can simulate the behavior of the concrete/rock specimen under compressive loadings as well as tensile loadings with a few model parameters requirements. The proposed model has excellent features, such as prefailure configuration of inside material, final failure mechanism, capability of seeing induced/inherent anisotropy and also any fabric effects on the material behavior. However, the

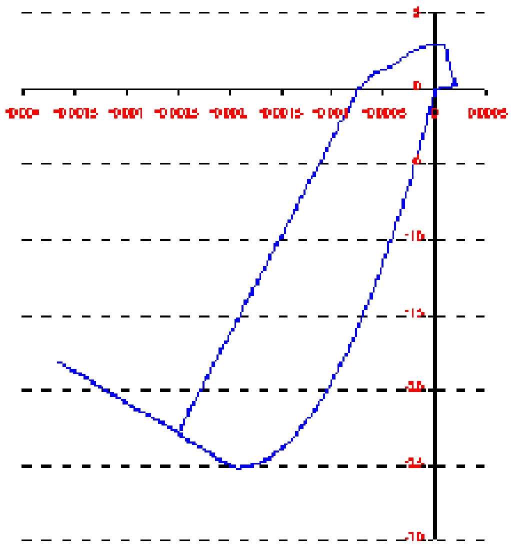

Fig. 22. Complete cyclic test simulation; axial strain (mm/mm) on the horizontal axis, axial stress (MPa) on the vertical axis (the sense on the cycle is clockwise).

basis of its formulation is simple, logical and has some physical insights that make it convenient to perceive.

References

[1] Batdorf, S. B., Budiansky, B., *A mathematical theory of plasticity based on the concept of slip*, Technical Note **1871**, National Advisory Committee for Aeronautics, 1949.

[2] Ramm, E., D'Addetta, G. A., Leukart, M., *From microscopic to macroscopic modeling of geomaterials*, European Congress on Computational Methods in Applied Sciences and Engineering, 2004.

[3] Bazant, Z.P., Gambarova, P.G., *Crack shear in concrete: Crack band micro plane model*, J. Struct. Eng., ASCE, **110**(1984), 2015-2036.

[4] Bazant, Z., Oh, B., *Micro plane model for progressive fracture of concrete and rock*, J. E. Mech., **111**(1985), 559-582.

[5] Bazant, Z., Prat, P., *Micro plane model for brittle plastic material: Part I & II*. J. E. Mech., 114, pp.1672-1702, 1988.

[6] Carol, I., Bazant, Z., *Damage and plasticity in micro plane theory*, Int. J. Solids & Structures., **34**(1997), 3807-3835.

[7] Carol, I., Bazant, Z. P., Prat, P., *New explicit microplane model for concrete: Theoretical aspects and numerical implementation*, Int. J. Solids & Structures, **29**(1992), 1173-1191.

[8] Carol, I., Jirasek, M., Bazant, Z. P., *A thermodynamically consistent approach to micro plane theory. Part I: Free energy and consistent micro plane stresses*, Int. J. Solids & Structures, **38**(2001), 2921-2931.

[9] Kuhl, E., Ramm, E., de Borst, R., *An anisotropic gradient damage model for quasi-brittle materials*, Comp. Meth. Appl. Mech. Eng., **183**(2000), 87-103.

[10] Kuhl, E., Ramm, E., *Micro plane modeling of cohesive frictional materials*, Eur. J. Mech." A/Solids, **19**(2000), S121-S143.

[11] Simo, J., Ju, J., *Strain and stress based continuum damage models: Part I-Formulation, Part II-Computational aspects*, Int. J. Solids and Structures **23**(1987), 821-869.

[12] Bazant, Z. P., Adley, M. D., Carol, I., Jirasek, M., Akers, S.A., Rohani, B., Cargile, J.D., Caner, F.C., *Large-strain generalization of micro plane constitutive model for concrete and application*, ASCE, J. Engrg. Mech. 126(9)(2000a), 971-980.

[13] Bazant, Z. P., Caner, F. C., Carol, I., Adley, M.D., Akers, S.A., *Micro plane model M4 for concrete: I. Formulation with work-conjugate deviatoric stress*, ASCE, J. Engrg. Mech. **126**(9)(2000b), 944-953.

[14] Bazant, Z. P., Caner, F. C., *Micro plane M4 for concrete: II. Algorithm and calibration*, ASCE, J. Engrg. Mech. **126**(2000), 954-961.

[15] Ozbolt, J., Li, Y., Kozar, I., *Micro plane model for concrete with relaxed kinematic constraint*, Int. J. Solids Struct., **38**(2001), 2683-2711.

[16] Pijaudier-Cabot, G., Bazant, Z. P., *Non local damage theory*, J. Engrg. Mech. ASCE, **113**(1987), 1512-1533.

[17] Mazars, J., *A description of micro and macro scale damage of concrete structures*, J. Engrg. Fracture Mech., **25**(1986), 729-737.

[18] Meschke, G., Lackner, R., Mang, H., *An anisotropic elastoplastic-damage model for plane concrete*, Int. J. Numerical Methods in Engrg., **42**(1998), 703-727.

[19] Yazdani, S., Schreyer, H.L., *An anisotropic damage model with dilatation for concrete*, Mechanics of Materials **7**(1988), 231-244.

[20] Lubarda, V. A., Krajcinovic, D., *Damage tensor and the crack density distribution*, Int. J. Solids Structures, **30**(20)(1993), 2859-2877.

ROMAI J., **4**, 2(2008), 169–175

TWO REDUCTION SCHEMES IN INVESTIGATION OF STABILITY BY LYAPUNOV AND ASYMPTOTIC STABILITY FOR ABSTRACT PARABOLIC DIFFERENTIAL EQUATIONS

Vladilen A. Trenogin

Moscow State Steel and Alloys Institute, Russia

vtrenogin@mail.ru

Abstract In order to investigate stability questions two reduction methods for nonlinear equations are suggested going back to A. M. Lyapunov and E. Schmidt. In this way an extension of the Lyapunov idea to deduce the stability of the solution of differential equation (DEq) from the linear approximation for this DEq is obtained. The investigation was supported by International grant Romania-Russia $07-0-91680-PA-a$.

Keywords: abstract parabolic differential equation, stability by Lyapunov, asymptotic stability, two reduction methods.

2000 MSC: 47J35, 377K45

1. INTRODUCTION

Let X be a real or complex Banach space. The differential equation

$$\dot{x} = Ax + R(x) \tag{1}$$

is considered assuming that the following conditions are fulfilled.

I. A is a closed linear operator, mapping its dense in X domain $D(A)$ in X.

II. The nonlinear operator $R(x)$ is defined and continuous at all x belonging to the open ball $S \subset X$ of the radius p with center at the origin, and also $R(0) = 0$. There exist constants $K > 0$ and $\beta > 0$ such that the inequality

$$||R(x_1) - R(x_2)|| \leq Kmax^{\beta}(||x_1||, ||x_2||)||x_1 - x_2||$$

holds for all $t \in \mathbb{R}^+$, $x_1, x_2 \in S$.

Remark 1. From condition II it follows that for all $x \in S$ and any $t \in \mathbb{R}^+$

the inequality $||R(x)|| \leq K||x||^{1+\beta}$ holds.
By the classical solution of DEq (1) on the semiaxis $\mathbb{R}^+ = [0, \infty)$ we understand the continuously differentiable on $\mathbb{R}^+$ function $x(\cdot)$, with $x(t) \in D(A)$, identically satisfying (1) on $\mathbb{R}^+$. Together with the nonlinear DEq (1) consider its linearization, namely the linear DEq

$$\dot{x} = Ax. \tag{2}$$

Note that DEq (1) and DEq (2) have the classical trivial solution $x(t) = 0$.

For (1) and (2) consider the Cauchy problem: to find their classical solutions satisfying the initial condition

$$x(0) = a. \tag{3}$$

Problem (1), (3) generates an abstract dynamic system, its solutions correspond to trajectories in phase space X and the function $x(\cdot) = 0$ corresponds to an equilibrium point of (1).

We are interested in conditions under which the trivial solution of DEq (1) is Lyapunov stable or asymptotically stable. In this way we essentially generalize the Lyapunov theorem [1] about asymptotic stability upon linear approximation (2).

Previously we have considered this problem under the additional assumption that the operator A is the generator semigroup $U(t) = exp(At)$ of the class C_0.

In [3]-[4] it was established that if this additional condition is fulfilled, then the asymptotic stability of the trivial solution to DEq (1) takes place. Also the more complicated case was studied when the operator R depends on t. Even the increasing of R together with t was assumed, but it was compensated by the exponential decreasing of the semigroup [5], [6]. In particular, under the fulfilment of the restriction on the semigroup, the operator A is continuously invertible [2], i.e. its range is coincident with all space where the inverse of operator A is bounded.

2. REDUCTION METHODS FOR THE SOLVING OF THE PROBLEM

Here we study the case when the operator A is non-invertible. Apparently, here more typical is the case of the Lyapunov stability of trivial solution to DEq, but not the case of its asymptotic stability. Further, it is supposed that the operator A satisfies the following very general conditions.

III. The set $V = N(A)$ of zeroes of the operator A is nontrivial, closed and has in X a direct complement U, such that the space X can be represented in the form of direct sum $X = U \oplus V$. The range $W = R(A)$ of the operator A is nontrivial, closed and has in X a direct complement Z such that the space X can be represented in the form of direct sum $X = W \oplus Z$.

As the finite-dimensionality of the subspaces V and Z is not assumed, the problem of the generalization of the notion of Fredholm operator arises.

The projection method we use goes back to A.M. Lyapunov and to our extension to branching theory in the Banach spaces [8].

Let P be the projector of X on U, and Q the projector of X on W. Then $I-P$ is projector of X on V. Set in (1) $x = u+v$, where $u = Px$, $v = (I-P)x$ and project the obtained problems (1), (3) and (2), (3) on U and V to get the following system of Cauchy problems

$$\dot{u} = PAu + PR(u+v), \quad u(0) = Pa, \tag{4}$$

$$\dot{v} = (I-P)Au + (I-P)R(u+v), \quad v(0) = (I-P)a. \tag{5}$$

For the further investigation suppose the following additional condition.

IV. The restriction of the operator PA to the subspace U is the generator of the exponentially decreasing semigroup $U(t) = exp(At)$ of class C_0 such that there exist the constants $M > 0$ and $\alpha > 0$ such that for all $t \in \mathbb{R}^+ = [0, +\infty)$ the inequality $||U(t)|| \leq Mexp(-\alpha t)$ is fulfilled.

Using the semigroup $U(t)$ the system of DEqs (4)-(5) becomes the system of integral equations

$$u(t) = U(t)Pa + \int_0^t U(t-s)PR(u(s)+v(s))ds, \tag{6}$$

$$v(t) = (I - P)a + \int_0^t (I - P)[Au(s) + R(u(s) + v(s))]ds. \qquad (7)$$

If $(u(t), v(t))$ is the continuous on $\mathbb{R}^+$ solution to the integral equations (6)-(7) then $x(t) = u(t) + v(t)$ will be called the generalized solution of the Cauchy problem (1), (3).

Remark 2. From the conditions I-II it follows that for any continuous and bounded on $\mathbb{R}^+$ pair of functions $(u(t), v(t))$ the right-hand sides in the formulae (6)-(7) are also continuous on $\mathbb{R}^+$ functions. Our nearest aim is the study of the continuous and bounded solutions of the system of integral equations (6)-(7) on the positive axis. We are interested also in the case where $u(t)$ and $v(t)$ are exponentially decreasing at $t \to +\infty$. Consider the linear Cauchy problem (2), (3), which by using the projection method, becomes

$$u(t) = U(t)Pa, \quad v(t) = (I - P)a + \int_0^t (I - P)Au(s)ds.$$

Substitute $u(t)$ in the second equation and calculate the integral to obtain the generalized solution of linear the Cauchy problem in the form

$$x(t) = U(t)Pa + (I - P)a + (I - P)[U(t) - I]Pa. \qquad (8)$$

Due to the asymptotic behavior of $U(t)$, we have the exponential decreasing $U(t)Pa \to 0$ as $t \to +\infty$. The other components in the right-hand side are bounded. Consequently, the trivial solution of (2) is Lyapunov stable in the class of generalized solutions. It is not difficult to find conditions guaranteeing the asymptotic stability of trivial solution. Let the projectors P and Q be equal. Then $(I - P)A = 0$. If furthermore the additional condition $(I - P)a = 0$ is satisfied, then the stability of trivial solution will be asymptotical in the class of generalized solutions. It turns out that for the nonlinear equation (1) the situation can be analogous.
Following [3], introduce a convenient family of Banach spaces of abstract functions.

Definition. *Let $\gamma > 0$. The space of continuous functions $u(t)$ defined on $\mathbb{R}^+$ and taking values in X, with natural operations of addition and multiplication by scalars, having finite norm $|||u|||_\gamma = sup_{\mathbb{R}^+}||u(t)||exp(\gamma t)$ is called C_γ.*

Note that C_γ is a Banach space. For $\gamma = 0$ we have the limit case - the space C_0 of bounded on $\mathbb{R}^+$ continuous abstract functions. Write system (6)-(7) in the form of the operator equation

$$x = Da + F(x) \tag{9}$$

with unknown $x = (u, v)$, where $u \in C_\alpha, \quad v \in C_0$ and the parameter $a \in X$. Here $Da = (U(t)Pa, (I - P)a)$, while the operator $F(x)$ is defined by the pair of integral terms in the right-hand sides of integral equations. For the investigation of the equation (9) apply to it the implicit operator theorem without assumption about differentiability of the operator F, which was formulated and proved in [2]. As the partial illustration after some technical estimates we get the following assertion.

Theorem. *Let the conditions I-IV, $R(v) = 0, \forall v \in V$ be fulfilled and Q=P. Then there exist the numbers $r_* > 0, \quad \rho_* > 0$ such that for any a, $||a\ || \leq \rho_*$ the equation (8) has in the ball $||x|| \leq r_*$ the unique continuous bounded on $\mathbb{R}^+$ solution $x = x(t, a)$. This solution is continuous on a in the ball $||x_0|| \leq \rho_*$ and $x(0) = a$. If in addition $Pa = a$ then $x \in C_\alpha$.*

The proof of the theorem is carried out following the scheme described in detail in [3]. In the first part of the proof the Lyapunov stability for the trivial solution of (1), in the class of the generalized solutions is established. In the second part, under some additional restrictions, its asymptotic stability is proved. Analogously to [3], under Hölder property of the operator $R(x)$, the stability of trivial solution in the class of classical solutions can be proved too. We hope that the theorem conditions will be essentially weakened.

We now characterize another possible way of stability questions investigation. Postulate the boundedness of $v(t)$ on $\mathbb{R}^+$. Using the implicit operator theorem, for all sufficiently small $||Pa||$, from integral equation (6), find the function u as an operator depending of v, i.e. $u = u_v(t)$. Substitute this operator in (7). As a result of this we get the following operator-integral equation

$$v(t) = (I - P)a + \int_0^t (I - P)[Au_v(s) + R(u_v(s) + v(s))]ds. \qquad (10)$$

Any assertion about the stability of solution $v \in C_0$ of equation (10) goes to the corresponding assertion about Lyapunov stability for trivial solution of DEq(1).

In the stability questions, equation (10) or the analogous Cauchy problem for the DEq obtained by substituting $u = u_v$ to Cauchy problem (6) plays the same role as the Lyapunov-Schmidt branching equation in the branching theory of solutions of nonlinear equations.

Consider now the usually encountered in practical applications classical case of the Fredholm operator A. Here along with the projection method one can use another method going back to E. Schmidt and transferred by us to linear operators acting in Banach spaces [8]. Assume that in (1) the subspaces N(A) and $N(A^*)$ are n-dimensional with the bases $\{\varphi_i\}_1^n$ and $\{\psi_i\}_k^n$ respectively, and $\{\gamma_j\}_1^n$, $\{z_l\}_l^n$ are the bi-orthogonal to them systems. In [8] the following statement was established.

Lemma. *The operator $\tilde{A}\cdot = A\cdot + \sum_1^n < \cdot, \gamma_i > z_i$ is continuously invertible.*

This assertion was called by us the generalized Schmidt lemma in honor of the German mathematician Erhard Schmidt who has proved the analogous fact in the particular case of a linear integral operator acting in the space of continuous functions. The operator $\tilde{A}$, for which we propose the name of *regularizer of Fredholm operator A*, allows us to write the DEq (1) in the form

$$\dot{x} = \tilde{A}x + R(x) - \sum_1^n c_i(t) z_i. \qquad (11)$$

The functions $c_i(t)$ occurring in the right-hand side of (11), and depending on the unknown solution $x(t)$ of Cauchy problem (1)-(2), are functionals, determined by formulae

$$c_i(t) =< x(t), \gamma_i >, \quad i = 1, 2, ...n. \qquad (12)$$

In order to perform the computations of this functionals we proceed as follows. Applying to both parts of (11) the functional γ_k, $k = 1, 2...n$ we get

$$\dot{c_k} =< Ax, \gamma_k > + < R(x), \gamma_k >, \quad c_k(0) =< a, \gamma_k >, \quad k = 1, 2, ..n. \qquad (13)$$

Investigation of the systems (11)-(12) and (11)-(13) leads to different variants and interpretations of conclusions about stability of the trivial solution of DEq (1). The condition of equality of projectors P and Q, used in the above means simplicity of the Jordan structure of the operator A (all Jordan chains for zeroes of the operator A have unit lengths). However, it turns out to be appropriate to use the general form A-Jordan structure of the operator A, the field where is working the author group [7].

References

[1] A. M. Lyapunov, *Collection of works*, **2**, Moscow-Leningrad, 1956;

[2] V. A. Trenogin, *Functional analysis*, Fizmatlit, Moscow, 2002, 2007 (Nauka-1980, 1993), French translation: Mir, Moscow, 1985.

[3] V.A.Trenogin, *Lyapunov theorem about stability on linear approximation as consequence of implicit operator theorem*, Doklady Academii Nauk, **407**, 1(2006), 742-746.

[4] V. A. Trenogin, *First Lyapunov method for the abstract parabolic equations*, Proceedings of 5-th ISAAC-Congress (Univ. of Catania, 2005), World Scientific, Singapore, 2008, 83-90.

[5] V. A. Trenogin, *Asymptotic stability of trivial solution of DE in Banach space with unbounded nonlinearity*, Abstracts CAIM-2007, 61-62.

[6] V. A. Trenogin, *Asymptotic stability of trivial solution of DE in Banach space with unbounded nonlinearity*, ROMAI Journal, **3**, 1(2007), 207-212.

[7] V. A. Trenogin, N. N. Avxentieva, L. R. Kim-Tyan, *Use of Jordan chains in stability and bifurcation problems*, Abstracts of CAIM-2008.

[8] M. M. Vainberg, V. A. Trenogin, *Theory of branching of nonlinear equations*, Nauka, Moscow, 1969;, Academie-Verlag, Berlin 1973; Nordhoof Int. Publ., Leiden 1974.

[9] V. A. Trenogin, A*nalytic variant of Lyapunov theorem about stability on linear approximation for differential equation in Banach space*, Proc. Middle-Volga MATH, Saransk, SVMO, **9**, 1(2007), 48-52.

ROMAI J., **4**, 2(2008), 177–189

GENERALIZED QUATERNIONS, CORRESPONDING TO THEM SYSTEM OF EQUATIONS AND APPLICATIONS

Mukhamadi Zakhirov

Faculty of Mechanics and Mathematics, National University of Uzbekistan,

Tashkent, Uzbekistan

mukhamadi@yahoo.com

Abstract In topology it is proved that every two-dimensional compact, connected and oriented manifold is diffeomorphic to the sphere with $n \geq 0$. Three-dimensional manifolds are investigated very little. For example, so far it has not been proved if every compact one-connected three-dimensional manifold is diffeomorphic to the sphere S^3, (Poincaré's conjecture) or at least homeomorphic to it [1]. Poincaré's conjecture [2] about homeomorphism is positively solved [3]. The present paper deals with the analogue of Riemann's theorem on mappings in the three-dimensional space. Moreover, famous properties of Beltrami equations system (BES) solutions as well as new results concerning these systems and generalizations are revealed and essentially used.

Keywords: main curvatures, mixed equations system, manifold, fibration, layer, groups, quaternions, quasi-conformal mappings.

2000 MSC:53Z05.

BES is system of first-order linear elliptic equations of first order

$$\begin{cases} u_x = -\frac{g_{12}}{g} v_x + \frac{g_{11}}{g} v_y, \\ u_y = -\frac{g_{22}}{g} v_x + \frac{g_{12}}{g} v_y, \end{cases} \tag{1}$$

$$g^2 = g_{11} g_{22} - g_{12}^2.$$

It may be viewed as a condition that the mapping $(x, y) \to (u, v)$ be conformal with respect to Riemann's metric

$$ds^2 = g_{11}(x, y)dx^2 + 2g_{12}(x, y) + g_{22}(x, y)dy^2,\ g_{11} \neq 0,\ \forall (x, y) \in D \subset R^2$$

that is, in this mapping any angle θ on the plane (x, y), determined in Riemann's metrics is transformed to the angle θ on the plane (u, v), determined in the essential way. Two Riemann's metrics are named conformal-equivalent if their coefficients are proportional, where the proportionality multiplier can be a function from (x, y). The two metrics set the same BES [4]. BES can be thought of as a system connecting the old and new coordinate systems at rewriting the positively defined quadratic form in the canonical form.

Here, we follow some results of the author [5]. Consider another interpretation of the generalized mixed BES and demonstrate that these equations systems are related to the main curvatures of the surfaces and the theorema egregium (Gaussian curvature) [5]. Let k_1, k_2 be the main curvatures and Ox, Oy be directed along the corresponding main directions of the smooth surface M at the point O.

From the Euler's formula it follows

$$\begin{aligned} g_{11} &= k_1 \cos^2\theta + k_2 \sin^2\theta, \\ g_{12} &= (k_1 - k_2)\cos\theta \sin\theta, \\ g_{22} &= k_1 \sin^2\theta + k_2 \cos^2\theta, \end{aligned} \tag{2}$$

where $g_{11}g_{22} - g_{12}^2 = k_1k_2 = K$, where K is the Gaussian curvature. From (2) we obtain

$$\tan 2\theta = \frac{2g_{12}}{g_{11} - g_{22}}, \;\; k_{1,2} = \frac{g_{11} + g_{22} \pm \sqrt{(g_{11} - g_{22})^2 + 4g_{12}^2}}{2}. \tag{3}$$

Consider the first-order partial differential equations : $u_x = g_{12}v_x + g_{11}v_y$, $-\,u_y = g_{22}v_x + g_{12}v_y$, where $g_{11}g_{22} - g_{12}^2 = k_1k_2 = K$, which, in the matrix form reads

$$\begin{pmatrix} g_{12} & g_{22} \\ -\frac{g_{12}^2 - K}{g_{22}} & -\,g_{12} \end{pmatrix} \begin{pmatrix} w_x \\ w_y \end{pmatrix} = i_e \begin{pmatrix} w_x \\ w_y \end{pmatrix}. \tag{4}$$

where

$$w = u(x,y) + i_e v(x,y) + i_h r(x,y) + i_e i_h q(x,y) \Rightarrow w_x = u_x + i_e v_x + i_h r_x + i_e i_h q_x,$$

$$w_y = u_y + i_e v_y + i_h v_y + i_h r_y + i_e i_h q_y$$

(related to the solutions of system (4); see also [5]).

The system (4) is of: elliptic type if $g_{11}g_{22} - g_{12}^2 = k_1k_2 = K$ is positive; hyperbolic type if K is negative; parabolic type if K is equal to zero.

From the representation (2) it follows that if $g_{12}(x, y) = 0$, then the point (x, y) is the point of rounding where it is not possible to define main directions. Therefore hereinafter it is assumed that $g_{12} \neq 0$. Thus, the following is proved

Lemma. *Let the coefficients of system (4) be defined in a domain D of a smooth surface $M \subset R^3$. Then at any point $O(x, y) \in D$, at which the main curvatures of the surface k_1, k_2 and θ are determined, the coefficients of system (4) (and, consequently, the tensor of Riemann's metric g_{ij}) are defined by system (2) at the point $O(x, y) \in D$. Conversely, if g_{ij} are determined , then the main curvatures of the surface k_1, k_2 and θ are calculated with formula (3) at the point $O(x, y) \in D$.*

Remark. If we divide by $\sqrt{|K|}$ equality (4) (for $K \neq 0$) and introduce the notations

$$\gamma = \frac{g_{11}}{\sqrt{|K|}},\ \beta = \frac{g_{12}}{\sqrt{|K|}},\ \alpha = \frac{g_{22}}{\sqrt{|K|}}, \tag{5}$$

then system (5) reads

$$u_x = \beta v_x + \gamma v_y,\ -u_y = \alpha v_x + \beta v_y,\ \alpha\gamma - \beta^2 = signK,$$

or, in matrix form,

$$\begin{pmatrix} \beta & \gamma \\ -\frac{\beta^2 - signK}{\gamma} & -\beta \end{pmatrix} \begin{pmatrix} w_x \\ w_y \end{pmatrix} = i_e \begin{pmatrix} w_x \\ w_y \end{pmatrix}. \tag{6}$$

The equations systems (6) are called *mixed Beltrami equations* system. It belongs to: 1) elliptic type for $K > 0$, 2) hyperbolic type vor $K < 0$,
3) parabolic type for $K = 0$.

For the surfaces of hyperbolical type, instead of (2) it is possible to use the following equalities system:

$$\begin{aligned} g_{11} &= k_1 \cosh^2\theta + k_2 \sinh^2\theta, \\ g_{12} &= (k_1 - k_2)\cosh\theta \sinh\theta, \\ g_{22} &= k_1 \sinh^2\theta + k_2 \cosh^2\theta, \end{aligned} \tag{7}$$

where $g_{11}g_{22} - g_{12}^2 = k_1k_2 = K$, (theorema egregium of the surface), yielding

$$\tanh 2\theta = \frac{2g_{12}}{g_{11} + g_{22}},\ k_{1,2} = \frac{g_{11} - g_{22} \pm \sqrt{(g_{11} + g_{22})^2 - 4g_{12}^2}}{2}. \tag{8}$$

Mixed Beltrami equations system is denoted by *MES* (Mixed Equation System). Further we demonstrate that it is possible to obtain *MES* from the Beltrami equations system by using the statement of the famous main lemma.

From (2),(3), (6), (7) it follows an obvious, but very important

Theorem 1. *MES coefficients depend on surface points, at which they are defined, and do not depend on parameters of the introduced coordinate system.*

The next theorem can be considered as an analogue of Riemann's theorem on mappings, as a homeomorphic solution of *MES*.

Theorem 2. *Any three-dimensional closed smooth simply connected manifold with a smooth surface layer is diffeomorphic to the three-dimensional sphere and this diffeomorphism satisfies MES.*

Proof. Let M be the base of fiber bundle. It is a three-dimensional sphere S^3 in the space of quaternions H. In this case the fibration layers are the space of quaternions, i.e. we deal with quaternion fibration. The quaternions imaginary units are isomorphic to the matrices [7]

$$\mathbf{i} \to \begin{pmatrix} 0 & 1 \\ -1 & 0 \end{pmatrix} \equiv A^0 \equiv A^0_e, \;\; \mathbf{j} \to \begin{pmatrix} 0 & i_e \\ i_e & 0 \end{pmatrix} \equiv i_e B^0 \equiv B^0_e,$$

$$\mathbf{k} \to \begin{pmatrix} i_e & 0 \\ 0 & i_e \end{pmatrix} \equiv i_e A^0 B^0 \equiv A^0_e B^0_e \equiv C^0_e, \tag{9}$$

i.e. there exists the isomorphism $\mathbf{i} \to A^0_e, \mathbf{j} \to B^0_e, \mathbf{k} \to C^0_e$ between the imaginary units of quaternions and the operators.

Let $G^0 = \pm\{E, A^0_e, B^0_e, C^0_e\}$, where E is the unit matrix. It is known that G^0 is a group, where elements form the basis of the complex-valued 2×2 space of matrices.

Let M' be a three-dimensional smooth manifold, which can be considered the base of other fibration $p' : E' \to M'$ [8], where E' is a space, and let F' be the layer of this fibration. Assume that at on each point of M' the Riemann's metric (g_{ij}) is defined $\alpha = \alpha(x, y, z), \; \beta = \beta(x, y, z), \; \gamma = \gamma(x, y, z)$, where (x, y, z) are the coordinates of the points related to the atlas map of the manifold M'. Denote by $\widetilde{i}, \; \widetilde{j}, \; \widetilde{k}$ the generalized surface quaternions which are isomorphic to the matrices

$$\widetilde{i} \to \begin{pmatrix} \beta & \gamma \\ -\frac{\beta^2+1}{\gamma} & -\beta \end{pmatrix} \equiv A \equiv A_e, \ \widetilde{j} \to \begin{pmatrix} i_e\beta & i_e\gamma \\ -i_e\frac{\beta^2-1}{\gamma} & -i_e\beta \end{pmatrix} \equiv i_eB \equiv B_e,$$

$$\widetilde{k} \to \begin{pmatrix} i_e & 0 \\ -i_e\frac{2\beta}{\gamma} & -i_e \end{pmatrix} \equiv A_eB_e \equiv C_e. \tag{10}$$

Consequently, it is a fixed isomorphism between the imaginary units of the generalized quaternions and the matrices A_e, B_e, C_e. It is easy to prove that $A_e^2 = B_e^2 = C_e^2 = -E$. In terms of g_{ij}, equality (10) reads

$$\widetilde{i} \to \frac{1}{\sqrt{|K|}} \begin{pmatrix} g_{12} & g_{11} \\ -\frac{g_{12}^2+K}{g_{11}} & -g_{12} \end{pmatrix} \equiv I_e, \ \widetilde{j} \to \frac{i_e}{\sqrt{|K|}} \begin{pmatrix} g_{12} & g_{11} \\ -\frac{g_{12}^2-K}{g_{11}} & -g_{12} \end{pmatrix} \equiv J_e,$$

$$\widetilde{k} \to i_e \begin{pmatrix} 1 & 0 \\ -\frac{2g_{12}}{g_{11}} & -1 \end{pmatrix} \equiv K_e,$$

where K is the theorema egregium at the corresponding points of the manifold M'. The matrices $\pm\{E, I_e, J_e, K_e\}$, where E is the unit matrix, form a group. It is easy to prove that: 1) $I_e^2 = J_e^2 = K_e^2 = -E$; 2) $I_eJ_e = K_e, \ J_eK_e = -I_e, \ K_eI_e = J_e$; 3) $detI_e = detJ_e = detK_e = 1$.

However, for the sake of simplicity of calculations we use the identities (10), assuming $K = 1$. Consequently, it is established the isomorphism between the imaginary units of the generalized quaternions and the matrices A_e, B_e, C_e. Let $G \equiv \pm\{E, A_e, B_e, C_e\}$. Obviously, G forms a Lie group. Now, define the manifold corresponding to this group. As in the quaternion space the bases A_e^0, B_e^0, C_e^0 induce the families of orthonormalized repers at each point of S^3, the basis matrices A_e, B_e, C_e induce the triorthogonal system at the corresponding point of the manifold. The considered matrices act on the tangent planes M' and as the matrices A_e^0, B_e^0, C_e^0 act on the tangent planes of the sphere S^3. This statement follows from the representations (2), (6) of the *MES* coefficients. If $\beta = 0 \Rightarrow k_1 = k_2$, i.e the surface consists of rounding points, but it realizes in a two-dimensional sphere or in a two-dimensional plane on the Euclidean plane $k_1 = k_2 = 0$. However, the Cauchy-Riemann's system arises when of introducing the curvilinear system of coordinates into the plane (x, y). Moreover, from the representation (2), (6) we can conclude that the operators

A_e, B_e, A_eB_e act on tangent planes of the three-dimensional manifold, each point of which is characterized by the layer of manifold possessing main directions and curvatures and theorem egregium. These matrices possess the same properties of the multiplication table as the matrices A_e^0, B_e^0, C_e^0. From these matrices and unit matrix we have formed the group G. Obviously, assuming in $G : \beta = 0, \gamma = 1$ we obtain all elements of the group G^0 [5]. Conversely, it is possible to obtain G from G^0. We shall assume that the matrix $A_e^0 \in G^0$ corresponds to the matrix $T = \begin{pmatrix} t' & x' \\ y' & z' \end{pmatrix} \in G$.

If $(A_e^0)^2 = -E$, where E is the unit matrix, then the square of the corresponding to it matrix from G must be equal to the negative unit matrix too. We can obtain $z' = -t', y' = -\frac{t'^2+1}{x'}$ from it. If in matrix B_e^0 correspondingly we put the matrix $S = \begin{pmatrix} g_{12} & g_{11} \\ -\frac{g_{12}^2+K}{g_{11}} & -g_{12} \end{pmatrix}$ and equate its square to unit matrix, then we obtain $z'' = -t'', y'' = -\frac{t''^2-1}{x''}$.

Anticommutative relations between these matrices define $t' = t'', z' = z''$. Assuming $t' = \beta,\ x' = \gamma$ we obtain $T = A_e \in G,\ S = B_e$. In the same way the correspondence $A_e^0B_e^0 \to A_eB_e$ can be proved. Thus, G^0 and G are homeomorphic and the elements of these sets uniquely satisfy the group operations. Consequently, G^0 and G are isomorphic and form the Lie group. The elements of the group G act on the tangent planes of the manifold M'. These operators transform the field of tangent planes to itself, i.e. they are the symmetry operators. On one hand, these operators are the operators of *MES*. Consider these operators from another point of view. Any three-dimensional closed manifold M' is considered the Seifert's fibration only if it is possible to represent it in the form of lamination on a circumference. It means that M' is divided into non-intersecting in pairs circumferences, union of some parts of which define the neighborhoods which are isomorphic to the entire torus or nonorientable torus [2]. Relating to the map atlas, some manifolds act as a smooth surface. We will consider that the layer circumferences of Seifert's fibration are circumferences which define the main curvatures of the surface in two inter-orthogonal main directions at any point of M'. As a consequence of formulae (2), (3), (4) the operators A_e, B_e, C_e at these points of the manifold are essentially defined. From the fact that M' is representable in view of a fibration on circumferences it follows that the manifold M' is closed.

From the definition of the fibration $E' \to M'$ of the function gluings, define smooth mappings of the domain U_{ij} onto the group G, where $U_{ij} = U_i \bigcap U_j$ and U_i is the domain of base cover M'. Maps U_j are domains of definition of the functions $\alpha = \alpha(p), \beta = \beta(p), \gamma = \gamma(p), p \subset M'$.

The elements of the group G satisfy the conditions

$$1)\ A_eB_e = C_e = (B_eA_e)^{-1}, B_e(A_eB_e) = B_eC_e = ((A_eB_e)B_e)^{-1} = (C_eB_e)^{-1},$$

$$(A_eB_e)A_e = C_eA_e = (A_e(A_eB_e))^{-1} = (A_eC_e)^{-1}$$

$$2)\ A_eB_eB_e(A_eB_e)(A_eB_e)A_e = A_eB_eB_eC_eC_eA_e = -E, \tag{11}$$

$$3)\ detA_e = detB_e = detC_e = 1.$$

As the Lie groups are simultaneously manifold, the condition 2) is satisfied at the points of the threefold overlapping $U_{ijk} = U_i \bigcap U_j \bigcap U_k$. It is easily verified that the following relations for the Lie brackets of G group

$$\frac{1}{2}[A_e, B_e] = \frac{1}{2}(A_eB_e - B_eA_e) = A_eB_e \equiv C_e,$$
$$\frac{1}{2}[B_e, C_e] = \frac{1}{2}(B_eC_e - C_eB_e) = A_e, \tag{12}$$
$$\frac{1}{2}[C_e, A_e] - \frac{1}{2}(C_eA_e - A_eC_e) = B_e,$$

hold, i.e. the Lie brackets are expressed linearly by the elements of the same group G. The index e indicates that the corresponding points of the surface are of elliptic type. The corresponding operators are defined in the following way at the points of hyperbolic type: $A_h = i_eA,\ B_h = i_hB,\ C_h = i_ei_hC$.

Whence, the properties

$$1)\ A_h^2 = B_h^2 = C_h^2 = E;\ A_hB_h = C_h,\ B_hC_h = A_h,\ C_hA_h = B_h;$$

$$2)\ (A_hB_h)^{-1} = C_h^{-1} = A_hB_h,\ (B_hC_h)^{-1} = A_h^{-1} = B_hC_h,\ (C_hA_h)^{-1} = B_h^{-1} = C_hA_h; \tag{13}$$

$$3)\ A_hB_hB_hC_hC_hA_h = E; \qquad 4)\ detA_h = detB_h = detC_h = -1.$$

In the same way as in (11), condition 3) is satisfied at the points of the threefold overlapping $U_{ijk} = U_i \bigcap U_j \bigcap U_k$. The sign minus in the latest equality (11) and the signs plus in 1), 2) in (13) certify the existence of the spin structure [9], as they exist in any three-dimensional oriented manifolds.

From the equations systems (4), (6) and (10) we can conclude that the operators A, B are symmetry operators together with every following from them traces. From (13) we partially obtain the following properties of the operators A, B. Any operator A, B rotates ζ by 180° with respect to a certain center defined by the symmetry of the same operators. The operators A, B act on the fundamental domain - plane square. As after two times application of operator B to ζ, (see (4)), ζ is transformed into itself, it follows that the vector ζ is directed along the cylinder's parallel. The operator A if applied two times transforms ζ to $-\zeta$, and after its four times applications transforms ζ to itself, i.e. ζ is a spinor. We conclude that the flag ζ is directed to the parallel of the Möbius leaf. Consequently, a torus corresponds to the product $B \times B$, whereas a nonorientable torus corresponds to the product $A \times B$.

Formally, the operators B_e, C_e turned into the hyperbolic operators B, C by multiplying them by the imaginary unit i_e. This is why further we call B_e, C_e the operators of hyperbolic type.

Each point $p \subset M'$ is covered at least by two maps. From (7), (8) and the fact that U_i is the domain of definition of the functions α, β, γ, we deduce that (U_i, φ_i) defines one of the three matrices A_e, B_e, C_e rather than A_e, and from 1) (11) it follows that on U_i, the two matrices are defined. As the functions $w = u(p) + i_e v(p)$ in the representation (6) depend on the points of the base M', and do not depend on the introduced coordinate systems, it follows that the derivatives W_x, w_y are the Lie derivatives along two main directions of the base.

On the other hand, the operator B_e essentially arises from the following lemma.

Main lemma. [11] *If the linear operator* $L : W \to W$ *acting in complex or real linear space* W *is involute, i.e.* $L^2 = E$, *then its eigenvalues are equal to* ± 1 *and diagonalizable, i.e. the space* W *is considered the direct sum*

$W = W_+ \oplus W_-$, *of the eigenspace* W_+, *corresponding to the eigenvalue +1, and the eigenspace* W_- *corresponding to the eigenvalue -1.*

The operator A_e satisfies the condition of the main lemma, from the statement of which the operator B_e arises. In order to obtain the Lie group, considering its product we obtain the operator C_e. Thus, w possesses the representation

$$w = u(p) + i_e v(p) + i_h r(p) + i_e i_h q(p) = u(p) + i_e v(p) + i_e(r(p) - i_e q(p)).$$

This representation can be considered as a doubling of complex numbers with the imaginary unit i_h. The matrix A_e plays an important role in forming the group G. In the meanwhile the group G induces the triorthogonal system of coordinates. Therefore in (14) essentially occur the partial derivatives with respect to the two variables (x, y). From the invariance of the obtained results with respect to the transformations of coordinate systems, instead of the pair of variables (x, y) it is possible to consider any other pairs among (y, z), (z, x). Finally, we have three equations systems with six first order partial differential equations. All of them form the pair equations system in the three-dimensional manifold domain. In the three-dimensional space *MES* is represented as

$$D_m \begin{pmatrix} u_x + i_e v_x + i_h r_x + i_e i_h q_x \\ u_y + i_e v_y + i_h r_y + i_e i_h q_y \end{pmatrix} = i_m \begin{pmatrix} u_x + i_e v_x + i_h r_x + i_e i_h q_x \\ u_y + i_e v_y + i_h r_y + i_e i_h q_y \end{pmatrix}, \tag{14}$$

where $u, v, p, q : M' \to S^3$, i.e. they are functions of the points of the manifold M' and $u_x, v_x, \dots q_x$ are their Lie derivatives along the main directions M' in the definition point. D_m are real-valued functional matrices, and i_m are their eigenvalues. Simple calculations demonstrate that if $m = 1$ and $i_m = i_1 = i_e$, then D_1 turns into A, (see (10)), if $m = 2$ and $i_m = i_2 = i_h$, then D_2 turns into B, and if $m = 3$ and $i_m = i_3 = i_e i_h$, then we obtain the matrix D_3 in the form of $AB = C$ and conversely. System (14) consists of six equations whose pairs form one elliptic and two hyperbolic systems. Here the pairs $(u, v), (r, -q)$ satisfy the equations system of elliptic and conjugate to it elliptic type, the pairs $(u, r), (v, q)$ satisfy the equations system of hyperbolic and conjugate to it hyperbolic types, the pairs $(u, q), (v, -r)$ satisfy the second equations system hyperbolic and conjugate to hyperbolical types. We are interested in three-dimensional manifolds, therefore, one variable, for example r, can be considered dependent on total four variables and is subject to elimination. Therefore three types of brackets remain: $(u,v),(v,q),(q,u)$. Representing them as cartesian products of the corresponding maps and using (14) we obtain the mapping $F' \times U_{ij} \to G$ [12]. At every point $\mathbf{x} \in M'$ the functions $\beta = \beta(\mathbf{x}), \gamma = \gamma(\mathbf{x})$ are defined, and by means of (14), the layer F' is defined. For each fixed m, $m = 1,2,3$, the layer F' coincides with one of A_e, B_e, C_e at each point $\mathbf{x} \in M'$.

The fibration $p' : E' \to M'$ is called by us the generalized quaternion fibration. The system of equations (14) plays the same role for mappings in the three-dimensional space as in Riemann's theorem on quasiconformal mappings, Beltrami equations system and at $\beta = 0, \gamma = 1$ Cauchy-Riemann's equations system at conformal mappings in two-dimensional space. Let us come back to the Lie brackets. Assuming that at each point of the manifold M' the two-dimensional distribution A_e is defined, automatically using the abovestated procedure we obtain the distribution A_e, B_e, C_e, which satisfies relations (12). It means that the condition of Frobenius theorem is satisfied. From the theorem of Frobenius [12], [13] it follows that in manifold M' a layer is defined. It is known that a class of orthonormalized respects τ^3 in the fibration are extracted. Generally, from the anticommutative relations of the G group elements it follows that the defined layer is triorthogonal space families. Then, by Dupin's theorem, the surfaces of the triorthogonal systems intersect in pairs along the curvature lines of these surfaces. But it allows to build *MES* from which we obtain the matrices A_e, B_e, C_e. The elements of the group $G : A_e, B_e, C_e \in G$ correspond to three orthogonal (one elliptic, two hyperbolic) surface families which form a triorthogonal system. By means of the corresponding (4) *MES* these surfaces are mapped on three orthogonal planes round S^3. Essentially the 3-reper fibrations $p : E \to M$ [12] are defined, where the manifold E points are the pairs $(\mathbf{x}, \tau^3)$, consisting of the points $\mathbf{x} \in M$ and the tangent 3-reper τ^3 at the point $\mathbf{x}$. Here the layer F and a structural group G^0 coincide (main fibration). Taking into account that in the fibration $p' : E' \to M'$ the quaternion space is defined and consequently, any vector $\mathbf{\Omega} \in M'$ is represented in the form

$$\mathbf{\Omega} = G\mathbf{x} = Eu + A_e v + B_e r + C_e q = \begin{pmatrix} t^c & x^c \\ y^c & z^c \end{pmatrix} =$$

$$= \begin{pmatrix} u + \beta v + i_e \beta r + i_e q & \gamma(v + i_e r) \\ -\frac{\beta^2+1}{\gamma} v - \frac{\beta^2-1}{\gamma} r - 2i_e \frac{\beta}{\gamma} q & u - \beta v - i_e \beta r - i_e q \end{pmatrix}, \tag{15}$$

where $(u, v, r, q) \in S^3 \equiv M$ and $det\mathbf{\Omega} = 1$ (the sign shows that all these numbers are complex). By direct calculations we can find that $det\mathbf{\Omega} = u^2 + v^2 + r^2 + q^2 = 1$. This is the three-dimensional sphere S^3 in the four-dimensional space of quaternions H. Therefore, the real functions u, v, r, q are dependent. Solving the last matrix identity with respect to $(u, v, r, q) \in S^3 \equiv M$ we obtain

$$u = \frac{t^c + z^c}{2}, \ v = \frac{1}{\gamma} Rex^c, \ r = \frac{1}{\gamma} Imx^c, \ q = \frac{\gamma(t^c - z^c) - 2\beta x^c}{2\gamma i_e}. \tag{16}$$

We demonstrate that t^c, x^c, y^c, z^c form a three dimensional manifold. In general, the variables t^c, x^c, y^c, z^c are complex and possess eight real variables. From the last identity it follows that $t^c + z^c$ is constant, i.e. $Im(t^c + z^c) = 0$, which requires one condition from t^c, x^c, y^c, z^c. It is easy to calculate the equality

$$y = \frac{\beta^2 x^c - \overline{x}^c + \beta\gamma(z^c - t^c)}{\gamma^2}$$

from which it follows that the variable y is not considered to be dependent. It also requires two more conditions from t^c, x^c, y^c, z^c. Moreover, $det\mathbf{\Omega} = 1$ defines two conditions: $Re(t^c z^c - x^c y^c) = 1, \ Im(t^c z^c - x^c y^c) = 0$. We conclude that only three functions from the eight real and imaginary parts of the complex functions t^c, x^c, y^c, z^c are independent, namely: $t^c + z^c, Rex^c, Imx^c$. As for the triorthogonal system, at each point on M' there exist three orthogonal main directions along which the curvature lines are directed, i.e. coordinate lines. *BES* (4) satisfy these conditions which in matrix writing sets the matrix A_e. The operator A_e satisfies the conditions of the main lemma from statement of which the operator B_e arises. In the meanwhile, in order to obtain the Lie groups and considering their product we obtain the operator C_e. Consequently, the group G essentially arises only from the matrix A_e. In the meanwhile, the group G induces the triorthogonal system of coordinates.

Therefore, the partial derivatives with respect to x, y essentially participate in (14). The invariance of the obtained results concerning the coordinate system enables us to consider any other pairs among $(y, z), (z, x)$ instead of x, y.

As $v + i_e r$ realizes quasiconformal mappings of the maps $M' \supset U_i' \to U_k \subset S^3$ we can conclude that the second and the third equations of system (16) is solvable in U_k and looks like $x = x(v, r),\ y = y(v, r)$. Thus, at any point $(u, v, r, q) \in S^3 \equiv M$ we correspondingly put the points $(u, v, r, q, \alpha, \beta, \gamma) \subset R^6$ of the six-dimensional space. It means that the manifold M' is realized in the form of the three dimensional surface of six-dimensional space at least in a local manner [14]. Different points S^3 are correspondingly substituted by different points of the surface. Following this one-to-one correspondence we consider all possible points (t, x, y, z) corresponding to the points $(u, v, r, q) \in S^3 \equiv M$. The space of these points is denoted by M'. Simultaneously, as stated above, M' is the considered Seifert's fibration. Thus, M' is a three-dimensional closed manifold and any of the operators E, A_e, B_e, C_e acting on the tangent space M' form a cyclic group of four order cycle. Thus, the morphism between the fibrations

$$E' \to M',\ E \to M \equiv S^3,\ E \to E'$$

and an inverse mapping

$$M' \to E',\ M \to E,\ E' \to E,$$

i.e. the correspondence between the points M' and S^3 are established. Thus, the obtained two fibrations on the same base S^3 are quaternionic and generalized quaternionic.

In conclusion we note that Dirac's matrices and Yang-Mill's field can be generalized if we use in an appropriate way the matrices $B - i_e A,\ C = AB$ instead of Pauli's matrices.

References

1. Arnold, V. I., *Obiknovennie differentsialnie uravneniya*, Moscow, 1976.

2. Scott, P., *The geometries of 3-manifolds*, Moscow, Mir, 1986. (Russian) (English version- London Mathematics Society, 1983).

3. Morgan, J. W., *Recent progress on the Poincaré conjecture and the classification of 3-manifolds*, Bulletin (New Series) of the American Mathematical Society, **42**(2005), 57-78.

4. Bers, L., *Mathematical aspects of subsonic and transonic gas*, (Russian), IIL, Moscow, (1961). (Rusian) (English version- New York, 1958)

5. Zakhirov, M., *Imaginary units: use in analysis and applications*, ROMAI Journal, **2**, 2(2006), 227-255.

6. Zakhirov, M., *Generalized quaternions, satisfying a system and applications*, Proc. of the Intern. Conf. "Aktualnie voprosi compleksnogo analiza", Urgench, Khiva, Uzbekistan, 2008, 16-17.

7. Warden, Van der, B. L, *Algebra*, Nauka, Moscow, 1970. (Russian) (English version- Springer Berlin, Heidelberg, New York, 1967).

8. Husemoller, D., *Fibre bundles*, Mir, Moscow, 1970.(Russian)(English version- New York, 1966)

9. Green, B., John, H., Schwarz, J. H., Witten, E., *Superstrings theory*, Vol 2, Mir, Moscow, 1990.(Russian) (English version- Cambridge University Press, 1988)

10. Penrose, R., Rindler, W., *Spinors and space-time*, Mir, Moscow, 1987. (Russian)(English version - Cambridge, University Press)

11. Postnikov ,M. M., *Lie groups and algebras*, Nauka, Moscow, 1982.(Russian)

12. Dubrovin, B. A., Novikov, S. P., Fomenko, A. T., *Contemporary geometry*, Nauka, Moscow, 1979.(Russian)

13. Schuts, B., *Geometrical methods of mathematical physics*, Mir, Moscov, 1984.(Russian) (English version - Cambridge University Press, London, 1982).

14. Rashevskiy, P. K., *Riemann geometry and tensor analysis*, Moscow, Nauka, 1964.

ROMAI J., **4**, 2(2008), 191–203

A NUMERICAL METHOD FOR OBTAINING THE GENERALIZED DERIVATIVE OF NONDIFFERENTIABLE FUNCTIONS

M. Zamirian, A. V. Kamyad, A. M. Vaziri

Department of Mathematics, Islamic Azad University of Bojnourd, Iran

Department of Mathematics, Ferdowsi University of Mashhad, Iran

Department of Mathematics, Ferdowsi University of Mashhad, Iran

zamirianm@yahoo.com

Abstract A numerical method to achieve generalized derivative for continuous functions which are nondifferentiable, is introduced. At first, it is proved that the relation between a continuously differentiable function and its derivative can be shown with an infinite moment problem (IMP). Then, by approximating the IMP to a finite moment problem (FMP), we obtain the relation between continuous and nondifferentiable function and its generalized derivative. Thus, by solving the FMP with numerical method, the generalized derivative is achieved. Finally, efficiency of our approach is confirmed by some numerical examples.

Keywords: generalized derivative, non-differentiable functions, infinite moment problem, finite moment problem.

2000 MSC: 26A24, 26A27.

1. INTRODUCTION

There are some optimization problems that involve nondifferentiable functions. Since the algorithms that solve these problems require a derivative of these functions, it is necessary to obtain a generalized derivative for them. Clarck in [1], analytically, presented a generalized derivative for Lipschitz continuous functions. In this method the generalized derivative is pointwise defined and different values are obtained in nondifferentiable points.

In this paper, our purpose is to obtain a continuous function as a generalized derivative for non-differentiable functions on a set such as $X - \partial X \subset \mathbb{R}^m$, where $X = (x_1, ..., x_m)$, $a_i \leq x_i \leq b_i$, $i = 1, ..., m$, a_i, b_i are given real numbers and ∂X is the boundary of X. First, it is supposed that $g(.)$ is a continuous function on X. Then by using $g(.)$, we obtain a IMP and prove that its analytical solution is the derivative of $g(.)$. In this situation, $g(.)$ must be a continuously differentiable function on $X - \partial X$. At this point, the IMP is approximated with a FMP so that $g(.)$ can be a continuous and nondifferetiable function. Thus, by solving the FMP a continuous function is obtained which is defined as the generalized derivative of $g(.)$ on $X - \partial X$.

2. THE GENERALIZED DERIVATIVE OF NONDIFFERENTIABLE REAL-VALUED FUNCTIONS OF ONE VARIABLE

We suppose $g(x) : [0,1] \to \mathbb{R}$ is a continuous real-valued function.

Theorem 2.1. *Let $g(.)$ and $f(.)$ be two continuous real-valued functions on $[0,1]$ such that*

$$\int_0^1 (v(x)f(x) + \dot{v}(x)g(x))dx = 0, \tag{1}$$

for any $v(.) \in C^1(0,1)$ with $v(0) = v(1) = 0$.
Then $g(.) \in C^1(0,1)$ and $\dot{g}(x) = f(x)$ on $(0,1)$.

Proof. Define

$$F(x) = \int_0^x f(t)dt.$$

Then by using integration by parts from (1), we have $\int_0^1 (g(x) - F(x))\dot{v}(x)dx = 0$, also the boundary conditions imply $\int_0^1 c\dot{v}(x)dx = 0$, where c is a arbitrary constant real number. Then,

$$\int_0^1 (g(x) - F(x) - c)\dot{v}(x)dx = 0, \tag{2}$$

for any c. Now, define $v(x) = \int_0^x (g(t) - F(t) - c_0)dt$, where c_0 is a constant real number such that $v(1) = 0$; then $v(.) \in C^1(0,1)$ and $v(0) = v(1) = 0$. Replacing this particular $v(.)$ and c_0 in (2), we obtain $\int_0^1 (g(x) - F(x) - c_0)^2 dx = 0$, then $g(x) - F(x) = c_0$ on $(0,1)$, so $g(.) \in C^1(0,1)$ and $\dot{g}(x) = f(x)$ on $(0,1)$.

Remark 2.1. Choosing $[0,1]$ as interval is not restrictive. In case $x \in [a,b]$, the mapping $y = (x-a)/(b-a)$ changes the x variable to $y \in [0,1]$.

Now, we weaken the assumptions of theorem (1) by the following proposition and theorem.

Proposition 2.1. *Let $f(.)$ be a continuous real-valued function on $[0,1]$, such that*

$$\int_0^1 \cos n\pi x f(x)dx = 0,\ n = 0, 1, 2, ... \tag{3}$$

Then $f(x) = 0$ for any $x \in [0,1]$.

Proof. For any $m \in \mathbb{N} \cup \{0\}$, the function $h(x) = x^m$ on $[0,1]$ is extended on $[-1,1]$ as follows:

$$h_e(x) = \begin{cases} h(x), & 0 \leq x < 1; \\ h(-x), & -1 \leq x \leq 0, \end{cases}$$

the $h_e(x)$ is an even function on $[-1,1]$ obviously; therefore its Fourier series is as follows:

$$S(x) = \sum_{n=0}^{\infty} a_n \cos n\pi x.$$

Now, set

$S_N(x) = \sum\limits_{n=0}^{N} a_n \cos n\pi x$, where N is any positive integer.

Thus, $S_N(x)$ is uniform convergent to $h_e(.)$ on $[-1,1]$ and $h(.)$ on $[0,1]$, and $S_N(.)f(.)$ is uniform convergent to $x^m f(.)$, so

$$\lim_{N\to\infty} \int_0^1 S_N(x)f(x)dx = \int_0^1 x^m f(x)dx.$$

By using (3) for any N, $\int_0^1 S_N(x)f(x)dx = 0$, then

$$\int_0^1 x^m f(x)dx = 0,\ m = 0, 1, 2, ... \tag{4}$$

Since $f(.)$ is a continuous real-valued function, then there exists a sequence of polynomial functions $P_N(.)$, $N = 1, 2, ...$, uniform convergent to $f(.)$, hence $P_N(.)f(.)$ is uniform convergent to $f^2(.)$; therefore,

$$\lim_{N\to\infty} \int_0^1 P_N(x)f(x)dx = \int_0^1 f^2(x)dx.$$

By using (4), for any N, $\int_0^1 P_N(x)f(x)dx = 0$, then $\int_0^1 f^2(x)dx = 0$, so $f(.) = 0$ for any $x \in [0,1]$.

Proposition 2.2. Let $f(.)$ be a continuous real-valued function on $[0,1]$ and

$$\int_0^1 \sin n\pi x f(x)dx = 0, \;\; n = 0,1,2,.... \tag{5}$$

Then $f(x) = 0$ for any $x \in [0,1]$.

Proof. Define

$$F(x) = \int_0^x f(t)dt.$$

By integration by parts in (5), we have $\sin n\pi x F(x)|_0^1 - n\pi \int_0^1 \cos n\pi x F(x)dx = 0$, $n = 0,1,2,...$, or $\int_0^1 \cos n\pi x F(x)dx = 0, \;\; n = 0,1,2,...,$

According to Prop. 2.1, $F(.) = 0$ so $f(.) = 0$ on $[0,1]$.

Theorem 2.2. *Let $f(.)$ and $g(.)$ be two continuous real-valued functions on $[0,1]$ and*

$$\int_0^1 (\sin n\pi x f(x) + n\pi \cos n\pi x g(x))dx = 0, \;\; n = 0,1,2,\dots. \tag{6}$$

Then $g(.) \in C^1(0,1)$ and $\dot{g}(x) = f(x)$ for any $x \in (0,1)$.

Proof. Define

$$F(x) = \int_0^x f(t)dt.$$

By using integration by parts, from (6), we have

$$\sin n\pi x F(x)|_0^1 + n\pi \int_0^1 \cos n\pi x (g(x) - F(x))dx = 0, \;\; n = 0,1,2,...,$$

or $\int_0^1 \cos n\pi x (g(x) - F(x))dx = 0, \;\; n = 0,1,2,....$

Due to Proposition 2.1 $g(x) - F(x) = 0$ on $[0,1]$, then $g(.) \in C^1(0,1)$ and $\dot{g}(x) = f(x)$ for any $x \in (0,1)$. Now, we set

$$\alpha_n = -n\pi \int_0^1 \cos n\pi x g(x)dx;$$

and we obtain, from (6)

$$\int_0^1 \sin n\pi x f(x)dx = \alpha_n, \;\; n = 0,1,2,... \tag{7}$$

Remark 2.2. If $g(.)$ is given on $[0,1]$, then α_n is a known real number, so (7) is a IMP with unknown function $f(.)$ which is the derivative of $g(.)$.

Now, the IMP is approximated by a FMP as follows

$$\int_0^1 \sin n\pi x f(x)dx = \alpha_n,\ n = 0, 1, 2, \ldots, N,$$

where, $N$is a given positive integer.

Definition 2.1. *Let $g(.)$ be a continuous real-valued function defined on $[0,1]$ and $f(.)$ a function defined on (0,1) such that*

$$\int_0^1 \sin n\pi x f(x)dx = \alpha_n,\ n = 0, 1, 2, \ldots, N. \tag{8}$$

Then $f(.)$ is defined as the generalized derivative of $g(.)$ on $(0,1)$.

Remark In this situation, $g(.)$ can be nondifferentiable such that its derivative must be integrable.

In order to determine a function f that satisfies (8), we partition interval $[0,1]$ to N sub-intervals (where N is a given positive integer) and chose the points $x_k = (2k+1)/(2N),\ k = 0, ..., N-1$ in each sub-interval

$$1/N \sum_{k=1}^{N} \sin n\pi x_k f(x_k) = \alpha_n,\ n = 0, 1, 2, ..., N. \tag{9}$$

If N tend to infinity, then the solution of (9) and (7), $f(.)$, are the same.

The problem (9) is a system of linear equations with N equations and N unknowns, $f(x_k)$, $k = 1, ..., N$. Then, we may acquire its solution by many packages such as Matlab.

3. THE GENERALIZED DERIVATIVE OF NON-DIFFERENTIABLE REAL-VALUED FUNCTIONS OF M VARIABLES

First, the real-valued functions of two variables, is considered. Then it is generalized to m variables.

Theorem 3.1. *Let $f(x,y)$ and $g(x,y)$ be two continuous real-valued functions on $[0,1] \times [0,1] \subset \mathbb{R}^2$ such that*

$$\int_0^1 \int_0^1 (\sin m\pi x \sin n\pi y f(x,y) + m\pi \cos m\pi x \sin n\pi y g(x,y))dxdy = 0, \tag{10}$$

$n, m = 0, 1, 2, \ldots$ Then $\partial g(x,y)/\partial x$ is a continuous function and $\partial g(x,y)/\partial x = f(x,y)$ for any $x, y \in (0,1)$.

Proof. Define

$$F(x,y)=\int_0^x f(t,y)dt.$$

Now, by integration by parts, we obtain from (10)

$$\int_0^1 \sin n\pi y(\sin m\pi x F(x,y)|_0^1+\int_0^1 m\pi\cos m\pi x(g(x,y)-F(x,y))dx)dy=0,$$

$n,m=0,1,2,...$ Then

$$\int_0^1 \sin n\pi y\int_0^1 m\pi\cos m\pi x(g(x,y)-F(x,y))dxdy=0,\ \ n,m=0,1,2,....$$

For brevity, set $w_m(y)=\int_0^1 m\pi\cos m\pi x(g(x,y)-F(x,y))dx$. Then $\int_0^1\sin n\pi x w_m(x)dx=0,\ n=0,1,2,....$ Since $w_m(y)$ is a continuous function on $[0,1]$, by Prop. 2.2, $w_m(y)=0$ for any $y\in[0,1]$.

Thus, for any $y\in[0,1]$, $\int_0^1 m\pi\cos m\pi x(g(x,y)-F(x,y))dx=0,\ m=0,1,2,...,$ and due to proposition (1), $g(x,y)-F(x,y)=0$, then $\partial g(x,y)/\partial x$ is a continuous function and $\partial g(x,y)/\partial x=f(x,y)$ for any $x,y\in(0,1)$.

Similarly we can prove the following

Theorem 3.1'. *Within the hypotheses of theorem 3.1, if*

$$\int_0^1\int_0^1 \sin m\pi x\sin n\pi y f(x,y)+n\pi\cos m\pi y\sin m\pi x g(x,y)dxdy=0$$

$n,m=0,1,2,...,$ *then $\partial g(x,y)/\partial y$ is a continuous function and* $\partial g(x,y)/\partial y=f(x,y)$ *for any $x,y\in(0,1)$.*

If $g(x,y)=g_1(x)+g_2(y)$, then the following theorem which is easier to use than Theorem 3.1 in practical purposes, is proposed.

Theorem 3.2. *Let $f(x,y)$ and $g(x,y)$ be two continuous real-valued functions on $[0,1]\times[0,1]$ and $g(x,y)$ be a separable function of its variables, that is $g(x,y)=g_1(x)+g_2(y)$ and*

$$\int_0^1(\sin n\pi x f(x)+n\pi\cos n\pi x g_1(x))dx=0,\ \ n=0,1,2,.... \tag{11}$$

Then $\partial g(x,y)/\partial x$ is a continuous function and $\partial g(x,y)/\partial x=f(x)$ for all $x,y\in(0,1)$.

Proof. Define

$$F(x)=\int_0^x f(t)dt.$$

Then

$$\sin n\pi x F(x)|_0^1 + n\pi \int_0^1 \cos n\pi x(g_1(x) - F(x))dx = 0, \tag{12}$$

$n = 0, 1, 2, ...,$ or

$$\int_0^1 \cos n\pi x(g_1(x) - F(x))dx = 0,\ n = 0, 1, 2, ...$$

Now, for $m, n = 0, 1, 2, ...,$ we have

$$\int_0^1 \int_0^1 (\sin m\pi x \sin n\pi y f(x) + m\pi \cos m\pi x \sin n\pi y g(x, y))dxdy =$$

$$= \int_0^1 \sin n\pi y(m\pi \int_0^1 \cos m\pi x(g(x, y) - F(x))dx)dx =$$

$$= \int_0^1 m\pi \sin n\pi y(\int_0^1 \cos m\pi x(g_1(x) - F(x))dx + g_2(y) \int_0^1 \cos m\pi x dx)dy\,.$$

Since $\int_0^1 \cos m\pi x dx = 0$ and by (3.3) $\int_0^1 \cos m\pi x(g_1(x) - F(x))dx = 0$, then

$$\int_0^1 \int_0^1 (\sin m\pi x \sin n\pi y f(x) + m\pi \cos m\pi x \sin n\pi y g(x, y))dxdy = 0,$$

$n, m = 0, 1, 2, ...$.

Therefore, by using Theorem 3.1 $\partial g(x, y)/\partial x$ is a continuous function and $\partial g(x, y)/\partial x = f(x)$ for any $x, y \in (0, 1)$.

In the same way, we can prove

Theorem 3.2'. *Within the hypotheses of Theorem 3.2, if for* $n = 0, 1, 2, ...$ $\int_0^1 (\sin n\pi y f(y) + n\pi \cos n\pi y g_2(y))dy = 0,$ *then* $\partial g(x, y)/\partial y$ *is a continuous function and* $\partial g(x, y)/\partial y = f(y)$ *for all* $x, y \in (0, 1)$.

Now we extend our discussion to m variables.

Theorem 3.3. *Let* $f(.)$ *and* $g(.)$ *be two continuous real-valued functions on* $A = \prod_{j=1}^{m} [0, 1] \subset \mathbb{R}^m$ *and*

$$\int_A (\prod_{j=1}^{m} \sin n_j \pi x_j f(X) + n_i \pi \cos n_i \pi x_i \prod_{j=1,\, j\neq i}^{m} \sin n_j \pi x_j g(X))dX = 0, \tag{13}$$

$n_j = 0, 1, 2, ..., j = 1, 2, ..., m.$ *Then* $\partial g(X)/\partial x_i$ *is a continuous function and* $\partial g(X)/\partial x_i = f(X)$ for any $X \in A - \partial A$, *where* $X = (x_1, ..., x_m)$ *and* ∂A *is the boundary of* A.

Proof. Set $A_i = \prod_{j=1,\, j\neq i}^{m} [0,1] \subset \mathbb{R}^{m-1}$**,** $X_i = (x_1, ..., x_{i-1}, x_{i+1}, ..., x_m) \in A_i$ and $F(X) = \int_0^{x_i} f(x_1, ..., x_{i-1}, t, x_{i+1}, ...x_m)dt$**.** We use induction on m. For $m = 2$ by Theorem 3.2 the proof is complete. Now, we suppose the theorem for $m = k$ is true. Then, for $m = k+1$ from (13) we obtain

$$\int_0^1 \sin n_l \pi x_l \int_{A_l} (\prod_{j=1, j\neq l}^{k+1} \sin n_j \pi x_j f(X) + n_i \pi \cos n_i \pi x_i \prod_{j=1,\, j\neq i,\, l}^{k+1} \sin n_j \pi x_j g(X)) dX_l dx_l = 0,$$

$n_j = 0, 1, 2, ...,\ j = 1, 2, ..., k+1$, where $1 \leq l \leq k+1, l \neq i$.

For brevity, set

$w(x_l) = \int_{A_l} (\prod_{j=1, j\neq l}^{k+1} \sin n_j \pi x_j f(X) + n_i \pi \cos n_i \pi x_i \prod_{j=1,\, j\neq i,\, j\neq l,}^{k+1} \sin n_j \pi x_j g(X)) dX_l.$

Then, for any $n_l = 0, 1, 2, ...,$ we have $\int_0^1 \sin n_l \pi x_l w(x_l) dx_l = 0$. Since $w(x_l)$ is a continuous function then according to result 2.1, $w(x_l) = 0$ for any $x_l \in [0,1]$. Then, for any $x_l \in [0,1]$

$$w(x_l) = \int_{A_l} (\prod_{j=1, j\neq l,}^{k+1} \sin n_j \pi x_j f(X) + n_i \pi \cos n_i \pi x_i \prod_{j=1,\, j\neq i,\, j\neq l}^{k+1} \sin n_j \pi x_j g(X)) dX_l = 0,$$

$n_j = 0, 1, 2, ...,\ j = 1, ..., l-1, l+1, ..., k+1$.

Due to induction assumption, $\partial g(X)/\partial x_i$ is a continuous function and $\partial g(X)/\partial x_i = f(X)$ for any $X \in A - \partial A$. For simplicity, set $\alpha^i_{n_1 n_2 \ldots n_m} = -n_i \pi \int_A \cos n_i \pi x_i \prod_{j=1,\, j\neq i}^{m} \sin n_j \pi x_j g(X) dX$. Due to (13), we have

$$\int_A (\prod_{j=1}^{m} \sin n_j \pi x_j f(X) dX = \alpha^{i_m}_{n_1 n_2 \ldots n_m},\ n_j = 0, 1, 2, ...,\ j = 1, 2, ..., m. \quad (14)$$

Now, let $g(.)$ be given, that means $\alpha^i_{n_1 n_2 \ldots n_m}$ is a known real number, so (14) is a IMP with the unknown function of $f(.)$ which is the partial derivative of $g(.)$ with respect to x_i.

Now, the IMP is approximated by a FMP as follows:

$$\int_A \prod_{j=1}^{m} \sin n_j \pi x_j f(X) dX = \alpha^i_{n_1 n_2 \ldots n_m} m,\ n_j = 0, 1, 2, ..., N,\ j = 1, 2, ..., m,$$

where N is a given positive integer.

Definition 3.1. *Let $g(.)$ be a continuous real-valued functions and given on A and*

$$\int_A (\prod_{j=1}^{m} \sin n_j \pi x_j f(X) dX = \alpha^i_{n_1 n_2 \ldots n_m m}, \; n_j = 0, 1, 2, ..., N, \; j = 1, 2, ..., m. \tag{15}$$

Then $f(.)$ is defined as the generalized partial derivative of $g(X)$ with respect to x_i, $i = 1, ..., m$ on $A - \partial A$. In this situation, $g(X)$ can be non-differentiable function with respect to x_i, $i = 1, ..., m$, such that its partial derivative with respect to x_i, $i = 1, ..., m$, must be integrable.

For solving the moment problem (15), each of the intervals $[0, 1]$ in A is partitioned into N equal parts and then (15) is approximated as follows

$$\sum_{k_m}^{N} \ldots \sum_{k_2}^{N} \sum_{k_1}^{N} \prod_{j=1}^{m} (1/N \sin n_j \pi x_{jk_j}) f(x_{1k_1}, x_{2k_2}, ..., x_{mk_m}) = \alpha^i_{n_1 n_2 \ldots n_m}, \tag{16}$$

$n_j = 0, 1, 2, ...,\ j = 1, 2, ..., m$, where $x_{jk_j} = (2k_j+1)/(2N),\ k_j = 0, 1, ..., N-1$.

Now, it is obvious that if N tend to infinity then the solution of (14) and (16) are the same.

The system (16) is a system of N^m linear equations with N^m unknowns, $f(x_{1k_1}, x_{2k_2}, ..., x_{mk_m})$, $k_j = 0, 1, 2, ..., N - 1$, $j = 1, ..., m$, thus its solution may be acquired by many packages such as Matlab.

4. THE GENERALIZED DERIVATIVE OF NON-DIFFERENTIABLE VECTOR-VALUED FUNCTIONS OF VARIABLES

Theorem 4.1. *Let $\mathbf{g}(.) = (g_1(.), ..., g_n(.))$ and $\mathbf{f}(.) = (f_1(.), ..., f_n(.))$ be two continuous real vector-valued functions on $A = \prod_{j=1}^{m} [0, 1]$ and*

$$\int_A (\prod_{j=1}^{m} \sin n_j \pi x_j f(X) + n_i \pi \cos n_i \pi x_i \prod_{j=1,\, j \neq i}^{m} \sin n_j \pi x_j g(X)) dX = \mathbf{0}, \tag{17}$$

$n_j = 0, 1, 2, ...,\ j = 1, 2, ..., m$. Then $\partial \mathbf{g}(X)/\partial x_i$ is a continuous function and $\partial \mathbf{g}(X)/\partial x_i = \mathbf{f}(X)$ for any $X \in A$, where $\mathbf{0} = (0, ..., 0)$ is the null vector in $\mathbb{R}^n$.

Proof. Define

$$\mathbf{F}(X) = (F_1(X), ..., F_n(X)) =$$

$$= (\int_0^{x_i} f_1(x_1, ..., x_{i-1}, t, x_{i+1}, ..., x_n)dt, ..., \int_0^{x_i} f_n(x_1, ..., x_{i-1}, t, x_{i+1}, ..., x_n)dt).$$

By (17), for $k = 1, 2, ..., n$,

$$\int_A (\prod_{j=1}^{m} \sin n_j\pi x_j f_k(X) + n_i\pi \cos n_i\pi x_i \prod_{j=1, j\neq i}^{m} \sin n_j\pi x_j g_k(X))dX = 0, \quad (18)$$

$n_j = 0, 1, 2, ...,$ $j = 1, 2, ..., m$. Now, by using Theorem 3.3, $g_k(X) = F_k(X)$, $k = 1, 2, ..., n$, we obtain that $\partial g_k(X)/\partial x_i$ is a continuous real-valued function and $\partial g_k(X)/\partial x_i = f_k(X)$, $k = 1, 2, ..., n$, hence $\partial \mathbf{g}(X)/\partial x_i$ is a continuous function and $\partial \mathbf{g}(X)/\partial x_i = \mathbf{f}(X)$ for any $\mathbf{X} \in A$.

Definition 4.1. *Let* $\boldsymbol{g}(.)$ *and* $\boldsymbol{f}(.)$ *be two continuous real vector-valued functions on* A *and*

$$\int_A (\prod_{j=1}^{m} \sin n_j\pi x_j \mathbf{f}(X) + n_i\pi \cos n_i\pi x_i \prod_{j=1, j\neq i}^{m} \sin n_j\pi x_j \mathbf{g}(X))dX = \mathbf{0}, \quad (19)$$

$n_j = 0, 1, 2, ..., N$, $j = 1, 2, ..., m$. *Then* $\mathbf{f}(.)$ *is defined as the approximation of the partial derivative of* $g(.)$ *with respect to* x_i *for any* $X \in A$*, where* N *is a given positive integer.*

Then, due to (19) for every $k = 1, 2, ..., n$

$$\int_A (\prod_{j=1}^{m} \sin n_j\pi x_j f_k(X) + n_i\pi \cos n_i\pi x_i \prod_{j=1, j\neq i}^{m} \sin n_j\pi x_j g_k(X))dX = 0,$$

$n_j = 0, 1, 2, ..., N$, $j = 1, 2, ..., m$. Therefore, $f_k(.)$, $k = 1, ..., n$, are numerically achieved like in Section 3. Finally $\mathbf{f}(.)$ as the generalized partial derivative of $\mathbf{g}(.)$ with respect to x_i is achieved.

5. NUMERICAL EXAMPLES

In this section, we use our method for some non-differentiable functions.

Example 1. Suppose

$$g(x) = \begin{cases} |2x^2 - 4| & 0 \leq x \leq 2, \\ 12 - 4x & 2 \leq x \leq 3, \\ \cos(\pi x/2) & 3 \leq x \leq 4. \end{cases}$$

The exact derivative of $g(.)$, except in $x = \sqrt{2}$, 2, 3, where the function is non-differentiable, is shown in Fig. 1. Now, for obtaining the generalized

Fig. 1. the exact derivative of g(x) except x=$2^{1/2}$,2 and 3.

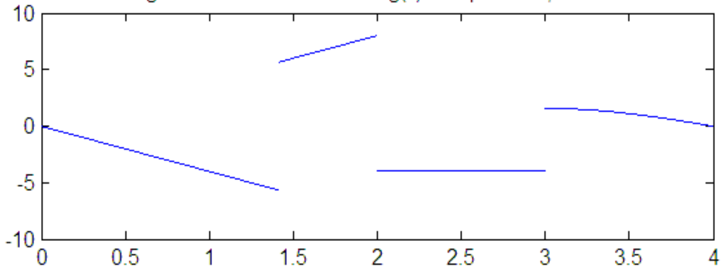

Fig. 2. the generalized derivative of g(x) on (0,4).

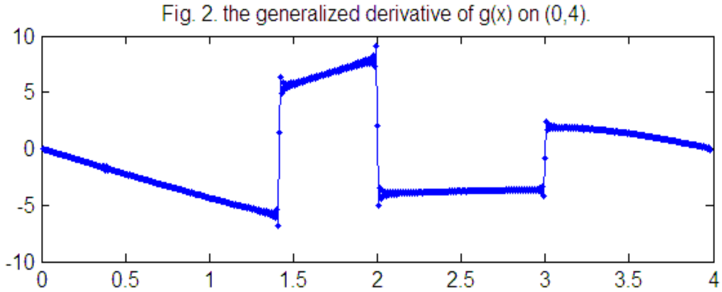

derivative of $g(.)$, we partition interval $[0, 4]$ to $N = 500$ equal subintervals. Then, by using (9) a system of linear equations with 500 variables and 500 equations is obtained. The generalized derivative of $g(.)$ obtained from the solution of this system, is shown in Fig. 2.

Example 2. Suppose

$$g(x) = |\sin(5\pi x)| \qquad 0 \leq x \leq 1.$$

The exact derivative of $g(.)$ except in $x = i/5$, $i = 1, ..., 4$, where the function is non-differentiable, is shown in Fig. 3.

Now, we choose $N = 575$. Then, the generalized derivative of $g(.)$ obtained from the solution of system (9), is shown in Fig. 4.

Example 3. Suppose

$$g(x, y) = |\sin(2\pi x)|\, y \qquad 0 \leq x \leq 1,\ 0 \leq y \leq 1.$$

The exact partial derivative of $g(.,.)$ with respect to x except in $(x, y) = (1/2, y)$, $0 < y < 1$, where the function is non-differentiable, is shown in Fig.5.

Fig. 3. the exact derivative of g(x) except x=i/5, i=1,...,4.

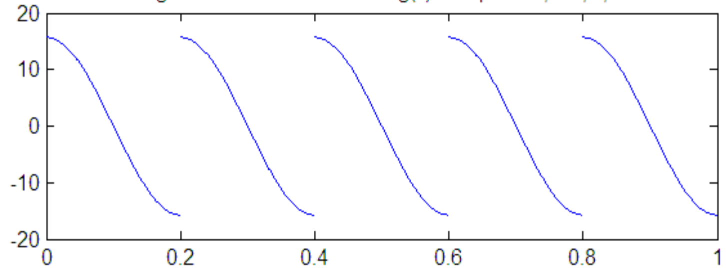

Fig. 4. the generalized derivative of g(x) on (0,1).

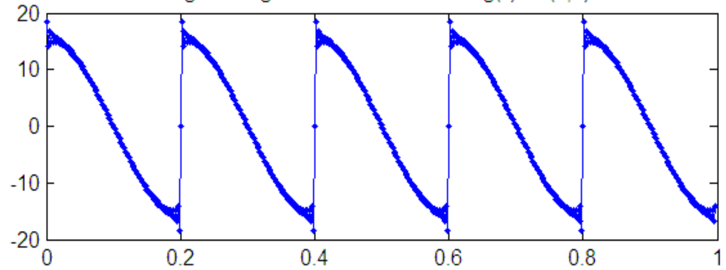

Fig. 5. the exact partial derivative of g(x,y) with respect to x except (x,y)=(0.5,y), 0<y<1.

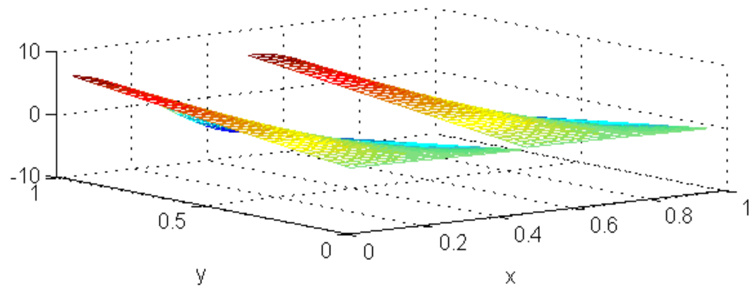

Fig. 6. the generalized partial derivative of g(x,y) with respect to x on 0<x,y<1.

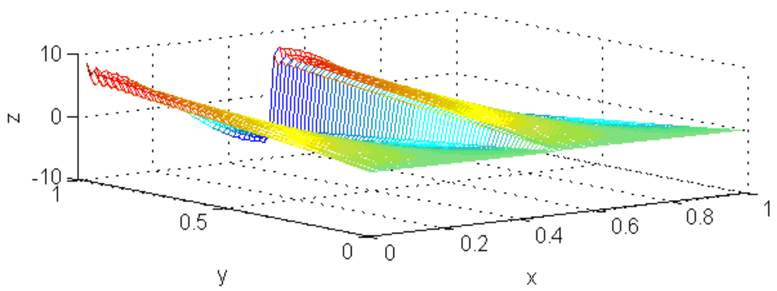

Now, we choose $N = 75$. Then, the generalized partial derivative of $g(.,.)$ with respect to x, obtained from the solution of system (16), $j = 2$, is shown in Fig. 6.

References

[1] Clarke, F. H. *Optimization and nonsmooth analysis*, J. Wiley, New York, 1983.